Development of Volume Translation Models for PC-SAFT Equation of State

by

Jialin Shi

A thesis submitted in partial fulfillment of the requirements for the degree of

Doctor of Philosophy

in

Petroleum Engineering

Department of Civil and Environmental Engineering
University of Alberta

ABSTRACT

Statistical associating fluid theory (SAFT)-type equations of states (EOSs) are commonly utilized in the chemical and petroleum industry to model the phase behavior of both pure and complex fluids because of its solid theoretical framework based on a perturbation theory. For the most SAFT-type EOSs (such as the perturbed-chain SAFT EOS (PC-SAFT EOS) proposed by Gross and Sadowski (2001)), one main drawback is that they fail to accurately describe the phase behavior of pure fluids near the critical region. They fail to reproduce the critical temperature and critical pressure of pure fluids, resulting in imprecise predictions of thermophysical properties (such as liquid density) in the vicinity of the critical point. This study aims to explore the development of more accurate volume translation models for PC-SAFT EOS that could work well at both near-critical and far-critical conditions.

Inspired by the re-parametrization method with the exact representation of critical temperature and critical pressure (Anoune *et al.*, 2021), we first develop a nonlinear temperature-dependent volume translation model in the PC-SAFT EOS for more accurate density predictions for CO_2 over a wide range of temperatures and pressures. The developed nonlinear temperature-dependent volume translation model can capture the general trend of the practically needed volume residuals for CO_2 (i.e., the molar volume calculated by the critical-point rescaled PC-SAFT EOS (CPPC-SAFT EOS) (Anoune *et al.*, 2021) minus the experimental one). Using the proposed volume translated PC-SAFT EOS, critical temperature and critical pressure of CO_2 can be exactly reproduced. In addition, more accurate predictions of liquid density and vapor pressure of CO_2 can be achieved with the proposed volume translated PC-SAFT EOS.

Although the above proposed nonlinear temperature-dependent volume translation model can partially remedy the prediction accuracy of critical properties, the accuracy of liquid density prediction is still compromised in the vicinity of the critical region. Thus, to further improve the prediction accuracy of thermodynamic properties near the critical region, we integrate a distance-function-based volume translation model into the CPPC-SAFT EOS, generating a volume-translated rescaled PC-SAFT EOS (VTR-PC-SAFT EOS). It is found that the proposed distance-function-based volume translation model can well capture the practically needed volume residuals. The proposed VTR-PC-SAFT EOS can exactly reproduce the critical temperature, critical pressure, and critical molar volume of a pure compound. Compared to the state-of-the-art PC-SAFT models in the literature (i.e., PC-SAFT EOS (Gross and Sadowski, 2001), I-PC-SAFT EOS (Moine *et al.*, 2019), and CPPC-SAFT EOS (Anoune *et al.*, 2021)), the VTR-PC-SAFT EOS yields more accurate predictions of several important thermodynamic properties (including saturated liquid density, liquid density, and vapor pressure) of 39 pure compounds at both critical and non-critical regions. In addition, we propose a generalized version of the VTR-PC-SAFT EOS model for *n*-alkanes (except CH_4). Furthermore, we explore if the proposed VTR-PC-SAFT EOS can also work well for more compounds that are not examined in the initial stage of the study. In the follow-up study, we examine the performance of the VTR-PC-SAFT EOS in correlating the vapor pressure, liquid density, vapor density, supercritical density, saturated-liquid density, and saturated-vapor density of 251 compounds from 20 chemical families. The testing results show that VTR-PC-SAFT EOS can yield a better performance in predicting both critical and non-critical properties in comparison to the other PC-SAFT-type EOSs.

Finally, we assess the performance of different PC-SAFT-type EOSs in reproducing various thermodynamic derivative properties of pure compounds, including thermal expansion coefficient, isothermal compressibility coefficient, heat capacities, Joule-Thomson coefficient, and speed of sound. The comparative analysis shows that the proposed VTR-PC-SAFT EOS outperforms the other models (PC-SAFT EOS, CPPC-SAFT EOS, and I-PC-SAFT EOS) in predicting most of the derivative properties. Specifically, it yields the smallest %AADs in reproducing thermal expansion coefficient, isothermal compressibility coefficient, Joule-Thomson coefficient, and speed of sound. However, the accuracy of VTR-PC-SAFT in reproducing the isobaric heat capacity is slightly lower than that of the original PC-SAFT EOS.

PREFACE

A version of **CHAPTER 2** has been published as J. Shi and H. Li, Modified temperature-dependent volume translation model in PC-SAFT equation of state for carbon dioxide, *Chemical Engineering Science* 263 (2022) 118107. J. Shi is responsible for the theoretical development, simulation results, analysis, and manuscript composition. H. Li is the supervisory author and gets involved in the concept formation, theoretical development, analysis, and manuscript composition.

A version of **CHAPTER 3** has been published as J. Shi and H. Li, An improved volume translation model for PC-SAFT EOS based on a distance function, *Chemical Engineering Science* 276 (2023) 118800. J. Shi is responsible for the theoretical development, simulation results, analysis, and manuscript composition. H. Li is the supervisory author and gets involved in the concept formation, theoretical development, analysis, and manuscript composition.

A version of **CHAPTER 4** will be submitted to an appropriate journal for possible publication. J. Shi is responsible for the theoretical development, simulation results, analysis, and manuscript composition. H. Li is the supervisory author and gets involved in the concept formation, theoretical development, analysis, and manuscript composition.

A version of **CHAPTER 5** will be submitted to an appropriate journal for possible publication. J. Shi is responsible for the theoretical development, simulation results, analysis, and manuscript composition. H. Li is the supervisory author and gets involved in the concept formation, theoretical development, analysis, and manuscript composition.

DEDICATION

To my parents, Jianbing Shi and Ju Zhang,

and to my wife Yuntao Feng.

ACKNOWLEDGMENTS

I would like to express my appreciation to my supervisor, Dr. Huazhou Li, for his invaluable guidance throughout my Ph.D. journey and for his continuous support in the preparation of this thesis. I am grateful to Dr. Daoyong Tony Yang for serving as the external examiner and providing constructive comments and suggestions on this thesis. I am also grateful to my committee members, Dr. Hongbo Zeng, Dr. Nobuo Maeda, Dr. Tayfun Babadagli, and Dr. Yuntong She, for their comments and suggestions on my PhD thesis.

I wish to thank the following individuals or organizations for supporting my PhD program:

- My family members (Jianbing Shi, Ju Zhang, Yubing Feng, Pei Tang, Yuntao Feng, and Lingmin Zhang, etc.) for their unconditional love and support;
- Natural Sciences and Engineering Research Council (NSERC) of Canada for a Discovery Grant to Dr. H. Li;
- The past and present group members in Dr. Li's research group; and
- All my friends for their endless help, encouragement, and love.

TABLE OF CONTENTS

LIST OF TABLES

LIST OF FIGURES

CHAPTER 1 INTRODUCTION

1.1 Research Background

Phase behavior modeling is critically important in various fields such as petroleum engineering and chemical engineering. For instance, during the Carbon Capture and Storage (CCS) process, CO_2 can exist in multiple phases, including vapor, liquid, and supercritical phases, depending on the different pressure and temperature conditions. The successful design of such process hinges on an in-depth and accurate modeling of the thermodynamic properties of CO_2 which is normally achieved through the use of equation of state (EOS) models.

1.1.1 Cubic EOS (CEOS)

In 1873, aiming to model the phase behavior of real fluids, van der Waals developed a CEOS by considering the repulsive and attractive forces between molecules. Since the proposal of the van der Waals EOS, the developments CEOSs have gained increasing tractions (Redlich and Kwong, 1949; Soave, 1972; Peng and Robinson, 1976). Among the various trials, the Redlich-Kwong-Soave EOS (SRK EOS) (Soave, 1972) and Peng-Robinson EOS (PR EOS) (Peng and Robinson, 1976) have emerged as two of the most effective and widely applied EOS models for phase equilibria and volumetric calculations relevant to real fluid mixtures. The detailed expression of SRK EOS is given as follows (Soave, 1972),

$$P = \frac{RT}{V-b} - \frac{a(T)}{V(V+b)} \tag{1-1}$$

where P, T, V, and R refer to pressure, temperature, molar volume, and universal gas constant; a and b are the two EOS parameters:

$$a(T)=\frac{0.42747R^2T_c^2}{P_c}\left[1+m\left(1-\sqrt{\frac{T}{T_c}}\right)\right]^2 \tag{1-2}$$

$$b=\frac{0.08664RT_c}{P_c} \tag{1-3}$$

where the subscript, *c*, denotes critical point; *m* is a function of acentric factor,

$$m=0.48+1.574\omega-0.176\omega^2 \tag{1-4}$$

Peng and Robinson (1976) proposed the following PR EOS:

$$P=\frac{RT}{V-b}-\frac{a(T)}{V^2+2bV-b^2} \tag{1-5}$$

PR EOS seems to yield a higher prediction accuracy of liquid density than SRK EOS. In **Eq. 1-5**, the expressions of $a(T)$ and b are written as,

$$a(T)=\frac{0.45724R^2T_c^2}{P_c}\left[1+m\left(1-\sqrt{\frac{T}{T_c}}\right)\right]^2 \tag{1-6}$$

$$m=\begin{cases}0.37464+1.54226\omega-0.26992\omega^2, \omega<0.49\\ 0.379642+1.48503\omega-0.164423\omega^2+0.016666\omega^3, \omega>0.49\end{cases} \tag{1-7}$$

$$b=\frac{0.0778T_c}{P_c} \tag{1-8}$$

Recently, Pina-Martinez *et al.* (2019) updated **Eq. 1-7** with the following one:

$$m=0.3919+1.4996\omega-0.2721\omega^2+0.1063\omega^3 \tag{1-9}$$

1.1.2 Perturbed-Chain Statistical Associating Fluid Theory EOS (PC-SAFT EOS)

Although CEOSs are invaluable tools that have found widespread use in both industrial and academic fields, they come with certain limitations. For example, CEOSs struggle to accurately model phase behavior affected by association and strong polar interactions. This highlights the need for a thermodynamic model underpinned by a more robust theoretical framework, particularly when considering the effect of hydrogen bonding on phase behavior (Kontogeorgis *et al.*, 1996). In this context, perturbation theories (Wertheim, 1984a,b; Wertheim, 1986a,b) can offer a solution to explicitly account

for these interactions. Among these theories, SAFT is gaining an increasing attention, laying a good foundation for the development of more accurate thermodynamic models.

In 1990, Chapman *et al.* (1990) introduced a new SAFT EOS based on an extended version of Wertheim's theory. The total intermolecular potential of a given molecule in this framework arises from three primary contributions: the repulsion-dispersion interaction among molecular segments, the potential energy due to chain formation between segments, and the contribution due to association between segments. The residual Helmholtz energy in this model can be expressed as follows (Chapman *et al.*, 1990),

$$a^r = a^{seg} + a^{chain} + a^{assoc} = a^{hs} + a^{disp} + a^{chain} + a^{assoc} \tag{1-10}$$

where a^r is the residual Helmholtz energy. a^{seg}, a^{chain}, and a^{assoc} correspond to the contributions from the monomeric segments, chain formation, and association sites, respectively. Moreover, a^{seg} consists of two parts: hard-sphere repulsion (a^{hs}) and dispersion term (a^{disp}). In 2001, Gross and Sadowski (2001) modified the SAFT EOS by introducing a hard-chain reference, leading to the so-called perturbed-chain SAFT EOS (PC-SAFT EOS). They utilized a Baker-Henderson-type perturbation theory (Baker and Henderson, 1967a,b) to capture the attractive interactions among these chains. There are three essential parameters in PC-SAFT EOS, namely, the segment number (m), segment diameter (σ), and energy parameter (ε/k_B; k_B is the Boltzmann constant). The residual Helmholtz energy, a^r, is given by (Gross and Sadowski, 2001),

$$a^r = a^{hc} + a^{disp} \tag{1-11}$$

where a^{hc} corresponds to the contribution from the hard-chain reference contribution (Gross and Sadowski, 2001),

$$a^{hc} = \bar{m}a^{hs} + a^{chain} = \bar{m}a^{hs} - \sum_{i=1}^{n_c} x_i \left(m_i - 1\right) \ln g_{ij}^{hs} \tag{1-12}$$

where $\bar{m}$ is the mean segment number for mixture, n_c is the number of components, and x_i is the mole fraction of component *i*. Additionally, g_{ij}^{hs} is the radial distribution function of the hard-sphere fluid and a^{hs} is the hard-sphere term. The expressions, a^{hs}, g_{ij}^{hs} and $\bar{m}$, can be written as (Gross and Sadowski, 2001),

$$a^{hs} = \zeta_0 \left[\frac{3\zeta_1\zeta_2}{1-\zeta_3} + \frac{3\zeta_2^3}{\zeta_3\left(1-\zeta_3\right)^2} + \left(\frac{\zeta_2^3}{\zeta_3^2} - \zeta_0 \right) \ln\left(1-\zeta_3\right) \right] \tag{1-13}$$

$$\bar{m} = \sum_i^{n_c} x_i m_i \tag{1-14}$$

$$g_{ij}^{hs} = \frac{1}{1-\zeta_3} + \frac{d_i d_j}{d_i + d_j} \frac{3\zeta_2}{\left(1-\zeta_3\right)^2} + \left(\frac{d_i d_j}{d_i + d_j} \right)^2 \frac{2\zeta_2^2}{\left(1-\zeta_3\right)^3} \tag{1-15}$$

where the coefficients ζ_n are defined by (Gross and Sadowski, 2001),

$$\zeta_n = \frac{\pi}{6} \tilde{\rho} \sum_{i=1}^{n_c} x_i m_i d_i^n \text{, } n\text{=0, 1, 2, 3} \tag{1-16}$$

In **Eq. 1-13**, $\tilde{\rho}$ and d_i are the number density of molecules and temperature-dependent segment diameter, respectively. d_i is shown as below (Gross and Sadowski, 2001),

$$d_i = \sigma_i \left[1 - 0.12 \exp\left(-\frac{3\varepsilon_i}{k_B T} \right) \right], \; i\text{=1, …, } n_c \tag{1-17}$$

In the dispersive term, a^{disp}, the impact of chain length on dispersion interactions is considered. The expression is detailed as follows (Gross and Sadowski, 2001),

$$a^{disp} = -2\pi\tilde{\rho} I_1\left(\eta, \bar{m}\right) \overline{m^2 \varepsilon \sigma^3} - \pi\tilde{\rho}\bar{m} C_1\left(\eta, \bar{m}\right) I_2\left(\eta, \bar{m}\right) \overline{m^2 \varepsilon^2 \sigma^3} \tag{1-18}$$

where C_1 is the compressibility expression. Additionally, $I_1\left(\eta, \bar{m}\right)$ and $I_2\left(\eta, \bar{m}\right)$ are integrals from perturbation theory. The expressions, $\overline{m^2 \varepsilon \sigma^3}$ and $\overline{m^2 \varepsilon^2 \sigma^3}$, are the mixing rules given by (Gross and Sadowski, 2001),

$$\begin{cases} \overline{m^2\varepsilon\sigma^3} = \sum_{i=1}^{n_c}\sum_{j=1}^{n_c} x_i \cdot x_j \cdot m_i \cdot m_j \left(\frac{\varepsilon_{ij}}{k_B T}\right)\sigma_{ij}^3 \\ \overline{m^2\varepsilon^2\sigma^3} = \sum_{i=1}^{n_c}\sum_{j=1}^{n_c} x_i \cdot x_j \cdot m_i \cdot m_j \left(\frac{\varepsilon_{ij}}{k_B T}\right)^2 \sigma_{ij}^3 \end{cases} \tag{1-19}$$

While PC-SAFT-type EOSs have found broad applications across various fields, these molecular-based EOSs continue to exhibit numerical issues and inaccuracies in predicting the properties of pure substances (Privat *et al.*, 2010). Consequently, further refinement of this version of PC-SAFT remains both necessary and significant.

1.1.3 Volume Translation Models

To address the notable deviation between the calculated molar volume by CEOS and the corresponding experimental value, Peneloux *et al.* (1982) proposed a constant volume translation correction based on an exact reproduction of saturated liquid densities when the reduced temperature equals 0.7. The volume translation term proposed by Peneloux *et al.* (1982) is given by,

$$V_{\text{corrected}} = V_{\text{EOS}} - c \tag{1-20}$$

where c is the volume translation term, while V_{EOS} and $V_{\text{Corrected}}$ are the uncorrected liquid molar volume calculated by EOSs and the corrected liquid molar volume, respectively. It is important to note that while introducing a constant volume translation into a CEOS will result in different molar volumes, the vapor pressure yielded by both the translated and untranslated models remains unchanged at a given temperature (Peneloux *et al.*, 1982).

1.1.3.1 Volume Translation Models in CEOS

Since the proposal of a constant volume translation correction by Peneloux *et al.* (1982), various frameworks for volume translation corrections have been incorporated into different CEOSs. From a mathematical perspective, these volume translations can be

categorized into three types: constant volume translation terms, temperature-dependent volume translation terms, and temperature/pressure-dependent volume translation terms.

Constant volume translation terms (Peneloux *et al.* 1982; Jaubert *et al.*, 2016) or temperature-dependent volume translation terms (Magoulas and Tassios, 1990; Monnery *et al.*, 1998; Lin and Duan, 2005; Lin *et al.*, 2006; Shi *et al.*, 2018) have been widely used in CEOSs. This is primarily because these types of volume translation terms can provide partially accurate liquid density predictions without affecting the vapor pressure or the predicted equilibrium conditions. However, it should be noted that these strategies are not guaranteed to provide accurate liquid density predictions for pure compounds near their critical points or at extremely high pressures.

To mitigate the limitations imposed by either constant or temperature-dependent volume translation terms, some researchers have concentrated on developing volume translation strategies that are dependent on both temperature and pressure. In 1989, Mathias *et al.* (1989) proposed a distance function correction, a dimensionless quantity related to the inverse of the isothermal compressibility, to improve density predictions near the critical region. Moreover, Chou and Prausnitz (1989) introduced a phenomenological volume translation correction that is dependent on both temperature and pressure. They further augmented the SRK EOS by adding a near-critical contribution to the residual Helmholtz energy, in an attempt to enhance the accuracy of molar volume predictions, particularly in the vicinity of the critical region. Abudour *et al.* (2012) incorporated a distance-function-based volume translation correction with one more component-dependent parameter into PR EOS for more accurate saturated and single-phase liquid density predictions. Then Chen and Li (2020 and 2021) modified such distance-function-

based correction with three component-dependent parameters in SRK EOS for the better representation of saturated and single-phase liquid densities. Recently, Matheis *et al.* (2016) demonstrated that the density predictions obtained by the method of Abudour *et al.* (2012), employing a distance-function-based volume translation, outperformed those by using the other volume translation approaches. This finding underscores the significant potential of the application of distance-function-based volume translation strategies in different types of EOSs.

1.1.3.2 Volume Translation Models in PC-SAFT EOS

Despite the widespread applications of volume translation strategies in CEOSs, an introduction of such strategy into PC-SAFT-type EOSs has been relatively rare. Recently, however, volume translation corrections have begun to receive attention in the realm of PC-SAFT-type EOSs. Palma *et al.* (2018) introduced a Peneloux-type constant volume translation in combination with a new parameterization method, which could exactly reproduce the experimental critical temperature and critical pressure, to enhance the description of the speed of sound, liquid density, and saturation pressure. However, while such PC-SAFT EOS can provide better predictions for some derivative properties, the basic volumetric properties are still not adequately reproduced. In 2019, an industrialized version of PC-SAFT EOS (i.e., the so-called I-PC-SAFT EOS) incorporating a constant volume translation was proposed by Moine *et al.* (2019) for non-associating compounds. While this approach leads to improvements in several areas, the prediction of liquid density near the critical region is still compromised. Additionally, Navarro *et al.* (2019) presented a temperature-dependent volume translation method specifically for ionic liquids, incorporated within the PC-SAFT-type EOS framework. It seems that their model could

provide a better description of liquid density than the original PC-SAFT EOS, but such model still faces challenges in accurately predicting properties near the critical region.

1.2 Problem Statement

Some technical problems still exist during the development of SAFT-type EOSs. Specifically, this thesis is focused on the following two research problems. Firstly, with the original PC-SAFT EOS, there is an overestimation of critical temperature and critical pressure. Such limitation brings about inaccurate prediction of thermodynamic properties such as density, resulting in a possible anomalous critical phenomenon prediction in the vicinity of the critical region. Secondly, although the three parameters in PC-SAFT-type EOSs (m, σ, and ε/k_B) can be adjusted to exactly reproduce the experimental critical temperature and experimental critical pressure of pure compounds, this re-parameterization can bring about undesirable consequences. These may include significant deviations in critical molar volume and inaccurate density predictions across the entire liquid phase region. It appears that incorporating volume translation into the PC-SAFT EOS is a useful methodology. Thus, developing and refining a volume-translated PC-SAFT EOS that provides an accurate framework for phase behavior calculations poses a formidable challenge to be tackled in this study.

1.3 Hypothesis

The first hypothesis is that the volume translation correction, which has been widely used in CEOSs, can be successfully transplanted into PC-SAFT-type EOSs. The second hypothesis is that introducing different types of volume translation models (including temperature-dependent volume translation and distance-function based volume

translation) into PC-SAFT EOS can lead to the improvement in the prediction accuracy of non-critical properties and critical properties.

1.4 Objectives

The objective of this research is to develop improved volume-translated PC-SAFT EOSs for an accurate description of thermodynamic properties over a wide range of temperature and pressure covering both the critical and the non-critical regions. The detailed objectives are listed as follows.

- Develop a nonlinear temperature-dependent volume translation model in PC-SAFT EOS for CO_2 based on the parametrization method that can reproduce the critical temperature and critical pressure of CO_2. The developed nonlinear temperature-dependent volume translation model is expected to capture the general trend of the practically needed volume residuals (i.e., the molar volume calculated by CPPC-SAFT EOS minus the experimental one). Using the proposed volume translated PC-SAFT EOS, the critical temperature and critical pressure of CO_2 are expected to be totally reproduced. In addition, the accuracy of liquid density predictions is expected to be improved.
- Develop a distance-function-dependent volume translation model in PC-SAFT EOS combined with the parametrization method that can reproduce critical temperature and critical pressure of pure compounds. The newly developed volume translation model is based on a distance function which measures the distance of the current condition from the critical point. Such strategy is expected to not only give a good match with the needed saturated-liquid molar volume residuals but also capture the variation trend of single-liquid molar volume

residuals at different pressures. Using the proposed volume-translated rescaled PC-SAFT EOS (VTR-PC-SAFT EOS), the critical temperature, critical pressure and critical molar volume are expected to be exactly reproduced. In addition, more accurate prediction of thermodynamic properties over a wide range of temperature and pressure covering both the critical region and non-critical regions is expected to be achieved.

- Develop a generalized version of the distance-function-based volume translation model in PC-SAFT EOS for *n*-alkanes. It is expected to generalize the parameters in the proposed volume-translated CPPC-SAFT EOS (i.e., m, σ, ε/k_B, and c) to make it applicable to the phase behavior prediction of uncharacterized compounds. All the parameters in the developed model are expected to be correlated with the experimental critical temperature, critical pressure, and acentric factor.
- Extend the application of the proposed VTR-PC-SAFT EOS to more compounds that are not examined in the initial stage of the study. We will evaluate the performance of the VTR-PC-SAFT EOS in correlating the vapor pressure, liquid density, vapor density, supercritical density, saturated-liquid density, and saturated-vapor density in comparison to the other PC-SAFT-type EOSs.
- Evaluate the reliability of various critical-point based PC-SAFT-type EOSs for the prediction of thermodynamic derivative properties of selected compounds. Their performance in predicting derivative properties such as heat capacities, Joule-Thomson coefficient, thermal expansion coefficient, isothermal compressibility coefficient, and speed of sound is expected to be analyzed.

1.5 Thesis Structure

This is a paper-based thesis. Six chapters are presented in this thesis and organized as follows:

CHAPTER 1 introduces the basic research background, the problem statement, and the major research objectives. In **CHAPTER 2**, a new nonlinear temperature-dependent volume translation model is developed in PC-SAFT EOS for a more accurate density prediction of CO_2 over a wide range of temperature and pressure. **CHAPTER 3** develops a distance-function-dependent volume translation model in PC-SAFT EOS for achieving better predictions of the thermodynamic properties of pure compounds close to and far from the critical region. Besides, a generalized version of VTR-PC-SAFT is developed for *n*-alkanes. In **CHAPTER 4**, we explore if the proposed VTR-PC-SAFT EOS can also work well for more compounds that are not examined in the initial stage of the study. The performance of the VTR-PC-SAFT EOS in predicting vapor pressure, liquid density, vapor density, supercritical density, saturated-liquid density, and saturated-vapor density is evaluated. In **CHAPTER 5**, the ability of various critical-point based PC-SAFT-type EOSs to predict thermodynamic derivative properties (i.e., heat capacities, Joule-Thomson coefficient, thermal expansion coefficient, isothermal compressibility coefficient, and speed of sound) is evaluated for selected compounds. **CHAPTER 6** summarizes the conclusions reached in the thesis and the recommendations for future work.

References

A. Peneloux, E. Rauzy, R. Freze, A consistent correction for Redlich-Kwong-Soave volumes, *Fluid Phase Equilibria* 8 (1982) 7–23.

A. Pina-Martinez, R. Privat, J.N. Jaubert, D.Y. Peng, Updated versions of the generalized Soave α-function suitable for the Redlich-Kwong and Peng-Robinson equations of state, *Fluid Phase Equilibria* 485 (2019) 264-269.

A.M. Abudour, S.A. Mohammad, R.L. Robinson, K.A.M. Gasem, Volume translated Peng-Robinson equation of state for saturated and single-phase liquid densities, *Fluid Phase Equilibria* 335 (2012) 74–87.

D.Y. Peng, D.B. Robinson, A new two-constant equation of state, *Industrial & Engineering Chemistry Fundamentals* 15 (1976) 59-64.

G. Soave, Equilibrium constants from a modified Redlich–Kwong equation of state, *Chemical Engineering Scienc*e 27 (1972) 1197-1203.

G.F. Chou, J.M. Prausnitz, A phenomenological correction to an equation of state for the critical region, *AIChE Journal* 35 (1989) 1487-1496.

G.M. Kontogeorgis, E.C. Voutsas, I.V. Yakoumis, D.P. Tassios, An equation of state for associating fluids, *Industrial & Engineering Chemistry Research* 35 (1996) 4310-4318.

H. Lin, Y. Duan, Empirical correction to the Peng-Robinson equation of state for the saturated region, *Fluid Phase Equilibria* 233 (2005) 194-203.

H. Lin, Y. Duan, T. Zhang, Z.M. Huang, Volumetric property improvement for the Soave-Redlich-Kwong equation of state, *Industrial & Engineering Chemistry Research* 45 (2006) 1829-1839.

J. Gross, G. Sadowski, Application of perturbation theory to a hard-chain reference fluid: an equation of state for square-well chains, *Fluid Phase Equilibria* 168 (2000) 183-199.

J. Gross, G. Sadowski, Perturbed-chain SAFT: An equation of state based on a perturbation theory for chain molecules, *Industrial & Engineering Chemistry Research* 40 (2001) 1244−1260.

J. Matheis, H. Müller, C. Lenz, M. Pfitzner, S. Hickel, Volume translation methods for real-gas computational fluid dynamics simulations, *The Journal of Supercritical Fluids* 107 (2016) 422-432.

J. Shi, H. Li, W. Pang, An improved volume translation strategy for PR EOS without crossover issue, *Fluid Phase Equilibria* 470 (2018) 164-175.

J.A. Barker, D. Henderson, Perturbation theory and equation of state for fluids: the square-well potential, *The Journal of Chemical Physics* 47 (1967) 2856-2861.

J.A. Barker, D. Henderson, Perturbation theory and equation of state for fluids. II. A successful theory of liquids, *The Journal of Chemical Physics* 47 (1967) 4714-4721.

J.N. Jaubert, R. Privat, Y. Le Guennec, L. Coniglio, Note on the properties altered by application of a Péneloux–type volume translation to an equation of state, *Fluid Phase Equilibria* 419 (2016) 88-95.

K. Magoulas, D. Tassios, Thermophysical properties of n-alkanes from C1 to C20 and their prediction for higher ones, *Fluid Phase Equilibria* 56 (1990) 119-140.

M.S. Wertheim, Fluids with highly directional attractive forces. I. Statistical thermodynamics, *Journal of Statistical Physics* 35 (1984) 19-34.

M.S. Wertheim, Fluids with highly directional attractive forces. II. Thermodynamic perturbation theory and integral equations, *Journal of Statistical Physics* 35 (1984) 35-47.

M.S. Wertheim, Fluids with highly directional attractive forces. III. Multiple attraction sites, *Journal of Statistical Physics* 42 (1986) 459-476.

M.S. Wertheim, Fluids with highly directional attractive forces. IV. Equilibrium polymerization, *Journal of Statistical Physics* 42 (1986) 477-492.

P.M. Mathias, T. Naheiri, E.M. Oh, A density correction for the Peng-Robinson equation of state, *Fluid Phase Equilibria* 47 (1989) 77-87.

R. Privat, R. Gani, J.N. Jaubert, Are safe results obtained when the PC-SAFT equation of state is applied to ordinary pure chemicals?, *Fluid Phase Equilibria* 295 (2010) 76-92.

O. Redlich, J.N.S. Kwong, On the thermodynamics of solutions. V. An equation of state. Fugacities of gaseous solutions, *Chemical Reviews* 44 (1949) 233-244.

W.D. Monnery, W.Y. Svrcek, M.A. Satyro, Gaussian-like volume shifts for the Peng-Robinson, *Industrial & Engineering Chemistry Research* 37 (1998) 1663-1672.

W.G. Chapman, K.E. Gubbins, G. Jackson, M. Radosz, New reference equation of state for associating liquids, *Industrial & Engineering Chemistry Research* 29 (1990) 1709-1721.

X. Chen, H. Li, An improved volume-translated SRK EOS dedicated to more accurate determination of saturated and single-phase liquid densities, *Fluid Phase Equilibria* 521 (2020) 112724.

X. Chen, H. Li, Improved prediction of saturated and single-phase liquid densities of water through volume-translated SRK EOS, *Fluid Phase Equilibria* 528 (2021) 112852.

CHAPTER 2 MODIFIED TEMPERATURE-DEPENDENT VOLUME TRANSLATION MODEL IN PC-SAFT EQUATION OF STATE FOR CARBON DIOXIDE

A version of this chapter has been published as J. Shi and H. Li, Modified temperature-dependent volume translation model in PC-SAFT equation of state for carbon dioxide, *Chemical Engineering Science* 263 (2022) 118107.

Abstract

Statistical associating fluid theory (SAFT)-type equations of states (EOSs) have been widely used to model the phase behavior of pure compounds (e.g., carbon dioxide). One issue with conventional SAFT-type EOSs is that they fail to accurately reproduce the critical pressure and critical temperature of pure compounds. To address this limitation, the three parameters in SAFT-type EOSs (i.e., m, σ, and ε/k) must be adjusted to exactly reproduce the critical temperature and critical pressure of pure compounds, leading to the development of the critical-point perturbed-chain SAFT (CPPC-SAFT). However, this is achieved by sacrificing the accuracy of the liquid-density predictions. As such, a fourth parameter, that is, the volume translation parameter, is indispensable for improving the accuracy of liquid density predictions. In this study, a new nonlinear temperature-dependent volume translation model was introduced into the perturbed-chain SAFT EOS (PC-SAFT EOS) for more accurate density predictions of CO_2. The newly developed volume-translated and critical-point PC-SAFT EOS (VT-CPPC-SAFT EOS) was found to be superior to previously developed models, such as the original PC-SAFT (Statistical associating fluid theory (SAFT)-type equations of states (EOSs) have been widely used to model the phase behavior of pure compounds (e.g., carbon dioxide). One issue with conventional SAFT-type EOSs is that they fail to accurately reproduce the critical pressure and critical temperature of pure compounds. To address this limitation, the three parameters in SAFT-type EOSs (i.e., m, σ, and ε/k) must be adjusted to exactly reproduce the critical temperature and critical pressure of pure compounds, leading to the development of the critical-point perturbed-chain SAFT (CPPC-SAFT). However, this is achieved by sacrificing the accuracy of the liquid-density predictions. As such, a fourth

parameter, that is, the volume translation parameter, is indispensable for improving the accuracy of liquid density predictions. In this study, a new nonlinear temperature-dependent volume translation model was introduced into the perturbed-chain SAFT EOS (PC-SAFT EOS) for more accurate density predictions of CO_2. The newly developed volume-translated and critical-point PC-SAFT EOS (VT-CPPC-SAFT EOS) was found to be superior to previously developed models, such as the original PC-SAFT (Gross and Sadowski, 2001), CPPC-SAFT (Anoune *et al.*, 2021), and industrialized version of PC-SAFT EOS (I-PC-SAFT) (Moine *et al.*, 2019), because it can provide more accurate density predictions for CO_2 in different phase states. In addition, the VT-CPPC-SAFT EOS accurately reproduced the critical pressure and critical temperature of CO_2), CPPC-SAFT, and industrialized version of PC-SAFT EOS (I-PC-SAFT), because it can provide more accurate density predictions for CO_2 in different phase states. In addition, the VT-CPPC-SAFT EOS accurately reproduced the critical pressure and critical temperature of CO_2.

Keywords: Carbon dioxide; Temperature-dependent volume translation; PC-SAFT EOS; Density prediction; Critical point

2.1 Introduction

The implementation of carbon capture, utilization, and storage technologies (CCUS) has confirmed to be an effective strategy for mitigating CO_2 emissions (Norhasyima and Mahlia, 2018; Tzirakis *et al.*, 2019). For engineers and practitioners working in the CCUS field, there is a huge demand for reliable experimental data and theoretical models associated with the thermophysical properties of CO_2. The thermodynamic properties (such as the density and vapor pressure of pure CO_2), as well as the relationship between the pressure, volume, and temperature (PVT) of CO_2-containing mixtures, are fundamental and critical for the design and optimization of CCUS operations. Therefore, it is necessary to develop an accurate but easy-to-implement thermodynamic model for CO_2.

Because the van der Waals equation of state (EOS) was proposed to describe PVT relationships, various mathematical frameworks have been developed and used to predict the phase behavior and thermodynamic properties of pure substances. Given their simplicity and reliability, cubic EOSs (CEOSs) have been widely applied in the petroleum and chemical industries. However, CEOSs (e.g., PR and SRK EOS (Soave, 1972; Peng and Robinson, 1976)) employ a universal critical compressibility factor, whereas the true critical compressibility factors vary between compounds. Using such constant compressibility factors in CEOSs lead to an inaccurate prediction of the liquid density of pure compounds (Li *et al.*, 2011; Vinhal *et al.*, 2017). In addition, these CEOS models do not provide accurate predictions of the thermodynamic properties of complex mixtures and frequently fail to model the multiphase equilibria of polar, highly asymmetric, and associated mixtures (Kordikowski *et al.*, 1995; Polishuk *et al.*, 2000).

To address this limitation of CEOSs, more advanced molecular thermodynamics-based models, such as the three-center Lennard-Jones (3CLJ) plus point quadrupole (3CLJQ) model (Merker *et al.*, 2010) and the statistical association fluid theory (SAFT) model (Wertheim, 1984a,b; Wertheim, 1986a,b), have been developed. Considering its wide applications in the industrial sector, the SAFT EOS proposed by Chapman *et al.* (1989) was selected as the theoretical model in this work, which was developed based on Wertheim's cluster expansion of Helmholtz energy and simplified perturbation theory (Wertheim, 1984a,b; Wertheim, 1986a,b). In SAFT, hard spheres form chain segments through covalent bonds, and chain segments interact with each other through dispersion and association forces. Although SAFT-type EOSs can provide extremely accurate predictions of liquid density, leading to a significant overestimation of critical points, that is, the values of the critical temperature and critical pressure calculated by SAFT-type EOSs are far greater than the experimental data (Pfohl *et al.*, 1998; Moine *et al.*, 2019). **Table 2-1** shows a comparison between the measured (Linstrom and Mallard, 2005) and calculated critical pressure/temperature values obtained using the original PC-SAFT. The three parameters (m, σ, and ε/k) in the PC-SAFT EOS were considered from the original reference (Gross and Sadowski, 2001). The values of critical temperature/pressure (T_c and P_c) calculated by PC-SAFT (Gross and Sadowski, 2001) and the measured values ($T_{c,exp}$ and $P_{c,exp}$) from the NIST database (Linstrom and Mallard, 2005) are presented in this table. As shown in **Table 2-1**, compared to the measured critical temperature and critical pressure, the calculated critical temperature and critical pressure were overestimated by the original PC-SAFT EOS with absolute relative deviation values (%ARDs) of 2.021 and 9.242, respectively. This indicates that the original PC-SAFT EOS

was not forced to reproduce the critical point. Meanwhile, the critical temperature and critical pressure calculated by the PC-SAFT EOS were much greater than the measured values for CO_2. This phenomenon can lead to inaccurate predictions of the thermophysical properties near the critical region. **Fig. 2-1** presents a comparison between the vapor-pressure curve and pressure-volume two-phase envelope (Linstrom and Mallard, 2005) and those calculated by the original PC-SAFT EOS (Gross and Sadowski, 2001). **Fig. 2-1** clearly shows that the overestimation of the critical temperature and critical pressure with the PC-SAFT EOS has a significant impact on the calculated molar volumes near the critical region.

Table 2-1. Comparison between the measured (Linstrom and Mallard, 2005) and calculated critical pressure/temperature values by the original PC-SAFT (Gross and Sadowski, 2001).

Compound	PC-SAFT					Measured values		$\%ARD_T$[a]	$\%ARD_P$[a]
	m	σ	ε/k	T_c	P_c	$T_{c,exp}$	$P_{c,exp}$		
CO_2	2.0729	2.7852	169.21	310.279	8.0591	304.13	7.3773	2.021	9.242

a: $\%ARD_T = 100\left|T_c - T_{c,exp}\right|/T_{c,exp}$; $\%ARD_P = 100\left|P_c - P_{c,exp}\right|/P_{c,exp}$

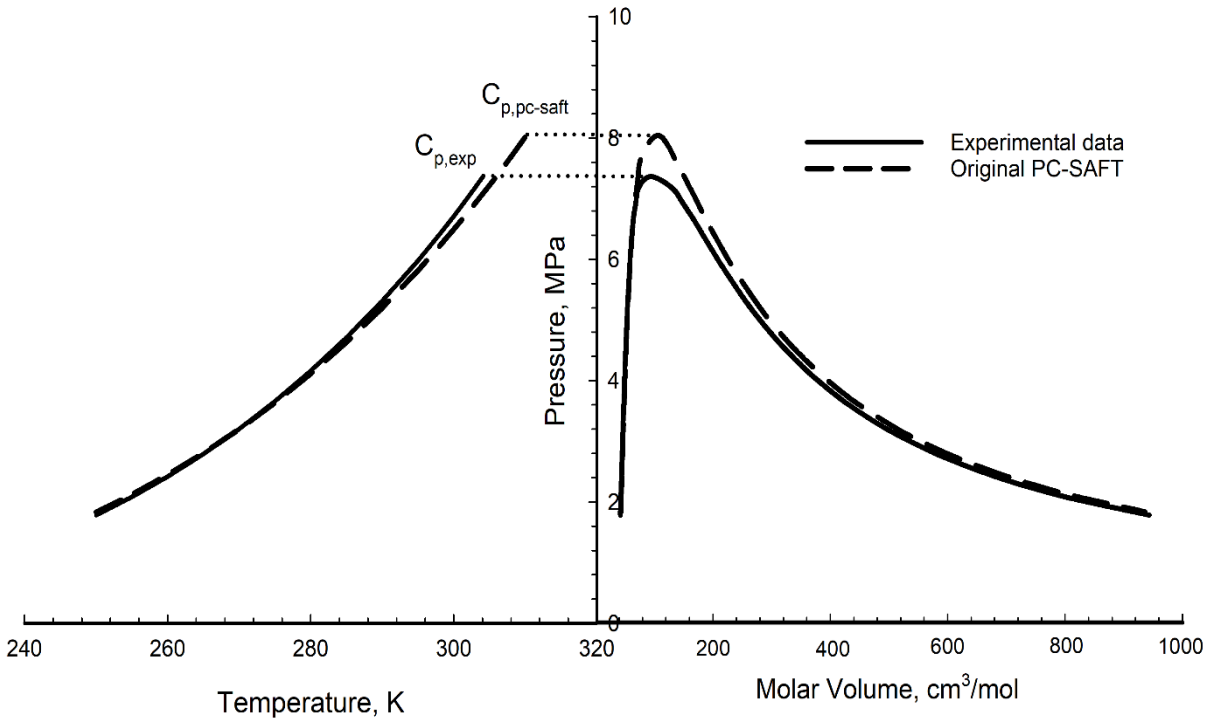

Fig. 2-1. Comparison between the vapor-pressure curve and pressure-volume two-phase envelope (Linstrom and Mallard, 2005) and those calculated by the original PC-SAFT EOS (Gross and Sadowski, 2001).

Without considering the density fluctuations in the critical region using the mean-field theory (Sengers, 1999), SAFT-type EOSs overpredict the critical temperatures and critical pressures of pure compounds. Meanwhile, because no constraints were applied to the critical region during the parameter regression process, the predictions of the vapor pressure and density near the critical region were not accurate. Thus, it is necessary and important for SAFT-type EOSs to exactly reproduce the critical temperature and critical pressure of a given pure compound during the parametrization of the SAFT EOS parameters. However, once such parametrization method is considered in the original

three-parameter PC-SAFT EOS, the predictions of other thermophysical properties may no longer be accurate.

In this study, the limitations of the three-parameter PC-SAFT EOS are presented, and the necessity of introducing one more parameter into the PC-SAFT EOS is analyzed. Moreover, coupled with the parametrization method, which can exactly reproduce the experimental critical points, a fourth temperature-dependent volume translation parameter was developed and introduced into the three-parameter PC-SAFT EOS. The newly developed model not only reproduces the true critical temperature and critical pressure but also provides a more accurate prediction of the CO_2 density in the liquid, vapor, and supercritical phases.

2.2 Literature Review and Motivation

2.2.1 Parametrization Methods in Three-parameter PC-SAFT EOSs

Over the past two decades, SAFT-type EOSs based on perturbation theory have gained increasing attention. For a non-associating pure component, three parameters, that is, the segment number, segment diameter, and energy parameter (m , σ , and ε/k), are required for SAFT-type EOSs. Because vapor pressure and liquid density data are used to fit these three input parameters in the original three-parameter PC-SAFT EOS proposed by Gross and Sadowski (2001), some researchers have focused on the development of the re-parametrization of the three parameters in the PC-SAFT EOS to obtain better predictions of thermophysical properties. Different parametrization procedures and objective functions used for fitting the three parameters can lead to different predictions of the thermodynamic properties of pure fluids. However, the existing parametrization methods used in SAFT-type EOSs tend to reduce the accuracy of critical-property predictions and high-pressure

phase equilibrium predictions (Gross and Sadowski, 2001; Chapman *et al.*, 1990; Gross and Sadowski, 2000; McCabe and Jackson, 1999; Tihic *et al.*, 2006).

The reproduction of critical points has always been of great significant importance in the development of EOSs s (Kontogeorgis *et al.*, 2020). Unfortunately, the SAFT EOS is based on the mean-field theory, while the effect of density fluctuations in the mean-field theory is neglected, especially near the critical region (Sengers, 1999). The mean-field theory fails to predict the correct thermodynamic properties near the critical region owing to the increasing effect of density fluctuations (Hu *et al.*, 2003). Most SAFT-type EOS models developed using various parametrization methods tend to overestimate the critical temperature and critical pressure of pure components. Meanwhile, the accuracy of the vapor-pressure and density predictions near the critical region by these SAFT-type EOSs is compromised.

To avoid this issue, attempts have been made to modify SAFT-type EOSs and improve their ability to represent critical points (Pfohl *et al.*, 1998; Anoune *et al.*, 2021; Pakravesh *et al.*, 2021; Cismondi *et al.*, 2005; Privat *et al.*, 2019; Polishuk, 2014; Polishuk, 2011). Polishuk (2014) proposed a standardized critical point-based numerical solution for the accurate prediction of densities using PC-SAFT, although there is a poor prediction of the vapor pressures of heavy components away from their critical points. In addition, to address the issue of SAFT-type EOS's numerical pitfalls and improve the prediction accuracy of the critical point, Polishuk (2011) attached SAFT using the attractive term of cubic EOS. In 1998, Pfohl *et al.* (1998) proposed a universal pure-component parametrization method to ensure the correct reproduction of critical temperature and critical pressure. Similarly, to mitigate the overestimation of critical pressure and critical

temperature, as well as the inaccurate predictions of the phase equilibria of mixtures, specifically in the critical regions, Anoune *et al.* (2021) presented a new approach that constrains the three model parameters to exactly reproduce the critical temperature and critical pressure of diverse pure compounds.

Although the critical temperature and critical pressure can be reproduced using the above parametrization methods, these SAFT-type EOSs fail to accurately predict the density. **Fig. 2-2** shows a comparison between the experimental saturation curve and two isotherms corresponding to $T_r = 0.9$ and $T_r = 1.1$ (Linstrom and Mallard, 2005) and those calculated by PC-SAFT with the re-parametrization method proposed by Anoune *et al.* (2021) for CO_2 (i.e., the so-called CPPC-SAFT EOS). Although the modified PC-SAFT EOS with the new parametrization method could reproduce the experimental critical point, there was a significant overestimation of the saturated liquid molar volume. In addition, the isotherms at $T_r = 0.9$ and $T_r = 1.1$ cannot be accurately represented with the CPPC-SAFT EOS, especially in the liquid and supercritical phases. Therefore, the exact reproduction of the critical point by the CPPC-SAFT EOS was achieved at the expense of sacrificing the accuracy of the liquid-density predictions.

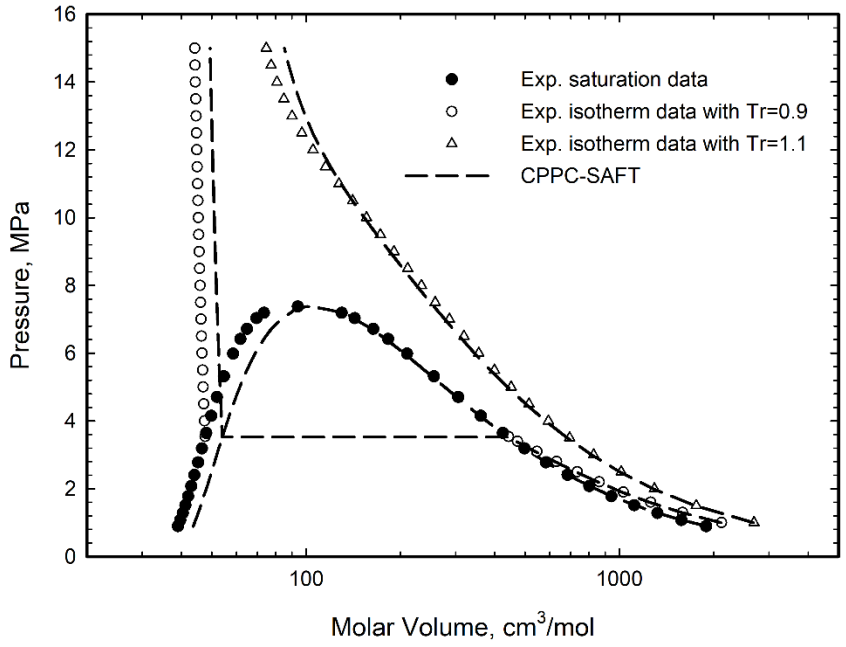

Fig. 2-2. Comparison between the experimental pressure-volume two-phase envelope and isotherms at T_r = 0.9 and T_r = 1.1 (Linstrom and Mallard, 2005) and those calculated by CPPC-SAFT EOS (Anoune *et al.*, 2021).

2.2.2 Volume Translation in PC-SAFT

As presented in the previous section, although the critical point can be exactly reproduced with the re-parametrization method, the three-parameter CPPC-SAFT EOS cannot provide an accurate prediction of the thermophysical properties of non-associated pure compounds. This makes the introduction of one more parameter necessary for the CPPC-SAFT EOS so that we not only reproduce the critical temperature and critical pressure but also obtain a more accurate prediction of the liquid-phase density.

The volume translation concept was first proposed by Martin (1979) and developed by Peneloux *et al.* (1982) with a constant correction term to overcome the limitations of two-parameter EOSs, such as PR EOS and SRK EOS (Soave, 1972; Peng and Robinson, 1976). This proposed term significantly improves the predictions of the liquid density in the low-temperature region without causing any changes in the vapor pressure calculations.

Because the proposal of the constant volume translation model by Peneloux *et al.* (1982), various volume translation models (such as temperature-dependent and temperature/density-dependent models) have been developed.

Although the volume translation model has been introduced into CEOS for almost 50 years (Shi *et al.*, 2018; Frey *et al.*, 2007; Young *et al.*, 2017; Ghoderao *et al.*, 2019; Lopez-Echeverry *et al.*, 2017), such a technique has only been incorporated into SAFT-type models by Palma *et al.* until recently (Palma *et al.*, 2018). They proposed a constant Peneloux-type volume shift in a PC-SAFT EOS to simultaneously improve the description of the speed of sound, liquid density, and saturation pressures. Previous research has demonstrated that the inaccurate calculation of the first derivative of pressure with respect to volume, $\left(\frac{dP}{dV}\right)_T$, in PC-SAFT EOS can result in an unsatisfactory prediction of the speed of sound; thus, Palma *et al.* (2018) first used both the saturation pressures and $\left(\frac{dP}{dV}\right)_T$ to fit the PC-SAFT parameters in the parametrization procedure and then introduced a constant volume translation term at a reduced temperature of 0.7. Their results indicate that there are better predictions of some derivative properties that are not directly associated with volumetric properties, and the liquid-density prediction is also improved with the newly proposed parametrization method. However, they indicated that, with the introduction of a constant volume translation model, there is real antagonism between the exact reproduction of isobaric expansivity and isothermal compressibility (Palma *et al.*, 2018) because an improvement in the prediction accuracy in $\left(\frac{dP}{dV}\right)_T$ can only be achieved

at the cost of a degradation in the prediction accuracy in $\left(\frac{dV}{dT}\right)_P$. Nevertheless, the performance of the model proposed by Palma *et al.* (2018) was compromised at high pressures. In 2019, Moine *et al.* (2019) developed an industrialized version of the volume-translated PC-SAFT EOS (I-PC-SAFT EOS) with a constant volume shift for non-associating compounds. In their work, two parametrization methods were proposed: one is to exactly reproduce the experimental critical temperature and critical pressure, and the other is to fit the three model parameters in the PC-SAFT EOS to the experimental vapor pressure, enthalpy of vaporization, saturated liquid heat capacity, and liquid molar volume. Using the new re-parametrization method, they introduced a constant volume translation term into the three-parameter PC-SAFT EOS. However, an accurate prediction of the liquid density cannot be obtained using the proposed constant volume translation, especially near the critical region. In addition to the introduction of constant volume translation terms into the PC-SAFT EOS, Navarro *et al.* (2019) recently presented a temperature-dependent volume translation term with the PC-SAFT EOS for some ionic liquids. This correction indeed leads to a better description of the density. However, their volume translation corrections could not reproduce the critical temperature and critical pressure.

2.2.3 Motivation

Most SAFT-type EOSs with three model parameters overestimate the critical temperatures and critical pressures of the pure components (Sengers, 1999). Thus, the introduction of a revised parametrization method is necessary to exactly reproduce the critical points from only the experimental critical pressure, critical temperature, and acentric factor (T_c, P_c, and ω) for pure substances. Furthermore, in three-parameter PC-SAFT EOSs, various parametrization methods can be exploited to improve the prediction

of various thermodynamic properties. However, this will yield contrary and negative effects on the prediction of other thermodynamic properties. The parameterization approach proposed by Anoune *et al.* (2021), for example, provides accurate vapor-pressure predictions and exactly reproduces T_c and P_c but yields inaccurate liquid-density predictions.

The needed volume shift is defined as the difference between the experimental volumes obtained from the NIST database (Linstrom and Mallard, 2005) and the values predicted by the EOS. **Fig. 2-3** shows the difference between the reference molar volumes (Linstrom and Mallard, 2005) and the molar volumes calculated by PC-SAFT for liquid-phase CO_2 at different constant reduced pressures. The PC-SAFT model uses a parametrization method that exactly reproduces experimental critical points (Anoune *et al.*, 2021). This figure clearly shows the trend of the needed volume shift in liquid density at different constant pressures. It can be observed that the needed volume shift increases significantly with temperature, especially at conditions close to the critical point. **Fig. 2-4** shows the needed volume shift over a wide range of temperatures at different constant reduced pressures. This clearly shows that there is an inferior reproduction of liquid-phase density and supercritical-phase density by the three-parameter PC-SAFT EOS with the parametrization approach proposed by Anoune *et al.* (2021). In addition, as the temperature increases, the needed volume shift gradually becomes constant.

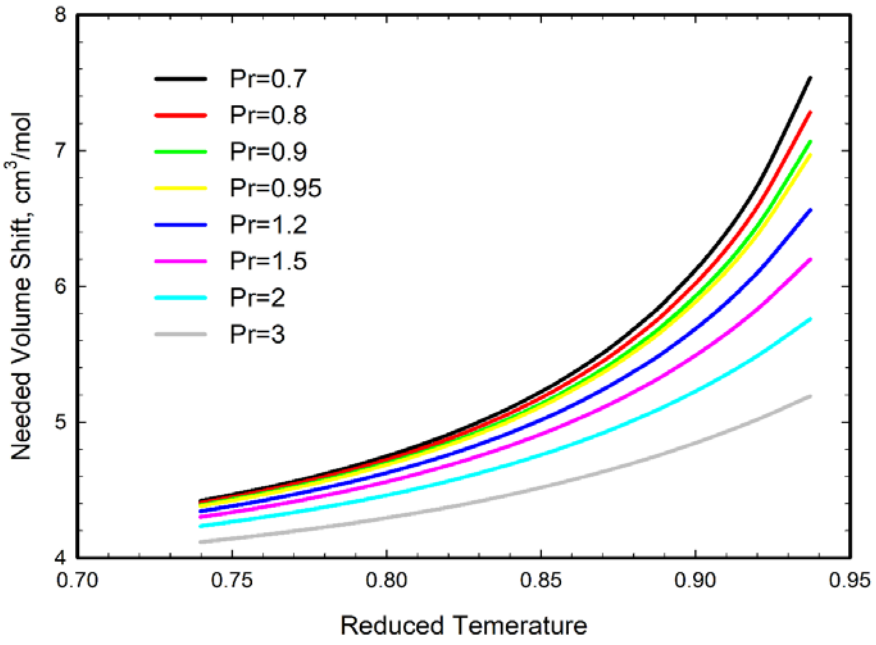

Fig. 2-3. Difference between the reference molar volumes (Linstrom and Mallard, 2005) and the molar volumes calculated by the CPPC-SAFT model (Anoune *et al.*, 2021) for liquid-phase CO_2 at different constant reduced pressures.

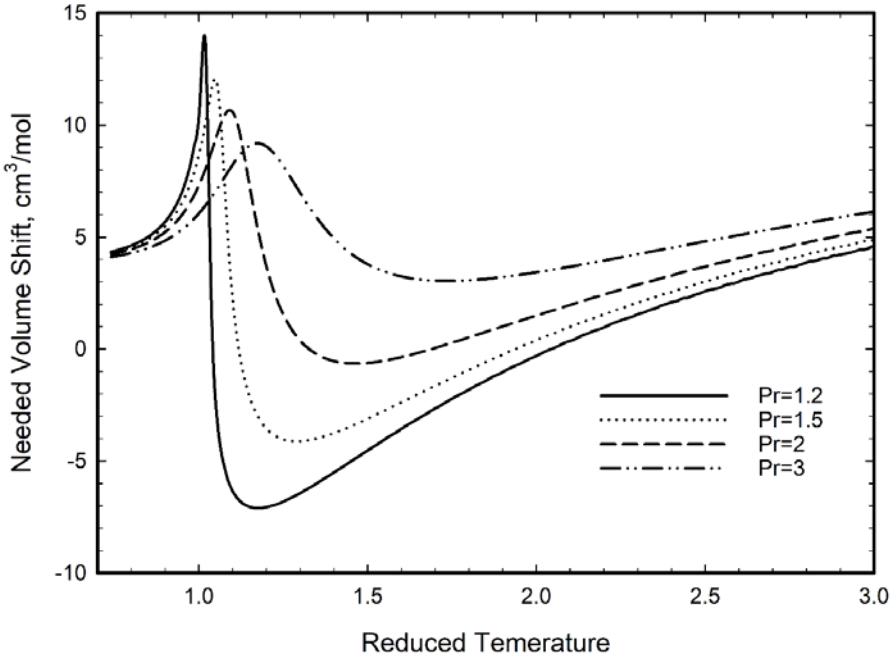

Fig. 2-4. Difference between the reference molar volumes (Linstrom and Mallard, 2005) and the molar volumes calculated by the CPPC-SAFT (Anoune *et al.*, 2021) for CO_2 over a wide range of temperatures at different constant reduced pressures.

Overall, exactly matching the experimental critical temperature and critical pressure with the three-parameter PC-SAFT EOS resulted in an overestimation of the liquid molar volumes, especially near the critical region. To achieve a more accurate density prediction over a wide range of temperatures and pressures and exactly reproduce the experimental critical temperature and pressure, a fourth parameter is essential to be introduced into the three-parameter PC-SAFT EOS. As shown in **Fig. 2-3** and **Fig. 2-4**, the overall trend of the needed volume shift over a wide range of temperatures cannot be exactly fitted with constant volume translation or linear temperature-dependent volume translation. A nonlinear temperature-dependent volume translation was necessary in this case. In summary, combined with the parametrization method with the representation of T_c and P_c, a fourth parameter (i.e., a nonlinear temperature-dependent volume translation) is proposed in this study to fit the overall trend of the needed volume shift and achieve a more accurate density prediction over a wide range of temperatures and pressures.

2.3 Methodology

2.3.1 Modified Volume Translated PC-SAFT Model

The residual Helmholtz energy in the original PC-SAFT EOS, as developed by Gross and Sadowski (2021), is expressed as follows,

$$a_{\text{res}} = a_{\text{hc}} + a_{\text{disp}} \tag{2-1}$$

where a_{res} is the residual Helmholtz free energy, while a_{hc} and a_{disp} are the hard-chain energy contribution and the dispersive energy contribution, respectively. There are three input parameters in SAFT-type EOSs, i.e., a segment number (m), a segment diameter (σ), and an energy parameter (ε/k).

A fourth parameter, temperature-dependent volume translation, is introduced to improve the accuracy of the thermodynamic properties based on the original three-parameter PC-SAFT EOS:

$$c(T) = V_{\mathrm{EOS}} - V_{\mathrm{exp}} \tag{2-2}$$

where $c(T)$ is the temperature-dependent volume translation term, V_{EOS} is the corrected molar volume, and V_{exp} is the experimental molar volume.

The parametrization proposed by Anoune *et al.* (2021) to exactly reproduce the experimental critical pressure and the critical temperature was selected as the parametrization method in this study. For a pure substance, the critical point can be reproduced by satisfying the following two constraints related to the first and second derivatives of pressure with respect to the volume,

$$\left(\frac{\partial P}{\partial V}\right)_T = 0 \tag{2-3}$$

$$\left(\frac{\partial^2 P}{\partial V^2}\right)_T = 0 \tag{2-4}$$

To adjust the PC-SAFT parameters to exactly reproduce the experimental critical pressure and critical temperature, in this parametrization method, the three parameters, critical pressure, critical temperature, and acentric factor (T_c, P_c, and ω) in the cubic EOS, were used to express the three PC-SAFT parameters (m , σ , and ε/k). The corresponding polynomial correlations and the obtained numerical values of PC-SAFT parameters for different substances were reported and presented by Anoune *et al.* (2021). Compared with the parameterization methods adopted by the original PC-SAFT EOS and

most other SAFT-type EOSs, the above method (CPPC-SAFT EOS) is more universal because the values of T_c, P_c, and ω are known for various substances.

As discussed in the previous sections, although the above parametrization method can be used to exactly reproduce the critical pressure and critical temperature, it leads to less accurate density predictions than the original PC-SAFT EOS. Aiming to improve the density, especially at conditions where the temperature is close to the critical point and capture the overall trend of the needed volume shift shown in **Fig. 2-3** and **Fig. 2-4**, we propose the use of a Gaussian-like function with a "bell curve" shape as a volume translation model in this work,

$$c\left(T_r\right) = A\exp\left[-\frac{(T_r-1)^2}{2B^2}\right] + C \tag{2-5}$$

Here, T_r is the reduced temperature, and A, B, and C are the coefficients to be determined for a specific pure component. A similar expression has been proposed for cubic EOS in previous works (Shi *et al.*, 2018; Monnery *et al.*, 1998). This mathematical function is symmetric with respect to $T_r = 1$. Thus, the proposed volume translation is a strong function of the temperature near the critical point, and then this term tends to be a constant value when the temperature is away from the critical temperature. The molar volume residuals, as shown in **Fig. 2-3** and **Fig. 2-4**, could be better fitted by this nonlinear temperature-dependent model, leading to more accurate density predictions over a wide range of temperatures and pressures.

The model parameters should be regressed based on the needed liquid volume translation, i.e., the liquid molar volume residuals. The three coefficients in **Eq. 2-5** are determined by minimizing the following objective function (OF),

$$\text{OF}=\frac{1}{N}\left(\sum_{1}^{N}\left|\frac{V_{\text{exp}}-V_{\text{EOS}}}{V_{EOS}}\right|\right) \tag{2-6}$$

where N denotes the number of data points. During the regression, the considered temperature ranges from $0.73T_c$ to $0.99T_c$ (225 K to 300 K), while the considered pressure ranges from $0.7P_c$ to $3P_c$ (5.164 MPa to 22.132 MPa). There are 236 data points along the eight isotherms. **Table 2-2** shows the re-optimized values of the three parameters in the CPPC-SAFT EOS (Anoune *et al.*, 2021), as well as the regressed coefficients A, B, and C shown in **Eq. 2-5** for CO_2.

Table 2-2. Parameters in PC-SAFT for CO_2 and values of the coefficients in **Eq. 2-5**.

Parameters	m [-]	σ [A]	ε/k [K]	A	B	C
	2.66827	2.61212	147.234	3.161	0.08094	4.398

2.3.2 Performance Evaluation of the Modified Volume Translated PC-SAFT

The average absolute percentage deviation (%AAD) was calculated to assess the performance of the PC-SAFT models in predicting various thermophysical properties,

$$\%\text{AAD}=\frac{100}{N}\sum_{i=1}^{N}\left|\frac{\text{Prop}_{i,\text{exp}}-\text{Prop}_{i,\text{calc}}}{\text{Prop}_{i,\text{exp}}}\right| \tag{2-7}$$

where N is the number of data points, $\text{Prop}_{i,\text{exp}}$ is the experimental property retrieved from the NIST database, and $\text{Prop}_{i,\text{calc}}$ is a property calculated using the EOS model. The performance of the new temperature-dependent volume-translated PC-SAFT coupled with Anoune *et al.*'s (2021) parametrization method, i.e., the so-called VT-CPPC-SAFT EOS, was compared with the performance of the other three EOSs: the original PC-SAFT (Gross and Sadowski, 2001), CPPC-SAFT S (Anoune *et al.*, 2021), and I-PC-SAFT EOS (Moine

et al., 2019). In particular, we are interested in applying these SAFT-type EOSs to predict the CO_2 density over a wide range of thermodynamic conditions, covering the liquid, vapor, and supercritical phases.

2.4 Results and Discussion

2.4.1 Prediction Accuracy of Vapor Pressure

For the most popular EOSs, including SAFT-type EOSs and cubic EOSs, with a constant volume translation or temperature-dependent volume translation, the original and translated EOSs give rise to the same vapor pressures. With the same volume translation applied for each isotherm in the pressure-volume phase diagram, the predicted molar volume curve is translated along the molar volume coordinate without causing any changes in the vapor pressure. Detailed calculations and similar conclusions can be found in previous studies (Péneloux *et al.*, 1982; Jaubert *et al.*, 2016; Frey *et al.*, 2007). Hence, the vapor pressures calculated with the VT-CPPC-SAFT EOS in this study should be the same as those predicted by the CPPC-SAFT EOS. **Fig. 2-5** compares the vapor-pressure curves calculated by the SAFT-type EOSs (Moine *et al.*, 2019; Gross and Sadowski, 2001) and the VT-CPPC-SAFT EOS developed in this work against the NIST vapor-pressure values. **Table 2-3** lists the average percentage absolute deviations (%AAD) in the vapor-pressure prediction for CO_2 using different models. **Fig. 2-5** and **Table 2-3** show that the VT-CPPC-SAFT model developed in this study provides a much more accurate vapor-pressure prediction for CO_2 than the original PC-SAFT model. In addition, as shown in **Fig. 2-5**, the two curves calculated by the I-PC-SAFT EOS and our model almost overlap, implying that a very small deviation in vapor-pressure predictions exists because of the different databases used in the development of the I-PC-SAFT EOS and our model. The results

demonstrate that our model with a %AAD of 0.247 for vapor-pressure prediction exhibits a slightly better performance than the I-PC-SAFT EOS with its %AAD of 0.489.

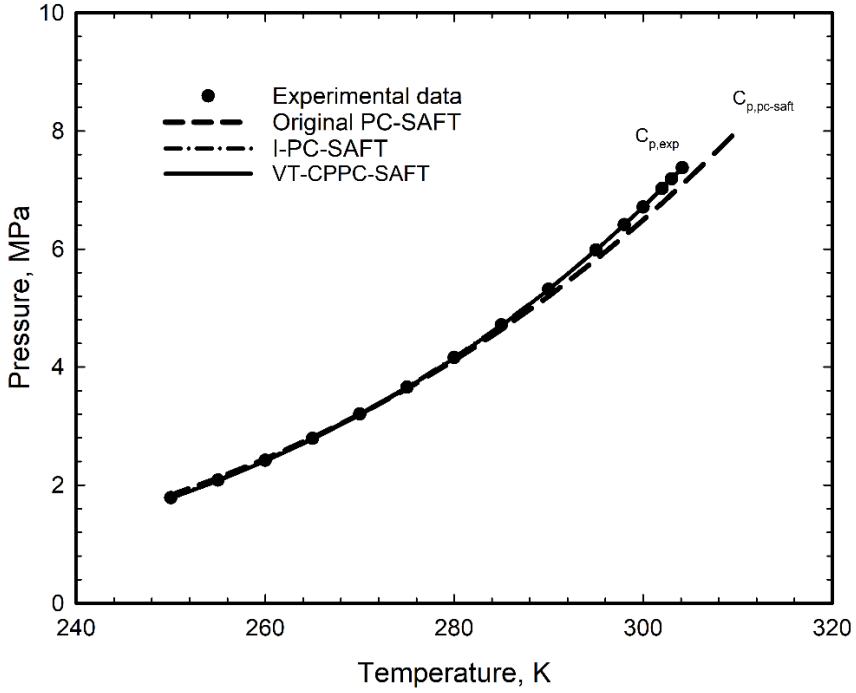

Fig. 2-5. Comparison between the experimental vapor-pressure values and those calculated by the SAFT-type EOSs (Moine *et al.*, 2019; Gross and Sadowski, 2001) and VT-CPPC-SAFT EOS developed in this work.

Table 2-3. %AADs in vapor-pressure predictions for CO_2 yielded by the different SAFT-type models and the VT-CPPC-SAFT EOS developed in this work.

	T_r range	N	PC-SAFT	I-PC-SAFT	VT-CPPC-SAFT
%AAD in vapor pressure	0.75-1	15	1.826%	0.489%	0.247%

2.4.2 Prediction Accuracy of Saturated Densities

Fig. 2-6 presents a comparison between the experimental pressure-volume two-phase envelope and those calculated by the CPPC-SAFT EOS and VT-CPPC-SAFT EOS for CO_2. **Fig. 2-6** shows that the VT-CPPC-SAFT EOS model can obviously provide an

improved prediction of the saturated liquid molar volumes. **Table 2-4** lists the %AADs in the predictions of the saturated-liquid density and saturated-vapor density yielded by the original PC-SAFT EOS, CPPC-SAFT EOS, I-PC-SAFT, and VT-CPPC-SAFT EOS. The original PC-SAFT, CPPC-SAFT, and I-PC-SAFT yield %AADs of 3.719, 15.073, and 4.254, respectively, in the saturated-liquid density predictions, whereas the VT-CPPC-SAFT developed in this study yields the smallest %AAD of 2.448. The original PC-SAFT EOS, CPPC-SAFT EOS, I-PC-SAFT, and VT-CPPC-SAFT yield the %AADs of 7.088, 1.216, 1.767, and 1.883 in the saturated-vapor density predictions, respectively. In terms of both the saturated-liquid and saturated-vapor density predictions, the original PC-SAFT, CPPC-SAFT, and I-PC-SAFT yield %AADs of 5.403, 8.144, and 3.011, respectively, while VT-CPPC-SAFT yields an overall %AAD of 2.165. Therefore, the VT-CPPC-SAFT developed in this study can provide more accurate predictions of saturated densities than the other PC-SAFT models.

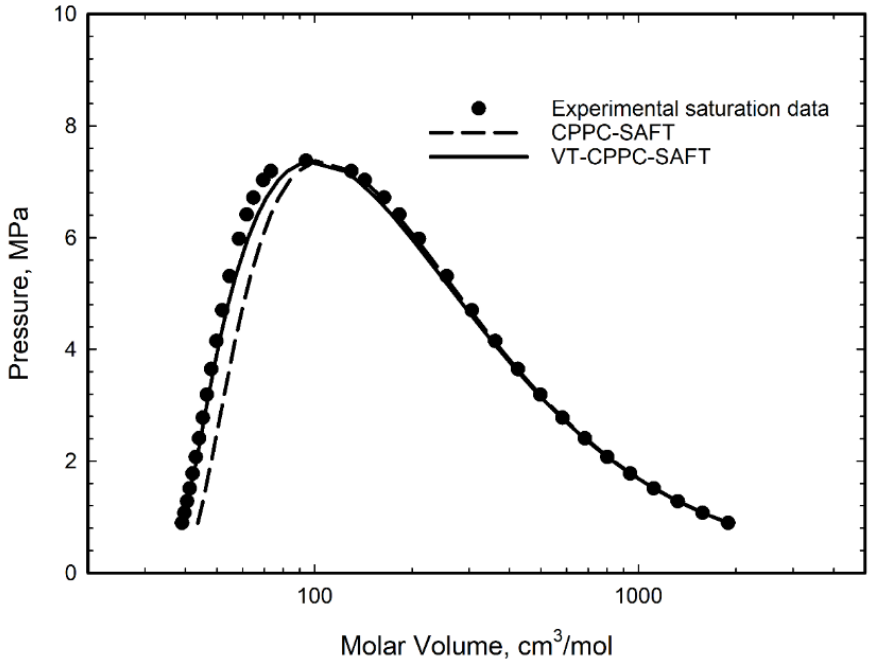

Fig. 2-6. Comparison between the experimental pressure-volume two-phase envelope and those calculated by CPPC-SAFT EOS (Anoune *et al.*, 2021) and VT-CPPC-SAFT EOS developed in this work.

Table 2-4. %AADs in the saturated density prediction for CO_2 yielded by the original PC-SAFT EOS, CPPC-SAFT EOS, I-PC-SAFT and VT-CPPC-SAFT EOS.

	T_r range	N	PC-SAFT	CPPC-SAFT	I-PC-SAFT	This work
%AAD in saturated liquid density	0.73-0.99	29	3.719%	15.073%	4.254%	2.448%
%AAD in saturated vapor density	0.73-0.99	29	7.088%	1.216%	1.767%	1.883%
Overall %AAD	0.73-0.99	58	5.403%	8.144%	3.011%	2.165%

2.4.3 Prediction Accuracy of Liquid-phase Density, Vapor-phase Density, and Supercritical-phase Density

Further, we evaluated the performance of the VT-CPPC-SAFT EOS in predicting the liquid-phase density, vapor-phase density, and supercritical-phase density of CO_2. **Fig. 2-7** shows a comparison between the needed volume shifts for liquid-phase CO_2 at different constant pressures of $0.7P_c$, $0.8P_c$, $0.9P_c$, $0.95P_c$, $1.2P_c$, $1.5P_c$, $2P_c$, and $3P_c$ and the volume shifts calculated using the proposed model. **Fig. 2-7** indicates that the proposed model can capture the general trend of the practically needed volume residuals. Considering the CO_2 density at various constant pressures of $0.7P_c$, $0.9P_c$, $1.2P_c$, and $1.5P_c$ as examples (see **Fig. 2-8**), the liquid density of CO_2 calculated with the VT-CPPC-SAFT EOS exhibits a better match with the experimental data than those calculated by the original PC-SAFT EOS, CPPC-SAFT EOS, and I-PC-SAFT EOS.

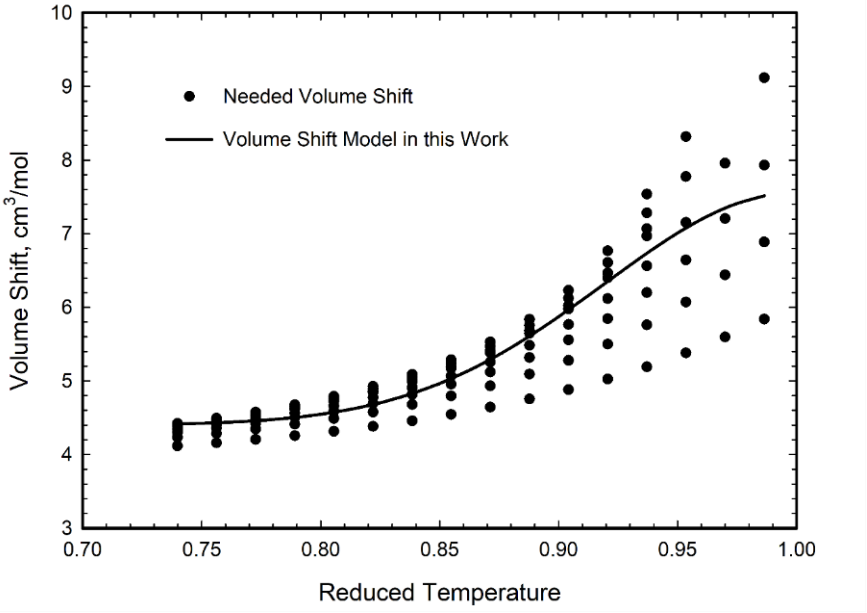

Fig. 2-7. Comparison between the needed volume shift for liquid-phase CO_2 at different constant pressures of $0.7P_c$, $0.8P_c$, $0.9P_c$, $0.95P_c$, $1.2P_c$, $1.5P_c$, $2P_c$, and $3P_c$ and those calculated by VT-CPPC-SAFT EOS.

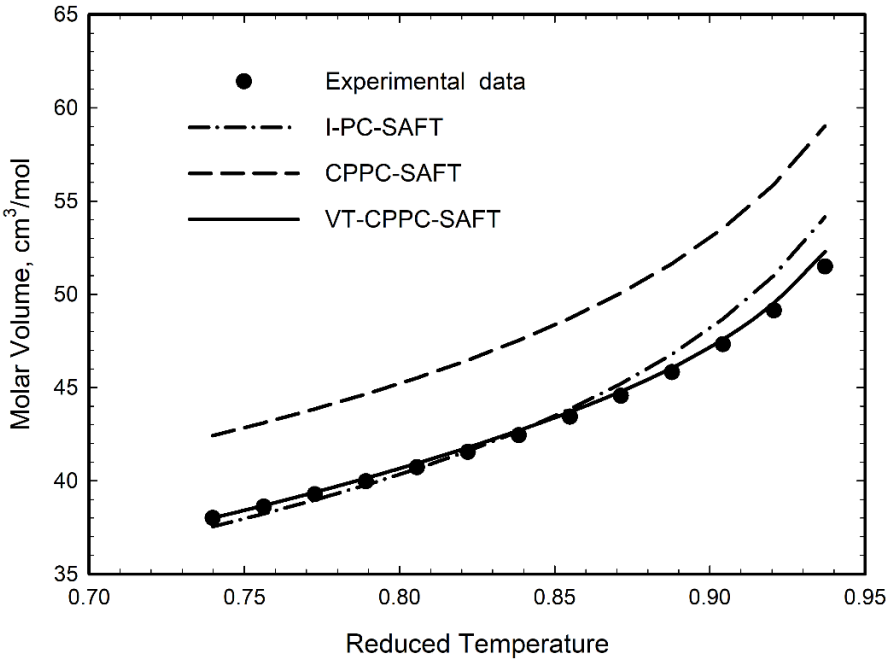

(a)

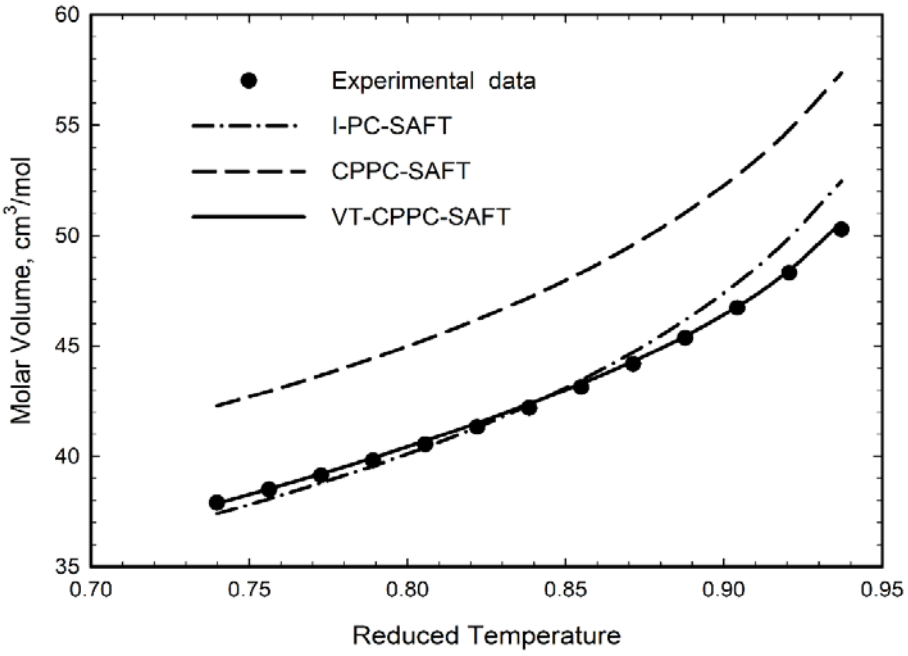
Experimental data
I-PC-SAFT
CPPC-SAFT
VT-CPPC-SAFT
Molar Volume, cm3/mol
Reduced Temperature
60
55
50
45
40
35
0.70
0.75
0.80
0.85
0.90
0.95

(b)

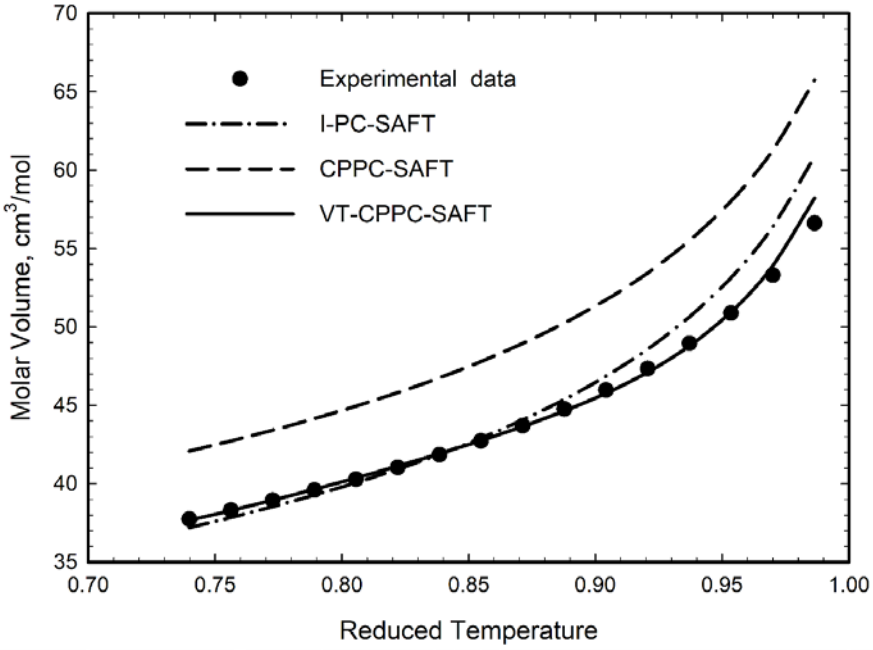
Experimental data
I-PC-SAFT
CPPC-SAFT
VT-CPPC-SAFT
Molar Volume, cm3/mol
Reduced Temperature
70
65
60
55
50
45
40
35
0.70
0.75
0.80
0.85
0.90
0.95
1.00

(c)

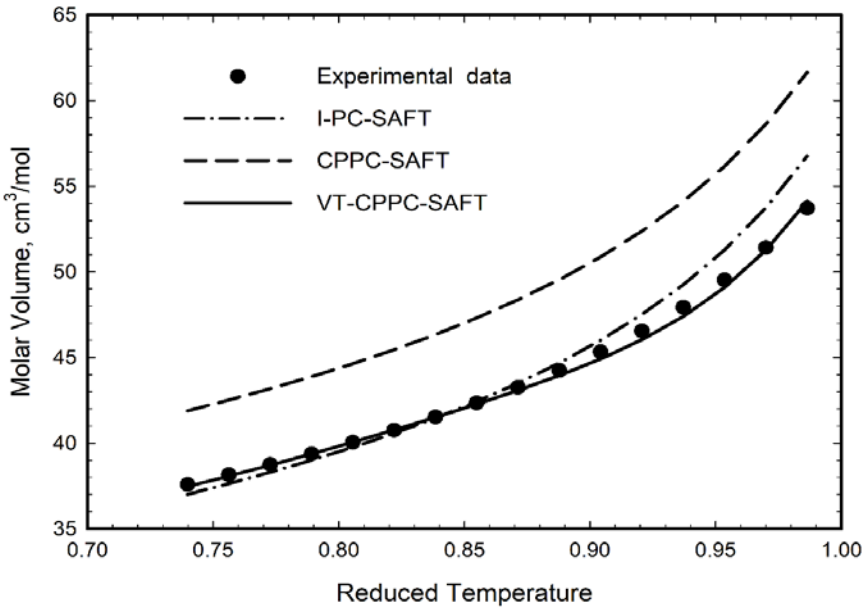

(d)

Fig. 2-8. Comparison between the experimental liquid density of CO_2 and those calculated by different models at constant pressures of (a) $0.7P_c$, (b) $0.9P_c$, (c) $1.2P_c$, and (d) $1.5P_c$.

Table 2-5 lists the %AADs in reproducing the liquid-phase density, vapor-phase density, and supercritical-phase density of CO_2 yielded by different models. For the liquid-phase density, the VT-CPPC-SAFT model yields the smallest %AAD of 0.697 among all the models considered in this study. Note that although CPPC-SAFT EOS can correctly reproduce the critical temperature and critical pressure of CO_2, it leads to a large %AAD of 12.173. For the vapor-phase density, all the considered models yield similar errors. For the supercritical density, the VT-CPPC-SAFT model provides the smallest %AAD of 1.282, although the other models give only slightly larger errors.

Table 2-5. %AAD in density predictions for various phases of CO_2 by different PC-SAFT models.

	T_r range	P_r range	N	PC-SAFT	CPPC-SAFT	I-PC-SAFT	VT-CPPC-SAFT
%AAD in liquid density	0.73-0.99	0.7-3	256	1.563%	12.173%	1.621%	0.697%
%AAD in vapor density	1.01-3	0.7-0.99	247	1.250%	1.132%	1.325%	1.263%
%AAD in supercritical density	1.01-3	1.01-3	246	1.449%	1.896%	1.475%	1.282%
Overall %AAD	0.73-3	0.7-3	759	1.424%	5.074%	1.477%	1.078%

Table 2-5 further shows that, considering the density predictions at different phase states, the performance in density predictions for CO_2 can be notably enhanced by the VT-CPPC-SAFT model developed in this work. The smallest overall %AAD of 1.078 is yielded by VT-CPPC-SAFT, while the overall %AADs yielded by the other three models are 1.424, 5.074 and 1.477, respectively. Although the proposed model in our work provides the smallest %AADs in density prediction and vapor-pressure prediction, the predictions of the first and second order thermodynamic derivative properties of pure components may not be more accurate than the other SAFT-type EOSs. The development of one SAFT-type EOS model for simultaneous and accurate description of a whole set of thermodynamic properties, including the density and the first and second order thermodynamic derivative properties, is still a necessary task.

Fig. 2-9 and **Fig. 2-10** show the pressure-volume saturation envelopes and three isotherms of CO_2 calculated with CPPC-SAFT, I-PC-SAFT, and VT-CPPC-SAFT. As

shown in **Fig. 2-9**, the temperature-dependent volume translation model used in VT-CPPC-SAFT translates the density predicted by CPPC-SAFT by a constant value along the molar volume coordinate in the pressure-volume diagram, yielding a better match with the experimental data than CPPC-SAFT. In addition, the CPPC-SAFT EOS significantly overestimated the saturated liquid molar volume and liquid molar volume near the critical region. Such deficiency, to some extent, has been remedied by our model. **Fig. 2-10** also shows that the VT-CPPC-SAFT model developed in this work has a slightly better performance, especially at conditions close to the critical point, than the I-PC-SAFT EOS with a constant volume translation.

In summary, the VT-CPPC-SAFT model developed in this study not only reproduces the critical temperature and critical pressure of CO_2 but also provides good accuracy in molar volume predictions.

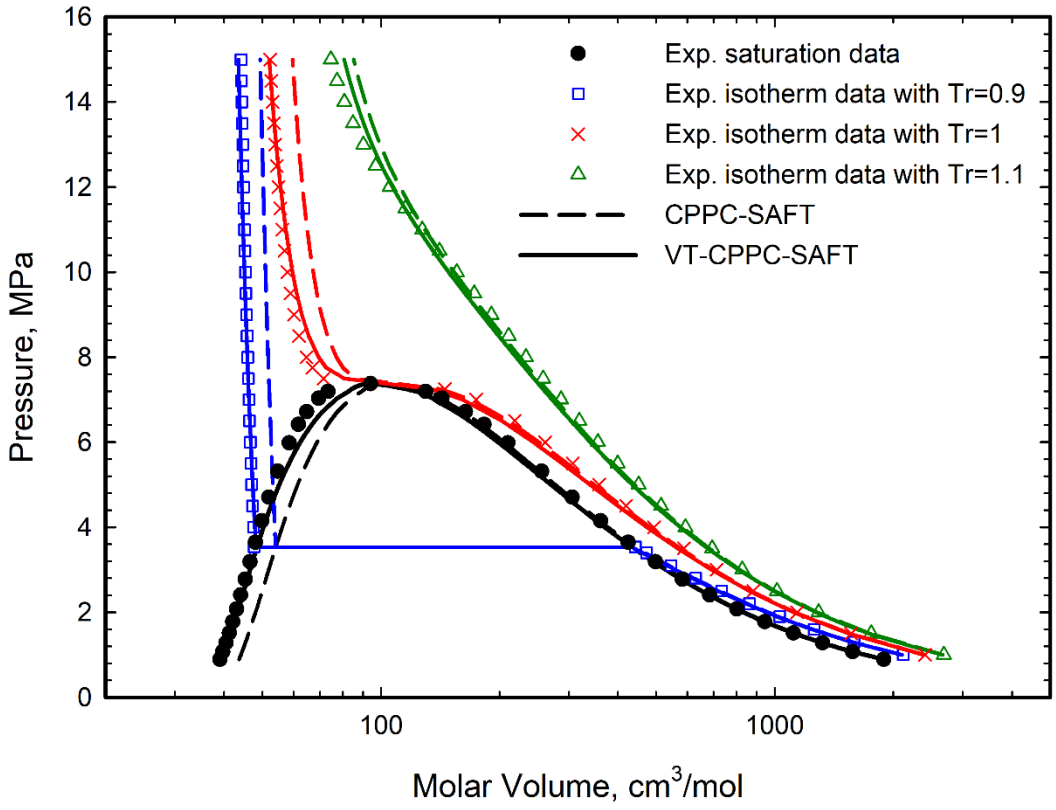

Fig. 2-9. Pressure-volume saturation envelopes and three isotherms of CO_2 calculated by CPPC-SAFT and VT-CPPC-SAFT.

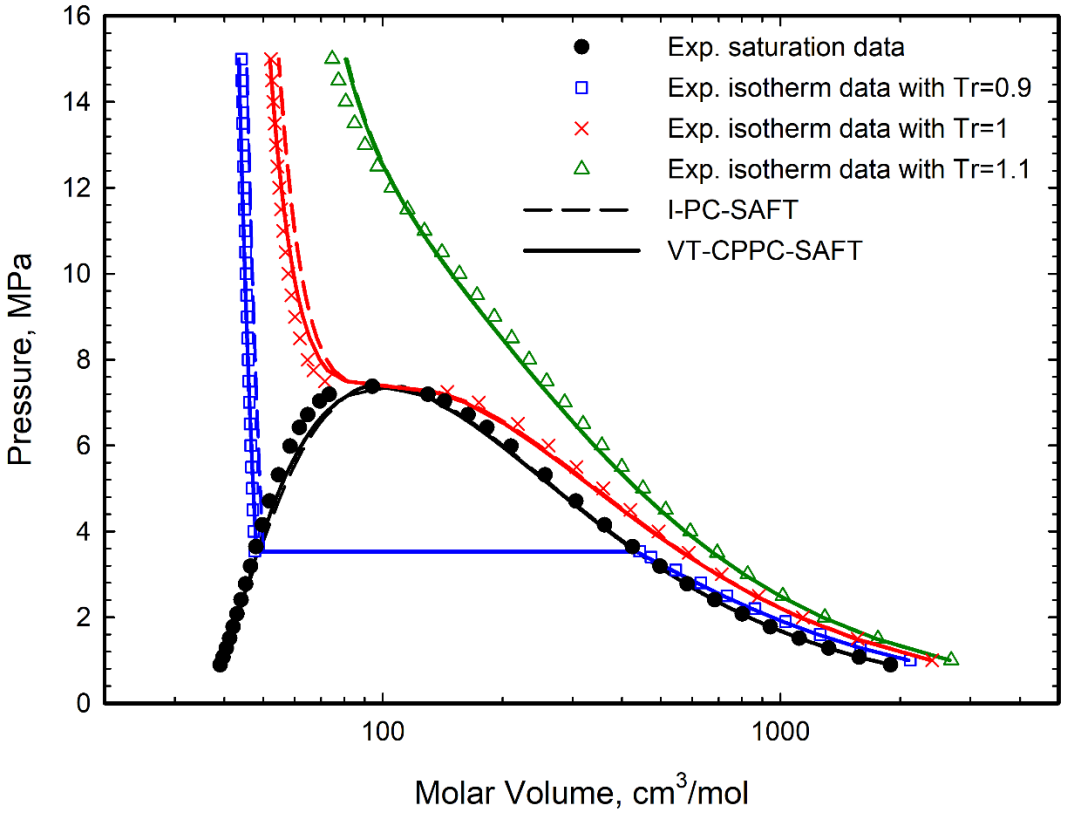

Fig. 2-10. Pressure-volume saturation envelopes and three isotherms of CO_2 calculated by I-PC-SAFT and VT-CPPC-SAFT.

2.4.4 Thermodynamic Consistency

The thermodynamic consistency issue has been widely discussed for SAFT-type EOSs (Polishuk, 2011; Kalikhman *et al.*, 2010; Polishuk, 2010) and volume-translated CEOS (Chen and Li, 2020, 2021; Pfohl, 1999; Shi *et al.*, 2018; Shi and Li, 2016; Young *et al.*, 2017). Polishuk (2011) reported that numerical pitfalls may exist in SAFT-type EOSs, resulting in multiple phase equilibria predicted for pure compounds (Polishuk, 2010), and possible negative heat capacities at very high pressures, as well as intersections of isotherms (Kalikhman *et al.*, 2010). Thus, more attention should be paid to such numerical pitfalls, especially at conditions where the pressure is extremely high. In addition, the

introduction of temperature-dependent volume translation into CEOS may cause the crossing of isotherms in the pressure-volume diagram because various degrees of volume shifts are required for the different isotherms along the molar volume coordinate. Such crossover phenomenon limits the application of these models and impedes their application in the calculation of other thermophysical properties. Similarly, such thermodynamic inconsistency may appear when a temperature-dependent volume translation technique is introduced into SAFT-type EOSs. Shi and Li (2016) developed a criterion to judge whether volume translation in CEOS can provide a consistent prediction of PVT relations over a wide range of temperatures and pressures. This criterion can also be applied to SAFT-type EOSs. To analyze the application range of the VT-CPPC-SAFT model, its thermodynamic consistency was tested to determine whether VT-CPPC-SAFT exhibits a crossover issue. **Fig. 2-11** presents the PV isotherms of CO_2 generated by VT-CPPC-SAFT at different temperatures and pressures below $10P_c$ (73.773 MPa). As shown in **Fig. 2-10**, there is no crossing of the pressure-volume isotherms at pressures below 73.773 MPa. However, a crossover issue appears at $12.335P_c$ (90.98 MPa) in the temperature range of $0.85T_c$-$0.9T_c$. Thus, the proposed VT-CPPC-SAFT model can be safely used only at pressures below 90.98 MPa.

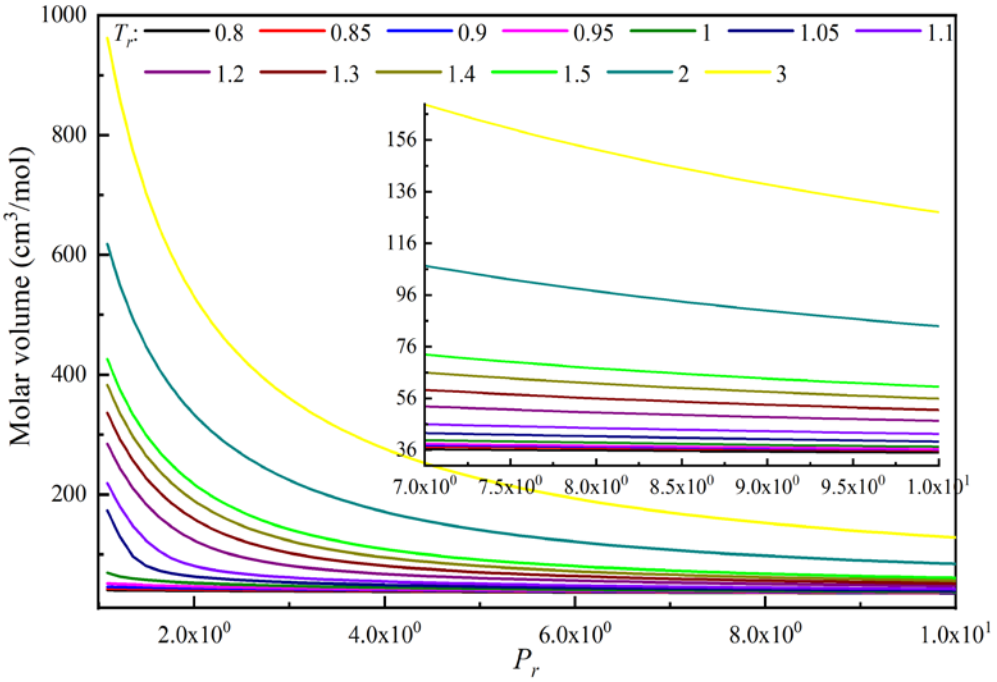

Fig. 2-11. Pressure-volume phase diagram at different temperatures generated by VT-CPPC-SAFT.

2.5 Conclusion

Three-parameter SAFT-type EOSs are unable to provide accurate predictions of density and critical properties simultaneously. Coupled with the parametrization method with the exact reproduction of the critical temperature and critical pressure, a fourth parameter, nonlinear temperature-dependent volume translation, was introduced to the PC-SAFT EOS to achieve a more accurate density prediction of CO_2. For the liquid-phase density and supercritical-phase density, the VT-CPPC-SAFT model developed in this work provided the smallest %AADs of 0.697 and 1.282, respectively, compared with the other three models (the original PC-SAFT, CPPC-SAFT, and I-PC-SAFT EOS). For the vapor-phase density, these models demonstrated a similar %AAD. Meanwhile, our model can provide the most accurate predictions of the vapor pressure and saturated density with the

smallest overall %AADs of 0.247 and 2.165, respectively. In addition, there was no crossover in the pressure-volume isotherms at pressures below 90.98 MPa. Overall, the model developed in this study not only provides accurate predictions of CO_2 density over a wide range of temperatures and pressures covering the liquid, vapor, and supercritical phases but also exactly reproduces the critical temperature and critical pressure of CO_2. The proposed strategy can be extended to other pure compounds in future studies.

Nomenclature

a	Helmholtz free energy
AAD	average absolute deviation
A, B and C	coefficients in Eq. 2-5
c	volume translation
CEOS	Cubic equation of state
P	pressure
SAFT	Statistical associating fluid theory
T	temperature
V	molar volume

Greek Letters

ω	acentric factor
m	segment number
σ	segment diameter
ε/k	energy parameter

Subscripts and superscripts

c	critical
cal	calculated property
disp	contribution due to dispersive attraction
exp	experimental
hc	hard-chain
N	number of data points
r	reduced
res	residual

References

A. Kordikowski, A.P. Schenk, R.M. Van Nielenand, C.J. Peters, Volume expansions and vapor-liquid equilibria of binary mixtures of a variety of polar solvents and certain near-critical solvents, *The Journal of Supercritical Fluids* 8 (1995) 205-216.

A. Pakravesh, F. Zarei, H. Zarei, PρT parameterization of SAFT equation of state: developing a new parameterization method for equations of state, *Fluid Phase Equilibri*a 538 (2021) 113024.

A. Peneloux, E. Rauzy, R. Freze, A consistent correction for Redlich-Kwong-Soave volumes, *Fluid Phase Equilibria* 8 (1982) 7-23.

A. Tihic, G.M. Kontogeorgis, N. Von Solms, M.L. Michelsen, Applications of the simplified perturbed-chain SAFT equation of state using an extended parameter table, *Fluid Phase Equilibria* 248 (2006) 29-43.

A.F. Young, F.L. Pessoa, V.R. Ahón, Comparison of volume translation and co-volume functions applied in the Peng-Robinson EoS for volumetric corrections, *Fluid Phase Equilibria* 435 (2017) 73-87.

A.M. Palma, A.J. Queimada, J.A. Coutinho, Using a volume shift in perturbed-chain statistical associating fluid theory to improve the description of speed of sound and other derivative properties, *Industrial & Engineering Chemistry Research* 57 (2018) 11804-11814.

A.P. Vinhal, W. Yan, G.M. Kontogeorgis, Evaluation of equations of state for simultaneous representation of phase equilibrium and critical phenomena, *Fluid Phase Equilibria* 437 (2017) 140-154.

C. McCabe, G. Jackson, SAFT-VR modelling of the phase equilibrium of long-chain n-alkanes, *Physical Chemistry Chemical Physics* 1 (1999) 2057-2064.

D.Y. Peng, D.B. Robinson, A new two-constant equation of state, *Industrial & Engineering Chemistry Fundamentals* 15 (1976) 59-64.

E. Moine, A. Piña-Martinez, J.N. Jaubert, B. Sirjean, R. Privat, I-PC-SAFT: an industrialized version of the volume-translated PC-SAFT equation of state for pure components, resulting from experience acquired all through the years on the parameterization of Saft-type and cubic models, *Industrial & Engineering Chemistry Research* 58 (2019) 20815-20827.

F. Tzirakis, I. Tsivintzelis, A.I. Papadopoulos, P. Seferlis, Experimental measurement and assessment of equilibrium behaviour for phase change solvents used in CO2 capture, *Chemical Engineering Science* 199 (2019) 20-27.

G. Soave, Equilibrium constants from a modified Redlich–Kwong equation of state, *Chemical Engineering Science* 27 (1972) 1197-1203.

G.M. Kontogeorgis, X. Liang, A. Arya, I. Tsivintzelis, Equations of state in three centuries. Are we closer to arriving to a single model for all applications? *Chemical Engineering Science: X* 7 (2020) 100060.

H. Li, J.P. Jakobsen, Ø. Wilhelmsen, J. Yan, PVTxy properties of CO2 mixtures relevant for CO2 capture, transport and storage: Review of available experimental data and theoretical models, *Applied Energy* 88 (2011) 3567-3579.

I. Anoune, Z. Mimoune, H. Madani, A. Merzougui, New modified PC-SAFT pure component parameters for accurate VLE and critical phenomena description, *Fluid Phase Equilibria* 532 (2021) 112916.

I. Polishuk, About the numerical pitfalls characteristic for SAFT EOS models, *Fluid Phase Equilibria* 298 (2010) 67-74.

I. Polishuk, Addressing the issue of numerical pitfalls characteristic for SAFT EOS models, *Fluid Phase Equilibria* 301 (2011) 123-129.

I. Polishuk, Hybridizing SAFT and cubic EOS: what can be achieved?, *Industrial & Engineering Chemistry Research* 50 (2011) 4183-4198.

I. Polishuk, J. Wisniak, H. Segura, A novel approach for defining parameters in a four-parameter EOS, *Chemical Engineering Science* 55 (2000) 5705-5720.

I. Polishuk, Standardized critical point-based numerical solution of statistical association fluid theory parameters: the perturbed chain-statistical association fluid theory equation of state revisited, *Industrial & Engineering Chemistry Research* 53 (2014) 14127-14141.

J. Gross, G. Sadowski, Application of perturbation theory to a hard-chain reference fluid: an equation of state for square-well chains, *Fluid Phase Equilibria* 168 (2000) 183-199.

J. Gross, G. Sadowski, Perturbed-Chain SAFT: An Equation of State Based on a Perturbation Theory for Chain Molecules, *Industrial & Engineering Chemistry Research* 40 (2001) 1244−1260.

J. Shi, H.A. Li, Criterion for determining crossover phenomenon in volume-translated equation of states, *Fluid Phase Equilibria* 430 (2016) 1-12.

J. Shi, H.A. Li, W. Pang, An improved volume translation strategy for PR EOS without crossover issue, *Fluid Phase Equilibria* 470 (2018) 164-175.

J.J. Martin, Cubic equations of state-which? *Industrial & Engineering Chemistry Fundamentals* 18 (1979) 81-97.

J.M.L. Sengers, Mean-field theories, their weaknesses and strength, *Fluid Phase Equilibria* 158 (1999) 3-17.

J.N. Jaubert, R. Privat, Y. Le Guennec, L. Coniglio, Note on the properties altered by application of a Péneloux–type volume translation to an equation of state, *Fluid Phase Equilibria* 419 (2016) 88-95.

J.S. Lopez-Echeverry, S. Reif-Acherman, E. Araujo-Lopez, Peng-Robinson equation of state: 40 years through cubics, *Fluid Phase Equilibria* 447 (2017) 39-71.

K. Frey, C. Augustine, R.P. Ciccolini, S. Paap, M. Modell, J. Tester, Volume translation in

equations of state as a means of accurate property estimation, *Fluid Phase Equilibria* 260 (2007) 316-325.

M. Cismondi, E.A. Brignole, J. Mollerup, Rescaling of three-parameter equations of state: PC-SAFT and SPHCT, *Fluid Phase Equilibria* 234 (2005) 108-121.

M.S. Wertheim, Fluids with highly directional attractive forces. I. Statistical thermodynamics, *Journal of Statistical Physics* 35 (1984) 19-34.

M.S. Wertheim, Fluids with highly directional attractive forces. II. Thermodynamic perturbation theory and integral equations, *Journal of Statistical Physics* 35 (1984) 35-47.

M.S. Wertheim, Fluids with highly directional attractive forces. III. Multiple attraction sites, *Journal of Statistical Physics* 42 (1986) 459-476.

M.S. Wertheim, Fluids with highly directional attractive forces. IV. Equilibrium polymerization, *Journal of Statistical Physics* 42 (1986) 477-492.

O. Pfohl, Letter to the editor: "Evaluation of an improved volume translation for the prediction of hydrocarbon volumetric properties", *Fluid Phase Equilibria* 163 (1999) 157-159.

O. Pfohl, T. Giese, R. Dohrn, G. Brunner, 1. Comparison of 12 equations of state with respect to gas-extraction processes: reproduction of pure-component properties when enforcing the correct critical temperature and pressure, *Industrial & Engineering Chemistry Research* 37 (1998) 2957-2965.

P. Navarro, A.M. Palma, J. García, F. Rodríguez, J.A. Coutinho, P.J. Carvalho, High-pressure density of bis(1-alkyl-3-methylimidazolium) tetraisothiocyanatocobaltate ionic liquids: experimental and PC-SAFT with volume-shift modeling, *Journal of Chemical & Engineering Data* 64 (2019) 4827-4833.

P.J. Linstrom, W.G. Mallard (Eds.), NIST Chemistry WebBook, NIST Standard Reference Database Number 69, National Institute of Standards and Technology, Gaithersburg, MD, 20899, http://webbook.nist.gov..

P.N. Ghoderao, V.H. Dalvi, M. Narayan, A five-parameter cubic equation of state for pure fluids and mixtures, *Chemical Engineering Science: X* 3 (2019) 100026.

R. Privat, E. Moine, B. Sirjean, R. Gani, J.N. Jaubert, Application of the corresponding-state law to the parametrization of statistical associating fluid theory (SAFT)-type models: Generation and use of "generalized charts", *Industrial & Engineering Chemistry Research* 58 (2019) 9127-9139.

R.S. Norhasyima and T.M.I. Mahlia, Advances in CO_2 utilization technology: A patent landscape review, *Journal of CO2 Utilization* 26 (2018) 323-335.

T. Merker, C. Engin, J. Vrabec, H. Hasse, Molecular model for carbon dioxide optimized to vapor-liquid equilibria, *The Journal of Chemical Physics* 132(2010) 234512.

V. Kalikhman, D. Kost, and I. Polishuk, About the physical validity of attaching the

repulsive terms of analytical EOS models by temperature dependencies, *Fluid Phase Equilibria* 293 (2010) 164-167.

W.D. Monnery, W.Y. Svrcek, M.A. Satyro, Gaussian-like Volume Shifts for the Peng−Robinson Equation of State, *Industrial & Engineering Chemistry Research* 37 (1998) 1663-1672.

W.G. Chapman, K.E. Gubbins, G. Jackson, M. Radosz, New reference equation of state for associating liquids, *Industrial & Engineering Chemistry Research* 29 (1990) 1709-1721.

W.G. Chapman, K.E. Gubbins, G. Jackson, M. Radosz, SAFT: equation-of-state solution model for associating fluids, *Fluid Phase Equilibri*a 52 (1989) 31-38.

X. Chen, H. Li, Improved prediction of saturated and single-phase liquid densities of water through volume-translated SRK EOS, *Fluid Phase Equilibria* 528 (2021) 112852.

Z.Q. Hu, J.C. Yang, Y.G. Li, Crossover SAFT equation of state for pure supercritical fluids, *Fluid Phase Equilibria* 205 (2003) 1-15.

CHAPTER 3 AN IMPROVED VOLUME TRANSLATION MODEL FOR PC-SAFT EOS BASED ON A DISTANCE FUNCTION

A version of this chapter has been published as J. Shi and H. Li, An improved volume translation model for PC-SAFT EOS based on a distance function, *Chemical Engineering Science* 276 (2023) 118800.

Abstract

In this work, we develop an improved volume-translation model for PC-SAFT EOS. The new volume translation model is based on a distance function which measures the distance of the current condition from the critical point. Such volume translation model is integrated into a particular version of PC-SAFT that can exactly reproduce the critical points of pure compounds. The proposed volume-translated PC-SAFT EOS is found to not only exactly reproduce the critical properties of pure compounds (including critical pressure, critical temperature, and critical molar volume), but also yield accurate reproductions of thermophysical properties of the selected 39 pure fluids over a wide range of temperature and pressure covering both the critical region and non-critical regions. Overall, the newly developed volume-translated SAFT EOS model yields average absolute percentage deviations (%AADs) of only 0.505%, 0.470%, and 0.676% in reproducing the saturated-liquid density, liquid density, and vapor pressure, respectively.

Keywords: Volume translation; Distance function; PC-SAFT EOS; Density prediction; Thermodynamic consistency

3.1 Introduction

A prerequisite for the design and simulation of industrial processes in the chemical and petroleum industry is a reliable knowledge of pressure-volume-temperature (PVT) relationships and thermophysical properties of pure fluids and mixtures (Nichita *et al.*, 2008; Seyf and Asgari, 2022). The development of a universal thermodynamic model for the accurate description of phase behavior and thermodynamic properties over a wide range of temperature and pressure conditions (including the near-critical region and the far-critical region) has always been one of the most challenging tasks (Anisimov and Wang, 2006; Wang and Anisimov, 2007; De Castro and Sollich, 2018; Song *et al.*, 2020; Papadopoulos *et al.*, 2021).

Since the proposal of the van der Waals equation of state (vdW EOS), extensive efforts have been devoted to developing EOSs in different mathematical frameworks, such as cubic EOSs (CEOSs) (Soave, 1972; Peng and Robinson, 1976) and non-cubic EOSs (Ghoderao *et al.*, 2018, 2019a,b). Although classic CEOSs such as SRK EOS (Soave, 1972) and PR EOS (Peng and Robinson, 1976) have been widely used in both academia and industry because of their simplicity and fairly good accuracy, the liquid density predicted by these two models deviates much from the experimental data. These classic CEOSs could not well capture the phase behavior of polar and associative compounds (Kontogeorgis *et al.*, 2020). Moreover, CEOSs are not sufficiently accurate in predicting the thermodynamic properties and performing phase equilibrium calculations near the critical region (Ji and Lempe, 1997; Kiselev, 1998; Saeed and Sattar, 2019).

Molecular-based EOSs, which are developed based on more sound theoretical analysis, have gained increasing attention recently. As one of the most successful

molecular-based EOSs, the SAFT-type EOSs, such as SAFT EOS proposed by Chapman *et al.* (1989) and perturbed-chain SAFT EOS (PC-SAFT EOS) proposed by Gross and Sadowski (2001), are envisioned as highly promising thermodynamic models that could potentially address the various issues exhibited by CEOSs (Wertheim, 1986a,b,c,d). In such SAFT-type EOSs, the effects of molecular shapes and interactions on the thermophysical properties can be more accurately captured and quantified.

Although SAFT-type EOSs such as PC-SAFT EOS (Gross and Sadowski, 2001) can well reproduce the measured liquid density data over a wide range of temperature and pressure, accurate predictions of the thermodynamic properties (including liquid density, saturated-liquid density, critical point, and vapor pressure) in the vicinity of the critical region cannot be realized. Taking *n*-butane as an example, **Fig. 3-1** compares the pressure-density two-phase envelope and isotherms at T =416.623K ($0.98T_{c,\mathrm{Exp}}$; $T_{c,\mathrm{Exp}}$ is the measured critical temperature) and T = 425.125K ($T_{c,\mathrm{Exp}}$) (retrieved from NIST database (Domalski *et al.*, 2015)) against those calculated by the original PC-SAFT EOS (Gross and Sadowski, 2001). In addition, the right panel of **Fig. 3-1** presents a partially enlarged view of the pressure-density phase diagram close to the critical region. From **Fig. 3-1**, it can be clearly seen that the original PC-SAFT model can provide accurate density predictions when temperature and pressure are away from the critical region. But imprecise liquid-density estimations by the original PC-SAFT model can be observed near the critical region. In addition, the original PC-SAFT model cannot provide accurate saturated-density prediction in the vicinity of the critical region. The isotherms, especially at temperatures approaching critical temperature, cannot be accurately reproduced by PC-SAFT EOS.

Fig. 3-2 compares the vapor-pressure curve calculated by PC-SAFT EOS against the experimental vapor pressure from NIST database for *n*-butane. From **Fig. 3-2**, we can clearly observe an overestimation of critical temperature and critical pressure by PC-SAFT EOS. **Fig. 3-3** shows the detailed average absolute percentage deviations (%AADs) yielded by the original PC-SAFT EOS in reproducing critical temperature, critical pressure, and critical molar volume of 13 compounds. It is evident that the original PC-SAFT is not accurate in predicting critical temperature, critical pressure, and critical molar volume of pure compounds. As a result, the performance of the original PC-SAFT EOS tends to be compromised near the critical region.

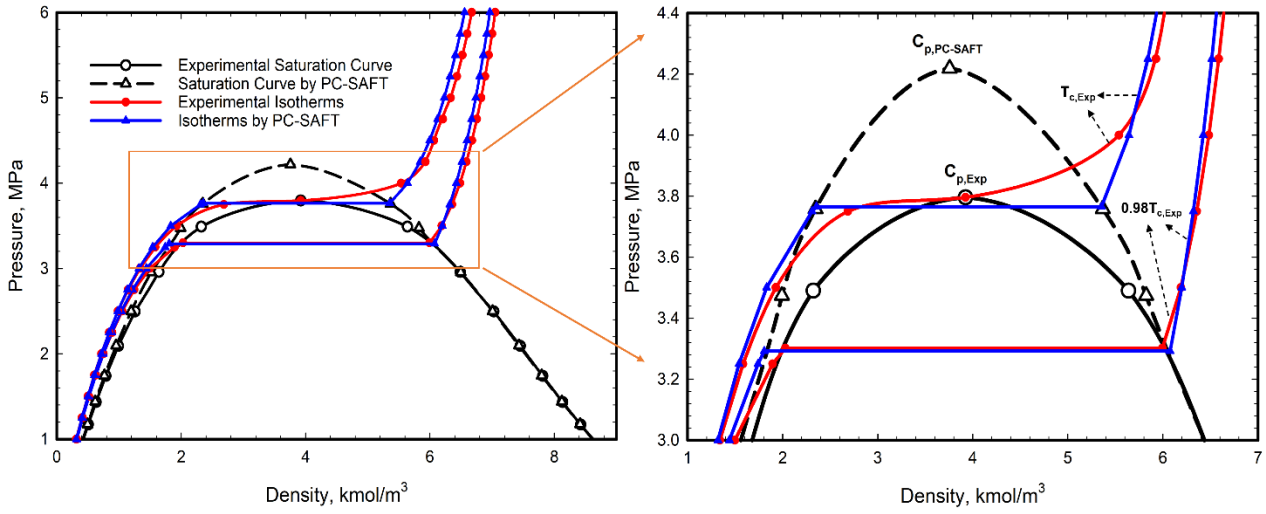

Fig. 3-1. Comparison of the experimental pressure-density two-phase envelope and isotherms at T =416.623K ($0.98T_{c,\mathrm{Exp}}$) and T = 425.125K ($T_{c,\mathrm{Exp}}$) (Domalski *et al.*, 2015) against those calculated by the original PC-SAFT EOS (Gross and Sadowski, 2001) for *n*-butane. $C_{\mathrm{p,PC\text{-}SAFT}}$ refers to the critical point predicted by the original PC-SAFT EOS, while $C_{\mathrm{p,Exp}}$ refers to the experimental critical point. The right panel shows a partially enlarged view of the pressure-density phase diagram close to the critical region.

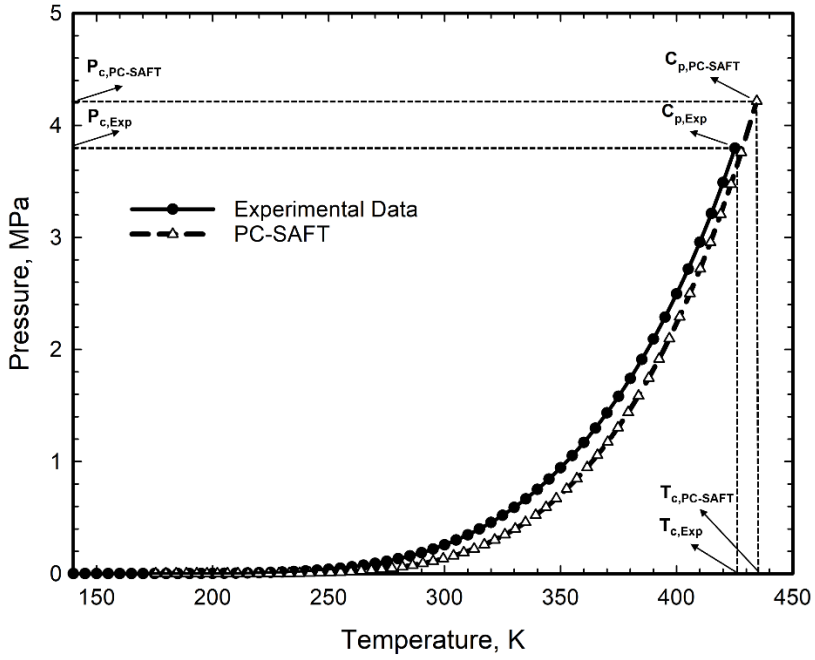

Fig. 3-2. Comparison between the experimental vapor-pressure values (Domalski *et al.*, 2015) and those calculated by the original PC-SAFT EOS (Gross and Sadowski, 2001) for *n*-butane.

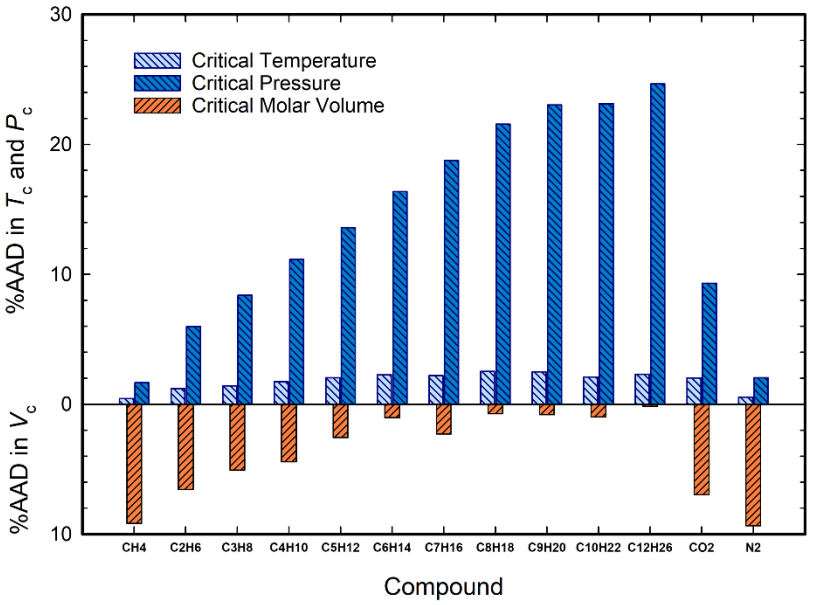

Fig. 3-3. %AADs yielded by the original PC-SAFT EOS (Gross and Sadowski, 2001) in reproducing critical temperature, critical pressure, and critical molar volume of 13 compounds.

3.2 Literature Review

Over the past three decades, the popularity of SAFT-type EOSs has substantially grown since the appearance of the first SAFT EOS (Chapman *et al.*, 1989) in 1989 (Müller and Gubbins, 2001). Despite their success, SAFT-type EOSs bear some limitations s (Sengers, 1999; Wyczalkowska *et al.*, 2004). As mentioned above, one significant limitation is that most of the SAFT-type EOSs cannot reproduce critical point of pure compounds, leading to significant deviations in reproducing liquid density, saturated liquid density, critical point, and vapor pressure near the critical region.

To address such limitation, some modifications of SAFT-type EOSs have been made in an attempt to obtain more accurate prediction of thermodynamic properties near the critical region. One approach is to reproduce the critical point with the re-parametrization method (Pfohl *et al.*, 1998; Cismondi *et al.*, 2005; Polishuk, 2014; Polishuk *et al.*, 2017a,b; Moine *et al.*, 2019; Privat *et al.*, 2019; Pakravesh *et al.*, 2021; Polishuk *et al.*, 2021; Anoune *et al.*, 2021). The three model parameters in SAFT-type EOSs are regressed from thermophysical properties (which normally include vapor pressure and density data) without imposing any restriction to the critical point. This leads to an overestimation of critical temperature and critical pressure (See **Fig. 3-2** and **Fig. 3-3**). Some researchers attempt to re-parameterize the original parameters used in SAFT-type EOSs such that critical point can be reproduced (Pfohl *et al.*, 1998; Cismondi *et al.*, 2005; Polishuk, 2014; Polishuk *et al.*, 2017a,b; Moine *et al.*, 2019; Privat *et al.*, 2019; Pakravesh *et al.*, 2021; Polishuk *et al.*, 2021; Anoune *et al.*, 2021). However, the exact reproduction of critical point by SAFT-type EOSs is achieved by sacrificing the prediction accuracy of other thermodynamic properties (Shi and Li, 2022). In addition, Cismondi *et al.* (2005)

demonstrated that, with the rescaled parameters based on the experimental critical point, the critical compressibility factor calculated by SAFT-type EOSs must be overestimated in order to obtain a better density description.

To remedy the above shortcomings of the re-parameterization methods for SAFT-type EOSs, some researchers (Palma *et al.*, 2018; Moine *et al.*, 2019; Navarro *et al.*, 2019; Shi and Li, 2022) try to introduce one more parameter, the so-called volume translation term (Martin, 1979; Peneloux *et al.*, 1982; Li *et al.*, 2017; Young *et al.*, 2017; Shi *et al.*, 2018; Chen and Li, 2020, 2021) that is widely used in CEOSs (Soave, 1972; Peng and Robinson, 1976), into three-parameter SAFT-type EOSs for the accurate prediction of liquid density and other properties. Palma *et al.* (2018) introduced a constant volume translation into PC-SAFT EOS to improve its accuracy in predicting speed of sound and other derivative properties. They demonstrated that the proposed approach leads to improved prediction of liquid-phase speed of sound and the first derivative of pressure with respect to volume. However, such strategy will worsen the description of the first derivative of volume with respect to temperature, engendering an inaccurate description of isobaric expansivity. Navarro *et al.* (2019) presented a temperature-dependent volume translation in PC-SAFT EOS for some ionic liquids. A better description of the density can be obtained especially at high pressures. But such an approach cannot be used over a wide range of temperature and pressure and its performance may be compromised near the critical point. Moine *et al.* (2019) proposed an industrialized version of the volume-translated PC-SAFT EOS (I-PC-SAFT EOS) based on a re-parameterization method that exactly reproduces the experimental critical point. A constant volume translation term was used by Moine *et al.* (2019). This model improves the prediction accuracy of saturated-

liquid density at conditions where the reduced temperature is less than 0.9. But the accuracy of saturated-liquid density prediction is compromised when the reduced temperature is greater than 0.9. In addition, their model gives a large error in critical density prediction. Shi and Li (2022) attempted to introduce a temperature-dependent volume translation term into PC-SAFT for more accurate density prediction of CO_2. But this model fails to provide accurate density predictions near the critical point. In summary, introducing a volume translation term into SAFT-type EOSs seems to be a very promising strategy to improve their density prediction accuracy, which is, however, faced with the challenge of inferior performance at near-critical conditions.

Another approach is to apply the renormalization group theory (RGT). This theory was first proposed by Wilson (Wilson, 1971, 1975; Wilson and Fisher, 1972) and then extended by White and his co-workers (Salvino and White, 1992; White, 1992; White and Zhang, 1993, 1995). Such strategy was explicitly applied into soft-SAFT EOS (Blas and Vega, 1997) to achiever more accurate prediction of critical properties, leading to the so-called crossover soft-SAFT EOS (Llovell *et al.*, 2004, 2006, Llovell and Vega, 2006a,b). Furthermore, some modifications of RGT have been incorporated into different SAFT-type EOSs for more accurate prediction of thermodynamic properties near critical point (Bymaster *et al.*, 2008; Smith *et al.*, 2022; Yang *et al.*, 2023). However, such crossover EOSs bear some limitations: their performance tends to deteriorate as the chain length increases (Llovell and Vega, 2006); an additional computational cost ensues because more extra parameters are required in the crossover model (Polishuk, 2011).

3.3 Mathematical Model

An exact reproduction of critical temperature and critical pressure is a cornerstone for achieving more accurate prediction of thermodynamic properties near the critical region. Such reproduction of critical point can be accomplished by the re-parameterization of the three parameters in the original SAFT-types EOSs. An example of a successful model is the critical-point rescaled perturbed-chain SAFT EOS (CPPC-SAFT EOS) proposed by Anoune *et al.* (2021). However, this is achieved at the expense of sacrificing the accuracy of liquid density predictions. **Fig. 3-4** compares the experimental pressure-density envelope and isotherms (at T = 416.623K ($0.98T_{c,\mathrm{Exp}}$) and T = 425.125K ($T_{c,\mathrm{Exp}}$)) of *n*-butane against those calculated by a critical-point rescaled perturbed-chain SAFT EOS (CPPC-SAFT EOS) (Anoune *et al.*, 2021). We can see from **Fig. 3-4** that the CPPC-SAFT EOS predicts a two-phase envelope that is much narrower than the NIST data. The CPPC-SAFT EOS also leads to a poor reproduction of the two isotherms. This finding indicates that, although the CPPC-SAFT EOS can exactly reproduce critical temperature and critical pressure, it cannot accurately describe the phase behavior of pure fluids. Thus, the CPPC-SAFT EOS, which is forced to reproduce critical temperature and critical pressure of a pure compound, leads to poor predictions of properties near and far from the critical region.

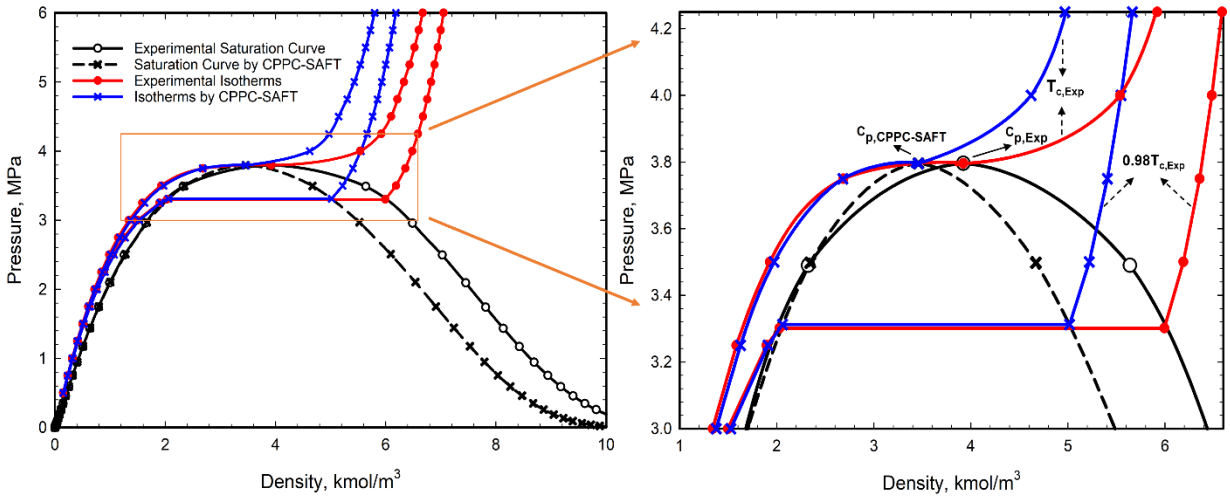

Fig. 3-4. Comparison of the experimental pressure-density envelope and isotherms (at T =416.623K ($0.98T_{c,\mathrm{Exp}}$) and T = 425.125K ($T_{c,\mathrm{Exp}}$)) (Domalski *et al.*, 2015) for *n*-butane against those calculated by CPPC-SAFT EOS (Anoune *et al.*, 2021).

In this work, we develop a pragmatic method to achieve significantly better density modeling performance with the SAFT-types EOSs. Herein, we propose to couple a distance-function-based volume translation model into CPPC-SAFT EOS (Anoune *et al.*, 2021). The critical point is exactly reproduced by CPPC-SAFT EOS (Anoune *et al.*, 2021), while the density prediction accuracy close to critical point is significantly improved with the distance-function-based volume translation model. The volume translation model needs to be forced to exactly reproduce the critical molar volume residuals ($V_{\mathrm{c,CPPC\text{-}SAFT}}$-$V_{\mathrm{c,Exp}}$; $V_{\mathrm{c,CPPC\text{-}SAFT}}$ is the critical molar volume predicted by CPPC-SAFT EOS and $V_{\mathrm{c,Exp}}$ is the experimental critical molar volume), which can ensure that the critical molar volume calculated by the proposed volume translated CPPC-SAFT EOS matches the true critical molar volume.

The original PC-SAFT EOS (Gross and Sadowski, 2001) is expressed as the sum of all the residual Helmholtz free energy contributions from different intermolecular effects:

$$a_{res} = a_{hc} + a_{disp} \tag{3-1}$$

where a_{res} is the residual Helmholtz free energy, while a_{hc} and a_{disp} represent the Helmholtz free energy due to hard-chain repulsion and dispersion for the non-associating compounds, respectively. Three model parameters, namely segment number (m), segment diameter (σ), and energy parameter (ε/k), are required in the original PC-SAFT EOS. In this work, we focus on a modified version of PC-SAFT EOS, i.e., the CPPC-SAFT EOS proposed by Anoune *et al.* (2021).

We introduce a volume translation term into CPPC-SAFT EOS:

$$c = V_{\text{CPPC-SAFT}} - V_{\text{Exp}} \tag{3-2}$$

where c is the volume translation term, while $V_{\text{CPPC-SAFT}}$ and V_{Exp} are the uncorrected saturated-liquid molar volume and the experimental saturated-liquid molar volume (Domalski *et al.*, 2015), respectively. To provide better corrections in saturated-liquid molar volumes near and far from the critical point as well as avoid the thermodynamic inconsistency (Shi and Li, 2016) in the development of volume translated PC-SAFT EOS, we propose the following volume translation function after evaluating several alternative functional forms:

$$c = \delta_c \exp\left(c_1 \gamma\right)\left(\frac{1}{1 + c_2 \gamma}\right) \tag{3-3}$$

where c_1 and c_2 refer to two compound-dependent parameters, and γ refers to a dimensionless distance function that is based on the first derivative of temperature with respect to molar volume at constant pressure:

$$\gamma = -\frac{R\rho^2}{P_c}\left(\frac{\partial T}{\partial \rho}\right)_P = \frac{R}{P_c}\left(\frac{\partial T}{\partial V}\right)_P \tag{3-4}$$

where R is universal gas constant and ρ is molar density. The dimensionless distance function is calculated from the untranslated CPPC-SAFT EOS to avoid iterations (Abudour *et al.*, 2012; Chou and Prausnitz, 1989; Frey *et al.*, 2009). It should be noted that, a different dimensionless distance expression, which is a function of the first derivative of pressure with respect of molar volume at constant temperature (i.e., $\left(\frac{\partial P}{\partial V}\right)_T$) has been previously adopted to develop volume-translated CEOSs (Chou and Prausnitz, 1989; Frey *et al.*, 2009; Abudour *et al.*, 2012; Chen and Li, 2020, 2021). But such technique has never been applied to the SAFT-type EOSs. We find that, compared to the $\left(\frac{\partial P}{\partial V}\right)_T$-dependent volume translations developed for CEOSs, the $\left(\frac{\partial T}{\partial V}\right)_p$-dependent volume translation strategy proposed here yields a much better performance in correcting the density predictions by CPPC-SAFT EOS. **Appendix 3-A.1** provides the detailed expression of $\left(\frac{\partial T}{\partial V}\right)_P$, as well as the detailed expressions of $\left(\frac{\partial T}{\partial P}\right)_V$ and $\left(\frac{\partial P}{\partial V}\right)_T$ based on PC-SAFT EOS.

The value of γ is zero at the critical point, resulting in the volume translation being equal to δ_c at the critical point:

$$\delta_c = V_{c,\text{CPPC-SAFT}} - V_{c,\text{Exp}} = \frac{N_A \pi m d_c^3}{6\eta_c} - \frac{z_{c,\text{Exp}} R T_c}{P_c} \tag{3-5}$$

where $V_{c,\text{CPPC-SAFT}}$ and $V_{c,\text{Exp}}$ are the calculated critical molar volume by CPPC-SAFT EOS (Anoune *et al.*, 2021) and the experimental critical molar volume from NIST database

(Domalski *et al.*, 2015), respectively. N_A is the Avogadro constant (6.022×10^{23} mol^{-1}), and d_c is the temperature-dependent hard segment diameter at critical point. The detailed expression of d_c can be found in the original PC-SAFT EOS paper (Gross and Sadowski, 2001) and **Appendix 3-A.1**. η_c refers to the packing fraction at critical point. The detailed values of η_c for different compounds are presented in **Table 3-1** (Anoune *et al.*, 2021). $z_{c,Exp}$ refers to the experimental critical compressibility factor. Since δ_c in **Eq. 3-5** is defined as the difference between the critical molar volume calculated by CPPC-SAFT EOS and the experimental one, we can guarantee that an exact reproduction of critical molar volume of each pure compound can be obtained with the introduction of such volume translation strategy.

It should be noted that the values of γ are always positive. It has a relatively high value at a low reduced temperature, while it has a relatively small value at a high reduced temperature. As such, with the aid of **Eq. 3-3**, we can achieve a relatively small correction at a low reduced temperature but a relatively high correction at a high reduced temperature. **Fig. 3-5** shows the relationship between molar volume residuals ($V_{CPPC\text{-}SAFT}$-V_{Exp}) yielded by CPPC-SAFT EOS for *n*-butane and the proposed distance function at different pressures. We select the curve of molar volume residuals versus distance function at saturation pressures as a benchmark. It can be seen from **Fig. 3-5** that the curves of molar volume residuals versus distance functions at different constant pressures tend to cluster around the benchmark curve. This implies that the molar volume residuals yielded by CPPC-SAFT EOS at different pressures correlate well with the proposed distance function.

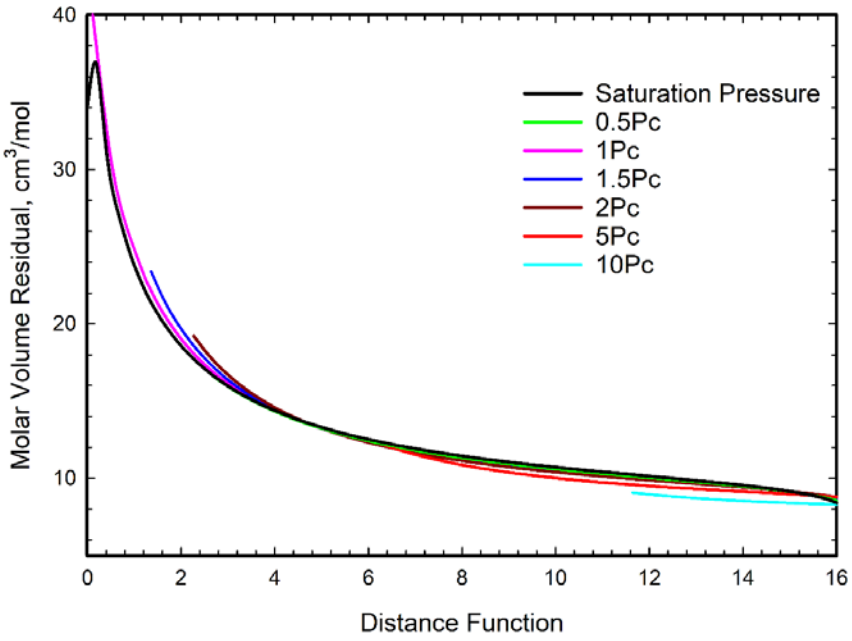

Fig. 3-5. Molar volume residuals ($V_{\text{CPPC-SAFT}}$-V_{Exp}) yielded by CPPC-SAFT EOS for *n*-butane versus distance function γ at different pressures.

To balance accuracy and generalizability, two compound-dependent values, i.e., c_1 and c_2, are adopted in the new volume translation correlation. The specific values of c_1 and c_2 are determined by performing nonlinear regression on the saturated-liquid molar volumes. The temperature range considered in the regression procedure is from triple point temperature to critical temperature with a step of 4K. **Table 3-1** presents the physical properties of pure compounds (i.e., m, σ, ε/k, T_c, P_c, z_c, η_c and ω (acentric factor)) and the optimized values of c_1 and c_2 in the volume-translated rescaled PC-SAFT EOS (VTR-PC-SAFT EOS) proposed in this work.

Table 3-1. Physical properties of pure compounds and optimized values of c_1 and c_2 in the volume-translated rescaled PC-SAFT EOS (VTR-PC-SAFT EOS).

Components	m [-]	σ [A]	ε/k [K]	c [cm^3/mol]		T_c [K]	P_c [MPa]	z_c	η_c	ω
				c_1	c_2					
Carbon dioxide	2.66827	2.61212	147.234	0.0784	0.5120	304.13	7.3773	0.2746	0.1295	0.22394
Sulfur dioxide	2.97081	2.76154	198.787	0.0848	0.4031	430.64	7.8866	0.2727	0.1281	0.256

Carbon monoxide	1.37867	3.19408	89.009	-1.0984	0.1444	132.86	3.494	0.2915	0.1349	0.0497
Carbonyl sulfide	1.72987	3.4255	226.049	0.1147	1.5979	378.77	6.37	0.2730	0.133	0.0978
Nitrogen	1.26985	3.26557	88.136	-0.9738	0.5280	126.192	3.3958	0.2894	0.136	0.0372
Methane	1.05059	3.64333	146.016	-0.3415	1.6143	190.564	4.5992	0.2863	0.1409	0.01142
Ethane	1.70277	3.50488	183.677	0.0553	1.0989	305.322	4.8722	0.2799	0.1331	0.0995
Propane	2.12134	3.62730	199.460	0.0568	0.6730	369.89	4.2512	0.2765	0.1317	0.1521
Butane	2.49164	3.73302	212.368	0.0484	0.4564	425.125	3.796	0.2738	0.1303	0.201
Pentane	2.90397	3.80482	218.979	0.0462	0.3798	469.7	3.3675	0.2686	0.1285	0.251
Hexane	3.31338	3.85201	223.812	0.0462	0.3546	507.82	3.0441	0.2664	0.1265	0.299
Heptane	3.72560	3.90169	227.084	0.0442	0.3287	540.2	2.73573	0.2614	0.1245	0.349
Octane	4.12817	3.94292	229.870	0.0447	0.3127	568.74	2.48359	0.2586	0.1226	0.398
Nonane	4.51670	3.97600	232.540	0.0403	0.2954	594.55	2.281	0.2549	0.1208	0.4433
Decane	4.89556	4.00817	234.891	0.0531	0.3844	617.7	2.103	0.2497	0.119	0.4884
Dodecane	5.62992	4.06224	238.987	0.0489	0.3262	658.1	1.817	0.2497	0.1159	0.574
Toluene	3.02633	3.78489	270.979	0.0512	0.3895	591.75	4.1263	0.2646	0.1279	0.2657
Benzene	2.63606	3.68774	273.586	0.0697	0.5359	562.02	4.907277	0.2692	0.1297	0.211
Propylene	2.0897	3.54472	197.841	0.0619	0.6731	364.211	4.555	0.2756	0.1318	0.146
Isopentane	2.71605	3.86698	221.087	0.0497	0.4873	460.35	3.378	0.2698	0.1293	0.2274
Cyclohexane	2.62447	3.908	270.027	0.0620	0.4959	553.6	4.0805	0.2750	0.1297	0.2096
Cyclopropane	1.95655	3.49076	223.481	0.0947	0.7991	398.3	5.5797	0.2743	0.1323	0.1305
Isobutane	2.38497	3.79437	207.923	0.0475	0.4905	407.81	3.629	0.2759	0.1307	0.184
Ethylene	1.65388	3.40992	172.389	0.0681	1.3332	282.35	5.0418	0.2812	0.1333	0.0866
Neopentane	2.48921	3.98124	216.77	0.0785	0.7881	433.74	3.196	0.2710	0.1303	0.1961
R11	2.43018	3.70738	238.091	0.0019	0.4340	471.11	4.407638	0.2790	0.1305	0.18875
R12	2.34661	3.58385	197.861	0.0127	0.5634	385.12	4.1361	0.1795	0.1308	0.17948
R21	2.59885	3.38341	221.204	0.0901	0.6148	451.48	5.1812	0.2700	0.1298	0.2061
R22	2.67514	3.17181	178.577	0.0975	0.5847	369.295	4.99	0.2683	0.1295	0.22082
R23	2.95578	2.88526	138.460	0.0987	0.4878	299.293	4.832	0.2582	0.1282	0.263
R32	3.01995	2.84472	160.998	0.0650	0.3546	351.255	5.782	0.2429	0.1279	0.2769
R114	2.92994	3.69232	194.505	-0.0883	0.1952	418.83	3.257	0.2756	0.1283	0.2523
R115	2.90397	3.54624	164.619	0.0300	0.6577	353.1	3.129	0.2678	0.1284	0.248
R123	3.19901	3.54145	204.313	0.0377	0.3722	456.831	3.6618	0.2681	0.127	0.28192
R124	3.24278	3.37	175.847	0.0367	0.3972	395.425	3.624296	0.2687	0.1268	0.2881
R125	3.37751	3.15657	148.305	-0.0020	0.2995	339.173	3.6177	0.2684	0.1262	0.3052
R134a	3.53622	3.08618	160.601	0.0778	0.4321	374.21	4.05928	0.2600	0.1254	0.32684
R141b	2.71152	3.63897	229.495	0.0687	0.4865	477.5	4.212	0.2706	0.1293	0.2195
R142b	2.77438	3.47533	195.165	0.0671	0.4427	410.26	4.055	0.26786	0.129	0.2321

We evaluate the performance of different PC-SAFT EOSs in predicting various properties with the following error index:

$$\begin{cases} \%\text{AAD}=\dfrac{100}{N}\displaystyle\sum_{i=1}^{N}\left|\dfrac{Prop_{i,\text{Exp}}-Prop_{i,\text{PC-SAFT}}}{Prop_{i,\text{Exp}}}\right| \\ \%\text{AD}=100\left|\dfrac{Prop_{i,\text{Exp}}-Prop_{i,\text{PC-SAFT}}}{Prop_{i,\text{Exp}}}\right| \end{cases} \tag{3-6}$$

where %AAD refers to the average absolute percentage deviation, %AD refers to the absolute percentage deviation and N refers to the number of data points. $Prop_{i,\text{Exp}}$ and $Prop_{i,\text{PC-SAFT}}$ are the experimental property corresponding to the ith data point retrieved from the NIST database (Domalski *et al.*, 2015) and the calculated one by a given PC-SAFT EOS, respectively.

3.4 Results and Discussion

3.4.1 Reproduction of Molar Volume Residuals

The distance-function-based volume translation model is found to well capture the molar volume residuals ($V_{\text{CPPC-SAFT}}$-V_{Exp}: the molar volume calculated by CPPC-SAFT EOS minus the experimental one). **Fig. 3-6** compares the molar volume residuals ($V_{\text{CPPC-SAFT}}$-V_{Exp}) and volume translations calculated by **Eq. 3-3** at different reduced temperatures for *n*-butane. It can be clearly observed from **Fig. 3-6** that the molar volume residuals depend on both pressure and temperature. The proposed volume translation strategy not only gives a good match with the needed saturated-liquid molar volume residuals but also captures the variation trend of single-liquid molar volume residuals at different pressures. Thus, with the introduction of the temperature/pressure-dependent volume translation strategy as shown in **Eq. 3-3**, accurate density predictions can be achieved with CPPC-SAFT EOS. As a result, although the two parameters in the proposed volume translation model are regressed only based on the saturated-liquid density, such strategy could provide a more accurate prediction of liquid density.

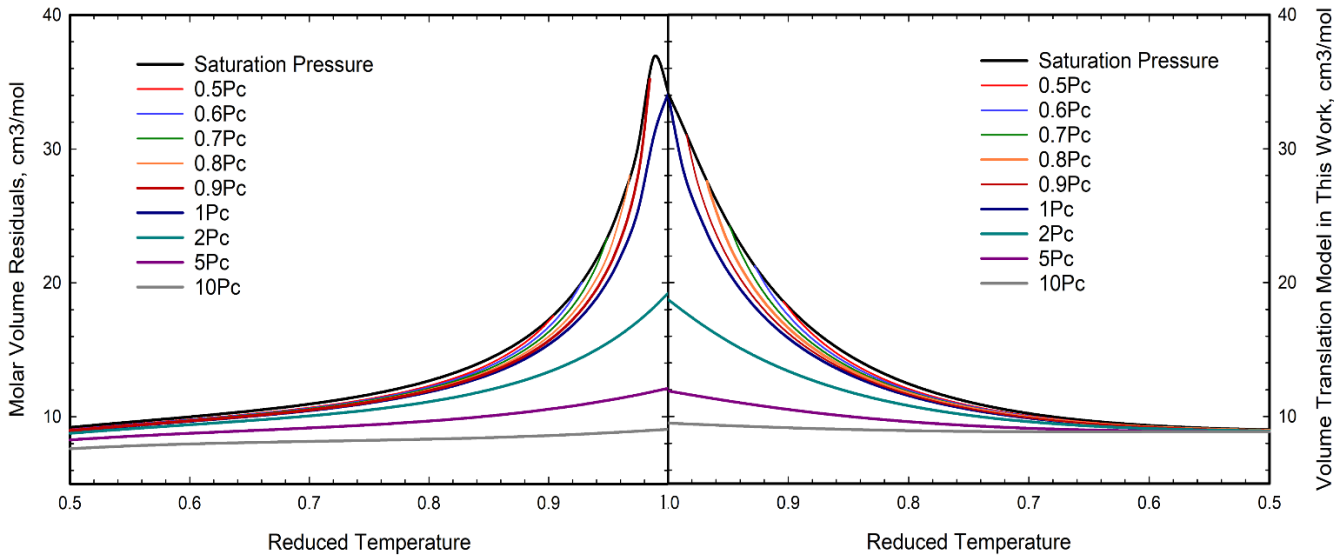

Fig. 3-6. Comparison between the molar volume residuals ($V_{\text{CPPC-SAFT}}$-V_{Exp}) yielded by CPPC-SAFT EOS for *n*-butane and the volume translations calculated by **Eq. 3-3** at different reduced temperatures.

3.4.2 Pressure-density Two-phase Envelope

Fig. 3-7 shows the comparison between the experimental pressure-density two-phase envelope and those calculated by different PC-SAFT EOSs for *n*-butane. As shown in **Fig. 3-7**, the pressure-density two-phase envelope calculated by the proposed volume-translated rescaled PC-SAFT EOS (VTR-PC-SAFT EOS) generally has a better match with the experimental data than those calculated by the original PC-SAFT EOS or CPPC-SAFT EOS. Although the issue of an overestimation of critical temperature and critical pressure with the original PC-SAFT EOS has been addressed by CPPC-SAFT EOS (Anoune *et al.*, 2021), the critical density calculated by CPPC-SAFT deviates much from the experimental one. In comparison, the critical density yielded by the VTR-PC-SAFT EOS can exactly reproduce the experimental one. **Table 3-2** and **Appendix 3-A.3** present the detailed errors yielded by different PC-SAFT EOSs in the non-critical and critical properties of 39 individual compounds. **Table 3-3** presents the overall errors. As seen from

Table 3-2 and **Appendix 3-A.3**, the VTR-PC-SAFT EOS can exactly reproduce critical temperature, critical pressure, and critical molar volume, whereas the other three PC-SAFT-type EOSs yield relatively large errors in reproducing these critical properties. Such large deviations can lead to an inaccurate density prediction at near-critical conditions (See **Fig. 3-1**). In addition, the VTR-PC-SAFT EOS developed in this work leads to much lower errors in reproducing saturated-density, single-liquid density, and saturation pressure than the original PC-SAFT EOS, CPPC-SAFT EOS, and I-PC-SAFT EOS.

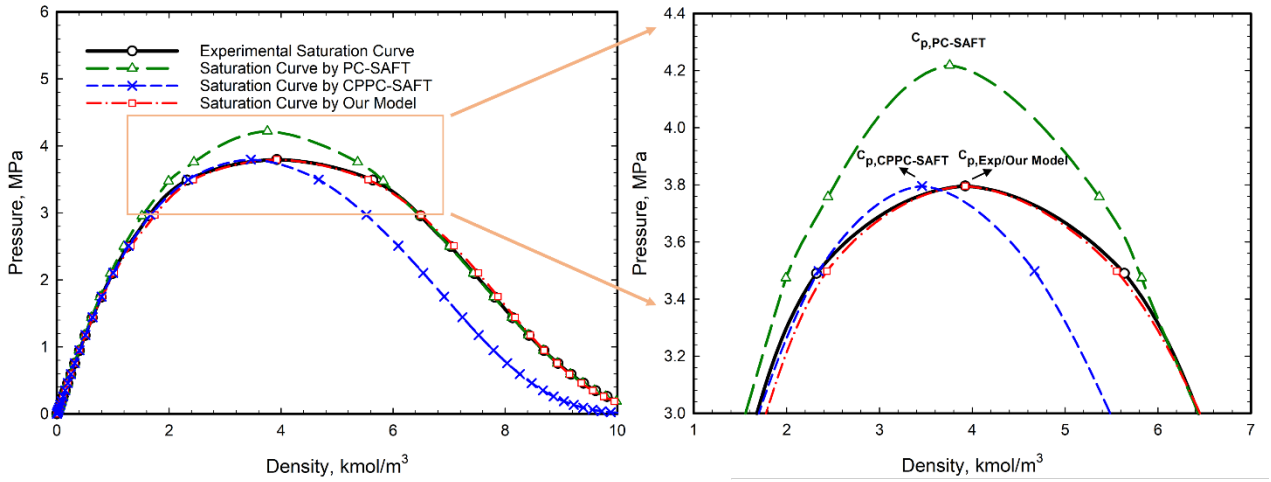

Fig. 3-7. Comparison between the experimental pressure-density two-phase envelope for *n*-butane and those calculated by different PC-SAFT EOSs.

Table 3-2. %AADs in non-critical property predictions (i.e., saturated-liquid molar volume, liquid molar volume, and vapor pressure) and %ADs in critical property predictions (i.e., critical temperature, critical pressure, and critical molar volume) yielded by the VTR-PC-SAFT EOS for 39 individual compounds.

Components	VTR-PC-SAFT EOS (this work)					
	%AAD in V_{SatL}	%AAD in V_{Liq}	%AAD in P_{Sat}	%AD in T_c	%AD in P_c	%AD in V_c
Carbon dioxide	0.368	0.324	0.276	0	0	0
Sulfur dioxide	0.258	0.218	0.412	0	0	0
Carbon monoxide	0.217	0.226	0.362	0	0	0
Carbonyl sulfide	0.216	0.231	0.386	0	0	0
Nitrogen	0.559	0.487	0.431	0	0	0
Methane	0.372	0.363	0.560	0	0	0
Ethane	0.409	0.397	1.042	0	0	0
Propane	0.537	0.431	0.731	0	0	0

Butane	0.614	0.560	0.782	0	0	0
Pentane	0.703	0.652	0.432	0	0	0
Hexane	0.691	0.673	0.412	0	0	0
Heptane	0.764	0.718	0.813	0	0	0
Octane	0.784	0.722	0.926	0	0	0
Nonane	0.674	0.563	1.421	0	0	0
Decane	0.807	0.738	1.762	0	0	0
Dodecane	0.940	0.782	1.903	0	0	0
Toluene	0.822	0.803	0.242	0	0	0
Benzene	0.379	0.345	0.725	0	0	0
Propylene	0.571	0.523	0.418	0	0	0
Isopentane	0.697	0.627	0.462	0	0	0
Cyclohexane	0.304	0.325	0.846	0	0	0
Cyclopropane	0.294	0.291	0.825	0	0	0
Isobutane	0.705	0.657	0.218	0	0	0
Ethylene	0.168	0.191	0.316	0	0	0
Neopentane	0.385	0.377	0.342	0	0	0
R11	0.460	0.472	0.192	0	0	0
R12	0.459	0.413	0.214	0	0	0
R21	0.278	0.265	0.672	0	0	0
R22	0.220	0.213	0.346	0	0	0
R23	0.326	0.321	1.012	0	0	0
R32	1.087	0.972	1.725	0	0	0
R114	0.463	0.413	0.423	0	0	0
R115	0.310	0.289	0.315	0	0	0
R123	0.533	0.512	0.782	0	0	0
R124	0.701	0.587	0.920	0	0	0
R125	0.740	0.671	0.989	0	0	0
R134a	0.370	0.375	0.762	0	0	0
R141b	0.315	0.326	0.788	0	0	0
R142b	0.395	0.369	0.296	0	0	0

3.4.3 Performance Evaluation

3.4.3.1 Prediction Accuracy of Saturated-liquid Density

Fig. 3-8 compares the saturated-liquid density (retrieved from NIST database (Domalski *et al.*, 2015)) against those calculated by different PC-SAFT EOSs for *n*-butane. It can be clearly observed that, our model can provide the most accurate saturated-liquid density estimates. In addition, the prediction of saturated-liquid density especially near the critical point is significantly improved with our proposed model. As seen from **Table 3-2**

and **Appendix 3-A.3**, the %AAD of only 0.614 is yielded by our model for *n*-butane, while the %AADs yielded by the other three models (i.e., PC-SAFT EOS, CPPC-SAFT EOS, and I-PC-SAFT) are much higher (i.e., 1.317, 13.172, and 3.592, respectively). The temperature range considered in the evaluation of saturated-liquid density is from triple point temperature to critical temperature with a step of 4K.

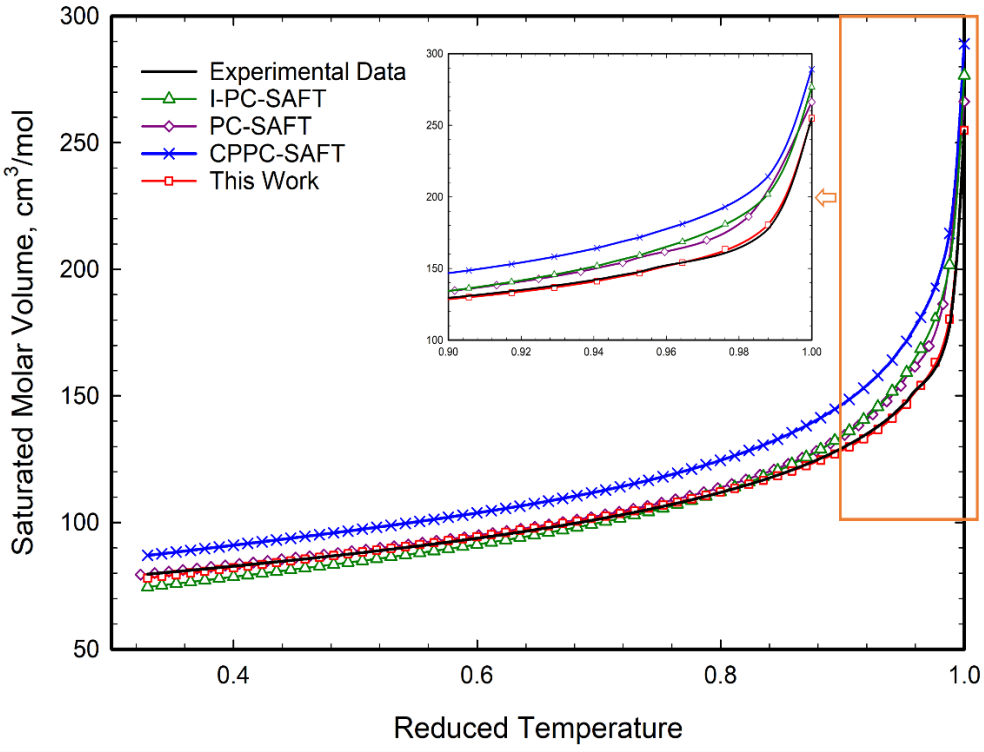

Fig. 3-8. Comparison between the experimental saturated-liquid molar volume (Domalski *et al.*, 2015) of *n*-butane and those calculated by different PC-SAFT EOSs.

3.4.3.2 Prediction Accuracy of Liquid Density

Besides the improvement in the prediction accuracy of saturated-liquid density as well as critical properties with the proposed VTR-PC-SAFT EOS, its performance in predicting liquid-density can also be notably enhanced over a wide range of temperature and pressure. **Fig. 3-9** compares the experimental liquid molar volume against that

calculated with different PC-SAFT EOSs at constant pressures of $0.5P_c$, $1P_c$, $1.5P_c$, $2P_c$, $5P_c$, and $10P_c$ for *n*-butane. As depicted in **Fig. 3-9**, overall, the liquid molar volume calculated by our model exhibits the best match with the experimental data. **Table 3-2** and **Appendix 3-A.3** present the detailed errors yielded by different PC-SAFT EOSs in reproducing the liquid molar volume of 39 individual compounds. The temperature range considered in the evaluation of liquid density is from triple point temperature to critical temperature with a step size of 4K, while the pressure range considered in the evaluation is from $0.25P_c$ to $10P_c$ with a step size of $0.25P_c$. The evaluation results show that the newly developed model yields the smallest %AAD of 0.560 in predicting the liquid molar volume for *n*-butane, whereas PC-SAFT EOS, CPPC-SAFT EOS, and I-PC-SAFT yield %AADs of 0.896, 11.663, and 2.989, respectively. In conclusion, a constant or temperature-dependent volume translation, to some extent, could provide a relatively good representation of liquid density when the reduced temperature is low. But their performance deteriorates as temperature approaches critical temperature. The distance-function-based volume translation strategy provides much more accurate liquid density prediction over a wide range of temperature and pressure.

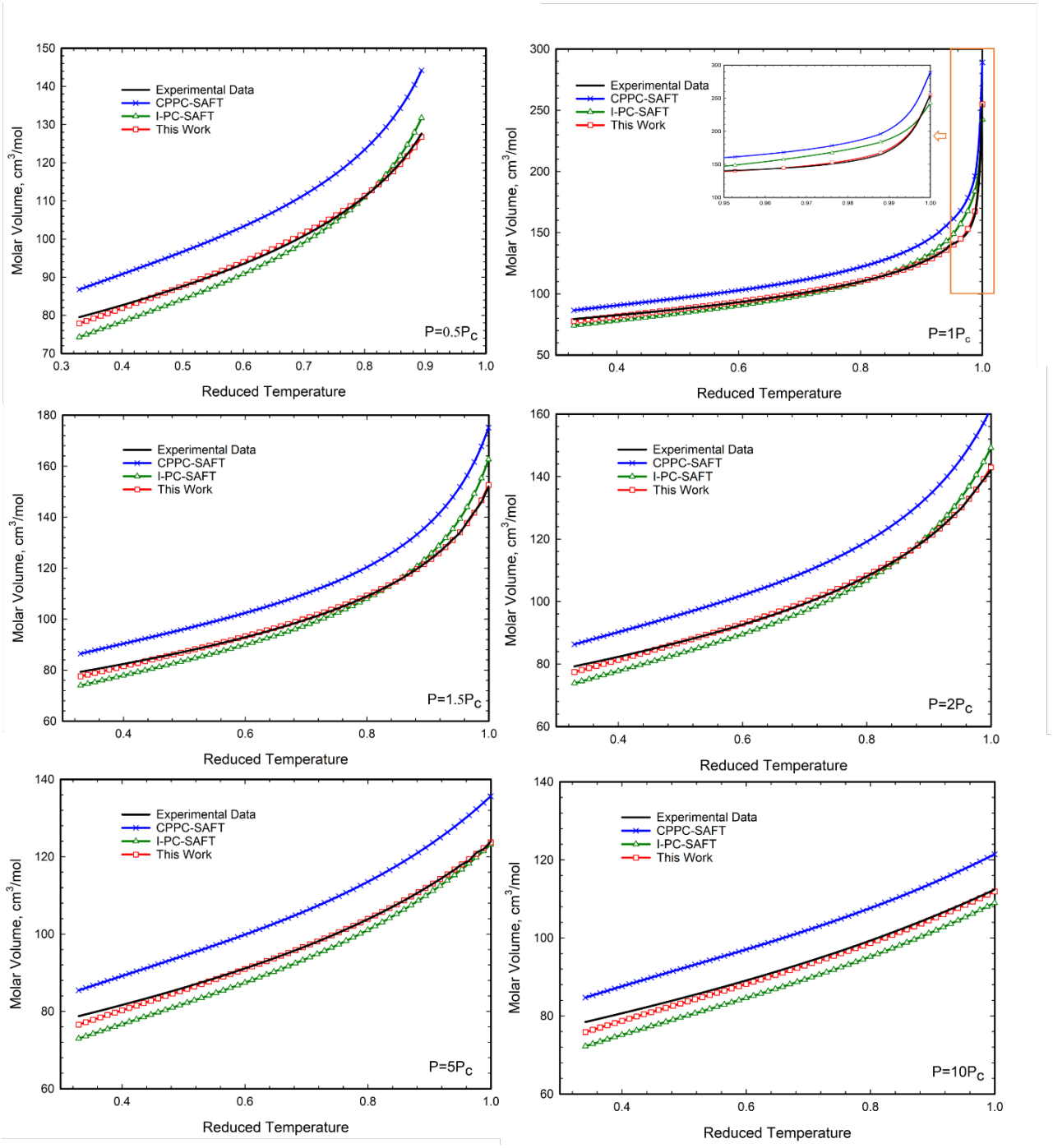

Fig. 3-9. Comparison between the experimental liquid molar volume (Domalski *et al.*, 2015) for *n*-butane and that calculated by different PC-SAFT EOSs at constant pressures of $0.5P_c$, $1P_c$, $1.5P_c$, $2P_c$, $5P_c$, and $10P_c$.

3.4.3.3 Prediction Accuracy of Vapor Pressure

Introducing a constant or temperature-dependent volume translation into an EOS does not alter the vapor pressure prediction (Peneloux *et al.*, 1982; Shi and Li, 2022). However, the distance-function-based volume translation used in CEOS could slightly alter the calculated vapor-pressure values (Frey *et al.*, 2009; Shi *et al.*, 2018). This is also applicable to the distance-function-based volume translation model developed in this study. **Fig. 3-10** compares the vapor-pressure curve of *n*-butane calculated by different PC-SAFT EOSs against the experimental vapor pressure from the NIST database (Domalski *et al.*, 2015). It indicates that the vapor-pressure curves predicted by our model, CPPC-SAFT EOS, and I-PC-SAFT EOS are almost identical and exhibit perfect match with the experimental vapor-pressure curve. **Table 3-2** and **Appendix 3-A.3** present the detailed errors yielded by different PC-SAFT EOSs in reproducing the vapor pressure of 39 individual compounds. The temperature range considered in the evaluation of vapor pressure is from triple point temperature to critical temperature with a step of 4K. It is obvious that the distance-function-based volume translation model in CPPC-SAFT EOS leads to negligible impact on the vapor-pressure predictions.

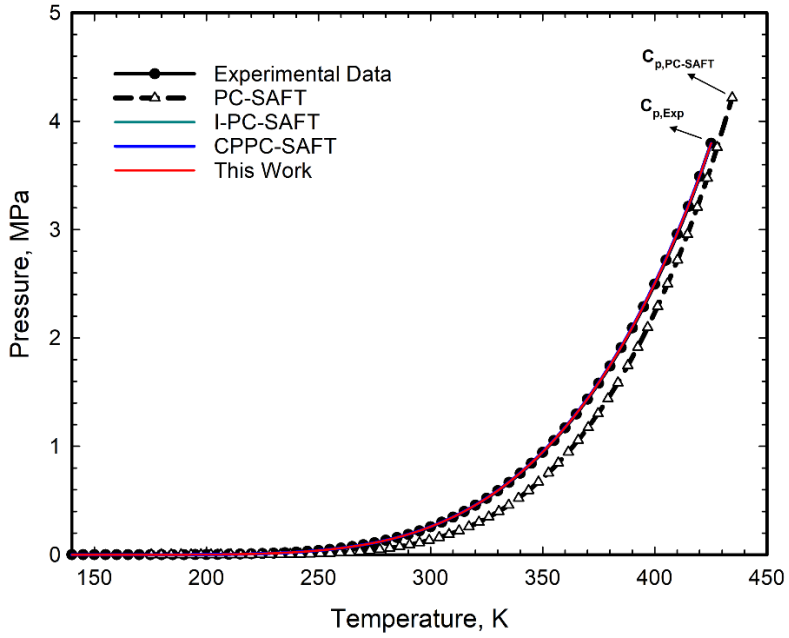

Fig. 3-10. Comparison between the experimental vapor-pressure values (Domalski *et al.*, 2015) of *n*-butane and those calculated by different PC-SAFT EOSs.

3.4.3.4 Overall Prediction Accuracy

Fig. 3-11 compares the two-phase envelope and pressure-density isotherms ($0.8T_c$, $0.85T_c$, $0.9T_c$, $0.98T_c$, $1T_c$, $1.02T_c$, $1.1T_c$, $1.2T_c$, and $1.3T_c$) of *n*-butane retrieved from NIST database (Domalski *et al.*, 2015) against those calculated by the VTR-PC-SAFT EOS model. **Fig. 3-11** proves that the proposed VTR-PC-SAFT EOS can generally well capture the phase behavior of *n*-butane both near and far from the critical region. Similar results have been obtained for the remaining 38 compounds. **Table 3-3** presents the overall %AADs in non-critical property predictions and %ADs in critical property predictions yielded by different PC-SAFT EOSs for the selected 39 compounds. Specifically, among all the models examined in this study, the VTR-PC-SAFT EOS yields the smallest %AADs of 0.505, 0.470, and 0.676 in reproducing saturated-liquid molar volume, liquid molar volume, and vapor pressure. Compared with the other PC-SAFT

EOSs, the VTR-PC-SAFT EOS leads to much more accurate reproduction of saturated-liquid molar volume and liquid molar volume, while it only yields a slightly higher accuracy in reproducing vapor pressure. In terms of critical property predictions, the VTR-PC-SAFT EOS can exactly reproduce the critical temperature, critical pressure, and critical molar volume, leading to a more accurate description of the phase behavior of pure compounds in the vicinity of critical point, as demonstrated in **Fig. 3-7** and **Fig. 3-11**. It is again worthwhile noting that, although the CPPC-SAFT EOS and I-PC-SAFT EOS can reproduce the critical temperature and critical pressure, they cannot reproduce the critical volume.

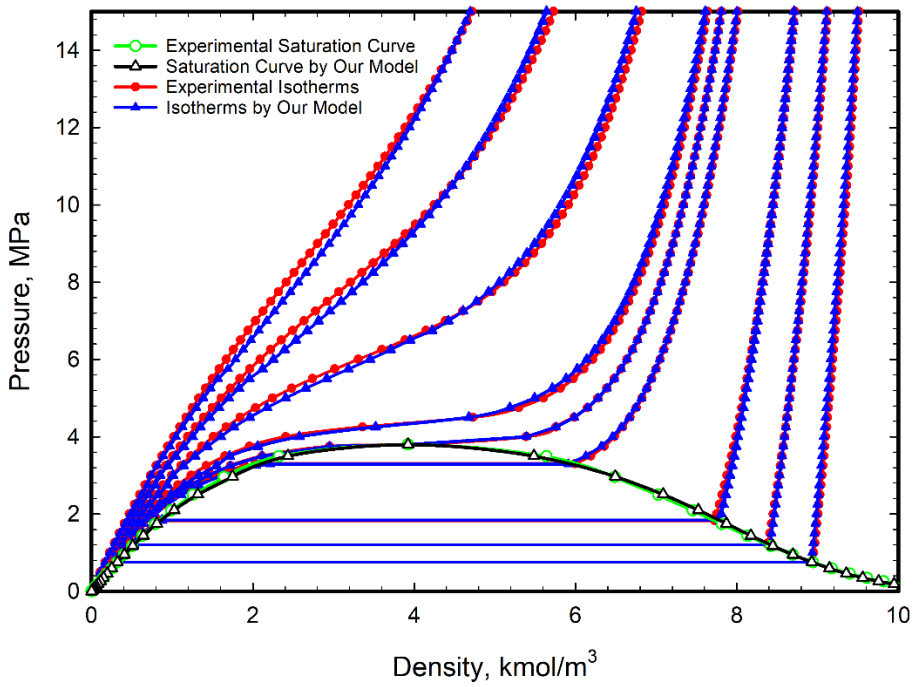

Fig. 3-11. Comparison of the experimental two-phase envelope and pressure-density isotherms ($0.8T_c$, $0.85T_c$, $0.9T_c$, $0.98T_c$, $1T_c$, $1.02T_c$, $1.1T_c$, $1.2T_c$, and $1.3T_c$) of *n*-butane retrieved from the NIST database (Domalski *et al.*, 2015) against those calculated by the VTR-PC-SAFT EOS.

Table 3-3. Overall %AADs in non-critical property predictions (i.e., saturated-liquid molar volume, liquid molar volume, and vapor pressure) and %ADs in critical property

predictions (i.e., critical temperature, critical pressure, and critical molar volume) yielded by different PC-SAFT EOSs for 39 individual compounds.

	PC-SAFT	CPPC-SAFT	I-PC-SAFT	VTR-PC-SAFT EOS (This work)
Overall %AAD in V_{SatL}	1.856	13.896	4.170	0.505
Overall %AAD in V_{Liq}	1.444	12.801	3.591	0.470
Overall %AAD in P_{Sat}	1.493	0.712	0.726	0.676
Overall %AD in T_c	1.790	0	0	0
Overall %AD in P_c	12.632	0	0	0
Overall %AD in V_c	4.408	15.075	10.771	0

Although the VTR-PC-SAFT EOS proposed in our work provides the smallest %AADs in non-critical property predictions (i.e., saturated-liquid molar volume, liquid molar volume, and vapor pressure), as well as the smallest %ADs in critical property predictions (i.e., critical temperature, critical pressure, and critical molar volume), further evaluation is needed to determine the reliability of the proposed VTR-PC-SAFT EOS in predicting derivative properties in future research.

3.4.4 Generalized Volume Translation Model for n-Alkanes

In addition to pure components (such as CH_4), crude oils produced from underground reservoirs also contain uncharacterized components (Kumar and Okuno, 2015, 2016; Venkatramani and Okuno, 2015; Zhao *et al.*, 2022). It is thus necessary to generalize the model parameters in the VTR-PC-SAFT EOS (i.e., m, σ, ε/k, c_1 and c_2) in order to make it applicable to the phase behavior prediction of uncharacterized components. We have learned from multiple trials that we could develop accurate correlations of the volume translation parameters only for *n*-alkanes (excluding CH_4). Some researchers

(Anoune *et al.*, 2021; Moine *et al.*, 2019), very recently, proposed correlations to determine the three PC-SAFT parameters (i.e., m, σ, ε/k) from $T_{c,\mathrm{Exp}}$, $P_{c,\mathrm{Exp}}$, and ω_{Exp}. In this work, we extend such method to generalize the five parameters in the VTR-PC-SAFT EOS (i.e., m, σ, ε/k, c_1 and c_2) for *n*-alkanes (except CH_4). **Fig. 3-12** shows the plots of m vs ω, $\sigma^3(P_c/T_c)$ vs $1/m$, and $(\varepsilon/k)/T_c$ vs $1/m$ for *n*-alkanes (except CH_4), while **Fig. 3-13** shows the plots of $c_1P_c/(T_cz_c)$ and $c_2P_c/(T_cz_c)$ vs $1/m$ for *n*-alkanes (except CH_4).

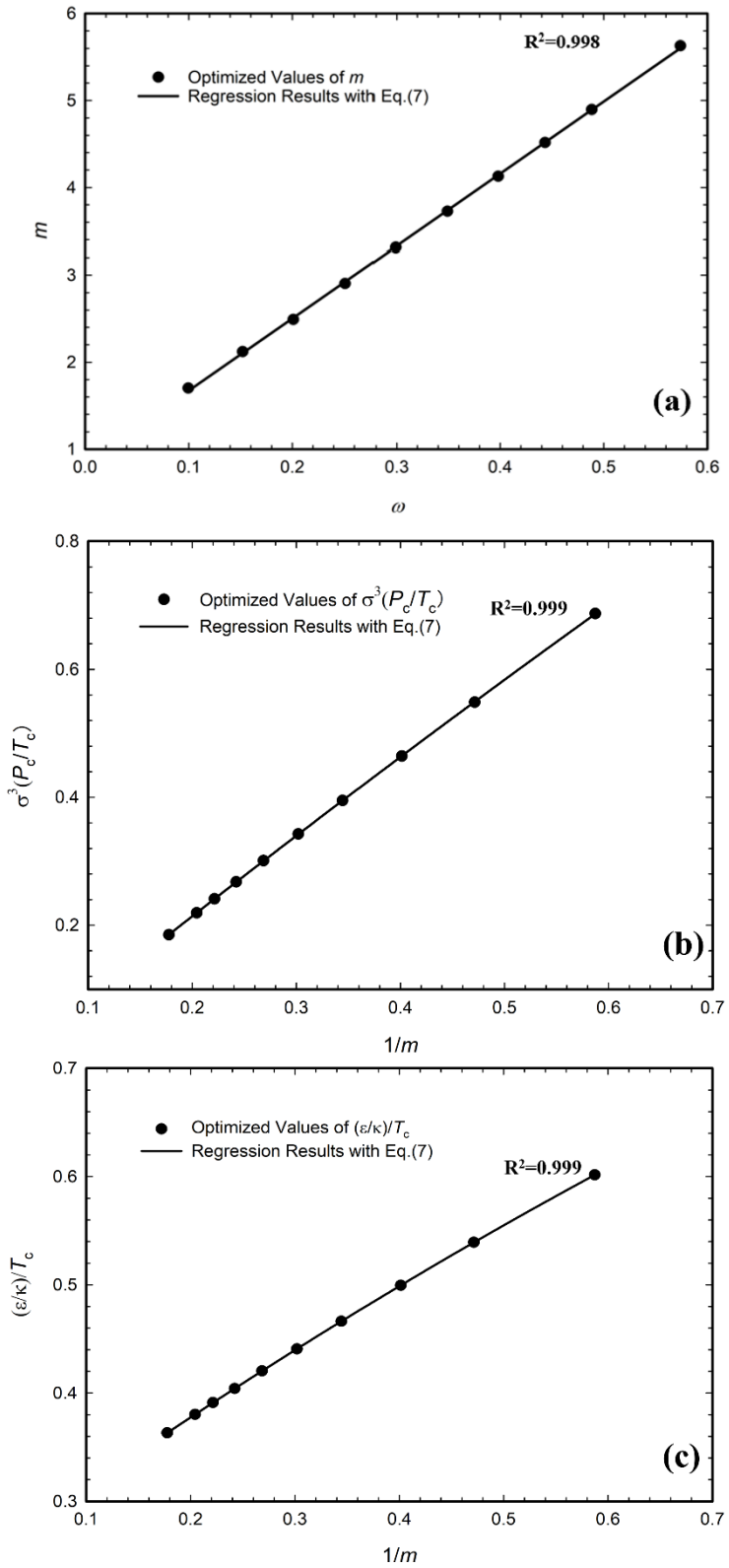

Fig. 3-12. Plots of m vs ω (a), $\sigma^3(P_c/T_c)$ vs $1/m$ (b), and $(\varepsilon/k)/T_c$ vs $1/m$ (c) for n-alkanes (except CH_4).

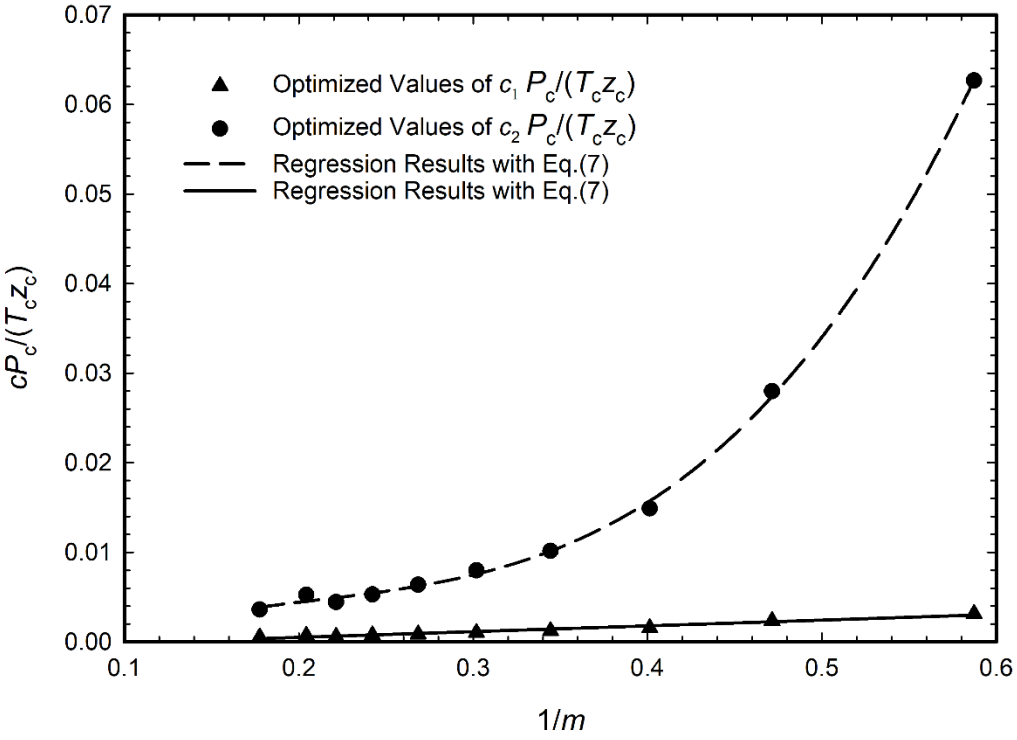

Fig. 3-13. Plots of $c_1P_c/(T_cz_c)$ and $c_2P_c/(T_cz_c)$ vs $1/m$ for *n*-alkanes (except CH_4).

By regressing the data shown in **Fig. 3-12** and **Fig. 3-13**, we obtain the following generalized correlations of the model parameters in the VTR-PC-SAFT EOS for *n*-alkanes (excluding CH_4):

$$\begin{cases} m = 8.286346\omega + 0.845451 \\ \sigma = \dfrac{T_c^{1/3}}{P_c^{1/3}}\left[-0.132356\left(\dfrac{1}{m}\right)^2 + 1.324604\dfrac{1}{m} - 0.045624\right]^{1/3} \\ \dfrac{\varepsilon}{k} = T_c\left[-0.148500\left(\dfrac{1}{m}\right)^2 + 0.695444\dfrac{1}{m} + 0.244382\right] \\ c_1 = \dfrac{T_c z_c}{P_c}\left(0.006434\dfrac{1}{m} - 0.000787\right) \\ c_2 = \dfrac{T_c z_c}{P_c}\left[0.889212\left(\dfrac{1}{m}\right)^3 - 0.549030\left(\dfrac{1}{m}\right)^2 + 0.136142\dfrac{1}{m} - 0.007954\right] \end{cases} \tag{3-7}$$

Note that, for uncharacterized components, the four properties (i.e., ω, T_c, P_c, and z_c) can be estimated with some empirical correlations.

3.4.5 Thermodynamic Consistency

Thermodynamic inconsistency (such as the crossing of pressure-volume isotherms) could appear in the development of volume-translated PC-SAFT EOSs (Kalikhman *et al.*, 2010; Polishuk, 2010, 2011; Shi and Li, 2022; Sun *et al.*, 2020; Yelash *et al.*, 2005). The crossing of pressure-volume isotherms for a pure compound may result in several numerical problems such as negative heat capacities and negative isobaric thermal expansivity (Kalikhman *et al.*, 2010; Polishuk, 2010; Yelash *et al.*, 2005). Such inconsistency could lead to anomalous prediction of multiphase equilibria, thus restricting the application scope of applications of the volume-translated PC-SAFT EOSs. In this work, we apply the criterion proposed by Shi and Li (2016) to judge if the VTR-PC-SAFT EOS leads to the crossing of pressure-volume isotherms. As stated by Shi and Li (2016), the first derivative of molar volume with respect to temperature calculated by the volume-translated PC-SAFT EOSs should be always positive if no crossing of isotherms occurs in the pressure-volume diagram,

$$D = \left(\frac{\partial V_{\text{Corrected}}}{\partial T}\right)_P = \left[\frac{\partial\left(V_{\text{CPPC-SAFT}} - c\right)}{\partial T}\right]_P = \left(\frac{\partial V_{\text{CPPC-SAFT}}}{\partial T}\right)_P - \left(\frac{\partial c}{\partial T}\right)_P > 0 \tag{3-8}$$

where D is the first derivative of corrected molar volume with respect to temperature, while $V_{\text{Corrected}}$ is the corrected molar volume by our proposed volume-translated PC-SAFT EOS. The first derivative of the volume translation term with respect to temperature, i.e., $\left(\frac{\partial c}{\partial T}\right)_P$, can be evaluated by,

$$\left(\frac{\partial c}{\partial T}\right)_p = \frac{c_1\left(1+c_2\gamma\right)-c_2}{\left(1+c_2\gamma\right)^2}\delta_c\left(\frac{\partial \gamma}{\partial T}\right)_p \exp\left(c_1\gamma\right) \tag{3-9}$$

where

$$\left(\frac{\partial \gamma}{\partial T}\right)_p = -\frac{R}{P_c}\left(\frac{\partial T}{\partial V}\right)_p^2\left(\frac{\partial^2 V}{\partial T^2}\right)_p \tag{3-10}$$

Here, we use **Eq. 3-8** to judge if the crossing of isotherms exists in the pressure-volume diagram for *n*-butane. The pressure range and temperature range considered in the evaluation are from 0 to $100P_c$ (379.6MPa) and from $0.317T_c$ (triple point temperature) to $5T_c$ (2125.625K), respectively. **Fig. 3-14** shows the relationship between the values of D and reduced temperature at $100P_c$ (379.6 MPa). As depicted in **Fig. 3-14**, at an isobaric pressure of $100P_c$, the values of D are always positive. Thus, it can be concluded that there is no crossing of pressure-volume isotherms at pressures equal to or below $100P_c$ for *n*-butane. Similarly, all the other compounds listed in **Table 3-1** are evaluated with such a thermodynamic consistency criterion, and no crossing of pressure-volume isotherms is detected at pressures equal to or below $100P_c$. Therefore, it can be concluded that the VTR-PC-SAFT EOS model developed in this work can be safely applied to describe the phase behavior of the selected 39 compounds over a wide range of temperature and pressure.

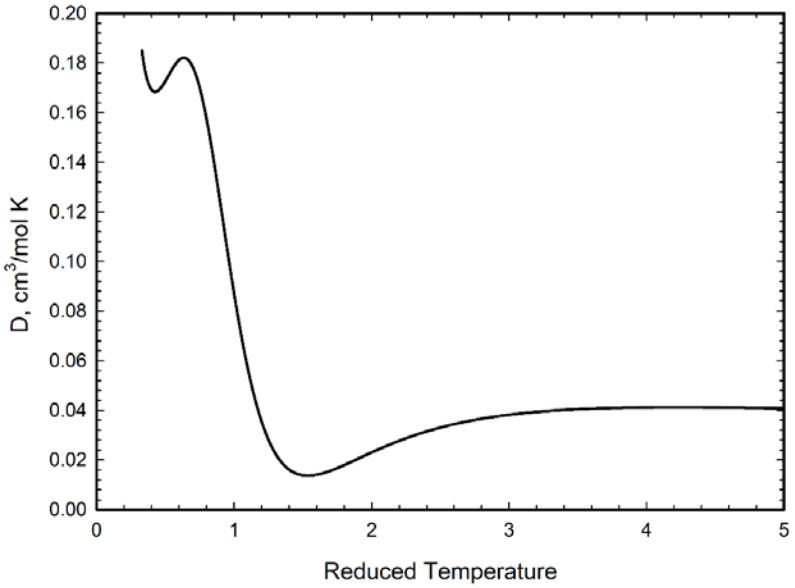

Fig. 3-14. Relationship between the first derivative of corrected molar volume with respect to temperature (D) and reduced temperature yielded by the VTR-PC-SAFT EOS for *n*-butane at $100P_c$ (379.6MPa).

3.5 Conclusion

We develop a volume translation model for CPPC-SAFT EOS based on a newly proposed distance-function. With the exact reproductions of critical temperature, critical pressure, and critical molar volume, the proposed model can well capture the phase behavior of pure compounds in the vicinity of the critical point. In addition, the proposed volume-translated rescaled-PC-SAFT EOS (VTR-PC-SAFT EOS) leads to significantly better predictions of thermodynamic properties of pure compounds both near and far from the critical region. Consequently, among all the PC-SAFT EOSs examined in this study, the proposed VTR-PC-SAFT EOS provides the smallest %AADs of 0.505, 0.470, and 0.676, respectively, in reproducing the saturated-liquid molar volume, liquid molar volume, and vapor pressure of 39 pure compounds. Furthermore, a generalized version of the VTR-PC-SAFT proposed in this work is developed for *n*-alkanes (except CH_4). Last but not least,

a thermodynamic consistency criterion, previously proposed by Shi and Li (2016), is applied to detect the potential crossing of pressure-volume isotherms that are calculated by the VTR-PC-SAFT EOS. The evaluation results show that the proposed VTR-PC-SAFT EOS does not lead to the crossover of pressure-volume isotherms at pressures up to $100P_c$ for the 39 compounds examined in this study.

References

A. Bymaster, C. Emborsky, A. Dominik, W.G. Chapman, Renormalization-group corrections to a perturbed-chain statistical associating fluid theory for pure fluids near to and far from the critical region, *Industrial & Engineering Chemistry Research* 47 (2008) 6264−6274.

A. Kumar, R. Okuno, A new algorithm for multiphase-fluid characterization for solvent injection, *SPE Journal* 21 (2016) 1688-1704.

A. Kumar, R. Okuno, Direct perturbation of the Peng–Robinson attraction and covolume parameters for reservoir fluid characterization, *Chemical Engineering Science* 127 (2015) 293-309.

A. Pakravesh, F. Zarei, H. Zarei, PρT parameterization of SAFT equation of state: developing a new parameterization method for equations of state, *Fluid Phase Equilibria* 538 (2021) 113024.

A. Peneloux, E. Rauzy, R. Freze, A consistent correction for Redlich-Kwong-Soave volumes, *Fluid Phase Equilibria* 8 (1982) 7-23.

A. Saeed, G. Sattar, Calculation of density, vapor pressure and heat capacity near the critical point by incorporating cubic SRK EoS and crossover translation, *Fluid Phase Equilibria* 493 (2019) 10-25.

A.F. Young, F.L.P. Pessoa, V.R.R Ahón, Comparison of volume translation and co-volume functions applied in the Peng-Robinson EoS for volumetric corrections, *Fluid Phase Equilibria* 435 (2017) 73-87.

A.I. Papadopoulos, F.A. Perdomo, F. Tzirakis, G. Shavalieva, I. Tsivintzelis, P. Kazepidis, E. Nessi, S. Papadokonstantakis, P. Seferlis, A. Galindo, G. Jackson, C.S. Adjiman, Molecular engineering of sustainable phase-change solvents: from digital design to scaling-up for CO2 capture, *Chemical Engineering Journal* 420 (2021) 127624.

A.K. Wyczalkowska, J.V. Sengers, M.A. Anisimov, Critical fluctuations and the equation of state of van der Waals, *Physica A: Statistical Mechanics and its Applications* 334 (2004) 482-512.

A.M. Abudour, S.A. Mohammad, R.L. Robinson, K.A.M. Gasem, Volume-translated Peng-Robinson equation of state for saturated and single-phase liquid densities, *Fluid Phase Equilibria* 335 (2012) 74-87.

A.M. Palma, A.J. Queimada, J.A. Coutinho, Using a volume shift in perturbed-chain statistical associating fluid theory to improve the description of speed of sound and other derivative properties, *Industrial & Engineering Chemistry Research* 57 (2018) 11804-11814.

A.V. Venkatramani, R. Okuno, Characterization of water-containing reservoir oil using an EOS for steam injection processes, *Journal of Natural Gas Science and Engineering* 26 (2015) 1091-106.

D.V. Nichita, F. García-Sánchez, and S. Gómez, Phase stability analysis using the PC-SAFT equation of state and the tunneling global optimization method, *Chemical Engineering Journal* 140 (2008) 509-520.

D.Y. Peng, D.B. Robinson, A new two-constant equation of state, *Industrial & Engineering Chemistry Fundamentals* 15 (1976) 59-64.

E. Moine, A. Piña-Martinez, J.N. Jaubert, B. Sirjean, R. Privat, I-PC-SAFT: an industrialized version of the volume-translated PC-SAFT equation of state for pure components, resulting from experience acquired all through the years on the parameterization of Saft-type and cubic models, *Industrial & Engineering Chemistry Research* 58 (2019) 20815-20827.

E.A. Müller, K.E. Gubbins, Molecular-based equations of state for associating fluids: A review of SAFT and related approaches, *Industrial & Engineering Chemistry Research* 40 (2001) 2193-2211.

F. Llovell, C.J. Peters, L.F. Vega, Second-order thermodynamic derivative properties of selected mixtures by the soft-SAFT equation of state, *Fluid Phase Equilibria* 248 (2006) 115-122.

F. Llovell, J.C. Pàmies, L.F. Vega, Thermodynamic properties of Lennard-Jones chain molecules: Renormalization-group corrections to a modified statistical associating fluid theory, *The Journal of Chemical Physics* 121 (2004) 10715-10724.

F. Llovell, L.F. Vega, Global fluid phase equilibria and critical phenomena of selected mixtures using the crossover soft-SAFT equation, *The Journal of Physical Chemistry B* 110 (2006) 1350-1362.

F. Llovell, L.F. Vega, Prediction of thermodynamic derivative properties of pure fluids through the soft-SAFT equation of state, *The Journal of Physical Chemistry B* 110 (2006) 11427-11437.

G. Soave, Equilibrium constants from a modified Redlich–Kwong equation of state, *Chemical Engineering Science* 27 (1972) 1197-1203.

G.F. Chou, J.M. Prausnitz, A phenomenological correction to an equation of state for the critical region, *AIChE Journal* 35 (1989) 1487-1496.

G.M. Kontogeorgis, X. Liang, A. Alay, T. Ioannis, Equations of state in three centuries. Are we closer to arriving to a single model for all applications? *Chemical Engineering Science: X* 7 (2020) 100060.

H. Zhao, C. Song, H. Zhang, C. Di, Z. Tian, Improved fluid characterization and phase behavior approaches for gas flooding and application on Tahe light crude oil system, *Journal of Petroleum Science and Engineering* 208 (2022) 109653.

I. Anoune, Z. Mimoune, H. Madani, A. Merzougui, New modified PC-SAFT pure component parameters for accurate VLE and critical phenomena description, *Fluid Phase Equilibria* 532 (2021) 112916.

I. Polishuk I, A. Chiko, E. Cea-Klapp, J.M. Garrido, Implementation of CP-PC-SAFT and CS-SAFT-VR-Mie for predicting thermodynamic properties of C1–C3 halocarbon systems. I. Pure compounds and mixtures with non-associating compounds, *Industrial & Engineering Chemistry Research* 60 (2021) 9624-9636.

I. Polishuk, About the numerical pitfalls characteristic for SAFT EOS models, *Fluid Phase Equilibria* 298 (2010) 67-74.

I. Polishuk, Addressing the issue of numerical pitfalls characteristic for SAFT EOS models, *Fluid Phase Equilibria* 301 (2011) 123-129.

I. Polishuk, H. Lubarsky, D. NguyenHuynh, Predicting phase behavior in aqueous systems without fitting binary parameters II: Gases and non-aromatic hydrocarbons, *AIChE Journal* 63 (2017) 5064-5075.

I. Polishuk, Hybridizing SAFT and cubic EOS: what can be achieved? *Industrial & Engineering Chemistry Research* 50 (2011) 4183-4198.

I. Polishuk, Standardized critical point-based numerical solution of statistical association fluid theory parameters: the perturbed chain-statistical association fluid theory equation of state revisited, *Industrial & Engineering Chemistry Research* 53 (2014) 14127-14141.

I. Polishuk, Y. Sidik, D. NguyenHuynh, Predicting phase behavior in aqueous systems without fitting binary parameters I: CP-PC-SAFT EOS, Aromatic Compounds, *AIChE Journal* 63 (2017) 4124-4135.

J. Gross, G. Sadowski, Perturbed-chain SAFT: An equation of state based on a perturbation theory for chain molecules, *Industrial & Engineering Chemistry Research* 40 (2001) 1244−1260.

J. Shi, H. Li, Modified temperature-dependent volume translation model in PC-SAFT equation of state for carbon dioxide, *Chemical Engineering Science* 263 (2022) 118107.

J. Shi, H.A. Li, Criterion for determining crossover phenomenon in volume-translated equation of states, *Fluid Phase Equilibria* 430 (2016) 1-12.

J. Shi, H.A. Li, W. Pang, An improved volume translation strategy for PR EOS without crossover issue, *Fluid Phase Equilibria* 470 (2018) 164-175.

J. Wang, M.A. Anisimov, Nature of vapor-liquid asymmetry in fluid criticality, *Physical Review E* 75 (2007) 051107.

J.A. White, Contribution of fluctuations to thermal properties of fluids with attractive forces of limited range: theory compared with PρT and Cv data for argon, *Fluid Phase Equilibria* 75 (1992) 53−64.

J.A. White, S. Zhang, Renormalization group theory for fluids, *The Journal of Chemical Physics* 99 (1993) 2012−2019.

J.A. White, S. Zhang, Renormalization theory of nonuniversal thermal properties of fluids, *The Journal of Chemical Physics* 103 (1995) 1922−1928.

J.J. Martin, Cubic equations of state-which? *Industrial & Engineering Chemistry Fundamentals* 18 (1979) 81-97.

J.M.L. Sengers, Mean-field theories, their weaknesses and strength, *Fluid Phase Equilibria* 158 (1999) 3-17.

J.Y. Seyf, M. Asgari, Parametrization of PC-SAFT EoS for solvents reviewed for use in pharmaceutical process design: VLE, LLE, VLLE, and SLE study, *Industrial & Engineering Chemistry Research* 61 (2022) 8252–8268.

K. Frey, M. Modell, J. Tester, Density-and-temperature-dependent volume translation for the SRK EOS: 1. Pure fluids, *Fluid Phase Equilibria* 279 (2009) 56-63.

K.G. Wilson, M.E. Fisher, Critical exponents in 3.99 dimensions, *Physical Review Letters* 28 (1972) 240-243.

K.G. Wilson, Renormalization group and critical phenomena. II. Phase-space cell analysis of critical behavior, *Physical Review B* 4 (1971) 3184-3205.

K.G. Wilson, The renormalization group: Critical phenomena and the Kondo problem, *Reviews of Modern Physics* 47 (1975) 773.

L. Yelash, M. Müller, W. Paul, K. Binder, Artificial multiple criticality and phase equilibria: an investigation of the PC-SAFT approach, *Physical Chemistry Chemical Physics* 7 (2005) 3728-3732.

L.W. Salvino, J.A. White, Calculation of density fluctuation contributions to thermodynamic properties of simple fluids, *The Journal of Chemical Physics* 96 (1992) 4559−4568.

M. Cismondi, E.A. Brignole, J. Mollerup, Rescaling of three-parameter equations of state: PC-SAFT and SPHCT, *Fluid Phase Equilibria* 234 (2005) 108-121.

M. Yang, T. Zhan, Y. Su, A. Dong, M. He, Y. Zhang, Crossover PC-SAFT equations of state based on White's method for the thermodynamic properties of CO2, n-alkanes and n-alkanols, *Fluid Phase Equilibria* 564 (2023) 113610.

M.A. Anisimov, J. Wang, Nature of asymmetry in fluid criticality, *Physical Review Letters* 97 (2006) 025703.

M.S. Wertheim, Fluids with highly directional attractive forces. I. Statistical thermodynamics, *Journal of Statistical Physics* 35 (1984) 19-34.

M.S. Wertheim, Fluids with highly directional attractive forces. II. Thermodynamic perturbation theory and integral equations, *Journal of Statistical Physics* 35 (1984) 35-47.

M.S. Wertheim, Fluids with highly directional attractive forces. III. Multiple attraction sites, *Journal of Statistical Physics* 42 (1986) 459-476.

M.S. Wertheim, Fluids with highly directional attractive forces. IV. Equilibrium polymerization, *Journal of Statistical Physics* 42 (1986) 477-492.

O. Pfohl, T. Giese, R. Dohrn, G. Brunner, 1. Comparison of 12 equations of state with respect to gas-extraction processes: reproduction of pure-component properties when enforcing the correct critical temperature and pressure, *Industrial & Engineering Chemistry Research* 37 (1998) 2957-2965.

P. De Castro, P. Sollich, Critical phase behavior in multi-component fluid mixtures: Complete scaling analysis, *The Journal of Chemical Physics* 149 (2018) 204902.

P. Navarro, A.M. Palma, J. García, F. Rodríguez, J.A. Coutinho, P.J. Carvalho, High-pressure density of bis(1-alkyl-3-methylimidazolium) tetraisothiocyanatocobaltate ionic liquids: experimental and PC-SAFT with volume-shift modeling, *Journal of Chemical & Engineering Data* 64 (2019) 4827-4833.

P.J. Linstrom, W.G. Mallard (Eds.), NIST Chemistry WebBook, NIST Standard Reference Database Number 69, National Institute of Standards and Technology, Gaithersburg, MD, 20899, http://webbook.nist.gov.

P.N. Ghoderao, V.H. Dalvi, M. Narayan, A five-parameter cubic equation of state for pure fluids and mixtures, *Chemical Engineering Science: X* 3 (2019) 100026.

P.N. Ghoderao, V.H. Dalvi, M. Narayan, A four parameter cubic equation of state with temperature dependent covolume parameter, *Chinese Journal of Chemical Engineering* 27 (2019) 1132-1148.

P.N. Ghoderao, V.H. Dalvi, M. Narayan, A four-parameter cubic equation of state for pure compounds and mixtures, *Chemical Engineering Science* 190 (2018) 173-189.

R. Privat, E. Moine, B. Sirjean, R. Gani, J.N. Jaubert, Application of the corresponding-state law to the parametrization of statistical associating fluid theory (SAFT)-type models: Generation and use of "generalized charts", *Industrial & Engineering Chemistry Research* 58 (2019) 9127-9139.

R. Privat, R. Gani, J.N. Jaubert, Are safe results obtained when the PC-SAFT equation of state is applied to ordinary pure chemicals? *Fluid Phase Equilibria* 295 (2010) 76-92.

S.A.M. Smith, J.T. Cripwell, C.E. Schwarz, Application of renormalization corrections to SAFT-VR Mie, *Industrial & Engineering Chemistry Research* 61 (2022) 12797-12812.

S.B. Kiselev, Cubic crossover equation of state, *Fluid Phase Equilibria* 147 (1998) 7-23.

V. Kalikhman, D. Kost, and I. Polishuk, About the physical validity of attaching the repulsive terms of analytical EOS models by temperature dependencies, *Fluid Phase Equilibria* 293 (2010) 164-167.

W. Song, L. Liu, D. Wang, Y. Li, M. Prodanović, J. Yao, Nanoscale confined multicomponent hydrocarbon thermodynamic phase behavior and multiphase transport ability in nanoporous material, *Chemical Engineering Journal* 382 (2020) 122974.

W.G. Chapman, K.E. Gubbins, G. Jackson, M. Radosz, SAFT: equation-of-state solution model for associating fluids, *Fluid Phase Equilibria* 52 (1989) 31-38.

W.R. Ji, D.A. Lempe, Density improvement of the SRK equation of state, *Fluid Phase Equilibria* 130 (1997) 49-63.

X. Chen, H. Li, An improved volume-translated SRK EOS dedicated to more accurate determination of saturated and single-phase liquid densities, *Fluid Phase Equilibria* 521 (2020) 112724.

X. Chen, H. Li, Improved prediction of saturated and single-phase liquid densities of water through volume-translated SRK EOS, *Fluid Phase Equilibria* 528 (2021) 112852.

X. Li, H. Han, D. Yang, X. Liu, J. Qin, Phase behavior of C_3H_8–CO_2–heavy oil systems in the presence of aqueous phase under reservoir conditions, *Fuel* 209 (2017) 358-370.

Y. Sun, Z. Zuo, A. Laaksonen, X. Lu, X. Ji, How to detect possible pitfalls in ePC-SAFT modelling: Extension to ionic liquids, *Fluid Phase Equilibria* 519 (2020) 112641.

Appendices of Chapter 3

3-A.1 Essential equations in PC-SAFT EOS (Gross and Sadowski, 2001; Privat *et al.*, 2010)

Table 3-A1. Essential equations in PC-SAFT EOS (Gross and Sadowski, 2001; Privat *et al.*, 2010).

Parameter	Equation	No.
Temperature-dependent segment diameter	$d_i = \sigma_i \left[1 - 0.12 \exp\left(-\frac{3\varepsilon_i}{k_B T} \right) \right]$, i=1, …, n_c (k_B is Boltzmann constant)	3-A1-1
Combining rules for a pair of unlike segments	$\begin{cases} \sigma_{ij} = \frac{1}{2}\left(\sigma_i + \sigma_j\right) \\ \frac{\varepsilon_{ij}}{k_B} = \sqrt{\frac{\varepsilon_i}{k_B} \cdot \frac{\varepsilon_j}{k_B}} \left(1 - k_{ij}\right) \end{cases}$, i, j=1, …, n_c	3-A1-2
Mixture's mean segment number	$\bar{m} = \sum_i^{n_c} x_i m_i$	3-A1-3
Expressions of coefficients a_i and b_i	$\begin{cases} a_i = a_{0i} + \frac{\bar{m}-1}{\bar{m}} a_{1i} + \frac{\bar{m}-1}{\bar{m}} \frac{\bar{m}-2}{\bar{m}} a_{2i} \\ b_i = b_{0i} + \frac{\bar{m}-1}{\bar{m}} b_{1i} + \frac{\bar{m}-1}{\bar{m}} \frac{\bar{m}-2}{\bar{m}} b_{2i} \end{cases}$, i=0, …, 6	3-A1-4
Number density of molecules	$\tilde{\rho} = \frac{6}{\pi} \eta \left(\sum_{i=1}^{n_c} x_i m_i d_i^3 \right)^{-1}$	3-A1-5
Reduced density	$\eta = \zeta_3$	3-A1-6
Definition of coefficients ζ_n	$\zeta_n = \frac{\pi}{6} \tilde{\rho} \sum_{i=1}^{n_c} x_i m_i d_i^n$, n=0, 1, 2, 3	3-A1-7
Definition of power series I_1 and I_2	$\begin{cases} I_1 = \sum_{i=0}^{6} a_i \eta^i \\ I_2 = \sum_{i=0}^{6} b_i \eta^i \end{cases}$	3-A1-8
Definition of coefficient C_1	$C_1 = \left[1 + \bar{m} \frac{8\eta - 2\eta^2}{(1-\eta)^4} + (1-\bar{m}) \frac{20\eta - 27\eta^2 + 12\eta^3 - 2\eta^4}{[(1-\eta)(2-\eta)]^2} \right]^{-1}$	3-A1-9
Molar volume (v in m^3/mol) and molar density (ρ)	$\begin{cases} v = 10^{-30} \frac{N_A}{\tilde{\rho}} \\ \rho = 1/v \end{cases}$ (N_A is Avogadro's number)	3-A1-10

The coefficient C_2	$\begin{cases} C_2 = \dfrac{\partial C_1}{\partial \eta} = -C_1^2 \cdot Q \\ Q = \bar{m}\dfrac{-4\eta^2+20\eta+8}{(1-\eta)^5} + (1-\bar{m})\dfrac{2\eta^3+12\eta^2-48\eta+40}{[(1-\eta)(2-\eta)]^3} \end{cases}$	3-A1-11
Radial distribution function of the hard-sphere fluid	$\begin{cases} g_{ij}^{hs} = \dfrac{1}{1-\zeta_3} + d_{ij}\dfrac{3\zeta_2}{(1-\zeta_3)^2} + d_{ij}^2\dfrac{2\zeta_2^2}{(1-\zeta_3)^3} \\ d_{ij} = \dfrac{d_i d_j}{d_i + d_j} \end{cases}$, i, j=1, …, n_c	3-A1-12
Dispersion contribution to the compressibility factor	$z^{disp} = -2\pi\tilde{\rho}\dfrac{\partial(\eta I_1)}{\partial\eta}\overline{m^2\varepsilon\sigma^3} - \pi\tilde{\rho}\bar{m}\left[C_1\dfrac{\partial(\eta I_2)}{\partial\eta} + C_2\eta I_2\right]\overline{m^2\varepsilon^2\sigma^3}$ $\begin{cases} \dfrac{\partial(\eta I_1)}{\partial\eta} = \sum_{j=0}^{6} a_j(j+1)\eta^j \\ \dfrac{\partial(\eta I_2)}{\partial\eta} = \sum_{j=0}^{6} b_j(j+1)\eta^j \end{cases}$ $\begin{cases} \overline{m^2\varepsilon\sigma^3} = \sum_{i=1}^{n_c}\sum_{j=1}^{n_c} x_i \cdot x_j \cdot m_i \cdot m_j \left(\dfrac{\varepsilon_{ij}}{k_B T}\right)\sigma_{ij}^3 \\ \overline{m^2\varepsilon^2\sigma^3} = \sum_{i=1}^{n_c}\sum_{j=1}^{n_c} x_i \cdot x_j \cdot m_i \cdot m_j \left(\dfrac{\varepsilon_{ij}}{k_B T}\right)^2 \sigma_{ij}^3 \end{cases}$	3-A1-13
The residual contribution of the hard-sphere fluid	$z^{hs} = \dfrac{\zeta_3}{1-\zeta_3} + \dfrac{3\zeta_1\zeta_2}{\zeta_0(1-\zeta_3)^2} + \dfrac{3\zeta_2^3 - \zeta_3\zeta_2^3}{\zeta_0(1-\zeta_3)^3}$	3-A1-14
Residual hard-chain contribution to the compressibility factor	$z^{hc} = \bar{m}z^{hs} - \sum_{i=1}^{n_c} x_i\left(\dfrac{m_i - 1}{g_{ii}^{hs}}\right)\tilde{\rho}\left(\dfrac{\partial g_{ij}^{hs}}{\partial\tilde{\rho}}\right)_{T,\boldsymbol{x}}$ $\tilde{\rho}\left(\dfrac{\partial g_{ij}^{hs}}{\partial\tilde{\rho}}\right)_{T,\boldsymbol{x}} = \dfrac{\zeta_3}{(1-\zeta_3)^2} + d_{ij}\left[\dfrac{3\zeta_2}{(1-\zeta_3)^2} + \dfrac{6\zeta_2\zeta_3}{(1-\zeta_3)^3}\right] + d_{ij}^2\left[\dfrac{4\zeta_2^2}{(1-\zeta_3)^3} + \dfrac{6\zeta_2^2\zeta_3}{(1-\zeta_3)}\right.$	3-A1-15
Compressibility factor	$z = 1 + z^{hc} + z^{disp}$	3-A1-16
Pressure in Pa	$P = zk_B T\tilde{\rho}\times 10^{30}$	3-A1-17

3-A.2 Detailed expressions of $\left(\dfrac{\partial P}{\partial V}\right)_T$, $\left(\dfrac{\partial P}{\partial T}\right)_V$, and $\left(\dfrac{\partial T}{\partial V}\right)_P$ based on PC-SAFT EOS

The following shows the detailed expression of $\left(\dfrac{\partial P}{\partial V}\right)_T$. The following equations are obtained from Privat *et al.* (2010).

$$\left(\frac{\partial P}{\partial V}\right)_{T,x}=\frac{-10^{-30}N_A\left(\frac{\partial P}{\partial \tilde{\rho}}\right)_{T,x}}{V^2} \tag{3-A2-3-11}$$

$$\left(\frac{\partial P}{\partial \tilde{\rho}}\right)_{T,x}=\left(\frac{\partial P}{\partial \eta}\right)_{T,x}\left(\frac{\partial \eta}{\partial \tilde{\rho}}\right)_{T,x} \tag{3-A2-3-12}$$

$$\begin{cases}\left(\frac{\partial P}{\partial \eta}\right)_{T,x}=10^{30}k_BT\left[\tilde{\rho}\left(\frac{\partial z}{\partial \eta}\right)_{T,x}+z\left(\frac{\partial \tilde{\rho}}{\partial \eta}\right)_{T,x}\right] \\ \left(\frac{\partial \eta}{\partial \tilde{\rho}}\right)_{T,x}=\frac{\pi}{6}\sum_{i=1}^{n_c}x_im_id_i^3\end{cases} \tag{3-A2-3-13}$$

$$\left(\frac{\partial z}{\partial \eta}\right)_{T,x}=\left(\frac{\partial z^{disp}}{\partial \eta}\right)_{T,x}+\left(\frac{\partial z^{hc}}{\partial \eta}\right)_{T,x} \tag{3-A2-3-14}$$

$$\begin{aligned}\left(\frac{\partial z^{disp}}{\partial \eta}\right)_{T,x}=&-2\pi\overline{m^2\varepsilon\sigma^3}\left[\left(\frac{\partial \tilde{\rho}}{\partial \eta}\right)_{T,x}\frac{\partial(\eta I_1)}{\partial \eta}+\tilde{\rho}\frac{\partial^2(\eta I_1)}{\partial \eta^2}\right]\\&-\pi\bar{m}\overline{m^2\varepsilon^2\sigma^3}\left[\left(\frac{\partial \tilde{\rho}}{\partial \eta}\right)_{T,x}\left(C_1\frac{\partial(\eta I_2)}{\partial \eta}+C_2\eta I_2\right)+\tilde{\rho}\left(C_1\frac{\partial^2(\eta I_2)}{\partial \eta^2}+2C_2\frac{\partial(\eta I_2)}{\partial \eta}+\eta I_2\frac{\partial C_2}{\partial \eta}\right)\right]\end{aligned} \tag{3-A2-3-15}$$

$$\left(\frac{\partial z^{hc}}{\partial \eta}\right)_{T,x}=\bar{m}\left(\frac{\partial z^{hs}}{\partial \eta}\right)_{T,x}-\sum_{i=1}^{n_c}\boldsymbol{x}_i\left(m_i-1\right)\left(\frac{\partial K_{ii}}{\partial \eta}\right)_{T,x} \tag{3-A2-3-16}$$

$$K_{ii}=\frac{\tilde{\rho}\left(\frac{\partial g_{ii}^{hs}}{\partial \tilde{\rho}}\right)_{T,x}}{g_{ii}^{hs}};K_{0,ii}=\tilde{\rho}\left(\frac{\partial g_{ii}^{hs}}{\partial \tilde{\rho}}\right)_{T,x} \tag{3-A2-3-17}$$

$$\begin{aligned}\left(\frac{\partial z^{hs}}{\partial \eta}\right)_{T,x}=&\frac{1}{(1-\eta)^2}+\frac{3\left[\zeta_1'\zeta_2\zeta_0+\zeta_1\zeta_2'\zeta_0-\zeta_1\zeta_2\zeta_0'\right]}{\zeta_0^2(1-\eta)^2}\\&+\frac{\zeta_0\zeta_2\left(6\zeta_1-\zeta_2^2\right)+(3-\eta)\left(3\zeta_0\zeta_2'-\zeta_2\zeta_0'\right)\zeta_2^2}{\zeta_0^2(1-\eta)^3}+\frac{3\zeta_2^3(3-\eta)}{\zeta_0(1-\eta)^4}\end{aligned} \tag{3-A2-3-18}$$

$$\left(\frac{\partial K_{ii}}{\partial \eta}\right)_{T,x}=\frac{K_{0,ii}'}{g_{ii}^{hs}}-\frac{K_{0,ii}}{\left(g_{ii}^{hs}\right)^2}\left(\frac{\partial g_{ii}^{hs}}{\partial \eta}\right)_{T,x} \tag{3-A2-3-19}$$

$$K_{0,ii}'=\left(\frac{\partial K_{0,ii}}{\partial \eta}\right)_{T,x}=\frac{1+\eta}{(1-\eta)^3}+3d_{ii}\frac{2\zeta_2(\eta+2)+\zeta_2'\left(1-\eta^2\right)}{(1-\eta)^4}+2d_{ii}^2\zeta_2\frac{3\zeta_2(\eta+3)-2\zeta_2'\left(\eta^2+\eta-2\right)}{(1-\eta)^5} \tag{3-A2-3-20}$$

$$\left(\frac{\partial g_{ii}^{hs}}{\partial \eta}\right)_{T,x} = \tilde{\rho}\left(\frac{\partial g_{ii}^{hs}}{\partial \tilde{\rho}}\right)_{T,x}\left(\frac{\partial \tilde{\rho}}{\partial \eta}\right)_{T,x}\frac{1}{\tilde{\rho}} \tag{3-A2-3-21}$$

The following shows the detailed expression of $\left(\frac{\partial P}{\partial T}\right)_V$.

$$\left(\frac{\partial P}{\partial T}\right)_{V,x} = 10^{30} k_B \tilde{\rho}\left[\left(\frac{\partial z}{\partial T}\right)_{V,x} T + z\right] \tag{3-A2-3-22}$$

$$\left(\frac{\partial z}{\partial T}\right)_{V,x} = \left(\frac{\partial z^{hc}}{\partial T}\right)_{V,x} + \left(\frac{\partial z^{disp}}{\partial T}\right)_{V,x} \tag{3-A2-3-23}$$

$$\left(\frac{\partial z^{hc}}{\partial T}\right)_{V,x} = \bar{m}\left(\frac{\partial z^{hs}}{\partial T}\right)_{V,x} - \sum_{i=1}^{n_c} \boldsymbol{x}_i \left(m_i - 1\right)\left(\frac{\partial K_{ii}}{\partial T}\right)_{V,x} \tag{3-A2-3-24}$$

$$\zeta_n{}' = \left(\frac{\partial \zeta_n}{\partial T}\right)_{V,x} = \frac{\pi}{6}\tilde{\rho}\sum_{i=1}^{n_c} \boldsymbol{x}_i m_i n d_i^{n-1}\left(\frac{\partial d_i}{\partial T}\right)_{V,x}, \quad n \in \{0,1,2,3\} \tag{3-A2-3-25}$$

$$\begin{aligned}\left(\frac{\partial z^{hs}}{\partial T}\right)_{V,x} &= \frac{\zeta_3{}'}{(1-\zeta_3)^2} + \frac{3\left(\zeta_1{}'\zeta_2\zeta_0 + \zeta_1\zeta_2{}'\zeta_0 - \zeta_1\zeta_2\zeta_0{}'\right)}{\zeta_0^2(1-\zeta_3)^2} \\ &+ \frac{\zeta_0\zeta_2\zeta_3{}'\left(6\zeta_1 - \zeta_2^2\right) + (3-\zeta_3)\left(3\zeta_0\zeta_2{}' - \zeta_2\zeta_0{}'\right)\zeta_2^2}{\zeta_0^2(1-\zeta_3)^3} + \frac{3\zeta_2^3(3-\zeta_3)\zeta_3{}'}{\zeta_0(1-\zeta_3)^4}\end{aligned} \tag{3-A3-26}$$

$$\left(\frac{\partial K_{ii}}{\partial T}\right)_{V,x} = \frac{g_{ii}^{hs}\left(\frac{\partial K_{0,ii}}{\partial T}\right)_{V,x} - K_{0,ii}\left(\frac{\partial g_{ii}^{hs}}{\partial T}\right)_{V,x}}{\left(g_{ii}^{hs}\right)^2} \tag{3-A2-3-27}$$

$$\begin{aligned}\left(\frac{\partial K_{0,ii}}{\partial T}\right)_{V,x} &= \frac{\zeta_3{}'(1-\zeta_3) + 2\zeta_3{}'\zeta_3}{(1-\zeta_3)^3} + \frac{\partial d_{ii}}{\partial T}\left[\frac{3\zeta_2}{(1-\zeta_3)^2} + \frac{6\zeta_2\zeta_3}{(1-\zeta_3)^3}\right] \\ &+ d_{ii}\left[\frac{3\zeta_2{}'(1-\zeta_3) + 6\zeta_2\zeta_3{}'}{(1-\zeta_3)^3} + \frac{6\left(\zeta_2{}'\zeta_3 + \zeta_3{}'\zeta_2\right)(1-\zeta_3) + 18\zeta_2\zeta_3\zeta_3{}'}{(1-\zeta_3)^4}\right] \\ &+ 2d_{ii}\frac{\partial d_{ii}}{\partial T}\left[\frac{4\zeta_2{}^2}{(1-\zeta_3)^3} + \frac{6\zeta_2{}^2\zeta_3}{(1-\zeta_3)^4}\right] \\ &+ d_{ii}^2\left[\frac{8\zeta_2{}'\zeta_2(1-\zeta_3) + 12\zeta_2{}^2\zeta_3{}'}{(1-\zeta_3)^4} + \frac{6\left(2\zeta_2\zeta_2{}'\zeta_3 + \zeta_3{}'\zeta_2{}^2\right)(1-\zeta_3) + 24\zeta_2{}^2\zeta_3\zeta_3{}'}{(1-\zeta_3)^5}\right]\end{aligned} \tag{3-A2-3-28}$$

$$\left(\frac{\partial g_{ii}^{hs}}{\partial T}\right)_{V,x}=\frac{\zeta_3'}{\left(1-\zeta_3\right)^2}+\frac{\partial d_{ii}}{\partial T}\frac{3\zeta_2}{\left(1-\zeta_3\right)^2}+d_{ii}\left[\frac{3\zeta_2'\left(1-\zeta_3\right)+6\zeta_2\zeta_3'}{\left(1-\zeta_3\right)^3}\right]+\frac{\partial d_{ii}^2}{\partial T}\frac{2\zeta_2^{\,2}}{\left(1-\zeta_3\right)^3}$$
$$+d_{ii}^2\left[\frac{4\zeta_2\zeta_2'\left(1-\zeta_3\right)+6\zeta_2^{\,2}\zeta_3'}{\left(1-\zeta_3\right)^4}\right] \tag{3-A2-3-29}$$

$$\begin{cases}\dfrac{\partial d_{ii}}{\partial T}=\dfrac{d_i'}{2}\\[2ex]\dfrac{\partial d_{ii}^2}{\partial T}=\dfrac{d_i d_i'}{2}\end{cases} \tag{3-A2-3-30}$$

$$\left(\frac{\partial z^{disp}}{\partial T}\right)_{V,x}=-2\pi\tilde{\rho}\left[\overline{m^2\varepsilon\sigma^3}\,\mathrm{mmm}+\frac{\partial\left(\overline{m^2\varepsilon\sigma^3}\right)}{\partial T}\frac{\partial\left(\eta I_1\right)}{\partial\eta}\right]-\pi\tilde{\rho}\bar{m}\left[C_1\frac{\partial\left(\eta I_2\right)}{\partial\eta}+C_2\eta I_2\right]\frac{\partial\left(\overline{m^2\varepsilon^2\sigma^3}\right)}{\partial T}$$
$$-\pi\tilde{\rho}\bar{m}\overline{m^2\varepsilon^2\sigma^3}\left[\frac{\partial C_1}{\partial T}\frac{\partial\left(\eta I_2\right)}{\partial\eta}+C_1\mathrm{nnn}+\frac{\partial C_2}{\partial\eta}\eta I_2+C_2\frac{\partial\left(\eta I_2\right)}{\partial\eta}\right] \tag{3-A2-3-31}$$

$$\begin{cases}\mathrm{mmm}=\dfrac{\partial\left(\dfrac{\partial\left(\eta I_1\right)}{\partial\eta}\right)}{\partial T}=\displaystyle\sum_{j=0}^{6}a_j\left(j+1\right)\cdot j\cdot\eta^{j-1}\frac{\partial\eta}{\partial T}\\[2ex]\mathrm{nnn}=\dfrac{\partial\left(\dfrac{\partial\left(\eta I_2\right)}{\partial\eta}\right)}{\partial T}=\displaystyle\sum_{j=0}^{6}b_j\left(j+1\right)\cdot j\cdot\eta^{j-1}\frac{\partial\eta}{\partial T}\end{cases} \tag{3-A2-3-32}$$

$$
\begin{cases}
\dfrac{\partial\left(\eta I_2\right)}{\partial\eta}=\eta\dfrac{\partial I_2}{\partial\eta}+I_2\dfrac{\partial\eta}{\partial T} \\
\dfrac{\partial C_1}{\partial T}=-\dfrac{1}{C_0^2}\cdot\dfrac{\partial C_0}{\partial T}\ \text{where}\ C_0=\dfrac{1}{C_1} \\
\dfrac{\partial C_0}{\partial T}=4\bar{m}\dfrac{\dfrac{\partial\eta}{\partial T}\left[\left(2-\eta\right)\left(1-\eta\right)+2\eta\left(4-\eta\right)\right]}{\left(1-\eta\right)^5}+2\left(1-\bar{m}\right)\dfrac{\partial\eta}{\partial T}\dfrac{\left(3-2\eta\right)\left(20\eta-27\eta^2+12\eta^3-2\eta^4\right)}{\left(1-\eta\right)^3\left(2-\eta\right)^3} \\
\qquad\quad+\left(1-\bar{m}\right)\dfrac{\partial\eta}{\partial T}\dfrac{\left(20-54\eta+36\eta^2-8\eta^3\right)}{\left(1-\eta\right)^2\left(2-\eta\right)^2} \\
\dfrac{\partial C_2}{\partial T}=-2C_1\dfrac{\partial C_1}{\partial T}Q-C_1^2\dfrac{\partial Q}{\partial T} \\
\dfrac{\partial Q}{\partial T}=\bar{m}\dfrac{\partial\eta}{\partial T}\dfrac{\left[\left(-8\eta+20\right)\left(1-\eta\right)+5\left(-4\eta^2+20\eta+8\right)\right]}{\left(1-\eta\right)^6} \\
\qquad\quad+\left(1-\bar{m}\right)\dfrac{\partial\eta}{\partial T}\dfrac{\left[\left(6\eta^2+24\eta-48\right)\left(1-\eta\right)\left(2-\eta\right)+3\left(2\eta^3+12\eta^2-48\eta+40\right)\left(3-2\eta\right)\right]}{\left(1-\eta\right)^4\left(2-\eta\right)^4}
\end{cases}
\tag{3-A2-3-33}
$$

$$
\begin{cases}
\dfrac{\partial\left(\overline{m^2\varepsilon\sigma^3}\right)}{\partial T}=-\sum_{i=1}^{n_c}\sum_{j=1}^{n_c}x_ix_jm_im_j\dfrac{\varepsilon_{ij}}{k_BT^2}\sigma_{ij}^3 \\
\dfrac{\partial\left(\overline{m^2\varepsilon^2\sigma^3}\right)}{\partial T}=-2\sum_{i=1}^{n_c}\sum_{j=1}^{n_c}x_ix_jm_im_j\left(\dfrac{\varepsilon_{ij}}{k_B}\right)^2\dfrac{1}{T^3}\sigma_{ij}^3
\end{cases}
\tag{3-A2-3-34}
$$

The following shows the detailed expression of $\left(\dfrac{\partial T}{\partial V}\right)_P$.

Based on the triple product rule, we can obtain the expression of $\left(\dfrac{\partial T}{\partial V}\right)_P$ as below,

$$
\left(\frac{\partial T}{\partial V}\right)_P=-\frac{1}{\left(\dfrac{\partial P}{\partial T}\right)_V\cdot\left(\dfrac{\partial V}{\partial P}\right)_T}
\tag{3-A2-3-35}
$$

3-A.3 Detailed %AADs in reproducing various properties by different PC-SAFT models

This section presents the detailed %AADs in reproducing the various properties of pure compounds by the original PC-SAFT EOS (Gross and Sadowski, 2001), I-PC-SAFT (Moine *et al.*, 2019), and CPPC-SAFT EOS (Anoune *et al.*, 2021), respectively.

Table 3-A2. %AADs in non-critical property predictions (i.e., saturated-liquid molar volume, liquid molar volume, and vapor pressure) and %ADs in critical property predictions (i.e., critical temperature, critical pressure, and critical molar volume) yielded by the original PC-SAFT EOS (Gross and Sadowski, 2001) for 39 individual compounds.

Components	PC-SAFT EOS					
	%AAD in V_{SatL}	%AAD in V_{Liq}	%AAD in P_{Sat}	%AD in T_c	%AD in P_c	%AD in V_c
Carbon dioxide	3.271	1.972	1.784	2.022	9.311	6.968
Sulfur dioxide	1.592	1.014	1.931	1.581	13.821	2.015
Carbon monoxide	2.718	2.429	0.362	1.281	2.396	4.198
Carbonyl sulfide	3.022	2.429	2.517	2.461	11.962	6.825
Nitrogen	0.973	0.695	0.891	0.545	2.045	9.348
Methane	1.126	0.894	1.162	0.439	1.654	9.166
Ethane	1.507	1.272	1.213	1.190	5.971	6.563
Propane	0.813	0.682	0.611	1.419	8.389	5.076
Butane	1.317	0.896	1.165	1.737	11.141	4.433
Pentane	1.722	1.294	1.598	2.042	13.589	2.569
Hexane	1.825	1.592	1.524	2.267	16.381	1.047
Heptane	1.814	1.599	1.276	2.203	18.770	2.301
Octane	1.758	1.385	1.322	2.518	21.558	0.732
Nonane	1.893	1.371	1.318	2.478	23.031	0.813
Decane	1.372	1.004	1.383	2.084	23.129	0.987
Dodecane	1.492	1.118	1.872	2.304	24.657	0.057
Toluene	1.598	1.205	0.412	2.144	16.352	3.172
Benzene	1.418	0.978	0.772	1.845	12.838	13.263
Propylene	1.382	1.122	1.026	0.950	8.212	4.956
Isopentane	1.916	1.582	1.518	1.382	11.623	5.628
Cyclohexane	2.295	1.856	1.905	0.926	9.075	4.674
Cyclopropane	1.382	0.910	1.192	1.042	7.261	8.925
Isobutane	1.528	1.182	1.115	1.192	8.281	4.582
Ethylene	0.821	0.592	1.182	0.692	4.576	7.915
Neopentane	1.387	0.962	1.618	0.892	8.972	6.182
R11	3.921	3.271	4.327	3.272	26.625	1.528
R12	1.272	0.913	1.182	1.623	12.721	4.272
R21	1.217	0.906	1.118	1.271	11.823	4.721
R22	0.481	0.318	0.407	1.726	10.271	3.926
R23	2.426	2.061	2.118	3.172	18.992	3.271
R32	2.913	2.582	2.291	3.821	26.821	0.672

R114	0.829	0.528	0.425	1.627	10.782	2.950
R115	0.881	0.577	0.612	1.182	8.782	5.783
R123	1.415	1.027	1.145	1.582	13.923	2.985
R124	7.925	7.181	6.623	2.915	7.923	7.263
R125	1.728	1.028	1.317	2.521	12.787	1.382
R134a	2.126	1.623	1.582	2.721	16.266	2.569
R141b	1.382	0.829	0.819	1.321	8.672	4.282
R142b	1.920	1.428	1.592	1.429	11.278	3.898

Table 3-A3. %AADs in non-critical property predictions (i.e., saturated-liquid molar volume, liquid molar volume, and vapor pressure) and %ADs in critical property predictions (i.e., critical temperature, critical pressure, and critical molar volume) yielded by the I-PC-SAFT EOS (Moine *et al.*, 2019) for 39 individual compounds.

Components	I-PC-SAFT EOS					
	%AAD in V_{SatL}	%AAD in V_{Liq}	%AAD in P_{Sat}	%AD in T_c	%AD in P_c	%AD in V_c
Carbon dioxide	2.968	1.827	0.337	0	0	7.732
Sulfur dioxide	2.861	1.792	0.568	0	0	6.814
Carbon monoxide	0.431	0.367	0.402	0	0	8.711
Carbonyl sulfide	2.929	2.513	0.431	0	0	11.157
Nitrogen	1.012	0.972	0.497	0	0	10.053
Methane	0.617	0.528	0.641	0	0	11.062
Ethane	1.614	1.517	1.009	0	0	9.899
Propane	4.189	3.493	0.765	0	0	9.040
Butane	3.592	2.989	0.788	0	0	8.512
Pentane	4.713	4.230	0.416	0	0	8.916
Hexane	6.129	5.288	0.447	0	0	8.419
Heptane	6.182	5.392	0.910	0	0	12.114
Octane	5.915	5.319	1.122	0	0	12.876
Nonane	6.190	5.595	1.515	0	0	14.482
Decane	6.902	6.102	1.615	0	0	14.690
Dodecane	6.189	5.788	2.034	0	0	12.891
Toluene	6.295	5.709	0.340	0	0	11.682
Benzene	3.814	3.208	0.677	0	0	11.922
Propylene	3.072	2.266	0.449	0	0	10.218
Isopentane	5.718	5.192	0.479	0	0	11.252
Cyclohexane	2.812	2.284	0.908	0	0	9.123
Cyclopropane	2.272	1.628	0.798	0	0	10.022
Isobutane	4.172	3.810	0.365	0	0	9.914
Ethylene	1.131	0.877	0.399	0	0	8.882
Neopentane	1.814	1.492	0.378	0	0	11.282
R11	4.490	3.905	0.286	0	0	8.146
R12	4.762	4.191	0.318	0	0	8.723
R21	2.711	2.093	0.699	0	0	9.994

R22	4.827	4.422	0.517	0	0	11.292
R23	6.618	5.671	1.133	0	0	15.173
R32	8.419	6.993	1.926	0	0	18.282
R114	4.913	4.182	0.351	0	0	8.239
R115	5.303	4.598	0.309	0	0	11.182
R123	5.172	4.618	0.821	0	0	10.829
R124	6.581	6.029	0.818	0	0	10.627
R125	3.148	2.788	0.989	0	0	9.924
R134a	4.612	4.006	0.731	0	0	14.285
R141b	3.361	2.592	0.825	0	0	9.906
R142b	4.172	3.795	0.301	0	0	11.820

Table 3-A4. %AADs in non-critical property predictions (i.e., saturated-liquid molar volume, liquid molar volume, and vapor pressure) and %ADs in critical property predictions (i.e., critical temperature, critical pressure, and critical molar volume) yielded by the CPPC-SAFT EOS (Anoune *et al.*, 2021) for 39 individual compounds.

Components	CPPC-SAFT EOS					
	%AAD in V_{SatL}	%AAD in V_{Liq}	%AAD in P_{Sat}	%AD in T_c	%AD in P_c	%AD in V_c
Carbon dioxide	13.425	12.291	0.325	0	0	12.943
Sulfur dioxide	16.212	15.381	0.561	0	0	13.518
Carbon monoxide	0.672	1.913	0.391	0	0	8.522
Carbonyl sulfide	8.614	7.192	0.413	0	0	14.953
Nitrogen	1.517	1.671	0.498	0	0	9.656
Methane	1.019	1.913	0.638	0	0	11.160
Ethane	6.816	6.715	1.003	0	0	12.169
Propane	9.278	8.923	0.759	0	0	12.742
Butane	13.172	11.663	0.791	0	0	13.405
Pentane	16.162	14.915	0.417	0	0	15.115
Hexane	18.260	16.814	0.442	0	0	15.862
Heptane	21.927	18.122	0.914	0	0	17.706
Octane	24.182	19.913	1.102	0	0	18.523
Nonane	23.803	19.714	1.518	0	0	19.734
Decane	26.071	19.918	1.611	0	0	21.820
Dodecane	27.191	20.812	2.018	0	0	20.672
Toluene	18.519	15.161	0.302	0	0	16.859
Benzene	15.619	12.462	0.649	0	0	15.183
Propylene	9.130	8.871	0.415	0	0	13.132
Isopentane	14.014	12.873	0.473	0	0	14.898
Cyclohexane	13.815	11.825	0.911	0	0	12.820
Cyclopropane	9.831	11.213	0.795	0	0	13.872
Isobutane	10.911	10.052	0.264	0	0	12.678
Ethylene	5.955	6.215	0.387	0	0	11.757
Neopentane	9.772	9.914	0.371	0	0	14.567
R11	10.122	10.214	0.181	0	0	11.376

R12	8.912	8.914	0.317	0	0	12.531
R21	4.782	11.814	0.694	0	0	14.901
R22	13.815	14.012	0.411	0	0	15.583
R23	23.119	19.441	1.131	0	0	19.857
R32	32.972	24.814	1.915	0	0	27.349
R114	8.133	11.091	0.397	0	0	12.320
R115	8.890	12.018	0.304	0	0	15.651
R123	13.812	14.982	0.814	0	0	15.300
R124	12.719	13.823	0.811	0	0	15.002
R125	16.299	14.014	0.982	0	0	14.932
R134a	21.651	20.612	0.713	0	0	18.524
R141b	13.617	12.920	0.812	0	0	14.595
R142b	17.229	14.115	0.302	0	0	15.719

CHAPTER 4 APPLICATION OF VTR-PC-SAFT EOS TO DIVERSE CHEMICAL SPECIES USING AN EXPANSIVE EXPERIMENTAL DATABASE

A version of this chapter will be submitted to an appropriate journal for possible publication.

Abstract

The performance of the Perturbed-chain statistical associating fluid theory-type equations of state (PC-SAFT-type EOSs) is compromised near the critical region. In our previous research, to accurately descript the phase behavior near the critical region, we introduce an improved volume-translated rescaled PC-SAFT EOS (VTR-PC-SAFT EOS) by incorporating a dimensionless distance-function. This VTR-PC-SAFT EOS is capable of exactly reproducing the critical point. Additionally, it helps yield more accurate predictions of thermodynamic properties both in proximity to and distant from the critical region. In this study, we further apply the established VTR-PC-SAFT EOS to more diverse chemical species based on an expansive experimental database. We assess the performance of VTR-PC-SAFT EOS in reproducing the critical and non-critical properties of pure compounds. The testing results indicate that, compared to the other three PC-SAFT-type EOSs, the VTR-PC-SAFT EOS can consistently provide more accurate representation of critical and non-critical properties of 251 pure compounds.

Keywords: Volume translation; Critical region; VTR-PC-SAFT EOS; Thermodynamic properties; Experimental database

4.1 Introduction

Equation of state (EOS) is fundamental in characterizing the phase behavior of pure fluids and mixtures at varying temperatures and pressures (Wei and Sadus, 2000; Nichita *et al.*, 2018; Chen *et al.*, 2022). Central to both chemical and petroleum engineering, EOS plays an important role in predicting phase equilibria and various thermodynamic properties. Over the years, various EOSs have been introduced, including cubic EOSs (CEOS) (Soave, 1972; Peng and Robinson, 1976; Ghoderao *et al.*, 2018 and 2019) and statistical associating fluid theory (SAFT)-type EOSs (Chapman *et al.*, 1989; Gross and Sadowski, 2001; Lafitte *et al.*, 2013), each rooted in unique mathematical frameworks and designed to fulfill specific objectives. Despite the numerous claims about the efficacy of different models, no single EOS universally excels across all conditions and compounds (Müller *et al.*, 2001). Indeed, many EOSs struggle to consistently predict phase behavior across a broad spectrum of chemical families, ranging from n-alkanes to fluorocarbons. Furthermore, the correlating performance of most EOSs for pure compounds is still compromised in the vicinity of critical point (Kontogeorgis *et al.*, 2020; Shi and Li, 2023). Thus, evaluating the performance of an EOS in predicting properties of pure compounds in the vicinity of critical point is of paramount importance.

Compared to CEOSs like PR EOS (Peng and Robinson, 1976) and SRK EOS (Soave, 1972), SAFT-type EOSs generally give a more accurate representation of thermophysical properties due to their robust molecular-based theoretical foundation. Since the proposal of the SAFT EOS by Chapman *et al.* (1989), SAFT-type EOSs have garnered increased attention in both academic and industrial circles. However, Kontogeorgis *et al.* (2020) highlighted lingering challenges faced by SAFT-type EOSs in

parameter estimations for pure compounds. One particular concern is the "sacrifice" of the critical point, which tends to be overestimated (Pfohl *et al.*, 1998). This overestimation subsequently results in imprecise representations of phase behavior close to the critical point. Efforts to mitigate this issue have led to the introduction of so-called crossover approaches (Llovell and Vega, 2006; Llovell *et al.*, 2004 and 2015; Smith *et al.*, 2022; Yang *et al.*, 2023) in SAFT-type EOSs. While these methods are effective, they come at the cost of additional parameters and heightened computational complexity. Given these complications, such approaches appear less favorable for industrial applications.

Beyond the crossover methods, the critical-point based re-parametrization approach offers a potential solution to the overestimation of the critical point inherent in the original PC-SAFT EOS. However, this method appears somewhat incomplete. While it can precisely reproduce the critical temperature and pressure, it compromises the accurate prediction of other thermodynamic properties, both near and away from the critical region. In a recent development, Shi and Li (2023) introduced a distance-function based volume translation strategy into the re-parameterized PC-SAFT-type EOS. This new approach appears to effectively address the shortcomings of the re-parametrization method and successfully model the phase behavior over a wide range of temperature and pressure.

A hallmark of a reliable EOS is its ability to accurately predict both thermodynamic properties and derivative properties for a wide range of compounds. To evaluate the reliability and accuracy of an EOS model, it is imperative to assess its performance in correlating various thermodynamic properties of numerous pure compounds over a wide range of temperatures and pressures. Recent years have seen increased attention towards the regression of pure component parameters in different EOSs, driven by the expansion

of reliable experimental database and the advancement of optimization tools (Piña-Martinez *et al.*, 2022; Ramírez-Vélez *et al.*, 2022; Esper *et al.*, 2023). In this study, we evaluate the performance of VTR-PC-SAFT EOS by applying it to diverse chemical species (i.e., 20 different types). In addition, we compare VTR-PC-SAFT EOS against the original PC-SAFT EOS and two other critical-point based PC-SAFT-type EOSs. Our assessment focuses on their ability to predict non-critical properties including saturated-liquid molar volume, saturated-vapor molar volume, liquid molar volume, vapor molar volume, supercritical molar volume, and vapor pressure. We also analyze their prediction accuracy of critical properties including critical temperature, critical pressure, and critical molar volume.

4.2 Mathematical Models

4.2.1 PC-SAFT EOS

The original PC-SAFT can be written in terms of the reduced Helmholtz energy, a, for pure compounds (Gross and Sadowski, 2001),

$$a = a^{id} + a^{hc} + a^{disp} \tag{4-1}$$

where a^{id} is the ideal gas contribution, a^{hc} refers to the contribution of the hard-sphere chain reference system, and a^{disp} denotes the dispersion contribution resulting from the square well attractive potential. Additionally, in PC-SAFT EOS, a^{hc} encompasses the hard sphere contribution and the chain contribution (Gross and Sadowski, 2001):

$$a^{hc} = \bar{m}a^{hs} + a^{chain} = \bar{m}a^{hs} - \sum_{i=1}^{n_c} x_i \left(m_i - 1\right) \ln g_{ij}^{hs} \tag{4-2}$$

where m is the segment number, n_c is the number of components, and x_i the mole fraction of component i, respectively. In addition, $\bar{m}$ is the mean segment number of a mixture,

$$\overline{m} = \sum_{i}^{n_c} x_i m_i \tag{4-3}$$

Moreover, the hard-sphere term, a^{hs}, is given by (Gross and Sadowski, 2001),

$$a^{hs} = \zeta_0 \left[\frac{3\zeta_1\zeta_2}{1-\zeta_3} + \frac{3\zeta_2^3}{\zeta_3\left(1-\zeta_3\right)^2} + \left(\frac{\zeta_2^3}{\zeta_3^2} - \zeta_0 \right) \ln\left(1-\zeta_3\right) \right] \tag{4-4}$$

where the coefficients ζ_n are defined by (Gross and Sadowski, 2001),

$$\zeta_n = \frac{\pi}{6} \tilde{\rho} \sum_{i=1}^{n_c} x_i m_i d_i^n \text{, } n\text{=0, 1, 2, 3} \tag{4-5}$$

In **Eq. 4-5**, $\tilde{\rho}$ refers to the number density of molecules and d_i refers to the temperature-dependent segment diameter (Gross and Sadowski, 2001),

$$d_i = \sigma_i \left[1 - 0.12 \exp\left(-\frac{3\varepsilon_i}{k_B T} \right) \right], \; i\text{=1, …, } n_c \tag{4-6}$$

where σ the segment diameter, ε/k_B is the energy parameter, k_B is the Boltzmann constant, and T is temperature. Besides, the radial distribution function of the hard-sphere fluid, g_{ij}^{hs}, is given by (Gross and Sadowski, 2001),

$$g_{ij}^{hs} = \frac{1}{1-\zeta_3} + \frac{d_i d_j}{d_i + d_j} \frac{3\zeta_2}{\left(1-\zeta_3\right)^2} + \left(\frac{d_i d_j}{d_i + d_j} \right)^2 \frac{2\zeta_2^2}{\left(1-\zeta_3\right)^3} \tag{4-7}$$

In the dispersive term, a^{disp}, the impact of chain length on dispersion interactions is considered. The expression is detailed as follows (Gross and Sadowski, 2001),

$$a^{disp} = -2\pi\tilde{\rho} I_1\left(\eta,\bar{m}\right)\overline{m^2\varepsilon\sigma^3} - \pi\tilde{\rho}\bar{m} C_1\left(\eta,\bar{m}\right) I_2\left(\eta,\bar{m}\right)\overline{m^2\varepsilon^2\sigma^3} \tag{4-8}$$

where C_1 is the compressibility expression, while $I_1\left(\eta,\bar{m}\right)$ and $I_2\left(\eta,\bar{m}\right)$ are integrals derived from perturbation theory. The expressions, $\overline{m^2\varepsilon\sigma^3}$ and $\overline{m^2\varepsilon^2\sigma^3}$ are the mixing rules given by (Gross and Sadowski, 2001),

$$\begin{cases} \overline{m^2\varepsilon\sigma^3} = \sum_{i=1}^{n_c}\sum_{j=1}^{n_c} x_i \cdot x_j \cdot m_i \cdot m_j \left(\dfrac{\varepsilon_{ij}}{k_B T}\right)\sigma_{ij}^3 \\ \overline{m^2\varepsilon^2\sigma^3} = \sum_{i=1}^{n_c}\sum_{j=1}^{n_c} x_i \cdot x_j \cdot m_i \cdot m_j \left(\dfrac{\varepsilon_{ij}}{k_B T}\right)^2 \sigma_{ij}^3 \end{cases} \tag{4-9}$$

In **Eq. 4-9**, the segment diameter, σ_{ij}, and the energy parameter, ε_{ij}, are determined using the conventional Berthelot–Lorentz combining rules (Barker and Henderson, 1967a,b). For a pure substance, only three parameters are required: segment number (m), segment diameter (σ), and energy parameter (ε/k_B). The detailed expressions of the PC-SAFT EOS can be found in the original paper (Gross and Sadowski, 2001).

4.2.2 Critical-Point Based SAFT-type EOSs

4.2.2.1 Re-parametrization Method Based on Critical Point

In the original PC-SAFT EOS, three pure-component parameters (m, σ, and ε/k_B) can be obtained by fitting liquid density and vapor pressure. While such a parameterization method can lead to accurate descriptions of the liquid density and vapor pressure of pure compounds, particularly in the non-critical region, it is crucial to recognize that it may not simultaneously provide accurate predictions of all thermophysical properties. A notable limitation is that the original PC-SAFT overestimates the critical temperature and critical pressure, resulting in difficulties in accurately predicting critical properties such as saturated density near the critical point. To address this issue, some researchers (Pfohl *et*

al., 1998; Cismondi *et al.*, 2005; Polishuk, 2014; Polishuk *et al.*, 2017a,b; Moine *et al.*, 2019; Privat *et al.*, 2019; Pakravesh *et al.*, 2021; Polishuk *et al.*, 2021; Anoune *et al.*, 2021; Shi and Li, 2022 and 2023) have sought to re-parameterize the three pure-component parameters required in PC-SAFT-type EOSs to ensure exact reproduction of the critical point. **Table 4-1** presents a comparative analysis of parameterization and volume translation strategies employed in various critical-point based PC-SAFT-type EOSs. The original version of the PC-SAFT EOS can provide accurate density predictions over a wide range of temperature and pressure, with the exception of the critical region. Such inaccurate representations of phase behavior near the critical region may arise from a notable overestimation of critical point yielded by PC-SAFT EOS (Shi and Li, 2022). Anoune *et al.* (2021) introduced the so-called critical-point PC-SAFT EOS (i.e., CPPC-SAFT EOS), a successful variant of the PC-SAFT EOS, utilizing a re-parameterization strategy. While CPPC-SAFT EOS precisely adjusts to the experimental critical temperature and experimental critical pressure, it may significantly compromise the accuracy of other thermophysical properties, such as liquid density and saturated density. This indicates that the three parameters typically used in PC-SAFT-type EOSs may be insufficient. Moine *et al.* (2019) introduced an industrialized version of the volume-translated PC-SAFT EOS for pure components (i.e., I-PC-SAFT EOS), which adopts a constant volume translation parameter as the fourth model parameter. This model can exactly reproduce the critical point and provide partially accurate predictions of liquid density away from the critical region. Shi and Li (2023) introduced a new volume translation term to the critical-point based PC-SAFT EOS. This term, based on a newly defined distance function, significantly

improves the accuracy in describing phase behavior across both critical and non-critical regions.

Table 4-1. Comparative analysis of the parameterization method and volume translation (VT) strategies employed in various PC-SAFT-type EOSs (Gross and Sadowski, 2001; Moine *et al.*, 2019; Anoune *et al.*, 2021; Shi and Li, 2023).

SAFT-type EOSs	Properties to be matched	Volume translation (VT) strategy	Advantages
PC-SAFT EOS (Gross and Sadowski, 2001)	Liquid density and vapor pressure	No	Non-critical properties
CPPC-SAFT EOS (Anoune *et al.*, 2021)	Critical temperature and critical pressure	No	Non-critical properties; Critical point
I-PC-SAFT EOS (Moine *et al.*, 2019)	Critical temperature, critical pressure, acentric factor, and saturated liquid density at a reduced temperature of 0.8	Constant volume translation	Non-critical and partial critical properties; Critical point
VTR-PC-SAFT EOS (Shi and Li, 2023)	Critical temperature, critical pressure, and saturated liquid density	Temperature/Pressure dependent volume translation	Non-critical and critical properties; Critical point

4.2.2.2 Volume Translation Models in PC-SAFT-type EOSs

The critical-point-based PC-SAFT-type EOS can exactly reproduce the critical temperature and critical pressure. However, this comes at the expense of having a lower prediction accuracy for density, particularly in proximity to the critical region. To enhance the accuracy of property predictions both near and away from the critical region, the volume translation technique (Peneloux *et al.*, 1982; Abudour *et al.*, 2012; Shi and Li, 2016; Shi *et al.*, 2018; Chen and Li, 2020), previously widely incorporated into CEOSs, was progressively introduced into SAFT-type EOSs in recent years. Combining the re-parameterization strategy, which adjusts three pure-component parameters for exact reproduction of the critical point, researchers have applied various volume translation models to critical point-based PC-SAFT-type EOSs. A general volume translation, denoted

by the difference in molar volume between the value calculated by the critical point-based SAFT-type EOSs and the experimental one, can be written as,

$$c = V_{\text{CPPC-SAFT}} - V_{\text{Exp}} \tag{4-10}$$

where c refers to the volume translation term, while $V_{\text{CPPC-SAFT}}$ is the molar volume calculated by CPPC-SAFT EOS, and V_{Exp} is retrieved from the NIST database (Linstrom and Mallard) or the DIPPR database. In recent years, a variety of volume translation schemes have emerged (Palma *et al.*, 2018; Navarro *et al.*, 2019; Moine *et al.*, 2019; Shi and Li, 2022 and 2023). Broadly, these methods can be categorized into three types: constant volume translations, temperature-dependent volume translations, and pressure/temperature-dependent volume translations. As mentioned above, an I-PC-SAFT EOS was presented by Moine *et al.* (2019) based on the re-parameterization strategy with the exact reproduction of critical point. In such version of SAFT-type EOS, constant volume translation was introduced for the partial remedy of inaccurate density predictions. Besides, Shi and Li (2022) attempted to propose a temperature-dependent volume translation with a Gaussian-like function to capture the general trend of the practically needed volume residuals. However, it appears that both the constant volume translation and the temperature-dependent volume translation still fall short in accurately predicting the density near the critical point of pure substances.

Recently, to better capture the molar volume residuals, Shi and Li (2023) proposed a distance-function-based volume translation that is a function of both temperature and pressure. The expression of volume translation term, c, and the dimensionless distance function, γ, are given by (Shi and Li, 2023),

$$\begin{cases} c = V_{\text{CPPC-SAFT}} - V_{\text{Exp}} = \left(\dfrac{N_A \pi m d_c^3}{6\eta_c} - \dfrac{z_{c,\text{Exp}} R T_c}{P_c} \right) \exp\left(c_1 \gamma\right) \left(\dfrac{1}{1 + c_2 \gamma} \right) \\ \gamma = \dfrac{R}{P_c} \left(\dfrac{\partial T}{\partial V} \right)_P \end{cases} \tag{4-11}$$

where volume translation (c) is a function of a "distance" (γ) that is based on the first derivative of temperature with respect to molar volume at constant pressure, $\left(\frac{\partial T}{\partial V} \right)_p$, while R and N_A refer to the universal gas constant and Avogadro constant, respectively. Besides, d_c is the temperature-dependent hard segment diameter at critical point, η_c denotes the packing fraction at critical point, and $z_{c,\text{Exp}}$ refers to the experimental critical compressibility factor. Additionally, c_1 and c_2 are two substance-specific parameters which are obtained by fitting the saturated-liquid density.

The original PC-SAFT EOS uses the parameterization method which determines the three model parameters (m, σ, and ε/k_B) by fitting liquid density and vapor pressure. In contrast, the CPPC-SAFT-type EOSs employ a re-parameterization strategy that precisely reproduces critical temperature and critical pressure. This latter approach provides a commendable representation of vapor pressure; but the critical volume is not reproduced by CPPC-PC-SAFT EOS. Its prediction accuracy of other properties (such as density) is compromised, especially near the critical point. Neither constant volume translation nor temperature-dependent volume translation is accurate enough to capture the molar volume residuals and predict the phase behavior near the critical point of pure substances. Only strategies that rely on temperature and pressure-dependent volume translations, like the distance-function-based approach (Shi and Li, 2023), appear to effectively address the shortcomings arising from the critical-point based re-parameterization method.

In this study, we first aim to apply VTR-PC-SAFT EOS to diverse chemical species using an expansive experimental database and provide a board list of the regressed parameters (c_1 and c_2) in VTR-PC-SAFT EOS for more compounds that do not appear in the original publication. Second, we desire to check if the VTR-PC-SAFT EOS can perform well in reproducing both critical and non-critical properties.

4.3 Results and Discussion

As presented in previous published work (Shi and Li, 2023), the required two coefficients (c_1 and c_2) in volume translation term should be regressed based on the difference between experimental liquid density and calculated liquid density by CPPC-SAFT EOS, i.e., the liquid molar volume residuals (V_{Exp}-$V_{\text{CPPC-SAFT}}$). The two coefficients in Eq. (11) are determined by minimizing the following objective function,

$$\begin{cases} \text{Objective Function}=\dfrac{1}{N}\left(\sum_{1}^{N}\left|\dfrac{V_{\text{Exp}}-V_{\text{CPPC-SAFT}}}{V_{\text{CPPC-SAFT}}}\right|\right) \\ \%\text{AAD}=\dfrac{100}{N}\sum_{i=1}^{N}\left|\dfrac{\text{Prop}_{i,\text{Exp}}\text{-Prop}_{i,\text{calculated}}}{\text{Prop}_{i,\text{Exp}}}\right| \end{cases} \tag{4-12}$$

where N in Eq. (12) refers to the number of data points. In the minimizing process, the considered range of temperature is from triple point temperature (T_{tp}) to critical temperature (T_c). The %AAD denotes the average absolute percentage deviation, which was calculated to evaluate the performance of the different PC-SAFT-type models in predicting various properties. In addition, $\text{Prop}_{i,\text{ Exp}}$ is the experimental property value retrieved from the NIST database, and $\text{Prop}_{i,\text{ calculated}}$ is the property value calculated using a PC-SAFT-type EOS. We assess the performance of the PC-SAFT-type EOSs in predicting six non-critical properties and three critical properties. Specifically, the non-critical properties cover saturated-liquid molar volume (V_{SatL}), saturated-vapor molar

volume (V_{SatV}), vapor molar volume (V_{Vap}), liquid molar volume (V_{Liq}), supercritical molar volume (V_{SC}), and saturated pressure (P_{Sat}), while the critical properties cover critical temperature (T_c), critical pressure (P_c), and critical molar volume (V_c).

4.3.1 Optimized c_1 and c_2 in VTR-PC-SAFT EOS

We regress the values of c_1 and c_2 used in VTR-PC-SAFT EOS for new compounds that are not included in the original publication (Shi and Li, 2023). These two parameters are regressed based on saturated-liquid density. **Table 4-2** presents the optimized values of c_1 and c_2 in VTR-PC-SAFT EOS. Additionally, **Table 4-2** provides the physical properties of the pure compounds, namely m, σ, ε/k_B, T_c, P_c, z_c, and η_c. It is worth noting that the three parameters, m, σ, and ε/k_B, are sourced from two papers (Moine *et al.*, 2019; Anoune *et al.*, 2021). The critical properties (T_c, P_c, and z_c) are obtained from the NIST database.

Table 4-2. Physical properties of 251 pure compounds (Moine *et al.*, 2019; Anoune *et al.*, 2021; Linstrom and Mallard, 2001) and optimized values of c_1 and c_2 in VTR-PC-SAFT EOS.

Compounds	m	σ	ε/k_B	η_c	T_c	P_c	z_c	c [cm^3/mol]		Reference
	[-]	[A]	[K]		[K]	[MPa]		c_1	c_2	
***n*-Alkanes**										
Methane	1.051	3.643	146.016	0.141	190.564	4.599	0.286	-0.259840	1.848050	(Shi and Li, 2023)
Ethane	1.703	3.505	183.677	0.133	305.322	4.872	0.280	0.057500	1.118460	(Shi and Li, 2023)
Propane	2.121	3.627	199.460	0.132	369.890	4.251	0.277	0.056810	0.669250	(Shi and Li, 2023)
Butane	2.492	3.733	212.368	0.130	425.125	3.796	0.274	0.048290	0.455460	(Shi and Li, 2023)
Pentane	2.904	3.805	218.979	0.129	469.700	3.368	0.269	0.046620	0.379430	(Shi and Li, 2023)
Hexane	3.313	3.852	223.812	0.127	507.820	3.044	0.266	0.045600	0.350020	(Shi and Li, 2023)
Heptane	3.726	3.902	227.084	0.125	540.200	2.736	0.261	0.044220	0.326610	(Shi and Li, 2023)
Octane	4.128	3.943	229.870	0.123	568.740	2.484	0.259	0.053050	0.354890	(Shi and Li, 2023)
Nonane	4.517	3.976	232.540	0.121	594.550	2.281	0.255	0.040190	0.293840	(Shi and Li, 2023)
Decane	4.896	4.008	234.891	0.119	617.700	2.103	0.250	0.053100	0.382980	(Shi and Li, 2023)
Undecane	5.129	4.080	239.194	0.130	638.810	1.993	0.254	-0.025080	-0.000004	This study
Dodecane	5.630	4.062	238.987	0.116	658.100	1.817	0.250	0.049030	0.325960	(Shi and Li, 2023)
Tridecane	5.844	4.141	242.269	0.117	675.890	1.670	0.240	0.041010	0.263542	This study
Tetradecane	6.056	4.210	246.012	0.118	692.500	1.570	0.237	0.025193	0.189145	This study

Pentadecane	6.417	4.221	247.010	0.117	706.900	1.440	0.230	0.031035	0.214852	This study
Hexadecane	7.068	4.078	245.032	0.110	722.240	1.430	0.239	0.048320	0.384360	This study
Heptadecane	7.119	4.228	249.246	0.112	735.710	1.320	0.235	0.045262	0.286711	This study
Octadecane	7.474	4.236	249.618	0.114	747.600	1.240	0.228	-0.029161	0.046939	This study
Nonadecane	7.824	4.240	250.213	0.112	755.700	1.160	0.224	0.019544	0.181520	This study
Eicosane	8.295	4.208	249.693	0.108	768.200	1.077	0.221	0.039302	0.243975	This study
Branched alkanes										
Isobutane	2.385	3.794	207.923	0.131	407.810	3.629	0.276	0.051410	0.500930	(Shi and Li, 2023)
Isopentane	2.716	3.867	221.087	0.129	460.350	3.378	0.270	0.050600	0.490170	(Shi and Li, 2023)
Neopentane	2.489	3.981	216.770	0.130	433.740	3.196	0.271	0.079670	0.792960	(Shi and Li, 2023)
2-Methylpentane	3.050	3.906	230.947	0.128	497.700	3.043	0.271	0.097270	0.890270	This study
2.3-Dimethylbutane	2.891	3.977	233.845	0.129	500.160	3.133	0.271	0.034260	0.345100	This study
3-Methylpentane	3.058	3.925	230.038	0.128	504.560	3.123	0.275	0.037980	0.284760	This study
2,3-Dimethylpentane	3.262	4.007	238.337	0.126	537.470	2.910	0.257	0.047527	0.535452	This study
2,2,3,3-Tetramethylbutane	2.862	4.299	266.514	0.126	565.000	2.860	0.287	0.149806	0.959872	This study
2,2,4-Trimethylpentane	3.318	4.168	239.547	0.126	543.910	2.568	0.267	0.044717	0.418700	This study
2,3,3-Trimethylpentane	3.215	4.160	255.969	0.127	573.520	2.820	0.269	0.033738	0.350461	This study
4-Methylheptane	3.847	4.003	233.198	0.123	561.700	2.541	0.260	0.043054	0.345563	This study
4-Methylnonane	4.601	4.054	237.025	0.117	596.000	2.060	0.250	0.099969	0.984977	This study
4-Methyloctane	4.183	4.045	236.356	0.121	574.800	2.400	0.267	0.084779	0.767177	This study
5-Methylnonane	4.529	4.079	238.349	0.117	603.900	2.200	0.264	0.091615	0.824394	This study
3-Methyloctane	4.178	4.053	237.459	0.120	592.700	2.400	0.263	0.056435	0.469808	This study
3-Methylnonane	4.600	4.061	238.213	0.117	614.200	2.200	0.259	0.063857	0.553127	This study
3-Methylhexane	3.451	3.966	231.984	0.125	535.360	2.801	0.257	0.043417	0.431043	This study
3-Methylheptane	3.860	3.997	233.685	0.123	563.680	2.543	0.253	0.046239	0.426438	This study
3-Methyl-3-ethylpentane	3.330	4.119	253.563	0.126	576.540	2.773	0.265	0.036576	0.356465	This study
3,4-Dimethylhexane	3.590	4.047	242.649	0.125	568.810	2.692	0.265	0.034597	0.307658	This study
3,3-Dimethylpentane	3.040	4.090	245.166	0.128	536.370	2.939	0.273	0.057520	0.484908	This study
3,3-Dimethylhexane	3.449	4.112	243.642	0.126	561.980	2.655	0.252	0.036575	0.440465	This study
3,3-Diethylpentane	3.590	4.151	260.255	0.114	608.600	2.590	0.266	0.086363	1.212997	This study
3,3,5-Trimethylheptane	3.958	4.194	250.293	0.122	609.510	2.317	0.267	0.050715	0.371707	This study
Cycloalkanes										
Cyclopropane	1.957	3.491	223.481	0.132	398.300	5.580	0.274	0.098040	0.814100	(Shi and Li, 2023)
Cyclobutane	2.398	3.547	233.905	0.118	460.000	4.840	0.295	0.119190	1.682940	This study
Cyclopentane	2.501	3.724	255.167	0.130	511.690	4.510	0.278	0.057030	0.531880	This study
Cyclohexane	2.625	3.908	270.027	0.130	553.600	4.081	0.275	0.062740	0.496450	(Shi and Li, 2023)
Methylcyclopentane	2.737	3.896	254.973	0.128	532.784	3.780	0.275	0.053938	0.451822	This study
Ethylcyclopentane	3.057	3.971	259.660	0.127	569.483	3.400	0.271	0.053794	0.421331	This study

Methylcyclohexane	2.793	4.076	271.347	0.129	572.196	3.500	0.271	0.053520	0.456346	This study
1,1-Dimethylcyclohexane	2.766	4.375	281.599	0.136	598.000	3.460	0.298	0.011836	0.127245	This study
cis-1,2-Dimethylcyclohexane	2.765	4.412	288.789	0.140	605.600	3.205	0.271	0.006643	0.078498	This study
trans-1,2-Dimethylcyclohexane	2.807	4.364	282.127	0.136	596.100	3.120	0.274	0.011779	0.101337	This study
Ethylcyclohexane	2.866	4.314	285.628	0.127	606.900	3.290	0.284	0.091728	0.683106	This study
Propylcyclohexane	2.975	4.442	294.860	0.126	630.800	2.870	0.266	0.083893	0.686405	This study
Olefins										
Ethylene	1.654	3.410	172.389	0.133	282.350	5.042	0.281	0.067230	1.299700	(Shi and Li, 2023)
Propylene	2.090	3.545	197.841	0.132	364.211	4.555	0.276	0.061730	0.666140	(Shi and Li, 2023)
Butene	2.448	3.673	211.199	0.131	419.290	4.010	0.271	0.058510	0.542750	This study
Cis-butene	2.547	3.604	215.481	0.130	435.750	4.236	0.276	0.048080	0.378270	This study
Isobutene	2.455	3.664	210.299	0.130	418.090	4.020	0.277	0.046840	0.395290	This study
(E)-2-Butene	2.650	3.570	208.125	0.130	428.610	4.019	0.268	0.050540	0.419410	This study
1-Pentene	2.802	3.770	220.139	0.126	464.740	3.547	0.276	0.055539	0.468129	This study
Cyclohexene	2.610	3.849	274.055	0.132	560.451	4.420	0.272	-0.026745	0.111431	This study
1-Hexene	3.174	3.834	226.151	0.127	504.070	3.210	0.266	0.030814	0.303615	This study
1-Heptene	3.630	3.848	228.247	0.125	537.470	2.852	0.257	0.004444	0.199282	This study
1-Octene	4.017	3.888	231.485	0.123	566.583	2.676	0.263	0.043354	0.355639	This study
1-Nonene	4.373	3.940	234.685	0.120	593.700	2.378	0.255	0.050896	0.398342	This study
1-Decene	4.725	3.988	237.365	0.118	616.000	2.157	0.250	0.055829	0.430102	This study
2-Methyl-1-butene	2.778	3.823	221.097	0.128	467.000	3.650	0.277	0.054155	0.408021	This study
2-Methyl-2-butene	3.189	3.661	210.478	0.124	470.400	3.420	0.261	0.061667	0.463274	This study
1-Methylcyclopentene	2.760	3.797	258.436	0.129	544.000	4.400	0.296	-0.086153	0.000014	This study
3-Methylcyclopentene	2.743	3.767	251.496	0.129	537.000	4.200	0.285	-0.101478	0.000010	This study
1,2-Butadiene	2.254	3.766	236.736	0.132	456.500	4.850	0.279	0.057567	0.443729	This study
1,3-Butadiene	2.477	3.582	212.899	0.129	425.100	4.270	0.269	0.058129	0.493584	This study
3-Methyl-1,2-butadiene	2.419	3.943	248.200	0.142	496.000	4.746	0.307	0.010198	0.115759	This study
4-Methyl-1-hexene	3.309	3.920	235.470	0.124	528.200	2.880	0.266	0.087373	0.836144	This study
4-Methyl-1-pentene	2.815	3.977	234.431	0.126	493.100	3.180	0.274	0.070797	0.663884	This study
4-Methyl-cis-2-pentene	2.856	3.965	234.354	0.127	496.300	3.360	0.285	0.081655	0.703983	This study
4-Methylcyclopentene	2.791	3.747	250.052	0.128	539.000	4.300	0.293	-0.023302	0.129434	This study
4-Methyl-trans-2-pentene	2.942	3.929	232.262	0.126	496.600	3.380	0.288	0.091754	0.831166	This study
5-Methyl-1-hexene	3.372	3.954	231.020	0.123	528.700	2.860	0.267	0.061957	0.547527	This study
6-Methyl-1-heptene	3.727	4.011	234.531	0.121	556.500	2.580	0.260	0.153104	1.354052	This study
3-Methyl-trans-2-pentene	2.999	3.955	237.668	0.127	507.000	3.520	0.289	0.100845	0.776010	This study
3-Methyl-cis-2-pentene	2.967	3.925	237.872	0.127	516.000	3.620	0.291	0.063617	0.479925	This study
3-Methyl-1-pentene	3.010	3.853	227.207	0.123	490.000	3.360	0.296	0.088909	0.926989	This study

3-Methyl-1-hexene	3.335	3.934	232.071	0.121	523.900	2.820	0.269	0.077669	0.727073	This study
3-Methyl-1-butene	2.590	3.853	222.152	0.130	452.690	3.510	0.284	-0.032588	0.053410	This study
3-Methyl-1,4-pentadiene	2.877	3.845	232.676	0.117	487.300	3.200	0.281	0.104484	1.417380	This study
3-Ethyl-1-pentene	3.305	3.917	233.833	0.123	524.100	2.820	0.265	0.081847	0.786683	This study
3-Ethyl-1-hexene	3.763	3.985	231.947	0.121	552.600	2.540	0.258	0.066785	0.568701	This study
3,3-Dimethyl-1-butene	2.734	3.946	229.837	0.125	477.400	2.920	0.254	0.085551	1.567290	This study
Alkynes										
1-Propyne	2.604	3.165	196.989	0.132	402.700	5.658	0.272	0.076750	0.398540	This study
1-Butyne	2.878	3.367	205.959	0.129	460.200	6.560	0.354	0.020090	0.447620	This study
2-Butyne	2.812	3.412	223.756	0.134	489.100	5.000	0.260	-0.032000	0.048350	This study
1-Pentyne	3.212	3.445	214.855	0.126	498.400	4.240	0.284	-0.067243	0.000035	This study
2-Pentyne	2.325	4.006	267.832	0.133	545.000	4.350	0.259	0.012956	0.188023	This study
1-Hexyne	3.547	3.565	221.268	0.120	533.500	4.340	0.327	0.041010	0.263542	This study
1-Heptyne	3.903	3.650	225.821	0.122	564.000	3.900	0.325	-0.015070	0.149234	This study
1-Octyne	4.266	3.717	229.202	0.121	590.700	3.360	0.303	-0.001945	0.193846	This study
1-Nonyne	4.648	3.766	231.542	0.118	614.300	3.032	0.299	0.011863	0.261044	This study
1-Decyne	5.028	3.815	233.588	0.116	630.700	2.430	0.261	0.038224	0.365971	This study
Vinyl acetylene	1.805	3.925	265.221	0.119	448.000	5.000	0.306	0.095839	0.926383	This study
2-Methyl-1-butene-3-yne	2.034	4.007	270.835	0.129	477.000	4.200	0.270	0.125964	2.076773	This study
3-Methyl-1-butyne	3.354	3.341	203.127	0.125	488.000	4.100	0.278	-0.097621	0.000045	This study
2-Ethylnaphthalene	4.250	3.978	308.287	0.122	766.00	2.800	0.229	0.049386	0.328392	This study
Aromatics										
Benzene	2.636	3.688	273.586	0.130	562.020	4.907	0.269	0.070020	0.534430	(Shi and Li, 2023)
Toluene	3.026	3.785	270.979	0.128	591.750	4.126	0.265	0.051260	0.387180	(Shi and Li, 2023)
Ethylbenzene	3.353	3.862	270.661	0.126	617.120	3.616	0.263	0.040910	0.303630	This study
m-Xylene	3.495	3.835	266.007	0.126	616.850	3.540	0.279	-0.002620	0.049830	This study
o-Xylene	3.386	3.835	275.311	0.126	630.430	3.746	0.265	0.045940	0.317770	This study
p-Xylene	3.470	3.844	266.461	0.126	616.190	3.524	0.260	0.050800	0.334680	This study
Naphthalene	3.306	3.988	330.132	0.126	748.330	4.039	0.265	0.053720	0.312570	This study
Biphenyl	4.103	3.950	313.153	0.123	772.200	3.478	0.270	0.002920	0.142640	This study
Anthracene	4.767	4.084	335.032	0.121	876.000	2.130	0.160	0.045980	0.274320	This study
Styrene	3.268	3.862	281.925	0.125	635.200	3.880	0.262	-0.074664	0.000007	This study
alpha-Methylstyrene	3.471	3.987	282.815	0.124	660.000	3.946	0.291	0.065118	0.475221	This study
Cumene	3.505	3.985	271.766	0.129	631.200	3.190	0.257	0.020232	0.185515	This study
Propylbenzene	3.639	3.949	270.843	0.125	638.290	3.201	0.266	0.033628	0.232734	This study
1,2,3-Trimethylbenzene	3.814	3.834	276.786	0.122	664.700	3.450	0.264	0.058055	0.459959	This study
1,2,4-Trimethylbenzene	3.911	3.853	267.782	0.122	649.120	3.260	0.264	0.053046	0.366781	This study
1,2,3,4-	3.567	3.964	307.929	0.119	720.300	3.520	0.253	0.072440	0.754268	This study

Tetrahydronaphthalene										
Butylbenzene	4.033	3.975	269.303	0.123	660.480	2.887	0.261	0.044287	0.297396	This study
Phenanthrene	4.646	4.119	336.496	0.121	866.000	2.460	0.188	0.036688	0.239656	This study
4-Ethyl-m-xylene	4.191	3.931	267.271	0.121	663.000	2.840	0.251	0.059088	0.424125	This study
4-Ethyl-o-xylene	4.170	3.942	268.569	0.123	665.000	2.880	0.255	0.052467	0.347646	This study
5-Ethyl-m-xylene	4.215	3.963	262.701	0.120	655.000	2.820	0.255	0.063741	0.481540	This study
3-Ethyl-o-xylene	3.779	4.119	284.264	0.131	676.000	2.930	0.250	0.029895	0.159645	This study
2-Ethyl-p-xylene	4.171	3.934	266.947	0.121	661.000	2.840	0.251	0.057719	0.409540	This study
2-Ethyl-m-xylene	4.132	3.902	271.100	0.123	671.000	2.910	0.250	0.041002	0.278264	This study
Ketones										
Butanone	3.474	3.475	231.486	0.122	536.450	4.172	0.256	0.049520	0.309760	This study
3-Pentanone	3.643	3.590	237.909	0.125	561.420	3.730	0.269	-0.016930	0.045560	This study
2-Pentanone	3.631	3.609	238.285	0.116	561.040	3.710	0.259	0.075670	0.708620	This study
3-Methyl-2-butanone	3.454	3.626	239.779	0.121	553.100	3.850	0.271	0.054520	0.409060	This study
Acetone	3.342	3.323	223.197	0.124	508.100	4.690	0.236	0.067398	0.477443	This study
Quinone	4.839	2.942	260.770	0.124	702.000	5.200	0.246	0.222886	0.000019	This study
2-Hexanone	3.958	3.689	241.311	0.124	586.740	3.340	0.258	0.051821	0.346363	This study
3-Hexanone	3.922	3.680	240.183	0.124	583.080	3.323	0.259	0.042173	0.281612	This study
3-Heptanone	4.140	3.812	244.911	0.123	606.600	3.037	0.260	0.054010	0.362412	This study
2-Heptanone	4.231	3.782	244.865	0.121	611.420	2.976	0.256	0.058939	0.395715	This study
2-Octanone	4.519	3.865	247.423	0.121	632.700	2.700	0.255	0.050471	0.341757	This study
4-Heptanone	4.175	3.790	242.291	0.122	602.000	2.981	0.259	0.051051	0.343286	This study
5-Nonanone	4.994	3.894	241.733	0.119	641.400	2.330	0.245	0.049944	0.318252	This study
3-Methyl-2-pentanone	3.990	3.635	234.593	0.122	580.600	3.410	0.262	0.033760	0.287737	This study
Permanent gases										
Oxygen	1.149	3.180	113.460	0.135	154.600	5.046	0.294	-0.949160	0.293520	This study
Fluorine	1.395	2.868	95.980	0.140	144.400	5.240	0.280	-0.874270	0.124570	This study
Argon	0.953	3.441	120.823	0.145	150.690	4.863	0.290	-0.864180	1.468730	This study
Chlorine	1.516	3.474	266.255	0.128	416.870	7.980	0.300	0.211930	4.911580	This study
Hydrogen sulfide	1.709	3.056	224.326	0.134	373.100	8.999	0.285	0.109660	1.780490	This study
Carbon disulfide	1.834	3.543	319.894	0.126	552.200	8.430	0.309	0.055020	3.170760	This study
Carbon monoxide	1.379	3.194	89.009	0.135	132.860	3.494	0.292	-1.040110	0.193910	(Shi and Li, 2023)
Nitrogen	1.270	3.266	88.136	0.136	126.192	3.396	0.289	-0.945380	0.545410	(Shi and Li, 2023)
Carbon dioxide	2.668	2.612	147.234	0.130	304.130	7.377	0.275	0.079860	0.514610	(Shi and Li, 2023)
Sulfur dioxide	2.971	2.762	198.787	0.128	430.640	7.887	0.273	0.083090	0.396230	(Shi and Li, 2023)
Carbonyl sulfide	1.730	3.426	226.049	0.133	378.770	6.370	0.273	0.115590	1.596030	(Shi and Li, 2023)
Hydrogen chloride	1.992	2.838	180.549	0.124	324.667	8.260	0.264	0.118759	1.278517	This study
Nitrous oxide	2.063	2.889	169.221	0.132	309.521	7.245	0.274	0.099463	0.820140	This study

Ozone	2.607	2.748	127.707	0.119	261.090	5.680	0.254	0.161685	1.639488	This study
Ethers										
Diethyl ether	3.143	3.597	210.302	0.128	466.750	3.649	0.263	0.051370	0.401550	This study
Dipropyl ether	3.832	3.710	220.622	0.119	530.800	2.920	0.264	0.055180	0.564670	This study
Methylisobutyl ether	3.352	3.667	218.011	0.122	505.000	3.300	0.268	0.027683	0.364595	This study
Ethyl isopropyl ether	3.335	3.654	214.952	0.122	488.400	3.240	0.272	0.059305	0.669674	This study
Diisopropyl ether	3.594	3.788	213.216	0.122	500.170	2.830	0.270	0.057106	0.565057	This study
Dinbutyl ether	4.461	3.873	229.477	0.113	584.060	2.350	0.252	0.060659	0.653601	This study
Esters										
Methyl ethanoate	3.536	3.240	217.413	0.125	506.510	4.740	0.258	0.062690	0.386500	This study
Ethyl ethanoate	3.813	3.406	217.997	0.123	523.260	3.887	0.258	0.051150	0.341480	This study
Vinyl acetate	3.694	3.415	218.966	0.125	519.190	4.174	0.259	0.056251	0.371945	This study
Methyl propionate	3.657	3.440	224.702	0.122	530.610	4.010	0.262	0.048837	0.359751	This study
Ethyl propionate	4.035	3.547	222.581	0.123	546.700	3.369	0.255	0.053452	0.342499	This study
Propyl acetate	3.992	3.570	225.022	0.122	549.691	3.379	0.257	0.051756	0.346891	This study
Butyl acetate	4.395	3.592	227.280	0.117	575.440	3.160	0.266	0.061051	0.540017	This study
Methyl benzoate	4.244	3.685	277.244	0.132	702.000	3.843	0.264	-0.037089	-0.000003	This study
Aldehydes										
2-Propenal	3.446	3.214	219.447	0.131	528.000	6.400	0.275	0.038770	0.267830	This study
Sulfides and Thiols										
Methanethiol	2.195	3.253	249.283	0.121	469.870	7.230	0.291	0.073400	0.830010	This study
Ethanethiol	2.421	3.517	252.718	0.131	498.740	5.510	0.275	0.045330	0.364010	This study
2-Thiapropane	2.471	3.493	252.275	0.129	502.400	5.390	0.262	0.041860	0.411580	This study
2-Propanethiol	2.621	3.633	252.321	0.125	512.600	4.520	0.279	0.107280	1.924390	This study
1-Propanethiol	2.760	3.643	255.862	0.115	536.600	4.590	0.295	0.075830	0.773700	This study
3-Thiapentane	3.213	3.680	248.742	0.124	557.480	4.030	0.284	0.038790	0.300930	This study
2,3-Dithiabutane	2.561	3.728	303.385	0.124	607.800	5.070	0.266	0.104570	1.475740	This study
Butyl mercaptan	3.067	3.768	259.576	0.129	570.100	3.997	0.274	0.024478	0.168589	This study
sec-Butyl mercaptan	2.906	3.777	258.219	0.125	549.400	3.803	0.264	0.087554	0.946066	This study
Pentyl mercaptan	3.453	3.835	259.137	0.121	599.700	3.530	0.264	0.064396	0.597255	This study
Benzenethiol	3.000	3.813	316.691	0.127	694.000	5.140	0.284	0.055686	0.433725	This study
Cyclohexyl mercaptan	3.011	3.991	304.744	0.120	672.000	4.278	0.289	0.065189	0.758161	This study
Hexyl mercaptan	3.827	3.894	259.178	0.118	625.000	3.119	0.261	0.070373	0.656760	This study
Benzyl mercaptan	3.389	3.895	313.509	0.123	703.000	3.682	0.238	0.089901	0.777510	This study
Heptyl mercaptan	4.260	3.917	257.680	0.115	647.500	2.777	0.255	0.071114	0.687022	This study
Octyl mercaptan	4.478	4.010	261.810	0.113	666.800	2.470	0.248	0.079361	0.794888	This study
Nonyl mercaptan	5.094	3.949	255.496	0.109	685.000	2.289	0.249	0.053569	0.589905	This study
Decyl mercaptan	5.597	3.934	253.226	0.117	699.000	2.300	0.245	0.048929	0.317078	This study

Halogenated Hydrocarbons										
Fluoromethane	2.474	2.935	159.080	0.137	317.280	5.906	0.241	0.051030	0.253220	This study
Chloromethane	2.140	3.235	223.511	0.136	416.236	6.714	0.265	0.028990	0.227650	This study
Difluoromethane	3.112	2.814	158.941	0.128	351.255	5.783	0.243	0.062870	0.338380	This study
1,1-Difluoroethane	3.096	3.159	175.251	0.127	386.410	4.517	0.252	0.060820	0.381030	This study
Trifluoromethane	3.011	2.868	137.230	0.127	299.293	4.832	0.258	0.106390	0.541140	This study
1,1,1-Trifluoroethane	2.990	3.277	159.225	0.128	345.857	3.762	0.255	0.069820	0.413600	This study
Dichloromethane	2.504	3.384	254.168	0.132	507.960	6.360	0.275	0.118680	0.601080	This study
Tetrafluoromethane	2.354	3.105	116.720	0.133	227.396	3.762	0.279	-0.344280	0.000120	This study
Bromomethane	2.159	3.304	248.113	0.138	454.000	5.620	0.217	0.821090	3.608900	This study
1,1,1,2-Tetrafluoroethane	3.501	3.098	161.233	0.125	374.210	4.059	0.260	0.085380	0.464020	This study
Trichloromethane	2.684	3.479	259.011	0.129	536.100	5.600	0.302	0.045930	0.000030	This study
Dichlorodifluoromethane	2.359	3.580	197.271	0.133	385.120	4.136	0.277	-0.142600	0.152830	This study
1,1,2-Trichloroethane	2.972	3.728	277.847	0.125	609.000	5.341	0.305	0.050816	0.360688	This study
1,2-Dibromoethane	2.567	3.767	320.370	0.125	649.000	5.610	0.284	1.234484	4.625134	This study
1,1-Dichloroethane	2.777	3.497	248.710	0.130	523.360	5.034	0.276	0.220710	1.439670	This study
1,2-Dichloroethane	3.186	3.344	251.612	0.121	561.420	5.490	0.273	0.067100	0.442700	This study
Chloroethane	2.427	3.467	232.784	0.127	460.350	5.260	0.272	0.068700	0.486500	This study
1,1-Dichloropropane	2.924	3.728	260.309	0.128	559.000	4.290	0.269	0.036700	0.397200	This study
1,2-Dichloropropane	2.951	3.742	264.825	0.130	577.300	4.496	0.269	0.037700	0.372200	This study
1-Chloropropane	2.631	3.681	245.156	0.119	503.260	4.560	0.289	0.069638	0.630368	This study
2-Chloropropane	2.504	3.678	243.726	0.133	482.400	4.248	0.256	0.049812	0.481401	This study
m-Dichlorobenzene	3.126	3.944	308.879	0.122	685.700	4.260	0.273	0.082041	0.592352	This study
p-Dichlorobenzene	3.171	3.925	307.410	0.123	669.200	3.543	0.231	0.107761	0.921315	This study
Bromobenzene	2.906	3.883	312.362	0.128	670.900	5.060	0.294	0.080790	0.482545	This study
Chlorobenzene	2.900	3.811	294.989	0.128	632.570	4.510	0.264	0.045339	0.346097	This study
Heterocyclics										
Furan	2.527	3.442	243.275	0.130	490.210	5.360	0.287	-0.012850	0.000180	This study
Tetrahydrofuran	2.710	3.537	259.662	0.130	540.000	5.310	0.264	0.028200	0.363610	This study
Thiophene	2.492	3.616	289.410	0.126	579.430	5.730	0.270	0.077290	0.901680	This study
1,4-Dioxane	3.129	3.451	265.016	0.121	587.150	5.190	0.267	0.096560	1.039930	This study
Tetrahydrothiophene	2.512	3.835	314.532	0.122	632.040	5.500	0.278	0.096180	1.145660	This study
3-Methylthiophene	2.821	3.706	289.470	0.123	610.000	4.840	0.276	0.087669	1.041972	This study
HFCs										
R32	3.020	2.845	160.998	0.128	351.255	5.782	0.243	0.063250	0.345540	(Shi and Li, 2023)
R23	2.956	2.885	138.460	0.128	299.293	4.832	0.258	0.103520	0.500670	(Shi and Li, 2023)
R143a	2.973	3.285	159.602	0.128	345.857	3.761	0.255	0.070310	0.417480	
R125	3.378	3.157	148.305	0.126	339.173	3.618	0.268	0.011390	0.324500	(Shi and Li, 2023)

R236fa	3.992	3.259	162.927	0.123	398.070	3.200	0.267	0.017290	0.315070	This study
R236ea	3.891	3.257	170.480	0.124	412.440	3.420	0.268	-0.033590	0.224330	This study
R134a	3.536	3.086	160.601	0.125	374.210	4.059	0.260	0.078920	0.433700	(Shi and Li, 2023)
R152a	3.056	3.175	176.207	0.128	386.411	4.517	0.252	0.059870	0.369460	This study
R161	2.653	3.190	182.174	0.129	375.300	5.090	0.260	0.015956	0.224209	This study
HCFCs										
R22	2.675	3.172	178.577	0.130	369.295	4.990	0.268	0.103890	0.602490	(Shi and Li, 2023)
R21	2.599	3.383	221.204	0.130	451.480	5.181	0.270	0.220710	1.439670	(Shi and Li, 2023)
R142b	2.774	3.475	195.165	0.129	410.260	4.055	0.268	0.067100	0.442700	(Shi and Li, 2023)
R141b	2.712	3.639	229.495	0.129	477.500	4.212	0.271	0.068700	0.486500	(Shi and Li, 2023)
R124	3.243	3.370	175.847	0.127	395.425	3.624	0.269	0.036700	0.397200	(Shi and Li, 2023)
R123	3.199	3.541	204.313	0.127	456.831	3.662	0.268	0.037700	0.372200	(Shi and Li, 2023)
CFCs										
R12	2.347	3.584	197.861	0.131	385.120	4.136	0.276	0.046950	0.633530	(Shi and Li, 2023)
R11	2.430	3.707	238.091	0.131	471.110	4.408	0.279	0.090265	0.634548	(Shi and Li, 2023)
R13	2.308	3.396	156.394	0.131	302.000	3.879	0.277	-0.026840	0.549830	This study
R115	2.904	3.546	164.619	0.128	353.100	3.129	0.268	0.030000	0.657700	(Shi and Li, 2023)
R114	2.930	3.692	194.505	0.128	418.830	3.257	0.276	-0.088300	0.195200	(Shi and Li, 2023)
R113	2.958	3.818	225.325	0.128	487.210	3.392	0.280	-0.142530	0.000010	This study
Fluorocarbons										
R14	2.341	3.109	117.008	0.131	227.510	3.750	0.279	-0.219950	0.392540	This study
R116	2.969	3.335	135.308	0.128	293.030	3.048	0.282	-0.208000	-0.000030	This study
R218	3.470	3.491	149.203	0.126	345.020	2.640	0.276	-0.261190	0.000020	This study
RC318	3.773	3.461	162.457	0.124	388.380	2.778	0.278	-0.166360	0.000040	This study
Acids										
Acetic anhydride	4.522	3.316	236.913	0.125	606.000	4.020	0.235	0.035127	0.230275	This study
Others										
Ethylene oxide	2.495	3.116	234.201	0.133	469.000	7.220	0.255	0.067547	0.392476	This study
Dimethyl sulfoxide	3.139	3.606	328.677	0.124	706.900	5.847	0.232	0.087899	0.639375	This study

4.3.2 Example Applications

In this section, we present three examples from different chemical families illustrating the PVT relationship calculated by the VTR-PC-SAFT EOS. One substance selected is hexane from the *n*-alkanes family, while the other two are neopentane and 1,1,1-Trifluoroethane from the branched alkanes family and haloalkanes family, respectively.

Fig. 4-1, **Fig. 4-2**, and **Fig. 4-3** compare the pressure-density two-phase envelopes of hexane, neopentane, and 1,1,1-Trifluoroethane calculated by various PC-SAFT-type EOSs against the experimental data. As shown in **Fig. 4-1**, **Fig. 4-2**, and **Fig. 4-3,** for hexane, neopentane, and 1,1,1-Trifluoroethane, the saturated-liquid density predicted by CPPC-SAFT EOS significantly deviates from the experimental data. With the introduction of the constant volume translation strategy, I-PC-SAFT EOS shows improved performance in predicting saturated-liquid density compared to CPPC-SAFT EOS. Furthermore, with the adoption of the distance-function-based volume translation, the saturation curve yielded by VTR-PC-SAFT EOS shows a particularly good match with the experimental one in both critical and non-critical regions. In addition, among the different versions of PC-SAFT EOS, only VTR-PC-SAFT EOS can exactly reproduce the experimental critical temperature, experimental critical pressure, and experimental critical molar volume.

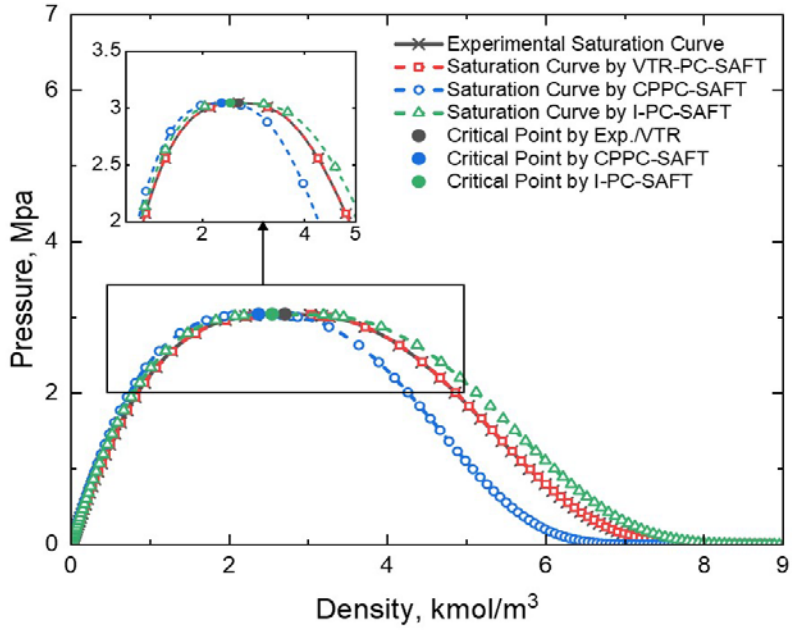

Fig. 4-1. Comparison between the pressure-density two-phase envelopes of hexane calculated by different PC-SAFT-type EOSs and the experimental one.

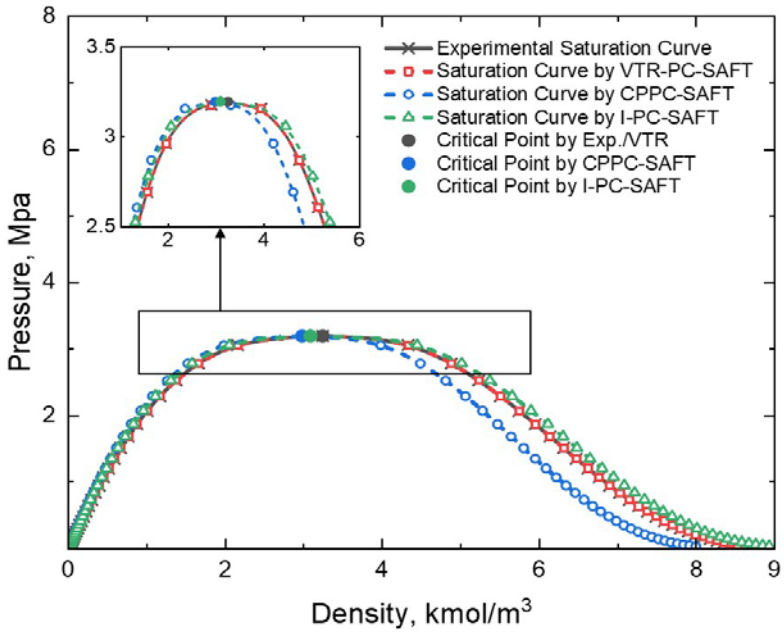

Fig. 4-2. Comparison between the pressure-density two-phase envelopes of neopentane calculated by different PC-SAFT-type EOSs and the experimental one.

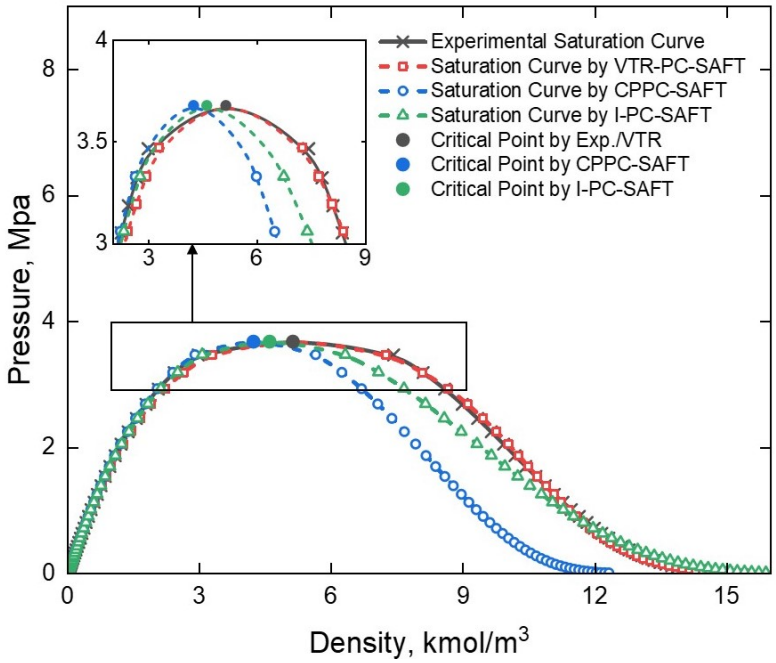

Fig. 4-3. Comparison between the pressure-density two-phase envelopes of 1,1,1-Trifluoroethane calculated by different PC-SAFT-type EOSs and the experimental one.

Fig. 4-4, Fig. 4-5, and **Fig. 4-6** further compare the pressure-density diagrams and isotherms calculated by VTR-PC-SAFT EOS against the experimental data for hexane,

neopentane, and 1,1,1-Trifluoroethane respectively. It can be clearly seen that the VTR-PC-SAFT EOS can generally well represent the phase behavior of these three compounds, whether near or away from the critical region. In addition, as illustrated in **Fig. 4-4**, **Fig. 4-5**, and **Fig. 4-6**, the VTR-PC-SAFT EOS can provide more precise estimations of isotherms at various constant temperatures when compared to both CPPC-SAFT EOS and I-PC-SAFT EOS. Specifically, **Table 4-A1** presents the detailed %AADs in non-critical property predictions (i.e., V_{SatL}, V_{SatV}, V_{Vap}, V_{Liq}, V_{SC}, and P_{Sat}) and %ADs in critical property predictions (i.e., T_c, P_c, and V_c) yielded by VTR-PC-SAFT EOS for the compounds covered in this study. Note that the %AADs and %ADs in predicting different properties by CPPC-SAFT EOS and I-PC-SAFT EOS can be found in **Table 4-A2** and **Table 4-A3**. Taking hexane, neopentane, and 1,1,1-Trifluoroethane as examples, we can see from **Table 4-A1**, **Table 4-A2**, and **Table 4-A3** that VTR-PC-SAFT EOS yields significantly more accurate reproduction of saturated-liquid molar volume (V_{SatL}), liquid molar volume (V_{Liq}), and vapor pressure (P_{Sat}) than the other counterpart models. Furthermore, it is evident that the three critical-point based PC-SAFT EOSs yield similar %AADs for the saturated-vapor molar volume (V_{SatV}) and supercritical molar volume (V_{SC}). However, the VTR-PC-SAFT EOS demonstrates a slightly diminished accuracy in reproducing the vapor molar volume (V_{Vap}). Again, only the VTR-PC-SAFT can exactly reproduce the experimental critical temperature, experimental critical pressure, and experimental critical molar volume.

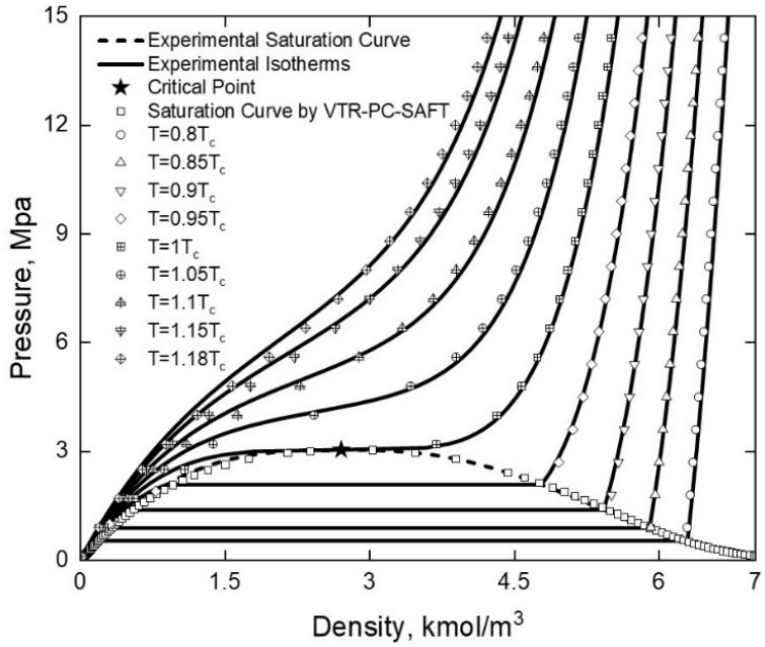

Fig. 4-4. Comparison between the pressure-density diagram and isotherms of hexane calculated by VTR-PC-SAFT EOS and the experimental data.

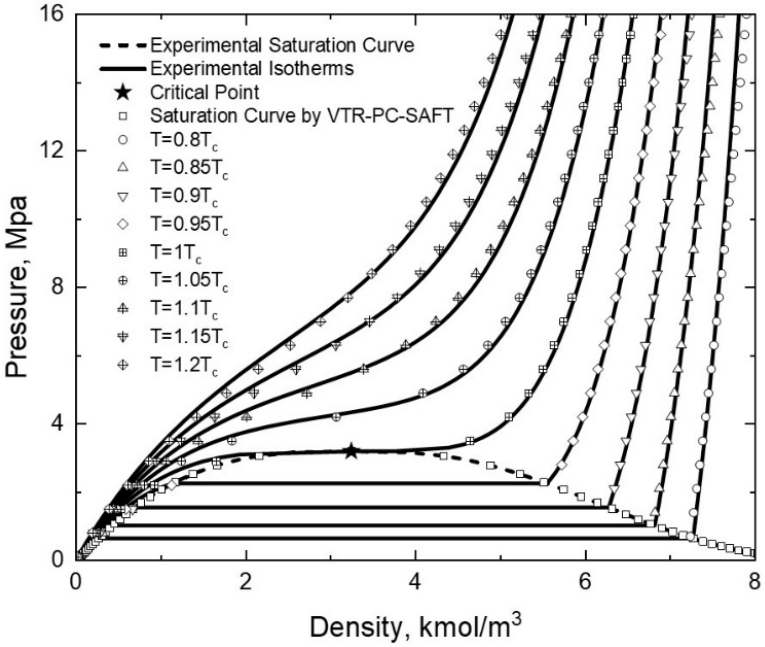

Fig. 4-5. Comparison between the pressure-density diagram and isotherms of neopentane calculated by VTR-PC-SAFT EOS and the experimental data.

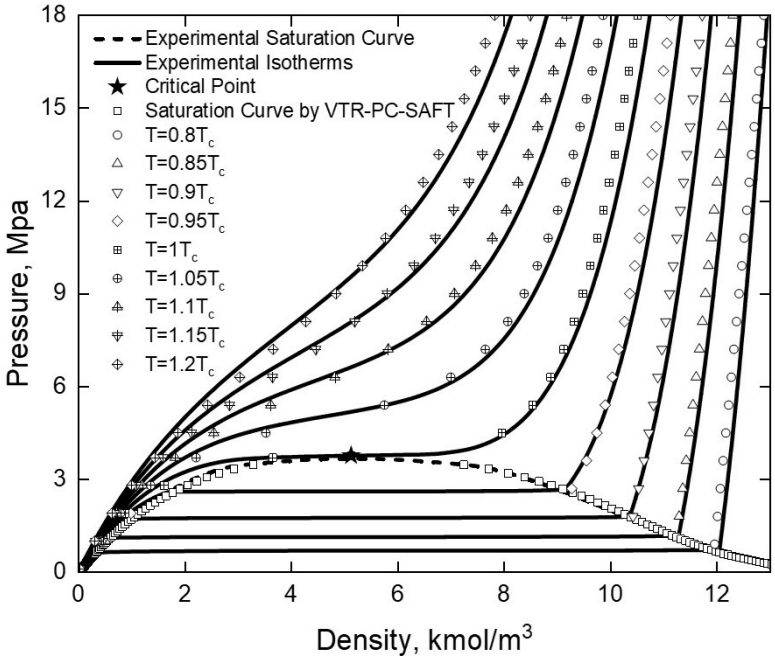

Fig. 4-6. Comparison between the pressure-density diagram and isotherms of 1,1,1-Trifluoroethane calculated by VTR-PC-SAFT EOS and the experimental data.

4.3.3 Overall Prediction Accuracy

Table 4-3 presents %AADs in non-critical property predictions and %ADs in critical property predictions yielded by the VTR-PC-SAFT EOS for the 20 chemical families, while **Table 4-A4** and **Table 4-A5** presents the detailed %AADs in reproducing non-critical properties and %ADs in reproducing critical properties by CPPC-SAFT EOS and I-PC-SAFT EOS, respectively. As seen from **Table 4-3**, VTR-PC-SAFT EOS yields a fairly good prediction of both critical and non-critical properties for the majority of the chemical families. But it yields relatively higher deviations in producing saturated-vapor density for some chemical families.

Table 4-3. %AADs in non-critical property predictions and %ADs in critical property predictions yielded by the VTR-PC-SAFT EOS for 20 chemical families.

Chemical groups	Number of compounds	%AADs in non-critical properties						%ADs in critical properties		
		V_{SatL}	V_{SatV}	P_{Sat}	V_{Liq}	V_{Vap}	V_{SC}	T_c	P_c	V_c
n-Alkanes	20	0.972	3.819	3.392	0.744	3.443	2.362	0	0	0

Branched alkanes	25	1.002	4.749	2.116	0.826	1.689	3.342	0	0	0
Cycloalkanes	12	1.116	4.749	3.774	1.073	1.792	2.156	0	0	0
Olefins	38	1.112	4.477	3.744	0.683	1.944	2.138	0	0	0
Alkynes	14	1.536	7.435	5.231	1.091	1.479	4.115	0	0	0
Aromatics	24	1.015	4.968	2.192	0.762	1.712	3.131	0	0	0
Ketones	14	1.436	5.028	3.451	1.219	3.297	-	0	0	0
Permanent gases	14	0.551	2.857	1.123	0.649	1.146	1.846	0	0	0
Ethers	6	0.708	7.466	3.688	0.606	0.970	-	0	0	0
Esters	8	1.138	5.828	3.858	0.939	2.283	-	0	0	0
Aldehydes	1	1.054	5.050	8.690	4.885	-	-	0	0	0
Sulfides and Thiols	18	1.390	6.269	2.391	-	2.087	-	0	0	0
Halogenated Hydrocarbons	24	1.170	5.179	1.798	1.634	1.507	4.267	0	0	0
Heterocyclics	6	1.371	4.753	3.329	0.961	0.863	-	0	0	0
HFCs	8	0.726	3.160	1.140	1.237	4.232	5.443	0	0	0
HCFCs	6	0.470	2.935	1.419	0.805	2.752	3.457	0	0	0
CFCs	6	0.429	4.738	0.993	1.154	3.449	3.584	0	0	0
Fluorocarbons	4	0.811	4.120	0.230	2.218	3.672	3.927	0	0	0
Acids	1	1.012	3.533	1.834	-	2.881	-	0	0	0
Others	2	2.376	5.730	3.245	3.317	0.708	-	0	0	0
Overall %AAD	251	1.074	4.864	2.784	0.925	2.086	2.392	0	0	0

Table 4-4 presents the overall %AADs for non-critical property predictions and %ADs for critical property predictions yielded by the various PC-SAFT EOSs. Among the four PC-SAFT-type EOSs (i.e., PC-SAFT EOS, I-PC-SAFT EOS, CPPC-SAFT EOS, and VTR-PC-SAFT), the VTR-PC-SAFT EOS demonstrates the best prediction accuracy for the 251 substances examined in this study. Specifically, it yields %AADs of 1.074, 0.925, 2.392, and 2.784 in predicting the saturated-liquid molar volume, liquid molar volume, supercritical molar volume, and vapor pressure, respectively. In contrast, the PC-SAFT EOS, CPPC-SAFT EOS, and I-PC-SAFT show larger deviations when reproducing these properties. Furthermore, the VTR-PC-SAFT EOS can exactly reproduce the experimental critical temperature, experimental critical pressure, and experimental critical molar volume. In addition, some researchers present that the PC-SAFT-type EOSs could have a significantly different performance in reproducing thermophysical properties of

non-self-associating and self-associating compounds. Taking the I-PC-SAFT EOS as an example, it appears to provide more accurate predictions for the thermodynamic properties of non-self-associating compounds than for self-associating compounds (Ramírez-Vélez *et al.*, 2022). In this study, we evaluate the efficacy of the VTR-PC-SAFT in reproducing the thermophysical properties of both non-self-associating and self-associating compounds. The results suggest that VTR-PC-SAFT EOS demonstrates good performance in predicting the thermophysical properties of both compound types, although the association contribution is not considered in the current version of VTR-PC-SAFT EOS.

Table 4-4. Overall %AADs in non-critical property predictions and %ADs in critical property predictions yielded by different PC-SAFT EOSs for 251 individual substances.

EOSs	%AADs in non-critical properties						%ADs in critical properties		
	V_{SatL}	V_{SatV}	P_{Sat}	V_{Liq}	V_{Vap}	V_{SC}	T_c	P_c	V_c
CPPC-SAFT	17.641	3.565	3.062	14.203	1.499	6.658	0	0	17.586
I-PC-SAFT	4.805	4.046	2.923	3.625	1.695	2.464	0	0	10.695
PC-SAFT	2.052	3.662	3.742	2.874	1.985	2.447	2.322	12.001	4.453
VTR-PC-SAFT	1.074	4.864	2.784	0.925	2.086	2.392	0	0	0

Fig. 4-7 presents a radar chart highlighting the overall prediction accuracy of various properties yielded by the four PC-SAFT-type EOSs. It can be seen from **Fig. 4-7** that the VTR-PC-SAFT EOS occupies the smallest area in the radar chart, further solidifying the conclusion that it significantly outperforms the other three EOS models.

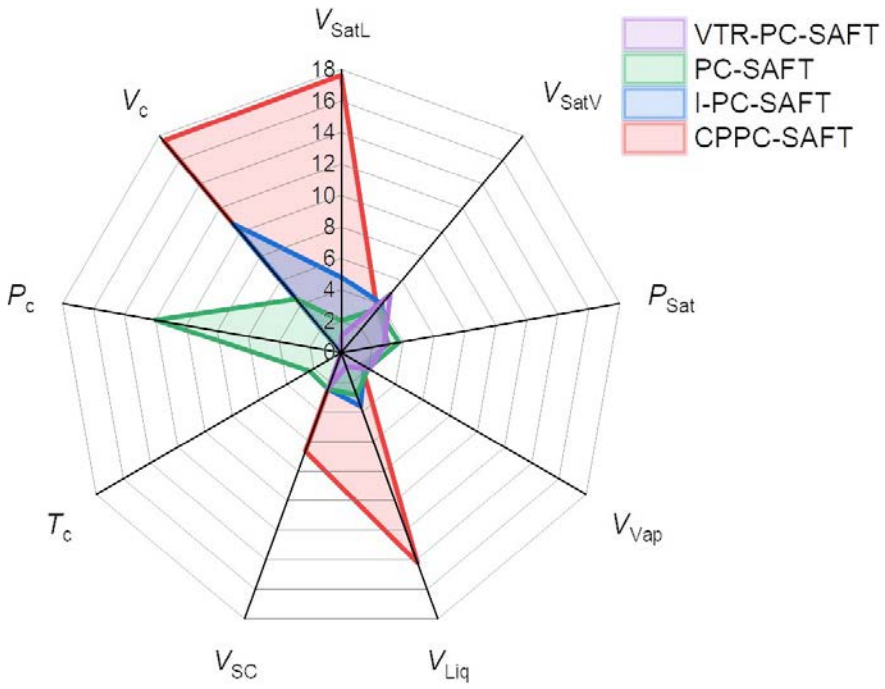

Fig. 4-7. Radar chart showing the overall prediction accuracy (%AAD) of the various properties of the 251 compounds yielded by different PC-SAFT-type EOSs.

4.4 Conclusions

In this study, we regress the two component-dependent parameters (c_1 and c_2) in the distance-function-based volume translation in the VTR-PC-SAFT EOS for a diverse group of chemical species. The VTR-PC-SAFT EOS is then applied to reproduce both non-critical and critical properties of 251 chemical compounds. Overall, VTR-PC-SAFT EOS can yield a significantly higher accuracy in predicting both non-critical and critical properties for the majority of the 251 chemical compounds in comparison to the other three PC-SAFT-type EOSs. For the non-critical properties, the VTR-PC-SAFT EOS achieves the smallest %AADs when predicting saturated-liquid molar volume, liquid molar volume, supercritical molar volume, and vapor pressure. While all the four PC-SAFT-type EOSs yield similar %AADs for the saturated-vapor molar volume, the VTR-PC-SAFT EOS has

a marginally lower accuracy in replicating the vapor molar volume than the other three PC-SAFT-type EOSs. For critical properties, only the VTR-PC-SAFT EOS can exactly reproduce the experimental critical temperature, experimental critical pressure, and experimental critical molar volume.

References

A. Pakravesh, F. Zarei, H. Zarei, PρT parameterization of SAFT equation of state: developing a new parameterization method for equations of state, *Fluid Phase Equilibria* 538 (2021) 113024.

A. Peneloux, E. Rauzy, R. Freze, A consistent correction for Redlich-Kwong-Soave volumes, *Fluid Phase Equilibria* 8 (1982) 7–23.

A. Piña-Martinez, R. Privat, J.N. Jaubert, Use of 300,000 pseudo-experimental data over 1800 pure fluids to assess the performance of four cubic equations of state: SRK, PR, tc-RK, and tc-PR, *AIChE Journal* 68 (2022) e17518.

A.M. Abudour, S.A. Mohammad, R.L. Robinson, K.A.M. Gasem, Volume translated Peng-Robinson equation of state for saturated and single-phase liquid densities, *Fluid Phase Equilibria* 335 (2012) 74–87.

A.M. Palma, A.J. Queimada, J.A. Coutinho, Using a volume shift in perturbed-chain statistical associating fluid theory to improve the description of speed of sound and other derivative properties, *Industrial & Engineering Chemistry Research* 57 (2018) 11804-11814.

D.V. Nichita, F. García-Sánchez, and S. Gómez, Phase stability analysis using the PC-SAFT equation of state and the tunneling global optimization method, *Chemical Engineering Journal* 140 (2008) 509-520.

D.Y. Peng, D.B. Robinson, A new two-constant equation of state, *Industrial & Engineering Chemistry Fundamentals* 15 (1976) 59-64.

DIPPR's Project 801 Database. DIPPR: Design Institute for Physical Properties, 2021. https://www.aiche.org/dippr.

E. Moine, A. Piña-Martinez, J.N. Jaubert, B. Sirjean, R. Privat, I-PC-SAFT: an industrialized version of the volume-translated PC-SAFT equation of state for pure components, resulting from experience acquired all through the years on the parameterization of Saft-type and cubic models, *Industrial & Engineering Chemistry Research* 58 (2019) 20815-20827.

E.A. Müller, K.E. Gubbins, Molecular-based equations of state for associating fluids: A review of SAFT and related approaches, *Industrial & Engineering Chemistry Research* 40 (2001) 2193-2211.

F. Llovell, J.C. Pàmies, L.F. Vega, Thermodynamic properties of Lennard-Jones chain molecules: Renormalization-group corrections to a modified statistical associating fluid theory, *The Journal of Chemical Physics* 121 (2004) 10715-10724.

F. Llovell, L.F. Vega, Global fluid phase equilibria and critical phenomena of selected mixtures using the crossover soft-SAFT equation, *The Journal of Physical Chemistry B* 110 (2006) 1350-1362.

F. Llovell, L.F. Vega, M.A. Anisimov, J.V. Sengers, Incorporating critical divergence of isochoric heat capacity into the soft-SAFT equation of state, *AIChE Journal* 61(2015) 3073-3080.

G. Soave, Equilibrium constants from a modified Redlich–Kwong equation of state, *Chemical Engineering Science* 27 (1972) 1197-1203.

G.M. Kontogeorgis, X. Liang, A. Alay, T. Ioannis, Equations of state in three centuries. Are we closer to arriving to a single model for all applications? *Chemical Engineering Science: X* 7 (2020) 100060.

I. Anoune, Z. Mimoune, H. Madani, A. Merzougui, New modified PC-SAFT pure component parameters for accurate VLE and critical phenomena description, *Fluid Phase Equilibria* 532 (2021) 112916.

I. Polishuk I, A. Chiko, E. Cea-Klapp, J.M. Garrido, Implementation of CP-PC-SAFT and CS-SAFT-VR-Mie for predicting thermodynamic properties of C1–C3 halocarbon systems. I. Pure compounds and mixtures with non-associating compounds, *Industrial & Engineering Chemistry Research* 60 (2021) 9624-9636.

I. Polishuk, H. Lubarsky, D. NguyenHuynh, Predicting phase behavior in aqueous systems without fitting binary parameters II: Gases and non-aromatic hydrocarbons, *AIChE Journal* 63 (2017) 5064-5075.

I. Polishuk, Standardized critical point-based numerical solution of statistical association fluid theory parameters: the perturbed chain-statistical association fluid theory equation of state revisited, *Industrial & Engineering Chemistry Research* 53 (2014) 14127-14141.

I. Polishuk, Y. Sidik, D. NguyenHuynh, Predicting phase behavior in aqueous systems without fitting binary parameters I: CP-PC-SAFT EOS, Aromatic Compounds, *AIChE Journal* 63 (2017) 4124-4135.

J. Gross, G. Sadowski, Perturbed-chain SAFT: An equation of state based on a perturbation theory for chain molecules, *Industrial & Engineering Chemistry Research* 40 (2001) 1244−1260.

J. Shi, H. Li, An improved volume translation model for PC-SAFT EOS based on a distance function, *Chemical Engineering Science* 276 (2023) 118800.

J. Shi, H. Li, Modified temperature-dependent volume translation model in PC-SAFT equation of state for carbon dioxide, *Chemical Engineering Science* 263 (2022) 118107.

J. Shi, H.A. Li, Criterion for determining crossover phenomenon in volume-translated equation of states, *Fluid Phase Equilibria* 430 (2016) 1-12.

J. Shi, H.A. Li, W. Pang, An improved volume translation strategy for PR EOS without crossover issue, *Fluid Phase Equilibria* 470 (2018) 164-175.

J.A. Barker, D. Henderson, Perturbation theory and equation of state for fluids: the square-well potential, *The Journal of Chemical Physics* 47 (1967) 2856-2861.

J.A. Barker, D. Henderson, Perturbation theory and equation of state for fluids. II. A successful theory of liquids, *The Journal of Chemical Physics* 47 (1967) 4714-4721.

M. Cismondi, E.A. Brignole, J. Mollerup, Rescaling of three-parameter equations of state: PC-SAFT and SPHCT, *Fluid Phase Equilibria* 234 (2005) 108-121.

M. Yang, T. Zhan, Y. Su, A. Dong, M. He, Y. Zhang, Crossover PC-SAFT equations of state based on White's method for the thermodynamic properties of CO2, *n*-alkanes and *n*-alkanols, *Fluid Phase Equilibria* 564 (2023) 113610.

N. Ramírez-Vélez, R. Privat, A. Piña-Martinez, J.N. Jaubert, Assessing the performance of non-associating SAFT-type equations of state to reproduce vapor pressure, liquid density, enthalpy of vaporization, and liquid heat capacity data of 1800 pure fluids, *AIChE Journal* 68 (2022) e17722.

O. Pfohl, T. Giese, R. Dohrn, G. Brunner, 1. Comparison of 12 equations of state with respect to gas-extraction processes: reproduction of pure-component properties when enforcing the correct critical temperature and pressure, *Industrial & Engineering Chemistry Research* 37 (1998) 2957-2965.

P. Navarro, A.M. Palma, J. García, F. Rodríguez, J.A. Coutinho, P.J. Carvalho, High-pressure density of bis(1-alkyl-3-methylimidazolium) tetraisothiocyanatocobaltate ionic liquids: experimental and PC-SAFT with volume-shift modeling, *Journal of Chemical & Engineering Data* 64 (2019) 4827-4833.

P.J. Linstrom, W.G. Mallard, NIST Chemistry WebBook, NIST Standard Reference Database Number 69, National Institute of Standards and Technology, Gaithersburg, MD, 20899, http://webbook.nist.gov.

P.N. Ghoderao, V.H. Dalvi, M. Narayan, A five-parameter cubic equation of state for pure fluids and mixtures, *Chemical Engineering Science: X* 3 (2019) 100026.

P.N. Ghoderao, V.H. Dalvi, M. Narayan, A four-parameter cubic equation of state for pure compounds and mixtures, *Chemical Engineering Science* 190 (2018) 173-189.

R. Privat, E. Moine, B. Sirjean, R. Gani, J.N. Jaubert, Application of the corresponding-state law to the parametrization of statistical associating fluid theory (SAFT)-type models: Generation and use of "generalized charts", *Industrial & Engineering Chemistry Research* 58 (2019) 9127-9139.

S. Dufal, T. Lafitte, A. Galindo, G. Jackson, A.J. Haslam, Developing intermolecular-potential models for use with the SAFT-VR Mie equation of state, *AIChE Journal* 61(2015) 2891-2912.

S.A.M. Smith, J.T. Cripwell, C.E. Schwarz, Application of renormalization corrections to SAFT-VR Mie, *Industrial & Engineering Chemistry Research* 61 (2022) 12797-12812.

T. Esper, G. Bauer, P. Rehner, J. Gross, PCP-SAFT parameters of pure substances using large experimental databases, *Industrial & Engineering Chemistry Research* 62 (2023) 15300-15310.

T. Lafitte, A. Apostolakou, C. Avendaño, A. Galindo, C.S. Adjiman, E.A. Müller, G. Jackson, Accurate statistical associating fluid theory for chain molecules from Mie segments, *The Journal of Chemical Physics* 139 (2013) 154504.

W.G. Chapman, K.E. Gubbins, G. Jackson, M. Radosz, SAFT: equation-of-state solution model for associating fluids, *Fluid Phase Equilibria* 52 (1989) 31-38.

X. Chen, H. Li, An improved volume-translated SRK EOS dedicated to more accurate determination of saturated and single-phase liquid densities, *Fluid Phase Equilibria* 521 (2020) 112724.

Y.S. Wei, R.J. Sadus, Equations of state for the calculation of fluid-phase equilibria, *AIChE Journal* 46 (2000) 169-196.

Appendices of Chapter 4

4-A.1 Detailed %AADs in reproducing non-critical properties and %ADs in reproducing critical properties by VTR-PC-SAFT EOS, CPPC-SAFT EOS, and I-PC-SAFT EOS

This section presents the detailed %AADs in reproducing the non-critical properties and %ADs in reproducing the critical properties for 251 substances by VTR-PC-SAFT EOS, CPPC-SAFT EOS (Anoune *et al.*, 2021) and I-PC-SAFT EOS (Moine *et al.*, 2019), respectively.

Table 4-A1. %AADs in non-critical property predictions (including saturated-liquid molar volume, saturated-vapor molar volume, liquid molar volume, vapor molar volume, supercritical molar volume, and vapor pressure) as well as %ADs in critical property predictions (including critical temperature, critical pressure, and critical molar volume) yielded by VTR-PC-SAFT EOS for 251 individual compounds.

Compounds	%AADs in non-critical properties						%AD in critical properties		
	V_{SatL}	V_{SatV}	P_{Sat}	V_{Liq}	V_{Vap}	V_{SC}	T_c	P_c	V_c
***n*-Alkanes**									
Methane	0.377	1.379	0.622	0.409	1.013	1.085	0	0	0
Ethane	0.353	2.266	1.407	0.488	1.475	1.341	0	0	0
Propane	0.548	2.081	1.198	0.970	1.989	1.573	0	0	0
Butane	0.663	2.599	1.478	0.666	2.999	1.713	0	0	0
Pentane	0.677	2.454	1.132	0.814	3.472	2.178	0	0	0
Hexane	0.724	2.146	0.932	0.675	4.188	1.950	0	0	0
Heptane	0.782	2.258	1.186	0.801	4.859	2.849	0	0	0
Octane	1.085	6.105	6.255	1.068	4.642	3.644	0	0	0
Nonane	0.666	2.265	1.396	0.651	4.689	2.149	0	0	0
Decane	0.901	2.456	1.806	1.050	5.970	4.350	0	0	0
Undecane	2.187	2.634	5.503	-	-	-	0	0	0
Dodecane	0.868	3.686	3.231	0.911	5.247	3.145	0	0	0
Tridecane	0.820	4.614	5.889	0.578	-	-	0	0	0
Tetradecane	0.764	7.539	5.603	-	3.037	-	0	0	0
Pentadecane	0.927	4.214	5.150	0.437	-	-	0	0	0
Hexadecane	0.570	5.581	3.124	0.807	-	-	0	0	0
Heptadecane	0.736	5.106	5.226	0.736	-	-	0	0	0
Octadecane	3.269	5.304	4.799	-	-	-	0	0	0

Nonadecane	1.724	5.404	6.158	-	1.173	-	0	0	0
Eicosane	0.796	6.285	5.761	0.840	-	-	0	0	0
Branched alkanes									
Isobutane	0.565	1.596	0.631	0.701	2.615	2.529	0	0	0
Isopentane	0.671	2.175	1.027	0.772	3.018	3.544	0	0	0
Neopentane	0.357	1.956	0.306	0.893	2.887	3.009	0	0	0
2-Methylpentane	1.779	5.778	5.798	1.784	3.098	4.287	0	0	0
2.3-Dimethylbutane	0.654	4.410	1.171	0.974	0.864	-	0	0	0
3-Methylpentane	0.543	5.446	0.577	0.452	1.048	-	0	0	0
2,3-Dimethylpentane	0.745	2.970	1.215	0.414	-	-	0	0	0
2,2,3,3-Tetramethylbutane	1.470	2.520	1.558	0.871	0.507	-	0	0	0
2,2,4-Trimethylpentane	0.653	5.541	0.778	0.570	-	-	0	0	0
2,3,3-Trimethylpentane	0.643	1.898	0.479	-	2.012	-	0	0	0
4-Methylheptane	0.760	4.862	2.079	-	-	-	0	0	0
4-Methylnonane	2.741	6.172	4.476	-	2.457	-	0	0	0
4-Methyloctane	1.124	5.215	4.419	-	-	-	0	0	0
5-Methylnonane	2.458	2.783	8.582	-	2.482	-	0	0	0
3-Methyloctane	1.006	6.282	1.319	-	-	-	0	0	0
3-Methylnonane	1.252	5.776	2.525	-	-	-	0	0	0
3-Methylhexane	0.756	5.096	1.737	-	0.699	-	0	0	0
3-Methylheptane	0.814	5.702	1.486	-	1.558	-	0	0	0
3-Methyl-3-ethylpentane	0.703	5.593	1.165	-	1.051	-	0	0	0
3-Ethylhexane	0.667	5.612	1.572	-	1.579	-	0	0	0
3,4-Dimethylhexane	0.747	5.212	1.224	-	1.429	-	0	0	0
3,3-Dimethylpentane	0.937	6.040	0.723	-	0.736	-	0	0	0
3,3-Dimethylhexane	0.847	7.087	0.822	-	1.232	-	0	0	0
3,3-Diethylpentane	1.297	7.668	1.546	-	1.125	-	0	0	0
3,3,5-Trimethylheptane	0.868	5.332	5.691	-	-	-	0	0	0
Cycloalkanes									
Cyclopropane	0.201	1.884	0.690	0.369	2.160	3.582	0	0	0
Cyclobutane	2.739	9.634	4.921	-	0.918	-	0	0	0
Cyclopentane	0.670	0.918	0.930	0.800	1.191	0.504	0	0	0
Cyclohexane	0.257	1.691	0.747	0.679	2.783	2.383	0	0	0
Methylcyclopentane	0.758	4.903	1.344	0.834	1.067	-	0	0	0
Ethylcyclopentane	0.800	4.954	0.538	-	0.904	-	0	0	0
Methylcyclohexane	0.717	1.976	1.326	0.958	4.235	-	0	0	0
1,1-Dimethylcyclohexane	1.177	6.876	5.908	-	1.825	-	0	0	0
cis-1,2-Dimethylcyclohexane	1.001	6.425	8.912	-	1.852	-	0	0	0
trans-1,2-Dimethylcyclohexane	0.894	4.605	6.289	-	1.663	-	0	0	0
Ethylcyclohexane	2.088	6.819	8.032	1.633	1.825	-	0	0	0
Propylcyclohexane	2.084	6.302	5.652	2.239	1.089	-	0	0	0
Olefins									

Ethylene	0.191	1.185	0.422	0.489	9.490	1.856	0	0	0
Propylene	0.593	1.261	0.403	0.537	2.030	2.077	0	0	0
Butene	0.628	1.455	0.540	0.755	2.528	2.626	0	0	0
Cis-butene	0.637	1.189	0.236	0.608	2.598	2.674	0	0	0
Isobutene	0.551	1.152	0.492	0.615	2.380	2.415	0	0	0
(E)-2-Butene	0.475	5.103	3.693	0.610	1.374	1.178	0	0	0
1-Pentene	0.763	4.572	2.236	0.368	1.296	-	0	0	0
Cyclohexene	1.897	2.376	1.183	-	-	-	0	0	0
1-Hexene	0.689	3.849	0.981	0.747	9.683	-	0	0	0
1-Heptene	1.313	6.444	2.008	0.907	-	-	0	0	0
1-Octene	0.583	5.698	1.432	0.448	2.138	-	0	0	0
1-Nonene	0.756	6.335	0.644	0.982	1.716	-	0	0	0
1-Decene	1.040	4.950	1.376	-	-	-	0	0	0
2-Methyl-1-butene	0.989	5.589	2.785	-	1.658	-	0	0	0
2-Methyl-2-butene	1.947	6.119	4.444	-	-	-	0	0	0
1-Methylcyclopentene	2.414	5.966	2.195	-	0.931	-	0	0	0
3-Methylcyclopentene	1.640	13.649	6.092	-	-	-	0	0	0
1,2-Butadiene	1.194	10.238	6.464	-	1.222	-	0	0	0
1,3-Butadiene	0.492	5.120	1.884	-	0.665	-	0	0	0
3-Methyl-1,2-butadiene	1.299	8.528	6.868	-	1.989	-	0	0	0
4-Methyl-1-hexene	1.326	1.730	5.040	-	-	-	0	0	0
4-Methyl-1-pentene	1.039	4.893	2.148	1.135	0.674	-	0	0	0
4-Methyl-cis-2-pentene	1.295	3.670	6.849	-	1.463	-	0	0	0
4-Methylcyclopentene	1.239	8.666	5.918	-	0.836	-	0	0	0
4-Methyl-trans-2-pentene	1.494	4.173	7.971	-	1.462	-	0	0	0
5-Methyl-1-hexene	1.100	6.674	0.862	-	1.031	-	0	0	0
6-Methyl-1-heptene	0.794	2.762	4.969	-	-	-	0	0	0
3-Methyl-trans-2-pentene	2.743	8.092	8.246	-	2.002	-	0	0	0
3-Methyl-cis-2-pentene	0.976	8.921	18.541	-	1.532	-	0	0	0
3-Methyl-1-pentene	1.287	2.323	3.310	-	0.675	-	0	0	0
3-Methyl-1-hexene	1.223	1.674	3.107	-	0.847	-	0	0	0
3-Methyl-1-butene	0.449	4.099	1.320	-	0.661	-	0	0	0
3-Methyl-1,4-pentadiene	1.334	1.963	8.465	-	0.899	-	0	0	0
3-Ethyl-1-pentene	1.110	0.732	3.364	-	0.746	-	0	0	0
3-Ethyl-1-hexene	1.252	3.643	1.119	-	-	-	0	0	0
3,3-Dimethyl-1-butene	0.916	1.834	6.349	-	0.663	-	0	0	0
2-Ethyl-1-pentene	1.306	2.260	2.760	-	-	-	0	0	0
2-Ethyl-1-butene	1.290	1.253	5.568	-	1.199	-	0	0	0
Alkynes									
1-Propyne	0.364	1.868	0.463	0.608	1.659	4.115	0	0	0
1-Butyne	1.411	5.207	2.246	-	3.164	-	0	0	0
2-Butyne	2.348	5.219	3.539	1.574	1.049	-	0	0	0

1-Pentyne	1.183	8.518	8.984	-	0.418	-	0	0	0
2-Pentyne	1.368	7.215	8.399	-	1.379	-	0	0	0
1-Hexyne	2.157	8.321	5.841	-	2.339	-	0	0	0
1-Heptyne	1.526	13.851	2.528	-	2.595	-	0	0	0
1-Octyne	1.585	9.185	3.800	-	-	-	0	0	0
1-Nonyne	1.331	9.042	2.958	-	-	-	0	0	0
1-Decyne	0.489	11.052	7.467	-	-	-	0	0	0
Vinylacetylene	2.272	4.612	6.129	-	0.962	-	0	0	0
2-Methyl-1-butene-3-yne	1.885	8.761	8.147	-	0.639	-	0	0	0
3-Methyl-1-butyne	2.487	9.416	7.170	-	0.113	-	0	0	0
2-Ethylnaphthalene	1.097	1.823	5.566	-	1.955	-	0	0	0
Aromatics									
Benzene	0.368	1.839	0.688	0.754	3.116	2.967	0	0	0
Toluene	0.820	1.373	0.582	0.879	2.659	3.295	0	0	0
Ethylbenzene	0.782	4.602	1.029	0.609	1.624	-	0	0	0
m-Xylene	0.586	4.049	0.552	0.376	0.657	-	0	0	0
o-Xylene	0.725	4.757	0.741	0.581	0.803	-	0	0	0
p-Xylene	0.540	5.593	0.567	0.689	1.756	-	0	0	0
Naphthalene	0.618	3.197	0.416	-	2.136	-	0	0	0
Biphenyl	1.593	5.822	3.444	1.119	2.983	-	0	0	0
Anthracene	0.743	-	1.553	-	-	-	0	0	0
Styrene	3.061	4.001	1.599	-	1.368	-	0	0	0
alpha-Methylstyrene	0.855	9.724	7.385	-	2.801	-	0	0	0
Cumene	0.808	4.043	2.134	0.420	1.549	-	0	0	0
Propylbenzene	0.684	5.548	0.692	0.366	2.486	-	0	0	0
1,2,3-Trimethylbenzene	0.926	7.209	1.476	-	1.430	-	0	0	0
1,2,4-Trimethylbenzene	1.160	7.261	1.425	0.570	1.381	-	0	0	0
1,2,3,4-Tetrahydronaphthalene	1.695	5.790	1.569	0.951	0.970	-	0	0	0
Butylbenzene	0.722	3.582	0.589	0.244	0.886	-	0	0	0
Phenanthrene	1.103	13.039	6.914	2.345	0.547	-	0	0	0
4-Ethyl-m-xylene	1.286	2.352	1.962	-	1.658	-	0	0	0
4-Ethyl-o-xylene	1.020	2.731	3.862	-	-	-	0	0	0
5-Ethyl-m-xylene	1.547	4.197	4.148	-	-	-	0	0	0
3-Ethyl-o-xylene	0.795	5.533	5.788	-	-	-	0	0	0
2-Ethyl-p-xylene	1.221	2.946	1.937	-	-	-	0	0	0
2-Ethyl-m-xylene	0.710	5.073	1.549	-	-	-	0	0	0
Ketones									
Butanone	0.358	2.668	0.658	1.002	0.923	-	0	0	0
3-Pentanone	1.646	3.838	1.996	1.005	-	-	0	0	0
2-Pentanone	1.954	6.204	2.373	-	8.444	-	0	0	0
3-Methyl-2-butanone	1.808	6.052	2.957	-	0.596	-	0	0	0
Acetone	2.317	5.391	3.071	2.233	4.221	-	0	0	0

Quinone	4.765	-	-	-	1.867	-	0	0	0
2-Hexanone	1.047	3.175	2.273	-	-	-	0	0	0
3-Hexanone	0.851	4.666	1.392	-	-	-	0	0	0
3-Heptanone	0.937	5.254	7.510	-	-	-	0	0	0
2-Heptanone	0.951	5.119	2.902	-	3.265	-	0	0	0
2-Octanone	0.782	5.017	7.648	0.637	4.232	-	0	0	0
4-Heptanone	0.796	4.346	3.418	-	3.215	-	0	0	0
5-Nonanone	0.917	6.751	2.332	-	2.916	-	0	0	0
3-Methyl-2-pentanone	0.974	6.881	6.330	-	-	-	0	0	0
Permanent gases									
Oxygen	0.189	1.728	0.794	0.344	0.299	0.404	0	0	0
Fluorine	0.402	6.609	0.788	1.106	0.319	2.467	0	0	0
Argon	0.046	2.843	0.790	0.632	0.255	0.435	0	0	0
Chlorine	0.813	4.736	2.503	-	0.707	-	0	0	0
Hydrogen sulfide	0.250	0.569	0.356	0.437	0.411	0.749	0	0	0
Carbon disulfide	0.451	3.202	1.837	-	0.736	-	0	0	0
Carbon monoxide	0.204	1.324	0.386	0.454	1.061	0.978	0	0	0
Nitrogen	0.523	1.407	0.492	0.896	1.062	1.474	0	0	0
Carbon dioxide	0.276	2.859	0.339	0.576	2.046	2.092	0	0	0
Sulfur dioxide	0.296	2.401	0.567	0.676	3.402	5.786	0	0	0
Carbonyl sulfide	0.216	2.450	0.633	0.675	1.633	2.229	0	0	0
Hydrogen chloride	1.509	2.989	0.707	1.161	0.878	-	0	0	0
Nitrous oxide	0.185	4.024	1.992	0.185	2.091	-	0	0	0
Ozone	2.358	-	3.536	-	-	-	0	0	0
Ethers									
Diethyl ether	0.694	3.563	2.229	-	1.459	-	0	0	0
Dipropyl ether	0.931	9.295	3.333	-	1.321	-	0	0	0
Methylisobutyl ether	0.655	8.146	6.812	-	0.651	-	0	0	0
Ethylisopropyl ether	0.454	8.007	5.074	-	0.414	-	0	0	0
Diisopropyl ether	0.548	9.395	1.990	0.456	1.004	-	0	0	0
Dinbutyl ether	0.968	6.391	2.694	0.757	-	-	0	0	0
Esters									
Methyl ethanoate	0.556	5.160	0.747	1.881	0.799	-	0	0	0
Ethyl ethanoate	0.640	4.331	2.148	0.683	0.858	-	0	0	0
Vinyl acetate	1.188	4.948	7.650	-	-	-	0	0	0
Methyl propionate	1.548	4.479	6.068	-	0.956	-	0	0	0
Ethyl propionate	0.880	5.959	2.535	0.845	0.846	-	0	0	0
Propyl acetate	1.030	6.117	4.882	-	2.320	-	0	0	0
Butyl acetate	0.687	8.299	5.031	0.712	9.034	-	0	0	0
Methyl benzoate	2.573	7.336	1.804	0.574	1.169	-	0	0	0
Aldehydes									
2-Propenal	1.054	5.050	8.690	-	4.885	-	0	0	0

Sulfides and Thiols									
Methanethiol	0.704	3.029	3.190	-	-	-	0	0	0
Ethanethiol	0.734	1.884	1.500	-	0.699	-	0	0	0
2-Thiapropane	0.885	8.344	1.513	-	0.961	-	0	0	0
2-Propanethiol	1.044	1.185	1.733	-	1.482	-	0	0	0
1-Propanethiol	1.547	7.014	0.362	-	0.603	-	0	0	0
3-Thiapentane	0.593	11.826	1.077	-	1.210	-	0	0	0
2,3-Dithiabutane	1.425	0.807	2.856	-	0.647	-	0	0	0
Butyl mercaptan	0.935	4.280	0.710	-	11.591	-	0	0	0
sec-Butyl mercaptan	1.404	1.474	1.749	-	-	-	0	0	0
Pentyl mercaptan	0.888	7.421	1.557	-	0.762	-	0	0	0
Benzenethiol	0.770	8.743	6.466	-	0.930	-	0	0	0
Cyclohexyl mercaptan	0.962	8.763	1.584	-	2.350	-	0	0	0
Hexyl mercaptan	1.560	8.616	0.859	-	2.339	-	0	0	0
Benzyl mercaptan	2.946	10.675	7.144	-	1.385	-	0	0	0
Heptyl mercaptan	1.707	9.142	0.774	-	2.770	-	0	0	0
Octyl mercaptan	2.427	5.479	2.648	-	-	-	0	0	0
Nonyl mercaptan	3.021	6.208	2.633	-	-	-	0	0	0
Decyl mercaptan	1.474	7.951	4.676	-	1.486	-	0	0	0
Halogenated Hydrocarbons									
Fluoromethane	1.057	4.767	3.232	1.455	1.215	5.042	0	0	0
Chloromethane	1.040	1.768	0.703	-	1.436	-	0	0	0
Difluoromethane	1.325	3.640	1.925	1.989	0.685	4.804	0	0	0
1,1-Difluoroethane	1.157	3.122	1.511	1.561	0.681	4.063	0	0	0
Trifluoromethane	0.380	2.925	0.306	1.305	0.659	4.077	0	0	0
1,1,1-Trifluoroethane	0.741	1.980	0.227	1.488	0.617	2.715	0	0	0
Dichloromethane	1.033	4.101	3.685	2.301	1.351	-	0	0	0
Tetrafluoromethane	1.098	6.349	0.218	1.828	0.455	3.284	0	0	0
Bromomethane	1.649	8.528	5.031	-	1.117	-	0	0	0
1,1,1,2-Tetrafluoroethane	0.250	2.891	0.558	1.836	0.924	5.202	0	0	0
Trichloromethane	4.303	1.584	1.907	-	0.529	-	0	0	0
Dichlorodifluoromethane	0.735	4.962	0.345	2.930	0.574	4.950	0	0	0
1,1,2-Trichloroethane	0.541	8.621	4.686	0.306	2.675	-	0	0	0
1,2-Dibromoethane	1.033	11.485	2.530	-	1.171	-	0	0	0
1,2-Dichloroethane	1.320	-	1.751	1.104	0.784	-	0	0	0
Chloroethane	1.143	2.712	1.348	1.489	0.605	-	0	0	0
1,1-Dichloropropane	0.631	3.434	2.363	-	1.909	-	0	0	0
1,2-Dichloropropane	0.864	9.413	1.333	-	1.801	-	0	0	0
1-Chloropropane	1.391	3.955	3.146	1.662	1.103	-	0	0	0
2-Chloropropane	0.693	4.542	1.544	-	-	-	0	0	0
m-Dichlorobenzene	1.633	6.822	1.106	-	0.864	-	0	0	0
p-Dichlorobenzene	3.233	12.876	1.494	-	11.752	-	0	0	0

Bromobenzene	0.233	5.584	1.374	-	1.166	-	0	0	0
Chlorobenzene	0.603	3.051	0.819	-	0.598	-	0	0	0
Heterocyclics									
Furan	2.028	5.139	5.874	1.713	0.341	-	0	0	0
Tetrahydrofuran	0.685	10.281	2.379	-	1.227	-	0	0	0
Thiophene	0.539	2.319	1.353	0.208	0.934	-	0	0	0
1,4-Dioxane	1.474	4.214	1.466	-	0.843	-	0	0	0
Tetrahydrothiophene	2.237	4.137	6.726	-	0.971	-	0	0	0
3-Methylthiophene	1.261	2.427	2.181	-	-	-	0	0	0
HFCs									
R32	1.384	1.348	1.899	1.899	3.256	6.059	0	0	0
R23	0.216	1.530	0.498	2.095	2.830	3.788	0	0	0
R125	0.555	5.125	0.727	1.407	4.108	4.803	0	0	0
R236fa	0.609	4.411	1.008	1.199	6.676	6.400	0	0	0
R236ea	0.746	3.747	0.938	0.655	6.855	4.493	0	0	0
R134a	0.322	3.096	0.859	0.561	5.143	6.344	0	0	0
R152a	1.127	1.923	1.059	1.328	4.008	6.216	0	0	0
R161	0.850	4.100	2.134	0.749	0.976	-	0	0	0
HCFCs									
R22	0.064	2.130	0.260	1.774	2.921	3.244	0	0	0
R21	0.814	7.389	5.763	1.260	2.803	2.368	0	0	0
R142b	0.395	1.342	0.275	0.369	2.113	3.211	0	0	0
R141b	0.315	1.423	0.738	0.326	3.435	4.113	0	0	0
R124	0.701	2.114	0.737	0.587	2.456	3.485	0	0	0
R123	0.533	3.214	0.740	0.512	2.784	4.321	0	0	0
CFCs									
R12	0.310	5.035	0.396	0.502	2.785	2.683	0	0	0
R11	0.003	5.891	4.253	2.698	2.551	3.866	0	0	0
R13	0.410	6.216	0.301	1.573	3.149	3.733	0	0	0
R115	0.310	3.112	0.276	0.289	4.331	2.113	0	0	0
R114	0.463	2.548	0.361	0.413	2.986	3.741	0	0	0
R113	1.079	5.626	0.373	1.447	4.894	5.366	0	0	0
Fluorocarbons									
R14	0.244	4.046	0.095	2.296	2.045	2.782	0	0	0
R116	1.067	3.140	0.084	1.937	3.574	4.025	0	0	0
R218	0.620	4.728	0.178	3.394	4.939	5.306	0	0	0
RC318	1.312	4.566	0.563	1.246	4.130	3.595	0	0	0
Acids									
Acetic anhydride	1.012	3.533	1.834	-	2.881	-	0	0	0
Others									
Ethylene oxide	0.878	3.095	1.306	-	0.708	-	0	0	0
Dimethyl sulfoxide	3.873	8.364	5.183	3.137	-	-	0	0	0

Table 4-A2. %AADs in non-critical property predictions (including saturated-liquid molar volume, saturated-vapor molar volume, liquid molar volume, vapor molar volume, supercritical molar volume, and vapor pressure) as well as %ADs in critical property predictions (including critical temperature, critical pressure, and critical molar volume) yielded by CPPC-SAFT EOS for 251 individual compounds.

Compounds	%AADs in non-critical properties						%ADs in critical properties		
	V_{SatL}	V_{SatV}	P_{Sat}	V_{Liq}	V_{Vap}	V_{SC}	T_c	P_c	V_c
***n*-Alkanes**									
Methane	1.674	0.569	0.684	0.656	0.401	1.013	0	0	11.160
Ethane	5.717	1.344	1.547	4.432	0.570	2.890	0	0	12.169
Propane	8.819	1.144	1.317	7.276	0.812	5.111	0	0	12.742
Butane	11.631	1.530	1.625	11.338	1.430	8.264	0	0	13.405
Pentane	14.706	1.451	1.245	13.041	1.702	10.588	0	0	15.115
Hexane	16.348	1.315	1.025	14.729	2.117	13.450	0	0	15.862
Heptane	19.131	1.430	1.304	17.312	2.578	15.189	0	0	17.706
Octane	20.629	5.300	6.879	19.179	2.426	15.984	0	0	18.523
Nonane	22.416	1.468	1.535	20.444	2.535	17.925	0	0	19.734
Decane	23.044	1.840	1.986	21.364	3.306	19.448	0	0	21.820
Undecane	23.953	1.776	6.052	-	-	-	0	0	10.960
Dodecane	24.172	3.115	3.553	22.386	2.638	18.989	0	0	20.672
Tridecane	26.794	2.411	6.476	24.913	-	-	0	0	21.540
Tetradecane	30.192	3.803	6.162	-	2.558	-	0	0	22.620
Pentadecane	29.012	6.437	5.663	26.818	-	-	0	0	22.420
Hexadecane	20.376	3.636	3.435	18.305	-	-	0	0	19.691
Heptadecane	26.801	3.180	5.747	25.406	-	-	0	0	21.520
Octadecane	32.555	4.712	5.277	-	-	-	0	0	20.770
Nonadecane	27.369	7.481	6.772	-	1.367	-	0	0	20.870
Eicosane	25.324	5.890	6.335	23.966	-	-	0	0	19.290
Branched alkanes									
Isobutane	10.410	0.849	0.694	9.161	1.216	6.414	0	0	12.678
Isopentane	12.260	1.209	1.129	10.929	1.293	7.726	0	0	14.898
Neopentane	10.601	0.633	0.336	8.801	1.316	5.842	0	0	14.567
2-Methylpentane	9.251	4.450	6.376	8.703	1.886	7.366	0	0	11.106
2.3-Dimethylbutane	12.197	1.011	1.288	9.668	0.958	-	0	0	13.219
3-Methylpentane	14.375	2.603	0.634	13.250	0.637	-	0	0	12.960
2,3-Dimethylpentane	15.493	3.519	1.336	13.258	-	-	0	0	20.580
2,2,3,3-Tetramethylbutane	9.990	2.791	1.713	10.050	0.358	-	0	0	10.500
2,2,4-Trimethylpentane	14.290	2.238	0.856	11.636	-	-	0	0	15.990
2,3,3-Trimethylpentane	13.475	2.929	0.527	-	2.064	-	0	0	14.750
4-Methylheptane	19.082	1.292	2.286	-	-	-	0	0	18.680
4-Methylnonane	17.713	5.580	4.922	-	1.817	-	0	0	22.840
4-Methyloctane	17.617	5.766	4.860	-	-	-	0	0	22.290

5-Methylnonane	19.128	5.354	9.437	-	1.791	-	0	0	22.930
3-Methyloctane	20.187	2.879	1.451	-	-	-	0	0	21.420
3-Methylnonane	21.031	2.564	2.777	-	-	-	0	0	23.440
3-Methylhexane	17.938	0.843	1.910	-	0.177	-	0	0	20.820
3-Methylheptane	19.396	1.651	1.634	-	0.908	-	0	0	21.670
3-Methyl-3-ethylpentane	14.590	2.217	1.281	-	0.555	-	0	0	15.670
3-Ethylhexane	19.098	1.424	1.729	-	0.929	-	0	0	21.730
3,4-Dimethylhexane	16.445	2.000	1.346	-	0.914	-	0	0	16.160
3,3-Dimethylpentane	11.607	3.282	0.795	-	0.377	-	0	0	12.900
3,3-Dimethylhexane	17.768	1.361	0.904	-	0.548	-	0	0	22.690
3,3-Diethylpentane	13.683	3.224	1.700	-	0.713	-	0	0	23.430
3,3,5-Trimethylheptane	17.044	2.054	6.258	-	-	-	0	0	16.200
Cycloalkanes									
Cyclopropane	11.333	0.591	0.759	10.349	0.768	5.895	0	0	13.872
Cyclobutane	9.043	6.707	5.412	-	0.656	-	0	0	13.610
Cyclopentane	8.386	0.992	1.023	7.338	0.323	5.919	0	0	10.104
Cyclohexane	11.816	0.928	0.822	10.147	1.260	8.035	0	0	12.820
Methylcyclopentane	12.447	1.938	1.478	11.850	0.852	-	0	0	13.510
Ethylcyclopentane	14.361	1.849	0.592	-	0.665	-	0	0	14.800
Methylcyclohexane	13.188	1.529	1.458	12.270	1.838	-	0	0	14.730
1,1-Dimethylcyclohexane	22.323	4.936	6.497	-	1.258	-	0	0	15.150
cis-1,2-Dimethylcyclohexane	25.572	7.990	9.800	-	1.326	-	0	0	15.510
trans-1,2-Dimethylcyclohexane	20.962	4.393	6.916	-	1.199	-	0	0	13.560
Ethylcyclohexane	19.274	7.568	8.833	19.649	1.151	-	0	0	19.940
Propylcyclohexane	19.866	5.500	6.215	19.905	0.477	-	0	0	22.770
Olefins									
Ethylene	5.291	0.559	0.464	4.347	11.683	3.272	0	0	11.757
Propylene	9.686	0.325	0.443	8.528	0.755	5.611	0	0	13.132
Butene	12.134	0.665	0.594	10.809	0.898	7.185	0	0	14.579
Cis-butene	12.868	0.649	0.260	11.516	1.050	7.773	0	0	12.842
Isobutene	11.639	0.733	0.541	10.420	0.953	7.206	0	0	12.284
(E)-2-Butene	12.348	4.162	4.061	10.977	0.537	10.826	0	0	13.230
1-Pentene	13.499	1.643	2.459	13.300	1.357	-	0	0	14.580
Cyclohexene	15.398	1.343	1.301	-	-	-	0	0	14.160
1-Hexene	15.723	0.571	1.079	14.171	6.973	-	0	0	15.870
1-Heptene	17.801	2.839	2.208	16.512	-	-	0	0	17.160
1-Octene	17.172	2.095	1.575	15.715	2.238	-	0	0	17.020
1-Nonene	18.512	2.869	0.708	17.061	1.568	-	0	0	18.500
1-Decene	20.215	1.567	1.513	-	-	-	0	0	20.280
2-Methyl-1-butene	19.371	1.880	3.063	-	1.014	-	0	0	18.980
2-Methyl-2-butene	20.656	1.844	4.887	-	-	-	0	0	20.850
1-Methylcyclopentene	15.579	3.021	2.414	-	0.595	-	0	0	11.560

3-Methylcyclopentene	7.962	12.006	6.699	-	-	-	0	0	8.280
1,2-Butadiene	21.757	5.190	7.108	-	0.480	-	0	0	21.910
1,3-Butadiene	13.321	1.723	2.072	-	0.394	-	0	0	14.920
3-Methyl-1,2-butadiene	19.985	9.616	7.553	-	1.473	-	0	0	13.560
4-Methyl-1-hexene	10.357	4.532	5.542	-	-	-	0	0	13.230
4-Methyl-1-pentene	12.062	8.433	2.362	11.543	0.451	-	0	0	14.960
4-Methyl-cis-2-pentene	12.938	4.122	7.532	-	0.946	-	0	0	15.280
4-Methylcyclopentene	9.001	7.104	6.508	-	0.736	-	0	0	8.450
4-Methyl-trans-2-pentene	12.729	6.004	8.765	-	0.934	-	0	0	15.680
5-Methyl-1-hexene	16.296	2.551	0.948	-	0.586	-	0	0	18.540
6-Methyl-1-heptene	18.242	1.788	5.464	-	-	-	0	0	21.150
3-Methyl-trans-2-pentene	20.030	7.663	9.068	-	1.280	-	0	0	21.490
3-Methyl-cis-2-pentene	16.997	5.251	20.389	-	0.928	-	0	0	17.370
3-Methyl-1-pentene	9.373	0.664	3.640	-	0.405	-	0	0	12.680
3-Methyl-1-hexene	12.449	1.627	3.417	-	0.614	-	0	0	15.350
3-Methyl-1-butene	10.972	2.124	1.452	-	0.477	-	0	0	8.450
3-Methyl-1,4-pentadiene	8.624	2.048	9.309	-	1.225	-	0	0	13.470
3-Ethyl-1-pentene	9.979	2.831	3.699	-	0.614	-	0	0	12.760
3-Ethyl-1-hexene	17.700	1.099	1.231	-	-	-	0	0	20.040
3,3-Dimethyl-1-butene	5.910	2.185	6.982	-	0.637	-	0	0	12.870
2-Ethyl-1-pentene	16.866	5.886	3.035	-	-	-	0	0	18.620
2-Ethyl-1-butene	14.919	4.349	6.123	-	0.834	-	0	0	16.150
Alkynes									
1-Propyne	14.507	1.077	0.509	13.191	0.800	7.943	0	0	12.390
1-Butyne	16.037	12.350	2.470	-	2.378	-	0	0	18.350
2-Butyne	19.618	12.011	3.892	12.985	0.788	-	0	0	13.210
1-Pentyne	10.334	7.300	9.880	-	0.233	-	0	0	6.960
2-Pentyne	24.095	7.780	9.236	-	1.017	-	0	0	20.630
1-Hexyne	14.287	6.560	6.423	-	1.804	-	0	0	13.410
1-Heptyne	14.839	11.549	2.780	-	2.104	-	0	0	12.420
1-Octyne	16.697	8.395	4.179	-	-	-	0	0	14.740
1-Nonyne	17.916	8.065	3.253	-	-	-	0	0	16.860
1-Decyne	18.098	9.037	8.211	-	-	-	0	0	19.590
Vinylacetylene	16.784	7.394	6.740	-	0.408	-	0	0	18.670
2-Methyl-1-butene-3-yne	9.736	7.518	8.959	-	0.361	-	0	0	17.510
3-Methyl-1-butyne	3.871	8.943	7.885	-	0.097	-	0	0	2.850
2-Ethylnaphthalene	20.934	2.077	6.121	-	1.860	-	0	0	19.040
Aromatics									
Benzene	13.929	1.022	0.757	12.439	1.409	9.905	0	0	15.183
Toluene	16.961	1.248	0.640	15.547	0.813	12.588	0	0	16.859
Ethylbenzene	18.836	0.550	1.132	16.832	0.490	-	0	0	17.233
m-Xylene	20.022	1.523	0.607	19.239	0.286	-	0	0	10.789

o-Xylene	18.477	1.415	0.815	16.903	0.365	-	0	0	16.646
p-Xylene	20.740	1.218	0.623	18.923	2.005	-	0	0	18.501
Naphthalene	19.935	0.754	0.457	-	1.161	-	0	0	16.490
Biphenyl	22.922	1.831	3.787	18.748	3.131	-	0	0	17.280
Anthracene	43.787	-	1.708	-	-	-	0	0	37.550
Styrene	32.295	1.147	1.758	-	0.898	-	0	0	20.750
alpha-Methylstyrene	25.870	6.768	8.121	-	1.919	-	0	0	25.000
Cumene	19.558	1.310	2.347	17.962	1.161	-	0	0	16.060
Propyl benzene	19.848	2.276	0.761	18.599	1.959	-	0	0	16.020
1,2,3-Trimethylbenzene	18.116	3.318	1.623	-	0.928	-	0	0	18.740
1,2,4-Trimethylbenzene	21.163	3.420	1.567	20.105	0.865	-	0	0	19.240
1,2,3,4-Tetrahydronaphthalene	17.873	1.431	1.725	16.486	0.621	-	0	0	23.800
Butylbenzene	20.040	0.738	0.648	19.021	0.430	-	0	0	17.280
Phenanthrene	45.642	7.924	7.603	41.059	0.301	-	0	0	37.100
4-Ethyl-m-xylene	22.714	2.268	2.158	-	1.001	-	0	0	21.990
4-Ethyl-o-xylene	22.817	3.935	4.247	-	-	-	0	0	20.380
5-Ethyl-m-xylene	25.736	3.370	4.562	-	-	-	0	0	25.810
3-Ethyl-o-xylene	27.720	8.010	6.365	-	-	-	0	0	19.030
2-Ethyl-p-xylene	22.629	4.754	2.130	-	-	-	0	0	21.650
2-Ethyl-m-xylene	20.271	1.809	1.703	-	-	-	0	0	17.450
Ketones									
Butanone	28.172	0.410	0.724	27.284	0.445	-	0	0	23.840
3-Pentanone	24.730	2.245	2.195	21.583	-	-	0	0	14.230
2-Pentanone	23.833	1.811	2.609	-	6.779	-	0	0	29.140
3-Methyl-2-butanone	21.344	6.685	3.252	-	0.578	-	0	0	20.390
Acetone	33.463	6.482	3.377	32.755	1.134	-	0	0	32.670
Quinone	11.802	-	-	-	1.879	-	0	0	5.716
2-Hexanone	23.091	1.555	2.500	-	-	-	0	0	20.690
3-Hexanone	21.973	1.574	1.531	-	-	-	0	0	18.560
3-Heptanone	24.780	2.921	8.259	-	-	-	0	0	22.230
2-Heptanone	23.964	1.443	3.191	-	2.616	-	0	0	21.970
2-Octanone	25.419	4.642	8.410	23.851	4.502	-	0	0	22.390
4-Heptanone	23.738	1.621	3.759	-	2.597	-	0	0	20.990
5-Nonanone	29.213	2.574	2.564	-	2.903	-	0	0	24.380
3-Methyl-2-pentanone	21.186	9.238	6.961	-	-	-	0	0	19.330
Permanent gases									
Oxygen	1.242	0.426	0.873	1.432	0.090	0.404	0	0	10.390
Fluorine	8.159	2.432	0.866	5.709	0.143	1.393	0	0	10.080
Argon	4.227	0.335	0.869	2.145	0.084	0.434	0	0	9.290
Chlorine	6.334	5.456	2.753	-	0.691	-	0	0	14.370
Hydrogen sulfide	5.084	1.054	0.392	4.940	0.228	4.250	0	0	10.400
Carbon disulfide	4.216	2.207	2.020	-	0.750	-	0	0	13.670

Carbon monoxide	1.244	0.647	0.424	0.618	0.494	0.807	0	0	8.523
Nitrogen	1.644	0.602	0.541	1.130	0.521	1.190	0	0	9.656
Carbon dioxide	13.536	0.923	0.373	11.486	0.872	7.215	0	0	12.948
Sulfur dioxide	17.075	1.106	0.624	16.733	1.698	10.553	0	0	13.518
Carbonyl sulfide	8.048	0.462	0.696	6.615	0.573	3.683	0	0	14.953
Hydrogen chloride	17.096	4.297	0.778	1.039	16.017	-	0	0	25.210
Nitrous oxide	11.216	1.929	2.191	9.151	0.760	-	0	0	13.770
Ozone	23.750	-	3.888	-	-	-	0	0	35.770
Ethers									
Diethyl ether	17.157	1.097	2.451	-	1.036	-	0	0	17.620
Dipropyl ether	13.835	5.926	3.665	-	0.837	-	0	0	17.200
Methyl isobutyl ether	11.665	8.749	7.491	-	0.484	-	0	0	13.620
Ethyl isopropyl ether	8.564	5.503	5.580	-	0.684	-	0	0	11.810
Diisopropyl ether	12.255	6.409	2.188	11.154	0.538	-	0	0	15.150
Dinbutyl ether	18.403	2.151	2.962	16.285	-	-	0	0	23.820
Esters									
Methyl ethanoate	22.170	1.045	0.821	20.380	1.003	-	0	0	19.790
Ethyl ethanoate	23.133	1.187	2.362	21.199	0.481	-	0	0	20.500
Vinyl acetate	26.872	3.476	8.412	-	-	-	0	0	24.250
Methyl propionate	21.675	2.140	6.673	-	0.491	-	0	0	20.230
Ethyl propionate	22.956	0.894	2.788	21.936	0.607	-	0	0	20.050
Propyl acetate	23.678	0.605	5.369	-	2.598	-	0	0	20.990
Butyl acetate	19.447	4.198	5.532	17.901	9.178	-	0	0	21.650
Methyl benzoate	25.426	4.821	1.984	23.153	0.762	-	0	0	12.690
Aldehydes									
2-Propenal	39.647	11.258	9.556	-	3.747	-	0	0	31.660
Sulfides and Thiols									
Methanethiol	11.825	1.986	3.508	-	-	-	0	0	16.050
Ethanethiol	13.478	2.813	1.650		0.618	-	0	0	13.450
2-Thiapropane	14.738	6.495	1.664	-	0.554	-	0	0	16.840
2-Propanethiol	5.140	1.561	1.906	-	1.241	-	0	0	10.490
1-Propanethiol	14.519	3.219	0.398	-	0.400	-	0	0	17.530
3-Thiapentane	15.216	8.652	1.184	-	0.746	-	0	0	13.590
2,3-Dithiabutane	9.983	3.950	3.141	-	0.389	-	0	0	17.460
Butyl mercaptan	17.172	1.644	0.781	-	12.085	-	0	0	12.500
sec-Butyl mercaptan	10.314	2.333	1.923	-	-	-	0	0	14.360
Pentyl mercaptan	19.374	2.916	1.712	-	0.579	-	0	0	23.020
Benzenethiol	18.505	4.882	7.110	-	0.922	-	0	0	18.650
Cyclohexyl mercaptan	15.228	7.475	1.742	-	1.598	-	0	0	21.140
Hexyl mercaptan	21.316	3.484	0.945	-	1.581	-	0	0	25.440
Benzyl mercaptan	20.395	15.318	7.856	-	1.118	-	0	0	23.550
Heptyl mercaptan	22.437	4.031	0.851	-	1.982	-	0	0	27.430

Octyl mercaptan	23.467	1.431	2.912	-	-	-	0	0	29.810
Nonyl mercaptan	24.887	6.244	2.895	-	-	-	0	0	30.210
Decyl mercaptan	38.701	6.455	5.142	-	0.592	-	0	0	31.260
Halogenated Hydrocarbons									
Fluoromethane	31.106	6.585	3.554	30.472	0.658	19.246	0	0	23.440
Chloromethane	16.956	3.737	0.773	-	1.480	-	0	0	14.490
Difluoromethane	33.793	4.418	2.117	33.044	0.466	16.054	0	0	26.850
1,1-Difluoroethane	25.561	2.736	1.662	24.401	0.353	12.635	0	0	22.730
Trifluoromethane	24.017	1.234	0.336	19.688	0.299	19.782	0	0	20.930
1,1,1-Trifluoroethane	23.704	1.601	0.250	22.099	0.285	10.081	0	0	21.180
Dichloromethane	18.883	4.819	4.052	18.808	0.789	-	0	0	17.020
Tetrafluoromethane	12.423	2.363	0.240	7.217	0.238	2.811	0	0	9.800
Bromomethane	12.743	21.534	5.532	-	1.433	-	0	0	14.110
1,1,1,2-Tetrafluoroethane	21.652	1.090	0.614	19.188	0.482	10.525	0	0	18.880
Trichloromethane	15.804	1.513	2.097	-	0.536	-	0	0	5.710
Dichlorodifluoromethane	13.055	1.610	0.379	9.384	0.294	4.540	0	0	11.140
1,1,2-Trichloroethane	28.021	7.332	5.153	23.962	1.780	-	0	0	22.990
1,2-Dibromoethane	15.643	5.216	2.782	-	0.697	-	0	0	17.060
1,2-Dichloroethane	17.168	-	1.926	15.569	0.609	-	0	0	22.070
Chloroethane	15.863	1.029	1.482	15.272	0.479	-	0	0	17.510
1,1-Dichloropropane	16.572	0.639	2.598	-	1.358	-	0	0	16.770
1,2-Dichloropropane	21.787	5.422	1.466	-	1.151	-	0	0	19.240
1-Chloropropane	18.615	2.287	3.460	18.325	0.484	-	0	0	20.650
2-Chloropropane	9.936	5.778	1.698	-	-	-	0	0	12.550
m-Dichlorobenzene	22.726	2.236	1.216	-	0.937	-	0	0	23.000
p-Dichlorobenzene	19.766	17.347	1.643	-	11.937	-	0	0	23.100
Bromobenzene	19.795	2.808	1.511	-	0.647	-	0	0	17.770
Chlorobenzene	17.567	1.913	0.901	-	0.466	-	0	0	16.900
Heterocyclics									
Furan	14.320	3.724	6.460	12.707	0.304	-	0	0	5.490
Tetrahydrofuran	17.237	6.106	2.616	-	1.438	-	0	0	19.720
Thiophene	12.129	1.019	1.488	11.744	1.093	-	0	0	20.010
1,4-Dioxane	14.928	1.720	1.612	-	0.539	-	0	0	21.660
Tetrahydrothiophene	17.928	4.698	7.396	-	0.539	-	0	0	26.940
3-Methylthiophene	10.921	1.340	2.398	-	-	-	0	0	16.460
HFCs									
R32	33.772	1.650	2.088	33.329	0.801	21.467	0	0	27.349
R23	22.633	1.235	0.548	21.611	0.917	12.723	0	0	19.857
R125	18.097	1.509	0.799	15.498	2.312	8.256	0	0	14.932
R236fa	18.386	1.524	1.108	15.977	4.042	8.159	0	0	15.138
R236ea	18.192	1.913	1.032	16.917	4.366	4.684	0	0	14.491
R134a	21.658	1.404	0.945	19.918	2.623	11.565	0	0	18.524

R152a	25.731	1.239	1.165	24.898	1.216	12.934	0	0	22.592
R161	22.371	3.985	2.347	19.042	0.671	-	0	0	21.020
HCFCs									
R22	15.829	0.715	0.286	14.507	1.276	9.193	0	0	15.583
R21	11.287	9.303	6.337	12.694	1.232	8.340	0	0	14.901
R142b	17.229	1.722	0.302	14.115	2.984	8.992	0	0	15.719
R141b	13.617	1.987	0.812	12.920	2.367	7.652	0	0	14.595
R124	12.719	1.548	0.811	13.823	1.562	7.435	0	0	15.002
R123	13.812	1.982	0.814	14.982	1.956	9.986	0	0	15.300
CFCs									
R12	12.645	1.481	0.436	9.355	1.320	5.702	0	0	12.531
R11	6.885	8.072	4.677	10.238	1.387	5.205	0	0	11.376
R13	12.588	2.337	0.331	9.167	1.607	4.697	0	0	12.361
R115	8.890	2.785	0.304	12.018	1.984	8.762	0	0	15.651
R114	8.133	2.971	0.397	11.091	1.673	9.461	0	0	12.320
R113	15.778	2.558	0.410	12.991	3.080	7.871	0	0	10.446
Fluorocarbons									
R14	12.010	2.769	0.104	7.422	1.037	2.982	0	0	11.579
R116	14.026	3.541	0.092	10.726	2.286	6.083	0	0	9.964
R218	15.589	2.590	0.196	12.862	3.281	6.987	0	0	11.936
RC318	16.111	4.733	0.619	12.300	2.830	6.239	0	0	10.804
Acids									
Acetic anhydride	33.605	3.592	2.017	-	2.324	-	0	0	26.480
Others									
Ethylene oxide	22.587	6.580	1.436	-	0.551	-	0	0	20.050
Dimethyl sulfoxide	43.889	7.339	5.700	46.498	-	-	0	0	46.010

Table 4-A3. %AADs in non-critical property predictions (including saturated-liquid molar volume, saturated-vapor molar volume, liquid molar volume, vapor molar volume, supercritical molar volume, and vapor pressure) as well as %ADs in critical property predictions (including critical temperature, critical pressure, and critical molar volume) yielded by I-PC-SAFT EOS for 251 individual compounds.

Compounds	%AADs in non-critical properties						%ADs in critical properties		
	V_{SatL}	V_{SatV}	P_{Sat}	V_{Liq}	V_{Vap}	V_{SC}	T_c	P_c	V_c
***n*-Alkanes**									
Methane	1.442	0.579	0.653	0.475	0.412	0.970	0	0	11.057
Ethane	2.153	1.428	1.477	1.840	0.802	1.222	0	0	9.949
Propane	2.842	1.638	1.257	3.316	1.240	1.509	0	0	9.031
Butane	3.656	1.939	1.551	5.123	2.084	2.292	0	0	8.514
Pentane	4.253	1.845	1.189	4.656	2.522	2.646	0	0	8.849
Hexane	5.208	1.683	0.979	5.626	3.160	3.020	0	0	8.544
Heptane	5.300	1.755	1.245	5.339	3.682	3.441	0	0	9.742

Octane	5.092	5.633	6.567	5.240	3.555	3.962	0	0	9.946
Nonane	5.812	1.744	1.465	5.464	3.553	2.654	0	0	10.807
Decane	4.726	1.913	1.896	3.293	4.365	6.382	0	0	13.762
Undecane	5.604	2.509	5.778	-	-	-	0	0	1.207
Dodecane	5.028	3.308	3.392	4.037	3.826	4.402	0	0	11.832
Tridecane	6.216	3.360	6.182	5.303	-	-	0	0	11.138
Tetradecane	7.189	5.548	5.883	-	2.876	-	0	0	11.462
Pentadecane	7.164	4.307	5.406	8.744	-	-	0	0	11.356
Hexadecane	10.761	4.711	3.279	16.984	-	-	0	0	8.641
Heptadecane	6.247	3.946	5.487	6.370	-	-	0	0	11.158
Octadecane	9.451	4.821	5.038	-	-	-	0	0	10.304
Nonadecane	7.806	5.657	6.465	-	1.159	-	0	0	10.601
Eicosane	5.436	5.886	6.048	5.500	-	-	0	0	10.053
Branched alkanes									
Isobutane	3.197	1.092	0.663	3.473	1.788	2.595	0	0	8.225
Isopentane	3.881	1.558	1.078	4.208	1.981	3.201	0	0	9.500
Neopentane	2.717	1.015	0.321	2.570	1.889	2.790	0	0	10.274
2-Methylpentane	6.167	4.028	6.087	7.457	2.669	6.198	0	0	5.100
2.3-Dimethylbutane	4.375	2.403	1.230	6.680	0.908	-	0	0	7.728
3-Methylpentane	4.385	4.039	0.605	4.561	0.830	-	0	0	6.685
2,3-Dimethylpentane	5.887	2.335	1.275	5.725	-	-	0	0	13.468
2,2,3,3-Tetramethylbutane	1.427	2.171	1.635	1.275	0.440	-	0	0	6.134
2,2,4-Trimethylpentane	4.616	3.548	0.817	5.452	-	-	0	0	9.790
2,3,3-Trimethylpentane	4.724	1.959	0.503	-	1.961	-	0	0	8.795
4-Methylheptane	5.650	2.752	2.182	-	-	-	0	0	10.477
4-Methylnonane	3.371	5.572	4.699	-	2.055	-	0	0	14.929
4-Methyloctane	4.714	5.284	4.640	-	-	-	0	0	13.995
5-Methylnonane	4.345	4.202	9.009	-	2.058	-	0	0	14.583
3-Methyloctane	5.380	4.146	1.385	-	-	-	0	0	13.207
3-Methylnonane	5.787	3.717	2.651	-	-	-	0	0	14.681
3-Methylhexane	6.282	2.551	1.823	-	0.314	-	0	0	12.800
3-Methylheptane	6.280	3.339	1.560	-	1.171	-	0	0	13.175
3-Methyl-3-ethylpentane	4.601	3.592	1.223	-	0.752	-	0	0	9.617
3-Ethylhexane	6.197	3.122	1.651	-	1.188	-	0	0	13.353
3,4-Dimethylhexane	5.216	3.483	1.285	-	1.146	-	0	0	9.029
3,3-Dimethylpentane	2.954	4.371	0.759	-	0.476	-	0	0	8.159
3,3-Dimethylhexane	6.990	3.499	0.863	-	0.806	-	0	0	14.417
3,3-Diethylpentane	4.956	4.649	1.623	-	0.810	-	0	0	17.127
3,3,5-Trimethylheptane	3.825	3.448	5.974	-	-	-	0	0	9.669
Cycloalkanes									
Cyclopropane	4.018	0.801	0.725	2.638	1.160	3.190	0	0	10.392
Cyclobutane	3.051	7.922	5.167	-	0.739	-	0	0	9.123

Cyclopentane	5.527	0.606	0.977	6.937	0.781	4.663	0	0	4.791
Cyclohexane	2.895	1.190	0.785	2.948	1.928	3.218	0	0	7.920
Methylcyclopentane	3.581	3.187	1.411	2.661	0.999	-	0	0	8.167
Ethylcyclopentane	4.290	3.240	0.565	-	0.816	-	0	0	8.432
Methylcyclohexane	3.488	1.524	1.392	3.468	2.830	-	0	0	9.250
1,1-Dimethylcyclohexane	4.952	5.917	6.203	-	1.590	-	0	0	6.359
cis-1,2-Dimethylcyclohexane	5.255	6.825	9.356	-	1.692	-	0	0	4.794
trans-1,2-Dimethylcyclohexane	4.997	4.137	6.603	-	1.509	-	0	0	4.573
Ethylcyclohexane	4.652	6.828	8.433	4.721	1.462	-	0	0	11.180
Propylcyclohexane	3.718	5.997	5.933	5.348	0.686	-	0	0	14.187
Olefins									
Ethylene	1.678	0.660	0.443	1.436	12.635	1.596	0	0	9.801
Propylene	2.359	0.550	0.423	1.588	1.170	2.266	0	0	9.670
Butene	3.048	0.878	0.567	2.754	1.502	2.442	0	0	9.854
Cis-butene	4.105	0.812	0.248	4.369	1.794	2.907	0	0	7.234
Isobutene	3.551	0.814	0.516	3.865	1.601	2.626	0	0	7.275
(E)-2-Butene	3.431	4.547	3.877	3.522	0.870	2.007	0	0	8.042
1-Pentene	3.654	2.734	2.348	1.214	1.325	-	0	0	9.025
Cyclohexene	5.889	1.089	1.242	-	-	-	0	0	8.856
1-Hexene	4.843	1.948	1.030	4.294	8.141	-	0	0	9.478
1-Heptene	6.235	4.315	2.108	3.570	-	-	0	0	10.364
1-Octene	4.946	3.631	1.504	3.503	2.185	-	0	0	9.950
1-Nonene	4.985	4.334	0.676	5.237	1.620	-	0	0	10.894
1-Decene	5.057	2.867	1.444	-	-	-	0	0	12.120
2-Methyl-1-butene	5.179	3.348	2.924	-	1.289	-	0	0	10.945
2-Methyl-2-butene	6.384	3.934	4.666	-	-	-	0	0	11.324
1-Methylcyclopentene	7.641	4.279	2.305	-	0.725	-	0	0	6.680
3-Methylcyclopentene	3.511	12.700	6.395	-	-	-	0	0	4.849
1,2-Butadiene	5.122	7.210	6.786	-	0.771	-	0	0	13.587
1,3-Butadiene	3.530	3.078	1.978	-	0.460	-	0	0	9.402
3-Methyl-1,2-butadiene	4.203	8.872	7.211	-	1.779	-	0	0	5.586
4-Methyl-1-hexene	3.066	3.334	5.291	-	-	-	0	0	8.256
4-Methyl-1-pentene	3.305	7.069	2.255	2.076	0.514	-	0	0	9.745
4-Methyl-cis-2-pentene	3.267	3.277	7.191	-	1.151	-	0	0	9.518
4-Methylcyclopentene	3.039	8.663	6.213	-	0.767	-	0	0	5.511
4-Methyl-trans-2-pentene	3.093	5.199	8.368	-	1.141	-	0	0	9.885
5-Methyl-1-hexene	4.738	4.185	0.905	-	0.724	-	0	0	11.653
6-Methyl-1-heptene	5.127	1.411	5.216	-	-	-	0	0	13.131
3-Methyl-trans-2-pentene	4.693	7.899	8.657	-	1.612	-	0	0	12.146
3-Methyl-cis-2-pentene	4.383	6.875	19.465	-	1.189	-	0	0	10.105
3-Methyl-1-pentene	2.629	1.078	3.475	-	0.485	-	0	0	8.352
3-Methyl-1-hexene	3.457	0.823	3.262	-	0.688	-	0	0	9.788

3-Methyl-1-butene	3.747	3.117	1.386	-	0.564	-	0	0	4.080
3-Methyl-1,4-pentadiene	3.799	1.809	8.887	-	1.101	-	0	0	9.021
3-Ethyl-1-pentene	2.573	1.827	3.531	-	0.654	-	0	0	8.253
3-Ethyl-1-hexene	5.024	1.800	1.175	-	-	-	0	0	12.270
3,3-Dimethyl-1-butene	1.986	1.590	6.666	-	0.631	-	0	0	10.194
2-Ethyl-1-pentene	3.247	4.340	2.897	-	-	-	0	0	11.415
2-Ethyl-1-butene	2.822	2.999	5.845	-	0.970	-	0	0	9.764
Alkynes									
1-Propyne	2.611	1.137	0.486	1.637	1.213	3.612	0	0	6.746
1-Butyne	5.545	13.642	2.358	-	2.638	-	0	0	12.489
2-Butyne	5.235	14.253	3.716	4.338	0.920	-	0	0	5.888
1-Pentyne	4.735	7.673	9.432	-	0.280	-	0	0	4.852
2-Pentyne	6.202	7.231	8.817	-	1.134	-	0	0	12.191
1-Hexyne	6.300	6.660	6.132	-	2.015	-	0	0	8.221
1-Heptyne	4.963	12.594	2.654	-	2.325	-	0	0	6.918
1-Octyne	5.697	8.602	3.990	-	-	-	0	0	8.545
1-Nonyne	5.827	8.255	3.106	-	-	-	0	0	10.360
1-Decyne	4.092	9.811	7.839	-	-	-	0	0	12.462
Vinylacetylene	2.515	6.278	6.435	-	0.556	-	0	0	12.516
2-Methyl-1-butene-3-yne	1.534	7.560	8.553	-	0.420	-	0	0	13.205
3-Methyl-1-butyne	3.488	8.996	7.528	-	0.095	-	0	0	2.537
2-Ethylnaphthalene	5.980	0.879	5.844	-	1.901	-	0	0	9.603
Aromatics									
Benzene	3.197	1.301	0.723	3.222	2.171	3.634	0	0	9.279
Toluene	4.871	0.880	0.611	5.117	1.622	4.089	0	0	9.489
Ethylbenzene	5.122	2.322	1.081	5.622	1.001	-	0	0	9.391
m-Xylene	3.915	3.422	0.579	4.641	0.564	-	0	0	2.713
o-Xylene	4.815	3.011	0.778	4.629	0.555	-	0	0	8.779
p-Xylene	4.998	3.400	0.595	5.141	1.873	-	0	0	9.714
Naphthalene	4.078	1.669	0.436	-	1.651	-	0	0	8.325
Biphenyl	6.754	3.538	3.615	9.107	3.027	-	0	0	8.548
Anthracene	12.482	-	1.631	-	-	-	0	0	24.829
Styrene	12.397	1.836	1.678	-	1.062	-	0	0	12.395
alpha-Methylstyrene	5.437	7.667	7.753	-	2.264	-	0	0	15.555
Cumene	5.200	2.553	2.241	3.453	1.339	-	0	0	8.277
Propylbenzene	4.441	3.815	0.727	4.160	2.201	-	0	0	8.582
1,2,3-Trimethylbenzene	6.269	5.185	1.549	-	1.137	-	0	0	10.294
1,2,4-Trimethylbenzene	5.420	5.274	1.496	6.718	1.069	-	0	0	10.414
1,2,3,4-Tetrahydronaphthalene	5.631	2.878	1.647	6.943	0.654	-	0	0	15.850
Butylbenzene	4.544	1.788	0.619	5.184	0.618	-	0	0	9.446
Phenanthrene	11.988	9.731	7.258	0.714	0.156	-	0	0	24.418
4-Ethyl-m-xylene	5.075	1.041	2.060	-	1.281	-	0	0	12.897

4-Ethyl-o-xylene	5.371	2.217	4.055	-	-	-	0	0	11.034
5-Ethyl-m-xylene	6.110	2.763	4.355	-	-	-	0	0	15.487
3-Ethyl-o-xylene	5.359	6.420	6.077	-	-	-	0	0	7.896
2-Ethyl-p-xylene	5.228	2.751	2.033	-	-	-	0	0	12.526
2-Ethyl-m-xylene	4.657	3.261	1.626	-	-	-	0	0	9.528
Ketones									
Butanone	4.127	1.114	0.691	3.639	0.611	-	0	0	13.308
3-Pentanone	5.423	3.102	2.096	4.107	-	-	0	0	5.530
2-Pentanone	4.995	3.434	2.491	-	7.656	-	0	0	19.527
3-Methyl-2-butanone	5.037	8.506	3.105	-	0.526	-	0	0	12.343
Acetone	5.950	5.605	3.224	4.420	1.912	-	0	0	20.292
Quinone	8.856	-	-	-	1.846	-	0	0	3.390
2-Hexanone	5.573	1.673	2.387	-	-	-	0	0	11.156
3-Hexanone	5.573	2.998	1.462	-	-	-	0	0	9.530
3-Heptanone	6.248	3.740	7.885	-	-	-	0	0	11.866
2-Heptanone	5.068	2.895	3.046	-	2.887	-	0	0	12.649
2-Octanone	5.727	4.100	8.029	4.062	4.378	-	0	0	12.683
4-Heptanone	5.429	2.639	3.589	-	2.864	-	0	0	11.720
5-Nonanone	6.419	4.507	2.448	-	2.899	-	0	0	13.066
3-Methyl-2-pentanone	5.818	10.859	6.646	-	-	-	0	0	11.078
Permanent gases									
Oxygen	1.355	0.399	0.833	1.475	0.086	0.329	0	0	10.577
Fluorine	7.653	2.575	0.827	5.138	0.149	1.466	0	0	9.737
Argon	4.952	0.248	0.830	2.955	0.075	0.380	0	0	9.754
Chlorine	2.819	4.775	2.628	-	0.684	-	0	0	11.424
Hydrogen sulfide	1.275	0.799	0.374	1.092	0.263	0.458	0	0	8.364
Carbon disulfide	3.142	2.108	1.928	-	0.745	-	0	0	13.120
Carbon monoxide	1.621	0.623	0.405	0.646	0.464	0.796	0	0	8.789
Nitrogen	1.628	0.561	0.516	0.645	0.479	1.076	0	0	10.067
Carbon dioxide	3.238	1.565	0.356	1.786	1.427	2.114	0	0	7.767
Sulfur dioxide	3.952	1.398	0.596	2.581	2.615	6.360	0	0	6.873
Carbonyl sulfide	2.768	1.040	0.664	2.596	0.993	1.673	0	0	11.163
Hydrogen chloride	3.256	2.773	0.743	1.196	0.949	-	0	0	18.757
Nitrous oxide	2.695	2.653	2.092	1.261	3.126	-	0	0	9.556
Ozone	5.354	-	3.712	-	-	-	0	0	24.819
Ethers									
Diethyl ether	4.614	1.914	2.340	-	1.202	-	0	0	10.334
Dipropyl ether	4.582	7.202	3.499	-	0.992	-	0	0	11.223
Methyl isobutyl ether	4.372	8.676	7.151	-	0.533	-	0	0	8.671
Ethyl isopropyl ether	2.273	6.261	5.327	-	0.600	-	0	0	8.584
Diisopropyl ether	3.843	7.537	2.089	3.200	0.699	-	0	0	9.890
Dinbutyl ether	5.621	3.439	2.828	5.782	-	-	0	0	16.447

Esters									
Methyl ethanoate	4.565	3.006	0.784	6.777	0.892	-	0	0	10.623
Ethyl ethanoate	5.417	2.450	2.255	4.704	0.617	-	0	0	11.178
Vinyl acetate	6.783	3.496	8.031	-	-	-	0	0	12.812
Methyl propionate	5.945	3.057	6.371	-	0.624	-	0	0	11.128
Ethyl propionate	5.507	3.126	2.662	4.513	0.693	-	0	0	10.556
Propyl acetate	5.893	3.121	5.126	-	2.454	-	0	0	11.282
Butyl acetate	5.592	5.824	5.281	4.107	9.119	-	0	0	13.671
Methyl benzoate	6.104	6.666	1.894	3.546	1.060	-	0	0	3.432
Aldehydes									
2-Propenal	7.844	13.299	9.123	-	4.224	-	0	0	18.637
Sulfides and Thiols									
Methanethiol	3.284	1.727	3.349	-	-	-	0	0	11.450
Ethanethiol	4.013	1.341	1.575	-	0.638	-	0	0	7.797
2-Thiapropane	5.080	8.079	1.589	-	0.647	-	0	0	10.345
2-Propanethiol	1.492	1.107	1.820	-	1.300	-	0	0	8.144
1-Propanethiol	3.707	4.496	0.380	-	0.431	-	0	0	12.000
3-Thiapentane	4.529	10.170	1.130	-	0.963	-	0	0	7.353
2,3-Dithiabutane	1.949	2.957	2.999	-	0.435	-	0	0	13.134
Butyl mercaptan	4.975	3.149	0.746	-	11.793	-	0	0	5.198
sec-Butyl mercaptan	2.591	1.274	1.836	-	-	-	0	0	9.804
Pentyl mercaptan	5.078	4.505	1.634	-	0.576	-	0	0	15.294
Benzenethiol	4.057	6.378	6.788	-	0.896	-	0	0	11.846
Cyclohexyl mercaptan	4.458	8.798	1.663	-	1.818	-	0	0	15.271
Hexyl mercaptan	6.026	5.443	0.902	-	1.839	-	0	0	16.537
Benzyl mercaptan	2.775	13.469	7.500	-	1.202	-	0	0	15.310
Heptyl mercaptan	6.090	5.892	0.812	-	2.241	-	0	0	18.273
Octyl mercaptan	6.048	2.404	2.780	-	-	-	0	0	20.167
Nonyl mercaptan	7.723	7.893	2.764	-	-	-	0	0	20.960
Decyl mercaptan	9.492	8.457	4.909	-	0.897	-	0	0	20.267
Halogenated Hydrocarbons									
Fluoromethane	5.352	5.492	3.393	4.828	0.793	4.081	0	0	10.947
Chloromethane	3.968	2.277	0.738	-	1.447	-	0	0	8.229
Difluoromethane	5.057	3.469	2.021	3.678	0.521	4.268	0	0	14.714
1,1-Difluoroethane	5.440	2.637	1.587	5.888	0.479	3.379	0	0	12.190
Trifluoromethane	5.211	1.348	0.321	1.082	0.452	3.599	0	0	11.580
1,1,1-Trifluoroethane	4.457	1.361	0.239	4.659	0.422	3.124	0	0	11.487
Dichloromethane	2.500	3.780	3.868	2.155	1.062	-	0	0	9.097
Tetrafluoromethane	8.263	3.435	0.229	4.475	0.301	1.629	0	0	7.077
Bromomethane	4.533	19.191	5.281	-	1.283	-	0	0	8.669
1,1,1,2-Tetrafluoroethane	4.435	1.751	0.586	3.881	0.670	3.773	0	0	10.444
Trichloromethane	7.770	1.443	2.002	-	0.518	-	0	0	1.806

Dichlorodifluoromethane	5.948	2.889	0.362	4.180	0.398	2.787	0	0	7.111
1,1,2-Trichloroethane	6.697	7.544	4.919	1.745	2.149	-	0	0	13.750
1,2-Dibromoethane	5.563	8.295	2.656	-	0.918	-	0	0	10.471
1,2-Dichloroethane	3.548	-	1.839	2.598	0.627	-	0	0	15.318
Chloroethane	4.224	1.015	1.415	2.287	0.493	-	0	0	10.847
1,1-Dichloropropane	5.893	1.813	2.480	-	1.636	-	0	0	8.324
1,2-Dichloropropane	5.168	7.297	1.400	-	1.449	-	0	0	10.581
1-Chloropropane	5.220	2.365	3.303	3.919	0.690	-	0	0	13.235
2-Chloropropane	3.438	5.276	1.621	-	-	-	0	0	7.854
m-Dichlorobenzene	4.137	3.878	1.161	-	0.847	-	0	0	14.840
p-Dichlorobenzene	2.072	15.410	1.569	-	11.864	-	0	0	14.561
Bromobenzene	4.032	3.635	1.443	-	0.848	-	0	0	10.057
Chlorobenzene	4.834	0.557	0.860	-	0.483	-	0	0	9.603
Heterocyclics									
Furan	3.316	5.136	6.167	5.275	0.341	-	0	0	0.027
Tetrahydrofuran	5.564	7.564	2.497	-	1.344	-	0	0	13.185
Thiophene	2.208	1.187	1.421	2.651	1.034	-	0	0	14.742
1,4-Dioxane	3.304	2.311	1.539	-	0.607	-	0	0	15.473
Tetrahydrothiophene	5.662	3.455	7.061	-	0.631	-	0	0	18.586
3-Methylthiophene	2.801	1.115	2.289	-	-	-	0	0	11.814
HFCs									
R32	4.272	1.002	1.993	3.675	1.811	5.956	0	0	15.210
R23	3.123	0.572	0.523	3.238	1.935	3.427	0	0	10.503
R125	6.420	3.026	0.763	3.176	3.154	4.405	0	0	8.611
R236fa	-	-	1.058	-	-	-	0	0	-
R236ea	-	-	0.985	-	-	-	0	0	-
R134a	4.605	2.029	0.902	2.729	3.895	5.511	0	0	10.087
R152a	5.375	1.257	1.112	4.840	2.596	5.413	0	0	12.049
R161	6.824	3.630	2.241	5.268	0.774	-	0	0	12.506
HCFCs									
R22	2.920	1.026	0.273	3.113	2.089	2.893	0	0	9.120
R21	1.357	10.005	6.050	2.960	1.969	3.326	0	0	9.419
R142b	4.172	2.098	0.288	3.795	2.896	4.997	0	0	11.820
R141b	3.361	1.342	0.775	2.592	1.985	3.986	0	0	9.906
R124	6.581	3.221	0.774	6.029	2.979	7.091	0	0	10.627
R123	5.172	2.076	0.777	4.618	1.976	4.873	0	0	10.829
CFCs									
R12	5.533	2.748	0.416	3.446	2.223	2.508	0	0	8.501
R11	1.588	9.028	4.465	3.141	1.984	2.559	0	0	7.309
R13	6.298	3.623	0.316	3.056	2.162	2.516	0	0	8.647
R115	5.303	2.761	0.290	4.598	2.981	4.012	0	0	11.182
R114	4.913	3.063	0.379	4.182	1.631	4.561	0	0	8.239

R113	6.499	4.066	0.391	3.363	3.985	4.031	0	0	5.445
Fluorocarbons									
R14	6.777	3.877	0.099	3.071	1.335	1.805	0	0	8.861
R116	4.190	4.854	0.088	3.888	2.774	3.886	0	0	6.457
R218	-	-	0.187	-	-	-	0	0	-
RC318	5.235	6.430	0.591	3.911	3.425	3.672	0	0	6.148
Acids									
Aceticanhydride	7.067	2.105	1.926	-	2.568	-	0	0	14.434
Others									
Ethyleneoxide	4.485	4.103	1.371	-	0.708	-	0	0	10.386
Dimethylsulfoxide	8.328	8.099	5.442	5.221	-	-	0	0	32.451

4-A.2 Overall %AADs in reproducing non-critical properties and %AADs in reproducing critical properties for 18 chemical families by CPPC-SAFT EOS and I-PC-SAFT EOS

This section presents the overall %AADs in non-critical property predictions and %ADs in critical property predictions for 20 chemical families by CPPC-SAFT EOS (Anoune *et al.*, 2021) and I-PC-SAFT EOS (Moine *et al.*, 2019), respectively.

Table 4-A4. %AADs in non-critical property predictions and %ADs in critical property predictions yielded by the CPPC-SAFT EOS for 20 chemical families.

Chemical groups	Number of compounds	%AADs in non-critical properties						%ADs in critical properties		
		V_{SatL}	V_{SatV}	P_{Sat}	V_{Liq}	V_{Vap}	V_{SC}	T_c	P_c	V_c
n-Alkanes	20	20.533	2.992	3.731	16.973	1.880	11.714	0	0	17.929
Branched alkanes	25	15.387	2.549	2.327	10.606	1.025	6.837	0	0	17.764
Cycloalkanes	12	15.714	3.743	4.150	13.073	0.981	6.616	0	0	15.031
Olefins	38	14.115	3.304	4.117	12.075	1.470	6.979	0	0	15.316
Alkynes	14	15.554	7.861	5.753	13.088	1.077	7.943	0	0	14.759
Aromatics	24	23.246	2.697	2.410	19.374	1.097	11.247	0	0	20.285
Ketones	14	24.051	3.323	3.795	26.368	2.604	-	0	0	21.180
Permanent gases	14	8.777	1.683	1.235	5.545	1.763	3.325	0	0	14.468
Ethers	6	13.647	4.973	4.056	13.720	0.716	-	0	0	16.537
Esters	8	23.170	2.297	4.243	20.914	2.160	-	0	0	20.019
Aldehydes	1	39.647	11.258	9.556	-	3.747	-	0	0	31.66
Sulfides and Thiols	18	17.594	4.716	2.629	-	1.743	-	0	0	20.154
Halogenated Hydrocarbons	24	19.715	4.576	1.977	19.802	1.212	11.959	0	0	18.162
Heterocyclics	6	14.577	3.101	3.662	12.226	0.783	-	0	0	18.380
HFCs	8	22.605	1.807	1.254	20.899	2.119	11.398	0	0	19.238
HCFCs	6	14.082	2.876	1.560	13.840	1.896	8.600	0	0	15.183
CFCs	6	10.819	3.367	1.093	10.810	1.842	6.950	0	0	12.448
Fluorocarbons	4	14.434	3.408	0.253	10.828	2.359	5.573	0	0	11.071
Acids	1	33.605	3.592	2.017	-	2.324	-	0	0	26.480
Others	2	33.238	6.960	3.568	46.498	0.551	-	0	0	33.03
Overall %AAD	251	17.641	3.565	3.062	14.203	1.499	6.658	0	0	17.586

Table 4-A5. %AADs in non-critical property predictions and %ADs in critical property predictions yielded by the I-PC-SAFT EOS for 20 chemical families.

Chemical groups	Number of compounds	%AADs in non-critical properties						%ADs in critical properties		
		V_{SatL}	V_{SatV}	P_{Sat}	V_{Liq}	V_{Vap}	V_{SC}	T_c	P_c	V_c
n-Alkanes	20	5.569	3.211	3.562	5.457	2.557	2.945	0	0	9.898
Branched alkanes	25	4.717	3.275	2.222	4.600	1.291	3.696	0	0	10.997
Cycloalkanes	12	4.202	4.015	3.963	4.103	1.349	3.690	0	0	8.264
Olefins	38	4.035	3.681	3.931	3.119	1.726	2.307	0	0	9.422
Alkynes	14	4.623	8.112	5.492	2.988	1.227	3.612	0	0	9.038
Aromatics	24	5.973	3.423	2.301	4.973	1.347	3.862	0	0	11.486
Ketones	14	5.732	4.244	3.623	4.057	2.842	-	0	0	12.010
Permanent gases	14	3.265	1.655	1.179	1.943	0.927	1.628	0	0	11.483
Ethers	6	4.218	5.838	3.872	4.491	0.805	-	0	0	10.858
Esters	8	5.726	3.843	4.051	4.729	2.208	-	0	0	10.585
Aldehydes	1	7.844	13.299	9.123	-	4.224	-	0	0	18.637
Sulfides and Thiols	18	4.632	5.419	2.510	-	1.834	-	0	0	13.286
Halogenated Hydrocarbons	24	4.907	4.616	1.887	3.490	1.320	3.330	0	0	10.533
Heterocyclics	6	3.809	3.461	3.496	3.963	0.791	-	0	0	12.305
HFCs	8	5.103	1.919	1.197	3.821	2.361	4.942	0	0	11.494
HCFCs	6	3.927	3.295	1.490	3.851	2.316	4.528	0	0	10.287
CFCs	6	5.022	4.215	1.043	3.631	2.494	1.682	0	0	8.221
Fluorocarbons	4	5.401	5.054	0.241	3.623	2.511	3.121	0	0	7.155
Acids	1	7.067	2.105	1.926	-	2.568	-	0	0	14.434
Others	2	6.407	6.101	3.407	5.221	0.708	-	0	0	21.419
Overall %AAD	251	4.805	4.046	2.923	3.625	1.695	2.464	0	0	10.695

CHAPTER 5 PREDICTION OF THERMODYNAMIC DERIVATIVE PROPERTIES OF PURE COMPOUNDS RELATED TO CARBON CAPTURE AND STORAGE BY VOLUME-TRANSLATED RESCALED PC-SAFT EOS

A version of this chapter will be submitted to an appropriate journal for possible publication.

Abstract

Thermodynamic models such as equations of state (EOS) are crucial for predicting phase behavior and thermophysical properties of pure substances in carbon capture and storage (CCS) processes. However, accurately describing the thermodynamic derivative properties of pure components over a wide range of temperature and pressure, especially near the critical region, remains a significant challenge for almost all EOS models. Very recently, a volume-translated rescaled perturbed-chain statistical associating fluid theory equation of state (VTR-PC-SAFT EOS) was developed for achieving accurate predictions of thermodynamic properties of pure compounds both near and far from the critical region. In this study, we apply VTR-PC-SAFT EOS to calculate the thermodynamic derivative properties of 16 selected pure compounds relevant to CCS. Specifically, we evaluate the performance of such model in predicting the various thermodynamic derivative properties (i.e., heat capacities, Joule-Thomson coefficient, thermal expansion coefficient, isothermal compressibility coefficient, and speed of sound). The evaluation results indicate that, compared to other state-of-the-art PC-SAFT-type EOSs assessed in this study, VTR-PC-SAFT EOS can generally provide more accurate derivative property predictions of CCS fluids.

Keywords: Carbon capture and storage; VTR-PC-SAFT EOS; Volume translation; Thermodynamic derivative properties; Prediction accuracy

5.1 Introduction

In recent years, carbon capture and storage (CCS) has garnered considerable attention, given their promising role in the mitigation of greenhouse gas emissions (Tzirakis *et al.*, 2019; Zhang *et al.*, 2023). In the realm of CCS, there is a substantial demand for dependable experimental data and theoretical models pertaining to the thermodynamic properties of pure compounds and mixtures in both industry and academia. Such need is especially critical in the design and operation of various CCS processes, such as compression, transportation, and storage. For instance, optimizing CO_2 transportation through pipelines can be achieved by using mixtures with higher CO_2 densities (Vitali *et al.*, 2021). Such a mechanism, which involves the phase behavior of CO_2, aids in decreasing the size requirements for pipelines.

Additionally, in CCS processes, transport properties such as viscosity and diffusion coefficients, as well as other thermophysical properties such as density and vapor pressure, are becoming increasingly significant for design and operational considerations. To address these needs, thermodynamic models such as equations of state (EOS) are widely used. These models are critical for accurately predicting thermodynamic properties under specific conditions. Various types of EOSs exist, including cubic EOSs (CEOS) and molecular-based EOSs, each characterized by a distinct mathematical framework. Among the various CEOSs, Peng-Robinson EOS (PR EOS) (Peng and Robinson, 1976) and Soave-Redlich-Kwong EOS (SRK EOS) (Soave, 1972) stand out and are extensively utilized in both industry and academia due to their commendable accuracy and simplicity. However, despite their success, CEOSs do have some limitations. One notable shortcoming is that they cannot accurately predict liquid density of pure components. To address such

limitation, an alternative route is to develop new thermodynamic models based on fundamental statistical mechanics. Since the development of statistical associating fluid theory EOS (SAFT EOS) based on a perturbation theory proposed by Wertheim (1984a,b; 1986a,b), various versions of SAFT EOSs have been developed. One of the classic SAFT EOS models, initially presented by Chapman *et al.* (1989), was subsequently modified by Gross and Sadowski (2001), resulting in the perturbed-chain SAFT EOS (PC-SAFT EOS). Such SAFT-type EOSs could potentially address the various issues associated with predicting thermodynamic properties, which are often encountered with CEOSs (Müller *et al.*, 2001).

While PC-SAFT-type EOS can potentially yield accurate phase equilibria predictions, a good precision in predicting derivative thermodynamic properties (such as heat capacities, the Joule-Thomson coefficient, thermal expansion coefficient, isothermal compressibility coefficient, and speed of sound) is not assured, as highlighted in the studies by Faradonbeh *et al.* (2013), Pakravesh and Zarei (2021), Zhang *et al.* (2020), Cea-Klapp *et al.* (2020), and Majdi *et al.* (2023). In this study, we evaluate the performance of various PC-SAFT-type EOSs in predicting the thermodynamic derivative properties of selected pure compounds. We have chosen 16 pure compounds, including CO_2 and several alkanes, for their relevance to CO_2 flooding and storage applications (Tzirakis *et al.*, 2019; Peletiri *et al.*, 2019; Vitali *et al.*, 2021; Zhang *et al.*, 2023).

5.2 Literature Review on the Prediction of Thermodynamic Derivative Properties

While numerous EOSs with various mathematical frameworks, such as cubic EOSs (Soave, 1972; Peng and Robinson, 1976; Ghoderao *et al.*, 2018 and 2019), SAFT-type EOSs (Chapman *et al.*, 1989; Gross and Sadowski, 2001; Lafitte *et al.*, 2013), and cubic-

plus-association (CPA)-type EOSs (Kontogeorgis *et al.*, 1996; Lundstrøm *et al.*, 2006), have been widely used to predict density and vapor pressure, there are limited published works reporting their applications to the calculation of derivative properties. Due to continued efforts in both academia and industry, SAFT-type EOSs have achieved notable success in predicting thermodynamic properties and phase equilibria for both pure fluids and mixtures. Starting with the original SAFT EOS (Chapman *et al.*, 1989), evolving to the PC-SAFT EOS (Gross and Sadowski, 2001), and then to the SAFT-VR Mie EOS (Lafitte *et al.*, 2013), various versions of SAFT-type EOSs have been proposed with subsequent modifications and extensions. However, while they can accurately reproduce thermodynamic properties such as liquid density in the non-critical region, they often lead to a compromised prediction accuracy near the critical region. This, in turn, results in less precise derivative property predictions in areas close to the critical region (De Villiers *et al.*, 2013).

Lafitte *et al.* (2013), for example, presented that the original PC-SAFT EOS and SAFT-Variable Range-type EOSs (SAFT-VR-type EOSs) are incapable of providing the accurate description of the derivative properties such as speed of sound and isothermal compressibility in the liquid region. In pursuit of enhancing the accuracy of second-order derivative property predictions, the SAFT-VR-Mie EOS was introduced, built on the *m*-*n* Mie potential function (Lafitte *et al.*, 2006). This molecular-based EOS has been demonstrated to accurately predict some derivative properties, including heat capacity and speed of sound. However, as emphasized by Polishuk and Garrido (2018), the SAFT-VR Mie EOS encounters some challenges, particularly when dealing with pure fluids near the critical region or complex mixtures.

To address the issues related to inaccuracies in property predictions near the critical region by SAFT-type EOSs, there has been a recent surging interest in the development of critical-point based SAFT-type EOSs. Chen and Mi (2001) proposed one SAFT-critical point EOS (SAFT-CP EOS) by considering the hard-convex-body reference term and excluding the intramolecular segment interaction in the dispersion term. Their model demonstrated accurate predictions of selected derivative properties for alkanes (Maghari and Sadeghi, 2007; Maghari *et al.*, 2008). However, it seems that the capability of such model to predict phase equilibria of mixtures requires further evaluation (Tan *et al.*, 2008). Vega and co-workers (Blas and Vega, 1998a,b; Llovell and Vega, 2006) proposed a soft-SAFT EOS by incorporating a crossover treatment, considering a renormalization group term with two parameters. Similarly, Yang *et al.* (2023) proposed a crossover PC-SAFT EOS based on White's method for CO_2, *n*-alkanes and *n*-alkanols. Such crossover strategy can effectively capture the phase behavior, particularly in the vicinity of the critical region, but might introduce significant deviations in the derivative properties such as speed of sound. Polishuk and co-workers (Polishuk, 2014 and 2015; Polishuk *et al.*, 2017a,b) introduced a standardized critical-point-based SAFT EOS by re-assessing the universal parameters matrix using the critical point as a foundation. Such model provides remarkable precision in predicting thermophysical properties like liquid density. However, they also highlighted its diminished accuracy in predicting the vacuum vapor pressures of heavy compounds, especially when distant from their critical point. Furthermore, the model provides a relatively accurate representation of derivative properties like heat capacities, with the exception of areas close to the critical region. Similar to the rescaling approach adopted by the critical-point-based SAFT EOSs (Polishuk, 2014 and 2015), some

researchers (Anoune *et al.*, 2021; Pakravesh *et al.*, 2021) attempted to use the re-parametrization method to exactly reproduce the critical point. However, an exact reproduction of critical point cannot guarantee the accurate reproduction of thermodynamic properties and phase behavior in the vicinity of the critical point. Contrarily, it appears that, in critical point-based SAFT EOSs (Shi and Li, 2022 and 2023), achieving exact reproductions of experimental critical temperature and experimental critical pressure comes at the cost of compromised density prediction accuracy both near and far from the critical region.

Unfortunately, rescaling the SAFT's molecular parameters typically results in significant deterioration in the prediction accuracy of both first-order and second-order properties. To address this issue, the volume translation strategy emerges as a beneficial and effective solution. Combining a re-parameterization method which can exactly reproduce the experimental critical point, Moine *et al.* (2019) proposed an industrialized version of the volume-translated PC-SAFT EOS, so-called I-PC-SAFT EOS. In such EOS, a constant volume translation term was incorporated into the re-parameterized PC-SAFT EOS for remedying the inaccurate liquid density predictions. However, such constant volume translation term still leads to compromised performance of I-PC-SAFT EOS in predicting the thermodynamic properties near the critical region. Similarly, Shi and Li (2022) incorporated a temperature-dependent volume translation into a CPPC- SAFT EOS (Anoune *et al.*, 2021) for carbon dioxide. While this temperature-dependent volume translated CPPC-SAFT EOS slightly enhances the accuracy in describing phase behavior both near and away from the critical region, its performance in predicting thermodynamic properties near the critical point appears to be suboptimal. Very recently, a volume-

translated rescaled PC-SAFT EOS (VTR-PC-SAFT EOS) was proposed by Shi and Li (2023). Their model yields significantly improved property prediction accuracy close to and away from the critical region. However, such VTR-PC-SAFT EOS has not yet undergone a systematic evaluation for the prediction of thermodynamic derivative properties of pure compounds.

In conclusion, the ability of SAFT-type EOSs to predict thermodynamic derivative properties remains a formidable challenge. This is primarily because the accuracy of derivative property predictions hinges on the precision of the basic PVT property predictions. Furthermore, derivative properties predicted by EOSs are inherently more sensitive compared to the basic PVT properties. This suggests that even minor inaccuracies in predicting PVT properties could lead to substantial deviations when predicting derivative properties. This study evaluates the ability of several benchmark PC-SAFT EOSs (including the original PC-SAFT EOS (Gross and Sadowski, 2001), CPPC-SAFT EOS (Anoune *et al.*, 2021), I-PC-SAFT EOS (Moine *et al.*, 2019), and VTR-PC-SAFT EOS (Shi and Li, 2023)) to predict derivative properties of pure compounds.

5.3 VTR-PC-SAFT EOS

The PC-SAFT-type EOS is written as (Gross and Sadowski, 2001),

$$a_{res} = a_{hc} + a_{disp} \tag{5-1}$$

where a_{res} is the residual Helmholtz free energy, while a_{hc} and a_{disp} refer to the contributions from hard-chain repulsion and dispersion, respectively.

To avoid the overestimation of critical pressure and critical temperature as well as exactly reproduce the critical point, three model parameters used in VTR-PC-SAFT EOS, i.e., segment number (m), segment diameter (σ), and energy parameter (ε/k), should be

rescaled and adjusted to exactly fit the experimental critical pressure and critical temperature. The detailed re-parametrization method can be found in the studies by Moine *et al.* (2019) and Anoune *et al.* (2021).

To exactly reproduce the critical molar volume as well as make the prediction of the saturated-liquid molar volumes and liquid molar volumes more accurate near and far from the critical point, a distance-function-based volume translation is introduced into CPPC-SAFT EOS (Anoune *et al.*, 2021), leading to the so-called VTR-PC-SAFT EOS (Shi and Li, 2023). The distance-function-based volume translation model in VTR-PC-SAFT is given as (Shi and Li, 2023),

$$c = V_{\text{CPPC-SAFT}} - V_{\text{Exp}} = \left(\frac{N_A \pi m d_c^3}{6\eta_c} - \frac{z_{c,\text{Exp}} R T_c}{P_c} \right) \exp\left(c_1 \gamma\right) \left(\frac{1}{1 + c_2 \gamma} \right) \tag{5-2}$$

where c is the volume translation term defined as the difference between the molar volume calculated by CPPC-SAFT EOS ($V_{\text{CPPC-SAFT}}$) and the experimental one from NIST database (V_{Exp}) (Linstrom and Mallard, 2001), while N_A, d_c, η_c, $z_{\text{c,Exp}}$ and R refer to the Avogadro constant, the temperature-dependent hard segment diameter at critical point, the packing fraction at critical point, the experimental critical compressibility factor, and the universal gas constant, respectively. c_1 and c_2 are two compound-dependent parameters, which are regressed based on the saturated-liquid density. Besides, γ is a dimensionless distance function, and its detailed expression is presented below (Shi and Li, 2023),

$$\gamma = -\frac{R\rho^2}{P_c}\left(\frac{\partial T}{\partial \rho}\right)_P = \frac{R}{P_c}\left(\frac{\partial T}{\partial V}\right)_P \tag{5-3}$$

where ρ is molar density, while $\left(\frac{\partial T}{\partial V}\right)_p$ is the first derivative of temperature with respect to to molar volume at constant pressure and can be calculated from the original CPPC-SAFT EOS. The so-called VTR-PC-SAFT EOS is shown to have the potential to address the issues found in other SAFT-type EOSs, providing a good representation of phase behavior across a broad range of temperature and pressure conditions (including both near-critical and far-critical regions).

5.4 Thermodynamic Derivative Properties

The derivative properties examined in this study include isothermal compressibility, isobaric thermal expansivity, isochoric heat capacity, isobaric heat capacity, Joule-Thomson coefficient, and speed of sound. The expressions of these derivative properties are given as (Llovell and Vega, 2006):

$$\beta_T = -\frac{1}{V}\left(\frac{\partial V}{\partial P}\right)_T \tag{5-4}$$

$$\alpha_P = \frac{1}{V}\left(\frac{\partial V}{\partial T}\right)_P \tag{5-5}$$

$$C_V = -T\left(\frac{\partial^2 a}{\partial T^2}\right)_V \tag{5-6}$$

$$C_P = C_V + \frac{TV\alpha_P{}^2}{\beta_T} \tag{5-7}$$

$$\mu_{\mathrm{JT}} = \frac{V\left(\alpha_P T - 1\right)}{C_P} = T\left(\frac{\partial P}{\partial T}\right)_V - \rho\left(\frac{\partial P}{\partial \rho}\right)_T = T\left(\frac{\partial P}{\partial T}\right)_V - \frac{1}{\beta_T} \tag{5-8}$$

$$u = \sqrt{-\frac{V^2}{M_w}\frac{C_P}{C_V}\left(\frac{\partial P}{\partial V}\right)_T} \tag{5-9}$$

where β_T refers to the isothermal compressibility, α_P refers to the isobaric thermal expansivity, C_V refers to the isochoric heat capacity, C_P refers to the isobaric heat capacity, μ_{JT} refers to the Joule-Thomson coefficient, and u refers to the speed of sound. Additionally, P, V, and T are pressure, molar volume, and temperature, respectively, while M_w and a denote molecular weight and the Helmholtz free energy per mole.

In this study, we assess the performance of various PC-SAFT EOSs in predicting derivative properties using the following error index,

$$\%\mathrm{AAD} = \frac{100}{N}\sum_{i=1}^{N}\left|\frac{Prop_{i,\mathrm{Exp}} - Prop_{i,\mathrm{SAFT\text{-}type}}}{Prop_{i,\mathrm{Exp}}}\right| \tag{5-10}$$

where %AAD is defined as the average absolute percentage deviation and N is the number of data points, $Prop_{i,\mathrm{Exp}}$ represents the experimental derivative property for the ith data point sourced from the NIST database, and $Prop_{i,\mathrm{SAFT\text{-}type}}$ is the derivative property calculated by a specific PC-SAFT EOS.

5.5 Results and Discussion

In this study, we evaluate the performance of the following representative versions of PC-SAFT EOS in predicting the thermodynamic derivative properties: CPPC-SAFT EOS (Anoune *et al.*, 2021), I-PC-SAFT EOS (Moine *et al.*, 2019), PC-SAFT EOS (Gross and Sadowski, 2001), and VTR-PC-SAFT EOS (Shi and Li, 2023). The predictive ability

of these EOSs is assessed at the non-critical region and near-critical region. **Table 5-1** presents the molecular parameters used in various PC-SAFT EOSs and compound-dependent parameters used in the volume translation strategies for the 16 compounds considered in this study. Note that CPPC-PC-SAFT EOS, I-PC-SAFT EOS, and VTR-PC-SAFT EOS use the same three molecular parameters.

Table 5-1. Molecular parameters used in various PC-SAFT-type EOSs (Gross and Sadowski, 2001; Moine *et al.*, 2019; Anoune *et al.*, 2021) and compound-dependent parameters used in the volume translation strategies.

Compounds	PC-SAFT EOS			CPPC SAFT EOS, I-PC-SAFT-EOS, and VTR-PC-SAFT			*c* in VTR-SAFT EOS		*c* in I-PC SAFT EOS
	m	σ [A]	ε/k [K]	*m*	σ [A]	ε/k [K]	c_1	c_2	*c* [cm^3/mol]
Hydrogen sulfide	1.669	3.035	229.00	1.709	3.056	224.326	0.1097	1.7805	1.9993
Oxygen	1.122	3.210	114.96	1.149	3.180	113.460	-0.9492	0.2935	-0.1402
Carbon dioxide	2.073	2.785	169.21	2.668	2.612	147.234	0.0784	0.5120	4.8763
Sulfur dioxide	2.861	2.683	205.35	2.971	2.762	198.787	0.0848	0.4031	8.2267
Carbon monoxide	1.310	3.251	92.15	1.379	3.194	89.009	-1.0984	0.1444	-0.2452
Nitrogen	1.205	3.313	90.96	1.270	3.266	88.136	-0.9738	0.5280	-0.3678
Methane	1.000	3.704	150.03	1.051	3.643	146.016	-0.3415	1.6143	0.1021
Ethane	1.607	3.521	191.42	1.703	3.505	183.677	0.0553	1.0989	3.2373
Propane	2.002	3.618	208.11	2.121	3.627	199.460	0.0568	0.6730	7.4213
Butane	2.332	3.709	222.88	2.492	3.733	212.368	0.0484	0.4564	12.4678
Pentane	2.690	3.773	231.20	2.904	3.805	218.979	0.0462	0.3798	19.5201
Hexane	3.058	3.798	236.77	3.313	3.852	223.812	0.0462	0.3546	27.0464
Heptane	3.483	3.805	238.40	3.726	3.902	227.084	0.0442	0.3287	34.1800
Octane	3.818	3.837	242.78	4.128	3.943	229.870	0.0447	0.3127	42.2321
Nonane	4.208	3.845	244.51	4.517	3.976	232.540	0.0403	0.2954	49.3187
Decane	4.663	3.838	243.87	4.896	4.008	234.891	0.0531	0.3844	56.7744

Table 5-2 lists the %AADs in predicting isothermal compressibility and isobaric thermal expansivity of the 16 compounds by different PC-SAFT EOSs. The results indicate that VTR-PC-SAFT EOS consistently outperforms its counterparts, providing the smallest %AADs of 3.47 for isothermal compressibility and 2.69 for isobaric thermal expansivity.

In **Eq. 5-4** and **Eq. 5-5**, isothermal compressibility and isobaric thermal expansivity are composed of two components: the molar volume value and its first derivative with respect to pressure ($\left(\frac{\partial V}{\partial P}\right)_T$) or temperature $\left(\frac{\partial V}{\partial T}\right)_p$. While I-PC-SAFT EOS introduces the constant volume translation into CPPC-SAFT EOS for improving the prediction accuracy of molar volume, the first derivatives with respect to pressure and temperature remain unaltered. This is because these derivatives are unaffected by the constant volume translation. The results shown in **Table 5-2** indicate that the introduction of the distance-function based volume translation brings about two benefits. Firstly, it refines the prediction accuracy of the molar volume. Secondly, it also enhances the prediction accuracy of the first derivatives with respect to pressure or temperature.

Table 5-2. %AADs in predicting isothermal compressibility (β_T) and isobaric thermal expansivity (α_P) by different PC-SAFT EOSs.

Compounds	PC-SAFT		CPPC-SAFT		I-PC-SAFT		VTR-PC-SAFT	
	β_T	α_P	β_T	α_P	β_T	α_P	β_T	α_P
Hydrogen sulfide	4.26	3.91	12.27	6.28	19.27	8.90	2.93	1.88
Oxygen	4.76	4.52	10.03	6.22	16.55	7.01	2.02	1.56
Carbon dioxide	5.98	4.80	19.72	8.91	31.27	19.22	4.86	2.95
Sulfur dioxide	5.12	5.08	14.29	9.94	18.29	10.20	3.23	2.57
Carbon monoxide	5.83	5.04	12.31	6.90	18.23	8.45	3.28	3.02
Nitrogen	3.77	2.81	8.93	5.26	10.44	6.38	2.05	1.47
Methane	4.89	4.66	8.45	6.70	11.27	5.94	2.73	2.06
Ethane	4.84	4.71	7.48	5.33	10.92	5.88	2.81	2.02
Propane	5.29	5.12	9.29	6.24	13.48	7.22	3.03	2.47
Butane	5.82	5.28	10.20	6.89	15.99	9.58	3.72	3.20
Pentane	5.29	5.23	12.38	7.92	17.28	9.93	3.03	3.21
Hexane	5.90	5.24	13.29	6.29	18.22	10.29	3.92	2.97
Heptane	5.82	5.10	15.28	8.70	20.72	12.25	4.02	3.50
Octane	6.29	5.78	15.02	9.18	23.01	12.92	4.14	3.28
Nonane	6.77	4.97	15.92	9.09	22.82	11.88	3.94	3.72
Decane	6.82	6.19	17.28	10.90	23.29	13.23	4.38	3.94
Over %AAD	5.84	5.03	13.89	8.22	18.20	10.92	3.47	2.69

We take CO_2 as an example to visualize the comparative evaluation results. **Fig. 5-1** compares the isothermal compressibility (β_T) at different constant temperatures calculated by CPPC-SAFT EOS, I-PC-SAFT EOS, and VTR-PC-SAFT EOS against the experimental data for CO_2. **Fig. 5-2** shows the isobaric thermal expansivity (α_P) of CO_2 at different constant pressures calculated by CPPC-SAFT EOS, I-PC-SAFT EOS, and VTR-PC-SAFT EOS. As seen from **Fig. 5-1** and **Fig. 5-2**, the VTR-PC-SAFT EOS offers a better match with the experimental isothermal compressibility and isobaric thermal expansivity than the other counterpart models.

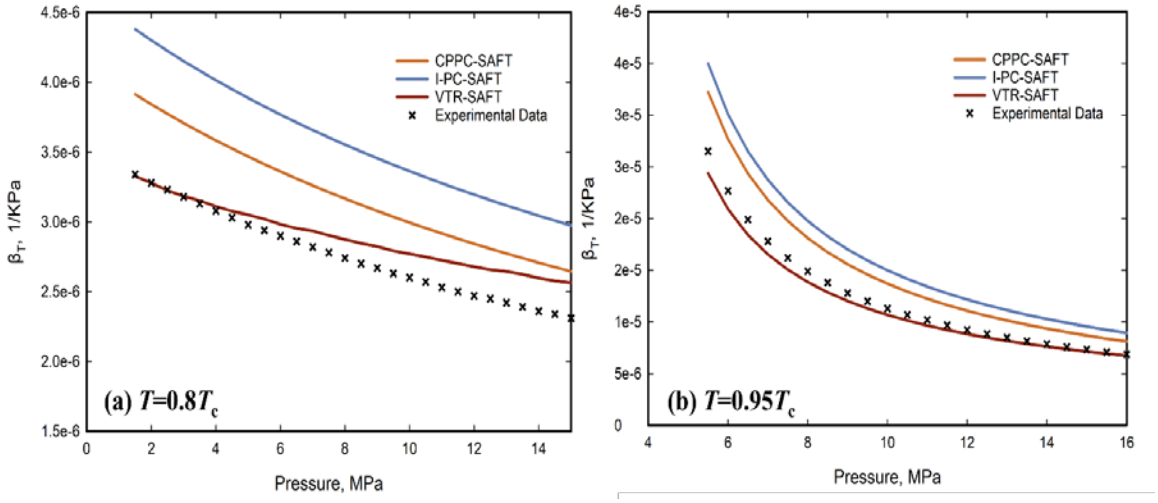

Fig. 5-1. Comparison of isothermal compressibility (β_T) of CO_2 at constant temperatures ($0.8T_c$ and $0.95T_c$) calculated by CPPC-SAFT EOS, I-PC-SAFT EOS, VTR-PC-SAFT EOS against the experimental data retrieved from NIST database.

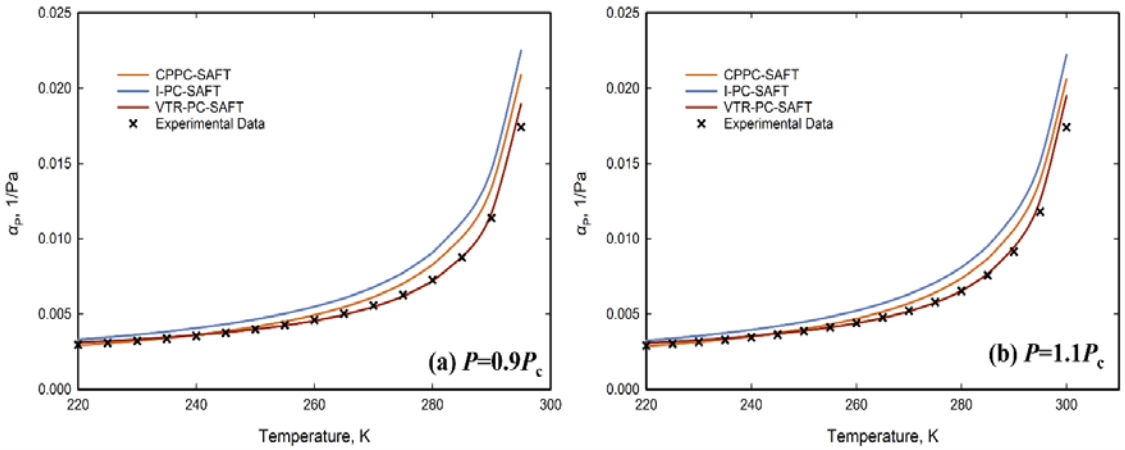

Fig. 5-2. Comparison of isobaric thermal expansivity (α_P) of CO_2 at constant pressures ($0.9P_c$ and $1.1P_c$) calculated by CPPC-SAFT EOS, I-PC-SAFT EOS, VTR-PC-SAFT EOS and experimental data retrieved from NIST database.

Table 5-3. %AADs in predicting isobaric heat capacity (C_P) by different PC-SAFT EOSs.

Compounds	PC-SAFT	CPPC-SAFT	I-PC-SAFT	VTR-PC-SAFT
	C_P	C_P	C_P	C_P
Hydrogen sulfide	3.28	7.21	10.28	3.05
Oxygen	3.20	5.89	8.04	2.38
Carbon dioxide	3.98	9.92	24.28	3.90
Sulfur dioxide	3.82	8.29	10.80	3.27
Carbon monoxide	3.48	5.24	8.27	3.04
Nitrogen	2.94	3.57	5.88	1.97
Methane	4.18	6.29	13.20	3.13
Ethane	3.92	7.05	10.28	3.30
Propane	3.72	6.82	14.32	3.82
Butane	2.01	7.91	15.29	3.92
Pentane	1.82	7.08	16.27	3.90
Hexane	1.79	6.27	14.77	3.77
Heptane	1.82	4.88	9.89	2.73
Octane	2.14	5.99	10.03	3.07
Nonane	1.90	6.85	11.82	3.24
Decane	2.67	7.12	12.88	2.86
Overall %AAD	2.89	7.02	14.98	3.03

Table 5-3 presents the detailed %AADs in predicting isobaric heat capacity (C_P) by different PC-SAFT EOSs. As shown in **Table 5-3**, the VTR-PC-SAFT EOS can provide

more precise estimation of isobaric heat capacity when compared to both CPPC-SAFT EOS and I-PC-SAFT EOS, while PC-SAFT EOS can provide a similar overall prediction accuracy as VTR-PC-SAFT EOS. Specifically, overall %AADs of only 2.89 and 3.03 are yielded by PC-SAFT EOS and VTR-SAFT EOS, respectively. In contrast, the CPPC-SAFT EOS and I-PC-SAFT EOS produce considerably higher %AADs (i.e., 7.02 and 14.98, respectively). Again, we take CO_2 as an example to visualize the comparative results. **Fig. 5-3** compares the isobaric heat capacity (C_P) of CO_2 at two constant pressures calculated by the CPPC-SAFT EOS, I-PC-SAFT EOS, and VTR-PC-SAFT EOS against the experimental data. It can be seen from **Fig. 5-2** that the VTR-PC-SAFT EOS can generally better represent the isobaric heat capacity of CO_2 over a wide range of temperature and pressure than CPPC-SAFT EOS and I-PC-SAFT EOS.

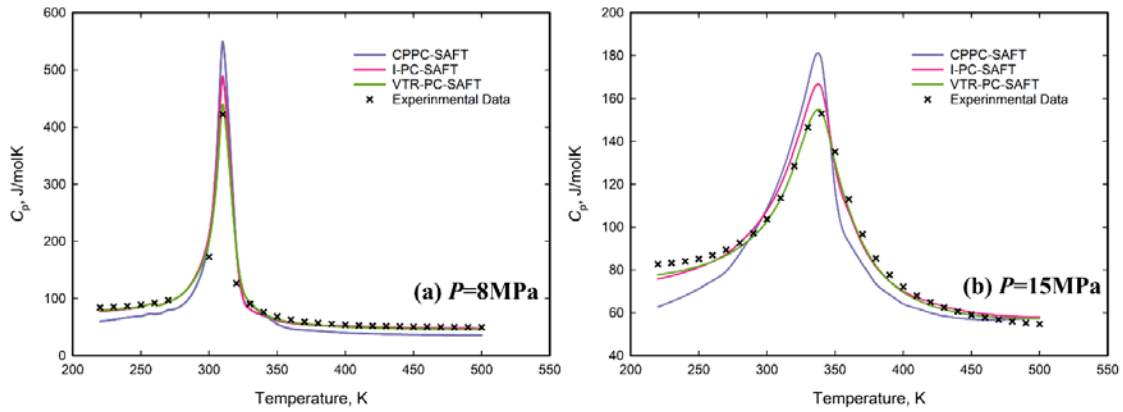

Fig. 5-3. Comparison of isobaric heat capacity (C_P) of CO_2 at two constant pressures (8 MPa and 15 MPa) calculated by CPPC-SAFT EOS, I-PC-SAFT EOS, VTR-PC-SAFT EOS against the experimental data retrieved from NIST database.

Table 5-4 lists the %AADs in predicting the Joule-Thomson coefficient and speed of sound by the four PC-SAFT EOSs. Notably, the VTR-PC-SAFT EOS achieves the lowest %AADs in predicting Joule-Thomson coefficient and speed of sound (i.e., 4.81 and

5.28, respectively). **Fig. 5-4** and **Fig. 5-5** compare Joule-Thomson coefficient (μ_{JT}) and speed of sound (u) of CO_2 calculated by CPPC-SAFT EOS, I-PC-SAFT EOS, and VTR-PC-SAFT EOS against the experimental data. Evident from these figures, the VTR-PC-SAFT EOS consistently offers the most accurate predictions for both Joule-Thomson coefficient and speed of sound, outperforming both CPPC-SAFT EOS and I-PC-SAFT EOS.

Table 5-4. %AADs in predicting Joule-Thomson coefficient (μ_{JT}) and speed of sound (u) by different PC-SAFT EOSs.

Compounds	PC-SAFT		CPPC-SAFT		I-PC-SAFT		VTR-PC-SAFT	
	μ_{JT}	u	μ_{JT}	u	μ_{JT}	u	μ_{JT}	u
Hydrogen sulfide	7.28	10.28	13.28	27.27	20.12	21.24	4.28	5.32
Oxygen	5.29	9.83	10.02	20.14	18.25	17.27	3.92	3.65
Carbon dioxide	6.90	8.27	12.93	21.32	26.28	19.28	4.99	4.92
Sulfur dioxide	9.28	10.54	13.28	22.65	22.39	19.92	4.05	5.26
Carbon monoxide	7.25	11.29	15.77	19.29	24.22	17.21	4.87	4.88
Nitrogen	5.02	8.41	9.45	17.05	16.90	15.03	2.39	4.85
Methane	8.02	10.28	15.29	25.28	23.29	20.93	5.28	4,07
Ethane	9.28	10.55	16.28	23.22	23.73	22.29	5.92	5.26
Propane	8.37	12.45	14.23	23.90	28.28	24.28	6.82	5.21
Butane	8.40	13.29	13.27	25.66	24.37	25.20	5.10	5.93
Pentane	10.27	13.02	14.92	24.21	25.90	23.43	4.92	5.18
Hexane	10.89	14.27	15.28	25.98	24.10	21.65	5.29	4.27
Heptane	12.24	13.05	14.74	23.76	22.88	21.58	5.59	5.55
Octane	11.28	12.88	14.90	26.80	22.04	24.21	5.82	5.10
Nonane	10.23	13.50	15.28	27.21	24.26	20.38	4.55	6.17
Decane	10.03	12.92	15.27	24.72	23.91	22.76	4.27	5.98
Overall %AAD	9.12	11.56	13.89	24.27	22.60	23.65	4.81	5.28

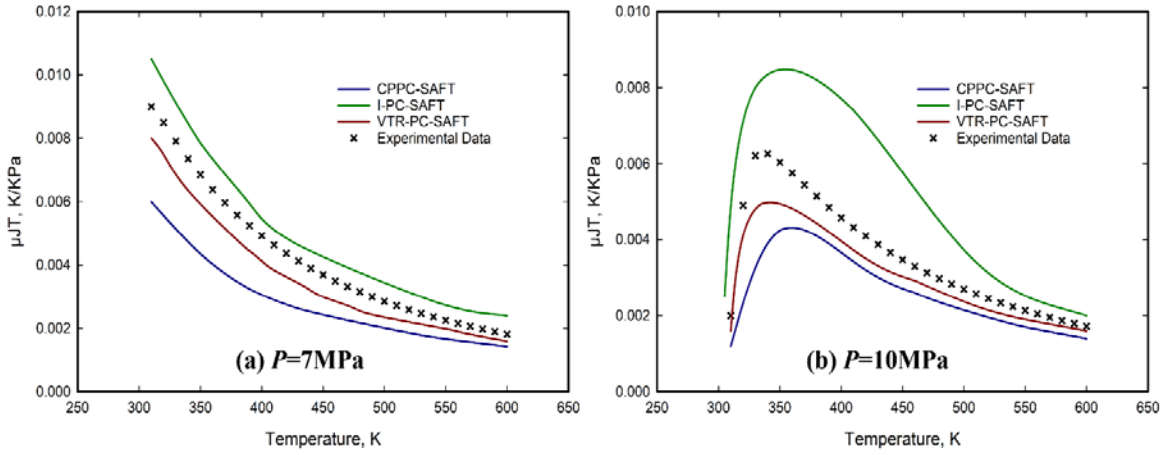

Fig. 5-4. Comparison of Joule-Thomson coefficient (μ_{JT}) of CO_2 at two constant pressures (7MPa and 10MPa) by CPPC-SAFT EOS, I-PC-SAFT EOS, and VTR-PC-SAFT EOS against the experimental data retrieved from NIST database.

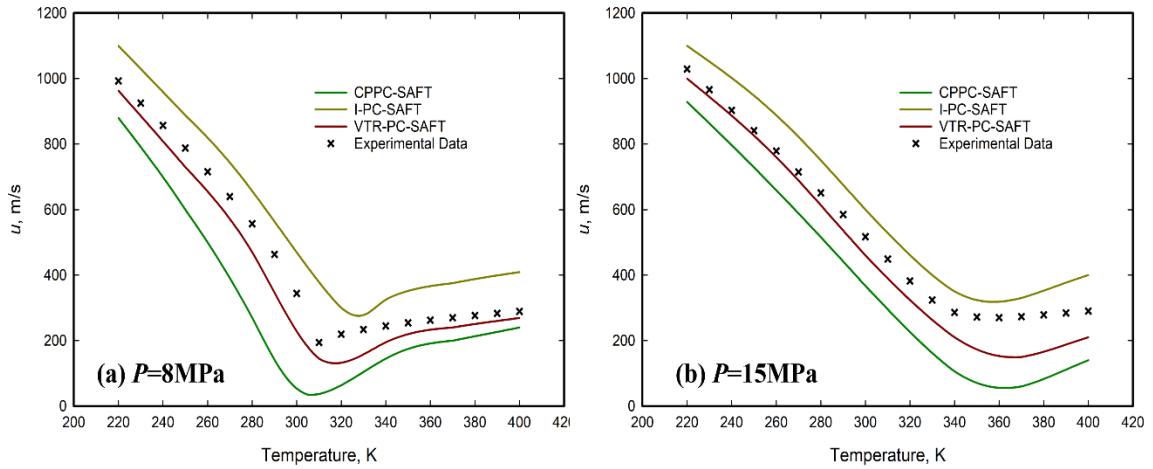

Fig. 5-5. Comparison of speed of sound (u) of CO_2 at two constant pressures (8MPa and 15MPa) with CPPC-SAFT EOS, I-PC-SAFT EOS, and VTR-PC-SAFT EOS against the experimental data retrieved from NIST database.

The derivative properties are influenced by contributions from molar volume values and the derivatives of pressure, molar volume, and temperature (i.e., $\left(\frac{\partial V}{\partial P}\right)_T$,

$\left(\frac{\partial V}{\partial T}\right)_p$, and $\left(\frac{\partial P}{\partial T}\right)_V$). PC-SAFT EOS, while being unable to accurately represent vapor pressure and phase behavior near the critical region, inherently struggles to precisely predict these derivative properties. Although the CPPC-SAFT EOS can exactly reproduce the critical temperature and critical pressure, it manifests significant deviations in predicting the liquid molar volume across various temperatures and pressures. This lack of precision in predicting liquid molar volume invariably affects the prediction accuracy of the derivative properties. The constant volume translation used by I-PC-SAFT EOS—a term independent of temperature and pressure—cannot effectively rectify the predicted values of $\left(\frac{\partial V}{\partial P}\right)_T$, $\left(\frac{\partial V}{\partial T}\right)_p$, and $\left(\frac{\partial P}{\partial T}\right)_V$ calculated by I-PC-SAFT EOS. The adoption of a distance-function-based volume translation term in VTR-PC-SAFT EOS appears to considerably enhance the prediction accuracy of these derivatives. This improvement, together with the improvement in molar volume predictions, translates into generally more accurate predictions of the various derivative properties. The only exception is regarding the prediction of isobaric heat capacity, for which PC-SAFT EOS shows a marginally better accuracy than VTR-PC-SAFT EOS.

5.6 Conclusions

In this study, we assess the performance of PC-SAFT EOS, CPPC-SAFT EOS, I-PC-SAFT EOS, and VTR-PC-SAFT EOS in predicting the thermodynamic derivative properties (including isothermal compressibility, isobaric thermal expansivity, heat capacity, Joule-Thomson coefficient, and speed of sound) of 16 selected pure compounds. The comparative results show that, among all the models considered in this study, VTR-PC-SAFT EOS generally outperforms the other counterpart models in predicting the

derivative properties. But regarding the isobaric heat capacity, the accuracy yielded by VTR-PC-SAFT is slightly lower than the original PC-SAFT EOS.

References

A. Maghari, M.S. Sadeghi, Prediction of sound velocity and heat capacities of n-alkanes from the modified SAFT-BACK equation of state, *Fluid Phase Equilibria* 252 (2007) 152-161.

A. Maghari, Z. Safaei, S. Sarhangian, Predictions of the Joule–Thomson inversion curves for polar and non-polar fluids from the SAFT-CP equation of state, *Cryogenics* 48 (2008) 48-55.

A. Pakravesh, F. Zarei, H. Zarei, PρT parameterization of SAFT equation of state: developing a new parameterization method for equations of state, *Fluid Phase Equilibria* 538 (2021) 113024.

A. Pakravesh, H. Zarei, Prediction of Joule–Thomson coefficients and inversion curves of natural gas by various equations of state, *Cryogenics* 118 (2021) 103350.

A.J. De Villiers, C.E. Schwarz, A.J. Burger, G.M. Kontogeorgis, Evaluation of the PC-SAFT, SAFT and CPA equations of state in predicting derivative properties of selected non-polar and hydrogen-bonding compounds, *Fluid Phase Equilibria* 338 (2013) 1-15.

B. Zhang, E. Wang, F. Meng, F. Zhang, C. Zhao, Prediction accuracy of thermodynamic properties using PC-SAFT for high-temperature organic Rankine cycle with siloxanes, *Energy* 204 (2020) 117980.

C. Lundstrøm, M. L. Michelsen, G.M. Kontogeorgis, K.S. Pedersen, H. Sørensen, Comparison of the SRK and CPA equations of state for physical properties of water and methanol, *Fluid Phase Equilibria* 247 (2006) 149-157.

D.Y. Peng, D.B. Robinson, A new two-constant equation of state, *Industrial & Engineering Chemistry Fundamentals* 15 (1976) 59-64.

E. Cea-Klapp, I. Polishuk, R.I. Canales, H. Quinteros-Lama, J.M. Garrido, Estimation of thermodynamic properties and phase equilibria in systems of deep eutectic solvents by PC-SAFT EoS, *Industrial & Engineering Chemistry Research* 59 (2020) 22292-22300.

E. Moine, A. Piña-Martinez, J.N. Jaubert, B. Sirjean, R. Privat, I-PC-SAFT: an industrialized version of the volume-translated PC-SAFT equation of state for pure components, resulting from experience acquired all through the years on the parameterization of Saft-type and cubic models, *Industrial & Engineering Chemistry Research* 58 (2019) 20815-20827.

E.A. Müller, K.E. Gubbins, Molecular-based equations of state for associating fluids: A review of SAFT and related approaches, *Industrial & Engineering Chemistry Research* 40 (2001) 2193-2211.

F. Llovell, L.F.Vega, Prediction of thermodynamic derivative properties of pure fluids through the soft-SAFT equation of state, *The Journal of Physical Chemistry B* 110 (2006) 11427-11437.

F. Tzirakis, I. Tsivintzelis, A.I. Papadopoulos, P. Seferlis, Experimental measurement and assessment of equilibrium behaviour for phase change solvents used in CO_2 capture, *Chemical Engineering Science* 199 (2019) 20-27.

F.J. Blas, L.F. Vega, Critical behavior and partial miscibility phenomena in binary mixtures of hydrocarbons by the statistical associating fluid theory, *The Journal of Chemical Physics* 109 (1998) 7405-7413.

F.J. Blas, L.F. Vega, Prediction of binary and ternary diagrams using the statistical associating fluid theory (SAFT) equation of state, *Industrial & Engineering Chemistry Research* 37 (1998) 660-674.

G. Soave, Equilibrium constants from a modified Redlich–Kwong equation of state, *Chemical Engineering Science* 27 (1972) 1197-1203.

G.M. Kontogeorgis, E.C. Voutsas, I.V. Yakoumis, D.P. Tassios, D. P, An equation of state for associating fluids, *Industrial & Engineering Chemistry Research* 35 (1996) 4310-4318.

G.M. Kontogeorgis, X. Liang, A. Alay, T. Ioannis, Equations of state in three centuries. Are we closer to arriving to a single model for all applications? *Chemical Engineering Science: X* 7 (2020) 100060.

H.S. Majdi, A.B.F. Raheem, S.J. Abdullah, I.M. Mohammed, Y. Yasin, A. Yadav, S.K. Hadrawi, R. Shariyati, Prediction of speed of sound and specific heat capacity of ionic liquids using predictive SAFT-based equation of state, *Chemical Engineering Science* 265 (2023) 118246.

I. Anoune, Z. Mimoune, H. Madani, A. Merzougui, New modified PC-SAFT pure component parameters for accurate VLE and critical phenomena description, *Fluid Phase Equilibria* 532 (2021) 112916.

I. Polishuk, A modeling framework for predicting and correlating viscosities of liquids in wide range of conditions, *Industrial & Engineering Chemistry Research* 54 (2015) 6999-7003.

I. Polishuk, H. Lubarsky, D. NguyenHuynh, Predicting phase behavior in aqueous systems without fitting binary parameters II: Gases and non-aromatic hydrocarbons, *AIChE Journal* 63 (2017) 5064-5075.

I. Polishuk, J.M. Garrido, Comparison of SAFT-VR-Mie and CP-PC-SAFT in predicting phase behavior of associating systems I. Ammonia-water, methanol, ethanol and hydrazine. *Journal of Molecular Liquids* 265 (2018) 639-653.

I. Polishuk, Standardized critical point-based numerical solution of statistical association fluid theory parameters: the perturbed chain-statistical association fluid theory equation of state revisited, *Industrial & Engineering Chemistry Research* 53 (2014) 14127-14141.

I. Polishuk, Y. Sidik, D. NguyenHuynh, Predicting phase behavior in aqueous systems without fitting binary parameters I: CP-PC-SAFT EOS, aromatic compounds, *AIChE Journal* 63 (2017) 4124-4135.

J. Chen, J.G. Mi, Equation of state extended from SAFT with improved results for non-polar fluids across the critical point, *Fluid Phase Equilibria* 186 (2001) 165-184.

J. Gross, G. Sadowski, Perturbed-chain SAFT: An equation of state based on a perturbation theory for chain molecules, *Industrial & Engineering Chemistry Research* 40 (2001) 1244−1260.

J. Shi, H.A. Li, Criterion for determining crossover phenomenon in volume-translated equation of states, *Fluid Phase Equilibria* 430 (2016) 1-12.

J. Shi, H.A. Li, W. Pang, An improved volume translation strategy for PR EOS without crossover issue, *Fluid Phase Equilibria* 470 (2018) 164-175.

J. Shi, H. Li, Modified temperature-dependent volume translation model in PC-SAFT equation of state for carbon dioxide, *Chemical Engineering Science* 263 (2022) 118107.

J. Shi, H. Li, An improved volume translation model for PC-SAFT EOS based on a distance function, *Chemical Engineering Science* 276 (2023) 118800.

M. Vitali, C. Zuliani, F. Corvaro, B. Marchetti, A. Terenzi, F. Tallone, Risks and safety of CO2 transport via pipeline: A review of risk analysis and modeling approaches for accidental releases, *Energies* 14 (2021) 4601.

M. Yang, T. Zhan, Y. Su, A. Dong, M. He, Y. Zhang. Crossover PC-SAFT equations of state based on White's method for the thermodynamic properties of CO2, n-alkanes and n-alkanols, *Fluid Phase Equilibria* 564 (2023) 113610.

M.R. Faradonbeh, J. Abedi, T.G. Harding, Comparative study of eight cubic equations of state for predicting thermodynamic properties of alkanes, *The Canadian Journal of Chemical Engineering* 91 (2013) 101-110.

M.S. Wertheim, Fluids with highly directional attractive forces. I. Statistical thermodynamics, *Journal of Statistical Physics* 35 (1984) 19-34.

M.S. Wertheim, Fluids with highly directional attractive forces. II. Thermodynamic perturbation theory and integral equations, *Journal of Statistical Physics* 35 (1984) 35-47.

M.S. Wertheim, Fluids with highly directional attractive forces. III. Multiple attraction sites, *Journal of Statistical Physics* 42 (1986) 459-476.

M.S. Wertheim, Fluids with highly directional attractive forces. IV. Equilibrium polymerization, *Journal of Statistical Physics* 42 (1986) 477-492.

P.J. Linstrom, W.G. Mallard, NIST Chemistry WebBook, NIST Standard Reference Database Number 69, National Institute of Standards and Technology, Gaithersburg, MD, 20899, http://webbook.nist.gov.

P.N. Ghoderao, V.H. Dalvi, M. Narayan, A five-parameter cubic equation of state for pure fluids and mixtures, *Chemical Engineering Science: X* 3 (2019) 100026.

P.N. Ghoderao, V.H. Dalvi, M. Narayan, A four-parameter cubic equation of state for pure compounds and mixtures, *Chemical Engineering Science* 190 (2018) 173-189.

S.P. Peletiri, I.M. Mujtaba, N. Rahmanian, Process simulation of impurity impacts on CO2 fluids flowing in pipelines, *Journal of Cleaner Production* 240 (2019) 118145.

S.P. Tan, H. Adidharma, M. Radosz, Recent advances and applications of statistical associating fluid theory, *Industrial & Engineering Chemistry Research* 47 (2008) 8063-8082.

T. Lafitte, A. Apostolakou, C. Avendaño, A. Galindo, C.S. Adjiman, E.A. Müller, G. Jackson, Accurate statisticalassociating fluid theory for chain molecules from Mie segments, *The Journal of Chemical Physics* 139 (2013) 154504.

T. Lafitte, D. Bessieres, M. Piñeiro, J.L. Daridon, Simultaneous estimation of phase behavior and second-derivative properties using the statistical associating fluid theory with variable range approach, *The Journal of Chemical Physics* 124 (2006) 024509.

W.G. Chapman, K.E. Gubbins, G. Jackson, M. Radosz, SAFT: equation-of-state solution model for associating fluids, *Fluid Phase Equilibria* 52 (1989) 31-38.

X. Chen, H. Li, An improved volume-translated SRK EOS dedicated to more accurate determination of saturated and single-phase liquid densities, *Fluid Phase Equilibria* 521 (2020) 112724.

Y. Zhang, L. Yu, K. Cui, H. Wang, T. Fu, Carbon capture and storage technology by steel-making slags: Recent progress and future challenges, *Chemical Engineering Journal* 455 (2023) 140552.

CHAPTER 6 CONCLUSIONS, CONTRIBUTIONS AND RECOMMENDATIONS

6.1 Conclusions and Scientific Contributions to the Literature

This thesis develops improved volume-translated PC-SAFT EOSs for achieving more accurate prediction of PVT properties and thermodynamic derivative properties at the non-critical region and near-critical region. Specifically, a temperature-dependent-volume translated PC-SAFT EOS and a distance-function-based volume translated PC-SAFT EOS (VTR-PC-SAFT EOS) are proposed in this study. VTR-PC-SAFT EOS is applied to diverse chemical species (i.e., 20 chemical species) to have a more comprehensive testing of its performance in correlating various thermodynamic properties. Moreover, the performance of VTR-PC-SAFT EOS in predicting the thermodynamic derivative properties is compared against the other three benchmark PC-SAFT EOSs. Generally, the results indicate that the VTR-PC-SAFT EOS outperform those benchmark PC-SAFT EOSs.

CHAPTER 2:

In this chapter, we develop a nonlinear temperature-dependent volume translation model based on CPPC-SAFT EOS. With the exact reproductions of critical temperature and critical pressure, the proposed strategy can provide a more accurate density prediction of CO_2. Consequently, among all the PC-SAFT EOSs examined in this study, for the liquid-phase density and supercritical-phase density, this model can provide the smallest %AADs compared with the other three models (the original PC-SAFT, CPPC-SAFT, and I-PC-SAFT EOS). For the vapor-phase density, these models demonstrate a

similar %AAD. Meanwhile, our model can provide the most accurate predictions of the vapor pressure and saturated density with the smallest overall %AADs.

CHAPTER 3:

In this chapter, we develop a volume translation model for CPPC-SAFT EOS based on a newly proposed distance-function. With the exact reproduction of critical temperature, critical pressure, and critical molar volume, the proposed strategy can not only give a good match with the needed saturated-liquid molar volume residuals but also capture the variation trend of single-liquid molar volume residuals at different pressures. In addition, the proposed volume-translated rescaled PC-SAFT EOS (VTR-PC-SAFT EOS) leads to significantly better predictions of thermodynamic properties of pure compounds both near and far from the critical region. Consequently, among all the PC-SAFT EOSs examined in this study, the proposed VTR-PC-SAFT EOS provides the smallest %AADs in reproducing the saturated-liquid molar volume, liquid molar volume, and vapor pressure of 39 pure compounds. Moreover, a generalized version of the VTR-PC-SAFT proposed in this work is developed for *n*-alkanes (except CH_4).

CHAPTER 4:

In this chapter, we further apply the established VTR-PC-SAFT EOS to more diverse chemical species. The two component-dependent parameters (c_1 and c_2) in the distance-function-based volume translation in the VTR-PC-SAFT EOS are further regressed for 251 chemical compounds. In addition, the performance of VTR-PC-SAFT EOS is assessed in reproducing the critical and non-critical properties of these pure compounds. The evaluation results show that, among all the PC-SAFT EOSs examined in

this study, the VTR-PC-SAFT EOS can yield a significantly higher accuracy in predicting both non-critical and critical properties for the majority of the 251 chemical compounds.

CHAPTER 5:

In this chapter, we assess the performance of VTR-PC-SAFT EOS in predicting the derivative properties including thermal expansion coefficient, isothermal compressibility coefficient, isobaric heat capacity, Joule-Thomson coefficient, and speed of sound. Pure compounds including CO_2 and *n*-alkanes relevant to CO_2 flooding and storage applications are investigated. Among all the PC-SAFT EOSs examined in this study, VTR-PC-SAFT EOS outperforms the other models in predicting most of the derivative properties. It yields the smallest %AADs in predicting thermal expansion coefficient, isothermal compressibility coefficient, Joule-Thomson coefficient, and speed of sound, but a marginally higher %AAD in predicting the isobaric heat capacity than the original PC-SAFT EOS.

6.2 Suggested Future Works

- We could extend the application of the VTR-PC-SAFT EOS (Shi and Li, 2023) to mixtures such as water-containing mixtures. It is crucial to select an appropriate mixing rule in this case. The hydrogen bonding behavior of water molecules should be also taken into account.
- We could develop a critical-point-rescaled PR EOS or SRK EOS coupled with a distance-function-based volume translation model. A new temperature and pressure dependent volume translation based on the distance function, which can reproduce the critical molar volume, is required for the accurate representation of phase behavior of pure substances near the critical point.

- We could further evaluate the possible numerical pitfalls (Sun *et al.*, 2020; Polishuk, 2011) existing in the various PC-SAFT-type EOSs due to the temperature dependencies of a segment packing fraction and the very high-polynomial orders in volume (Polishuk, 2010). The representative PC-SAFT EOSs (including CPPC-SAFT EOS (Anoune *et al.*, 2021), I-PC-SAFT EOS (Moine *et al.*, 2019), and VTR-PC-SAFT EOS (Shi and Li, 2023)) could be evaluated.
- Given that both the VTR-PC-SAFT EOS and crossover PC-SAFT EOS (Llovell *et al.*, 2004 and 2006; Smith *et al.*, 2022) are successful modifications of the PC-SAFT EOSs, providing commendable representations of phase behavior near the critical region, it is imperative to quantitatively compare their capability in predicting thermodynamic derivative properties. This assessment should place particular emphasis on both first-order and second-order derivative properties near the critical region.

References

E. Moine, A. Piña-Martinez, J.N. Jaubert, B. Sirjean, R. Privat, I-PC-SAFT: an industrialized version of the volume-translated PC-SAFT equation of state for pure components, resulting from experience acquired all through the years on the parameterization of Saft-type and cubic models, *Industrial & Engineering Chemistry Research* 58 (2019) 20815-20827.

F. Llovell, J.C. Pàmies, L.F. Vega, Thermodynamic properties of Lennard-Jones chain molecules: Renormalization-group corrections to a modified statistical associating fluid theory, *The Journal of Chemical Physics* 121 (2004) 10715-10724.

F. Llovell, L.F. Vega, Global fluid phase equilibria and critical phenomena of selected mixtures using the crossover soft-SAFT equation, *The Journal of Physical Chemistry B* 110 (2006) 1350-1362.

I. Anoune, Z. Mimoune, H. Madani, A. Merzougui, New modified PC-SAFT pure component parameters for accurate VLE and critical phenomena description, *Fluid Phase Equilibria* 532 (2021) 112916.

I. Polishuk, About the numerical pitfalls characteristic for SAFT EOS models, *Fluid Phase Equilibria* 298 (2010) 67-74.

I. Polishuk, Addressing the issue of numerical pitfalls characteristic for SAFT EOS models, *Fluid phase equilibria* 301 (2011) 123-129.

J. Shi and H. Li, An improved volume translation model for PC-SAFT EOS based on a distance function, *Chemical Engineering Science* 276 (2023) 118800.

S.A.M. Smith, J.T. Cripwell, C.E. Schwarz, Application of renormalization corrections to SAFT-VR Mie, *Industrial & Engineering Chemistry Research* 61 (2022) 12797-12812.

Y. Sun, Z. Zuo, A. Laaksonen, X. Lu, X. Ji, How to detect possible pitfalls in ePC-SAFT modelling: Extension to ionic liquids, *Fluid Phase Equilibria* 519 (2020) 112641.

BIBLIOGRAPHY

A. Bymaster, C. Emborsky, A. Dominik, W.G. Chapman, Renormalization-group corrections to a perturbed-chain statistical associating fluid theory for pure fluids near to and far from the critical region, *Industrial & Engineering Chemistry Research* 47 (2008) 6264−6274.

A. Kordikowski, A.P. Schenk, R.M. Van Nielenand, C.J. Peters, Volume expansions and vapor-liquid equilibria of binary mixtures of a variety of polar solvents and certain near-critical solvents, *The Journal of Supercritical Fluids* 8 (1995) 205-216.

A. Kumar, R. Okuno, A new algorithm for multiphase-fluid characterization for solvent injection, *SPE Journal* 21 (2016) 1688-1704.

A. Kumar, R. Okuno, Direct perturbation of the Peng–Robinson attraction and covolume parameters for reservoir fluid characterization, *Chemical Engineering Science* 127 (2015) 293-309.

A. Maghari, M.S. Sadeghi, Prediction of sound velocity and heat capacities of n-alkanes from the modified SAFT-BACK equation of state, *Fluid Phase Equilibria* 252 (2007) 152-161.

A. Maghari, Z. Safaei, S. Sarhangian, Predictions of the Joule–Thomson inversion curves for polar and non-polar fluids from the SAFT-CP equation of state, *Cryogenics* 48 (2008) 48-55.

A. Pakravesh, F. Zarei, H. Zarei, PρT parameterization of SAFT equation of state: developing a new parameterization method for equations of state, *Fluid Phase Equilibri*a 538 (2021) 113024.

A. Pakravesh, H. Zarei, Prediction of Joule–Thomson coefficients and inversion curves of natural gas by various equations of state, *Cryogenics* 118 (2021) 103350.

A. Peneloux, E. Rauzy, R. Freze, A consistent correction for Redlich-Kwong-Soave volumes, *Fluid Phase Equilibria* 8 (1982) 7-23.

A. Piña-Martinez, R. Privat, J.N. Jaubert, Use of 300,000 pseudo-experimental data over 1800 pure fluids to assess the performance of four cubic equations of state: SRK, PR, tc-RK, and tc-PR, *AIChE Journal* 68 (2022) e17518.

A. Saeed, G. Sattar, Calculation of density, vapor pressure and heat capacity near the critical point by incorporating cubic SRK EoS and crossover translation, *Fluid Phase Equilibria* 493 (2019) 10-25.

A. Tihic, G.M. Kontogeorgis, N. Von Solms, M.L. Michelsen, Applications of the simplified perturbed-chain SAFT equation of state using an extended parameter table, *Fluid Phase Equilibria* 248 (2006) 29-43.

A.F. Young, F.L. Pessoa, V.R. Ahón, Comparison of volume translation and co-volume functions applied in the Peng-Robinson EoS for volumetric corrections, *Fluid Phase Equilibria* 435 (2017) 73-87.

A.I. Papadopoulos, F.A. Perdomo, F. Tzirakis, G. Shavalieva, I. Tsivintzelis, P. Kazepidis, E. Nessi, S. Papadokonstantakis, P. Seferlis, A. Galindo, G. Jackson, C.S. Adjiman, Molecular engineering of sustainable phase-change solvents: from digital design to scaling-up for CO2 capture, *Chemical Engineering Journal* 420 (2021) 127624.

A.J. De Villiers, C.E. Schwarz, A.J. Burger, G.M. Kontogeorgis, Evaluation of the PC-SAFT, SAFT and CPA equations of state in predicting derivative properties of selected non-polar and hydrogen-bonding compounds, *Fluid Phase Equilibria* 338 (2013) 1-15.

A.K. Wyczalkowska, J.V. Sengers, M.A. Anisimov, Critical fluctuations and the equation of state of van der Waals, *Physica A: Statistical Mechanics and its Applications* 334 (2004) 482-512.

A.M. Abudour, S.A. Mohammad, R.L. Robinson, K.A.M. Gasem, Volume translated Peng-Robinson equation of state for saturated and single-phase liquid densities, *Fluid Phase Equilibria* 335 (2012) 74–87.

A.M. Palma, A.J. Queimada, J.A. Coutinho, Using a volume shift in perturbed-chain statistical associating fluid theory to improve the description of speed of sound and other derivative properties, *Industrial & Engineering Chemistry Research* 57 (2018) 11804-11814.

A.P. Vinhal, W. Yan, G.M. Kontogeorgis, Evaluation of equations of state for simultaneous representation of phase equilibrium and critical phenomena, *Fluid Phase Equilibria* 437 (2017) 140-154.

A.V. Venkatramani, R. Okuno, Characterization of water-containing reservoir oil using an EOS for steam injection processes, *Journal of Natural Gas Science and Engineering* 26 (2015) 1091-106.

B. Zhang, E. Wang, F. Meng, F. Zhang, C. Zhao, Prediction accuracy of thermodynamic properties using PC-SAFT for high-temperature organic Rankine cycle with siloxanes, *Energy* 204 (2020) 117980.

C. Lundstrøm, M. L. Michelsen, G.M. Kontogeorgis, K.S. Pedersen, H. Sørensen, Comparison of the SRK and CPA equations of state for physical properties of water and methanol, *Fluid Phase Equilibria* 247 (2006) 149-157.

C. McCabe, G. Jackson, SAFT-VR modelling of the phase equilibrium of long-chain n-alkanes, *Physical Chemistry Chemical Physics* 1 (1999) 2057-2064.

D.V. Nichita, F. García-Sánchez, and S. Gómez, Phase stability analysis using the PC-SAFT equation of state and the tunneling global optimization method, *Chemical Engineering Journal* 140 (2008) 509-520.

D.Y. Peng, D.B. Robinson, A new two-constant equation of state, *Industrial & Engineering Chemistry Fundamentals* 15 (1976) 59-64.

DIPPR's Project 801 Database. DIPPR: Design Institute for Physical Properties, 2021. https://www.aiche.org/dippr.

E. Cea-Klapp, I. Polishuk, R.I. Canales, H. Quinteros-Lama, J.M. Garrido, Estimation of thermodynamic properties and phase equilibria in systems of deep eutectic solvents by PC-SAFT EoS, *Industrial & Engineering Chemistry Research* 59 (2020) 22292-22300.

E. Moine, A. Piña-Martinez, J.N. Jaubert, B. Sirjean, R. Privat, I-PC-SAFT: an industrialized version of the volume-translated PC-SAFT equation of state for pure components, resulting from experience acquired all through the years on the parameterization of Saft-type and cubic models, *Industrial & Engineering Chemistry Research* 58 (2019) 20815-20827.

E.A. Müller, K.E. Gubbins, Molecular-based equations of state for associating fluids: A review of SAFT and related approaches, *Industrial & Engineering Chemistry Research* 40 (2001) 2193-2211.

F. Llovell, C.J. Peters, L.F. Vega, Second-order thermodynamic derivative properties of selected mixtures by the soft-SAFT equation of state, *Fluid Phase Equilibria* 248 (2006) 115-122.

F. Llovell, J.C. Pàmies, L.F. Vega, Thermodynamic properties of Lennard-Jones chain molecules: Renormalization-group corrections to a modified statistical associating fluid theory, *The Journal of Chemical Physics* 121 (2004) 10715-10724.

F. Llovell, L.F. Vega, Global fluid phase equilibria and critical phenomena of selected mixtures using the crossover soft-SAFT equation, *The Journal of Physical Chemistry B* 110 (2006) 1350-1362.

F. Llovell, L.F. Vega, M.A. Anisimov, J.V. Sengers, Incorporating critical divergence of isochoric heat capacity into the soft-SAFT equation of state, *AIChE Journal* 61 (2015) 3073-3080.

F. Llovell, L.F. Vega, Prediction of thermodynamic derivative properties of pure fluids through the soft-SAFT equation of state, *The Journal of Physical Chemistry B* 110 (2006) 11427-11437.

F. Tzirakis, I. Tsivintzelis, A.I. Papadopoulos, P. Seferlis, Experimental measurement and assessment of equilibrium behaviour for phase change solvents used in CO2 capture, *Chemical Engineering Science* 199 (2019) 20-27.

F.J. Blas, L.F. Vega, Critical behavior and partial miscibility phenomena in binary mixtures of hydrocarbons by the statistical associating fluid theory, *The Journal of Chemical Physics* 109 (1998) 7405-7413.

F.J. Blas, L.F. Vega, Prediction of binary and ternary diagrams using the statistical associating fluid theory (SAFT) equation of state, *Industrial & Engineering Chemistry Research* 37 (1998) 660-674.

G. Soave, Equilibrium constants from a modified Redlich–Kwong equation of state, *Chemical Engineering Scienc*e 27 (1972) 1197-1203.

G.F. Chou, J.M. Prausnitz, A phenomenological correction to an equation of state for the critical region, *AIChE Journal* 35 (1989) 1487-1496.

G.M. Kontogeorgis, E.C. Voutsas, I.V. Yakoumis, D.P. Tassios, D. P, An equation of state for associating fluids, *Industrial & Engineering Chemistry Research* 35 (1996) 4310-4318.

G.M. Kontogeorgis, X. Liang, A. Arya, I. Tsivintzelis, Equations of state in three centuries. Are we closer to arriving to a single model for all applications? *Chemical Engineering Science: X* 7 (2020) 100060.

H. Li, J.P. Jakobsen, Ø. Wilhelmsen, J. Yan, PVTxy properties of CO2 mixtures relevant for CO2 capture, transport and storage: Review of available experimental data and theoretical models, *Applied Energy* 88 (2011) 3567-3579.

H. Zhao, C. Song, H. Zhang, C. Di, Z. Tian, Improved fluid characterization and phase behavior approaches for gas flooding and application on Tahe light crude oil system, *Journal of Petroleum Science and Engineering* 208 (2022) 109653.

H.S. Majdi, A.B.F. Raheem, S.J. Abdullah, I.M. Mohammed, Y. Yasin, A. Yadav, S.K. Hadrawi, R. Shariyati, Prediction of speed of sound and specific heat capacity of ionic liquids using predictive SAFT-based equation of state, *Chemical Engineering Science* 265 (2023) 118246.

I. Anoune, Z. Mimoune, H. Madani, A. Merzougui, New modified PC-SAFT pure component parameters for accurate VLE and critical phenomena description, *Fluid Phase Equilibria* 532 (2021) 112916.

I. Khmelinskii, L.V. Woodcock, Supercritical fluid gaseous and liquid states: a review of experimental results, *Entropy* 22 (2020) 437.

I. Polishuk I, A. Chiko, E. Cea-Klapp, J.M. Garrido, Implementation of CP-PC-SAFT and CS-SAFT-VR-Mie for predicting thermodynamic properties of C1–C3 halocarbon systems. I. Pure compounds and mixtures with non-associating compounds, *Industrial & Engineering Chemistry Research* 60 (2021) 9624-9636.

I. Polishuk, A modeling framework for predicting and correlating viscosities of liquids in wide range of conditions, *Industrial & Engineering Chemistry Research* 54 (2015) 6999-7003.

I. Polishuk, About the numerical pitfalls characteristic for SAFT EOS models, *Fluid Phase Equilibria* 298 (2010) 67-74.

I. Polishuk, Addressing the issue of numerical pitfalls characteristic for SAFT EOS models, *Fluid Phase Equilibria* 301 (2011) 123-129.

I. Polishuk, H. Lubarsky, D. NguyenHuynh, Predicting phase behavior in aqueous systems without fitting binary parameters II: Gases and non-aromatic hydrocarbons, *AIChE Journal* 63 (2017) 5064-5075.

I. Polishuk, Hybridizing SAFT and cubic EOS: what can be achieved?, *Industrial & Engineering Chemistry Research* 50 (2011) 4183-4198.

I. Polishuk, J. Wisniak, H. Segura, A novel approach for defining parameters in a four-parameter EOS, *Chemical Engineering Science* 55 (2000) 5705-5720.

I. Polishuk, J.M. Garrido, Comparison of SAFT-VR-Mie and CP-PC-SAFT in predicting phase behavior of associating systems I. Ammonia-water, methanol, ethanol and hydrazine. *Journal of Molecular Liquids* 265 (2018) 639-653.

I. Polishuk, Standardized critical point-based numerical solution of statistical association fluid theory parameters: the perturbed chain-statistical association fluid theory equation of state revisited, *Industrial & Engineering Chemistry Research* 53 (2014) 14127-14141.

I. Polishuk, Y. Sidik, D. NguyenHuynh, Predicting phase behavior in aqueous systems without fitting binary parameters I: CP-PC-SAFT EOS, Aromatic Compounds, *AIChE Journal* 63 (2017) 4124-4135.

J. Chen, J.G. Mi, Equation of state extended from SAFT with improved results for non-polar fluids across the critical point, *Fluid Phase Equilibria* 186 (2001) 165-184.

J. Gross, G. Sadowski, Application of perturbation theory to a hard-chain reference fluid: an equation of state for square-well chains, *Fluid Phase Equilibria* 168 (2000) 183-199.

J. Gross, G. Sadowski, Perturbed-chain SAFT: An equation of state based on a perturbation theory for chain molecules, *Industrial & Engineering Chemistry Research* 40 (2001) 1244−1260.

J. Shi, H. Li, Modified temperature-dependent volume translation model in PC-SAFT equation of state for carbon dioxide, *Chemical Engineering Science* 263 (2022) 118107.

J. Shi, H.A. Li, Criterion for determining crossover phenomenon in volume-translated equation of states, *Fluid Phase Equilibria* 430 (2016) 1-12.

J. Shi, H.A. Li, W. Pang, An improved volume translation strategy for PR EOS without crossover issue, *Fluid Phase Equilibria* 470 (2018) 164-175.

J. Shi and H. Li, An improved volume translation model for PC-SAFT EOS based on a distance function, *Chemical Engineering Science* 276 (2023) 118800.

J. Wang, M.A. Anisimov, Nature of vapor-liquid asymmetry in fluid criticality, *Physical Review E* 75 (2007) 051107.

J.A. Barker, D. Henderson, Perturbation theory and equation of state for fluids: the square-well potential, *The Journal of Chemical Physics* 47 (1967) 2856-2861.

J.A. Barker, D. Henderson, Perturbation theory and equation of state for fluids. II. A successful theory of liquids, *The Journal of Chemical Physics* 47 (1967) 4714-4721.

J.A. White, Contribution of fluctuations to thermal properties of fluids with attractive forces of limited range: theory compared with PρT and Cv data for argon, *Fluid Phase Equilibria* 75 (1992) 53−64.

J.A. White, S. Zhang, Renormalization group theory for fluids, *The Journal of Chemical Physics* 99 (1993) 2012−2019.

J.A. White, S. Zhang, Renormalization theory of nonuniversal thermal properties of fluids, *The Journal of Chemical Physics* 103 (1995) 1922−1928.

J.J. Martin, Cubic equations of state-which? *Industrial & Engineering Chemistry Fundamentals* 18 (1979) 81-97.

J.M.L. Sengers, Mean-field theories, their weaknesses and strength, *Fluid Phase Equilibria* 158 (1999) 3-17.

J.N. Jaubert, R. Privat, Y. Le Guennec, L. Coniglio, Note on the properties altered by application of a Péneloux–type volume translation to an equation of state, *Fluid Phase Equilibria* 419 (2016) 88-95.

J.S. Lopez-Echeverry, S. Reif-Acherman, E. Araujo-Lopez, Peng-Robinson equation of state: 40 years through cubics, *Fluid Phase Equilibria* 447 (2017) 39-71.

J.Y. Seyf, M. Asgari, Parametrization of PC-SAFT EoS for solvents reviewed for use in pharmaceutical process design: VLE, LLE, VLLE, and SLE study, *Industrial & Engineering Chemistry Research* 61 (2022) 8252–8268.

K. Frey, C. Augustine, R.P. Ciccolini, S. Paap, M. Modell, J. Tester, Volume translation in equations of state as a means of accurate property estimation, *Fluid Phase Equilibria* 260 (2007) 316-325.

K. Frey, M. Modell, J. Tester, Density-and-temperature-dependent volume translation for the SRK EOS: 1. Pure fluids, *Fluid Phase Equilibria* 279 (2009) 56-63.

K.G. Wilson, M.E. Fisher, Critical exponents in 3.99 dimensions, *Physical Review Letters* 28 (1972) 240-243.

K.G. Wilson, Renormalization group and critical phenomena. II. Phase-space cell analysis of critical behavior, *Physical Review B* 4 (1971) 3184-3205.

K.G. Wilson, The renormalization group: Critical phenomena and the Kondo problem, *Reviews of Modern Physics* 47 (1975) 773.

L. Yelash, M. Müller, W. Paul, K. Binder, Artificial multiple criticality and phase equilibria: an investigation of the PC-SAFT approach, *Physical Chemistry Chemical Physics* 7 (2005) 3728-3732.

L.W. Salvino, J.A. White, Calculation of density fluctuation contributions to thermodynamic properties of simple fluids, *The Journal of Chemical Physics* 96 (1992) 4559−4568.

M. Cismondi, E.A. Brignole, J. Mollerup, Rescaling of three-parameter equations of state: PC-SAFT and SPHCT, *Fluid Phase Equilibria* 234 (2005) 108-121.

M. Vitali, C. Zuliani, F. Corvaro, B. Marchetti, A. Terenzi, F. Tallone, Risks and safety of CO2 transport via pipeline: A review of risk analysis and modeling approaches for accidental releases, *Energies* 14 (2021) 4601.

M. Yang, T. Zhan, Y. Su, A. Dong, M. He, Y. Zhang, Crossover PC-SAFT equations of state based on White's method for the thermodynamic properties of CO2, n-alkanes and n-alkanols, *Fluid Phase Equilibria* 564 (2023) 113610.

M.A. Anisimov, J. Wang, Nature of asymmetry in fluid criticality, *Physical Review Letters* 97 (2006) 025703.

M.R. Faradonbeh, J. Abedi, T.G. Harding, Comparative study of eight cubic equations of state for predicting thermodynamic properties of alkanes, *The Canadian Journal of Chemical Engineering* 91 (2013) 101-110.

M.S. Wertheim, Fluids with highly directional attractive forces. I. Statistical thermodynamics, *Journal of Statistical Physics* 35 (1984) 19-34.

M.S. Wertheim, Fluids with highly directional attractive forces. II. Thermodynamic perturbation theory and integral equations, *Journal of Statistical Physics* 35 (1984) 35-47.

M.S. Wertheim, Fluids with highly directional attractive forces. III. Multiple attraction sites, *Journal of Statistical Physics* 42 (1986) 459-476.

M.S. Wertheim, Fluids with highly directional attractive forces. IV. Equilibrium polymerization, *Journal of Statistical Physics* 42 (1986) 477-492.

N. Ramírez-Vélez, R. Privat, A. Piña-Martinez, J.N. Jaubert, Assessing the performance of non-associating SAFT-type equations of state to reproduce vapor pressure, liquid density, enthalpy of vaporization, and liquid heat capacity data of 1800 pure fluids, *AIChE Journal* 68 (2022) e17722.

O. Pfohl, Letter to the editor: "Evaluation of an improved volume translation for the prediction of hydrocarbon volumetric properties", *Fluid Phase Equilibria* 163 (1999) 157-159.

O. Pfohl, T. Giese, R. Dohrn, G. Brunner, 1. Comparison of 12 equations of state with respect to gas-extraction processes: reproduction of pure-component properties when enforcing the correct critical temperature and pressure, *Industrial & Engineering Chemistry Research* 37 (1998) 2957-2965.

P. De Castro, P. Sollich, Critical phase behavior in multi-component fluid mixtures: Complete scaling analysis, *The Journal of Chemical Physics* 149 (2018) 204902.

P. Navarro, A.M. Palma, J. García, F. Rodríguez, J.A. Coutinho, P.J. Carvalho, High-pressure density of bis(1-alkyl-3-methylimidazolium) tetraisothiocyanatocobaltate ionic liquids: experimental and PC-SAFT with volume-shift modeling, *Journal of Chemical & Engineering Data* 64 (2019) 4827-4833.

P.J. Linstrom, W.G. Mallard, NIST Chemistry WebBook, NIST Standard Reference Database Number 69, National Institute of Standards and Technology, Gaithersburg, MD, 20899, http://webbook.nist.gov (2001).

P.N. Ghoderao, V.H. Dalvi, M. Narayan, A five-parameter cubic equation of state for pure fluids and mixtures, *Chemical Engineering Science: X* 3 (2019) 100026.

P.N. Ghoderao, V.H. Dalvi, M. Narayan, A four parameter cubic equation of state with temperature dependent covolume parameter, *Chinese Journal of Chemical Engineering* 27 (2019) 1132-1148.

P.N. Ghoderao, V.H. Dalvi, M. Narayan, A four-parameter cubic equation of state for pure compounds and mixtures, *Chemical Engineering Science* 190 (2018) 173-189.

R. Privat, E. Moine, B. Sirjean, R. Gani, J.N. Jaubert, Application of the corresponding-state law to the parametrization of statistical associating fluid theory (SAFT)-type models: Generation and use of "generalized charts", *Industrial & Engineering Chemistry Research* 58 (2019) 9127-9139.

R. Privat, R. Gani, J.N. Jaubert, Are safe results obtained when the PC-SAFT equation of state is applied to ordinary pure chemicals? *Fluid Phase Equilibria* 295 (2010) 76-92.

R.S. Norhasyima and T.M.I. Mahlia, Advances in CO_2 utilization technology: A patent landscape review, *Journal of CO_2 Utilization* 26 (2018) 323-335.

S. Dufal, T. Lafitte, A. Galindo, G. Jackson, A.J. Haslam, Developing intermolecular-potential models for use with the SAFT-VR Mie equation of state, *AIChE Journal* 61 (2015) 2891-2912.

S.A.M. Smith, J.T. Cripwell, C.E. Schwarz, Application of renormalization corrections to SAFT-VR Mie, *Industrial & Engineering Chemistry Research* 61 (2022) 12797-12812.

S.B. Kiselev, Cubic crossover equation of state, *Fluid Phase Equilibria* 147 (1998) 7-23.

S.P. Peletiri, I.M. Mujtaba, N. Rahmanian, Process simulation of impurity impacts on CO2 fluids flowing in pipelines, *Journal of Cleaner Production* 240 (2019) 118145.

S.P. Tan, H. Adidharma, M. Radosz, Recent advances and applications of statistical associating fluid theory, *Industrial & Engineering Chemistry Research* 47 (2008) 8063-8082.

T. Lafitte, A. Apostolakou, C. Avendaño, A. Galindo, C.S. Adjiman, E.A. Müller, G. Jackson, Accurate statisticalassociating fluid theory for chain molecules from Mie segments, *The Journal of Chemical Physics* 139 (2013) 154504.

T. Merker, C. Engin, J. Vrabec, H. Hasse, Molecular model for carbon dioxide optimized to vapor-liquid equilibria, *The Journal of Chemical Physics* 132 (2010) 234512.

V. Kalikhman, D. Kost, and I. Polishuk, About the physical validity of attaching the repulsive terms of analytical EOS models by temperature dependencies, *Fluid Phase Equilibria* 293 (2010) 164-167.

W. Song, L. Liu, D. Wang, Y. Li, M. Prodanović, J. Yao, Nanoscale confined multicomponent hydrocarbon thermodynamic phase behavior and multiphase transport ability in nanoporous material, *Chemical Engineering Journal* 382 (2020) 122974.

W.D. Monnery, W.Y. Svrcek, M.A. Satyro, Gaussian-like Volume Shifts for the Peng−Robinson Equation of State, *Industrial & Engineering Chemistry Research* 37 (1998) 1663-1672.

W.G. Chapman, K.E. Gubbins, G. Jackson, M. Radosz, New reference equation of state for associating liquids, *Industrial & Engineering Chemistry Research* 29 (1990) 1709-1721.

W.G. Chapman, K.E. Gubbins, G. Jackson, M. Radosz, SAFT: equation-of-state solution model for associating fluids, *Fluid Phase Equilibria* 52 (1989) 31-38.

W.R. Ji, D.A. Lempe, Density improvement of the SRK equation of state, *Fluid Phase Equilibria* 130 (1997) 49-63.

X. Chen, H. Li, An improved volume-translated SRK EOS dedicated to more accurate determination of saturated and single-phase liquid densities, *Fluid Phase Equilibria* 521 (2020) 112724.

X. Chen, H. Li, Improved prediction of saturated and single-phase liquid densities of water through volume-translated SRK EOS, *Fluid Phase Equilibria* 528 (2021) 112852.

X. Li, H. Han, D. Yang, X. Liu, J. Qin, Phase behavior of C_3H_8–CO_2–heavy oil systems in the presence of aqueous phase under reservoir conditions, *Fuel* 209 (2017) 358-370.

Y. Sun, Z. Zuo, A. Laaksonen, X. Lu, X. Ji, How to detect possible pitfalls in ePC-SAFT modelling: Extension to ionic liquids, *Fluid Phase Equilibria* 519 (2020) 112641.

Y. Zhang, L. Yu, K. Cui, H. Wang, T. Fu, Carbon capture and storage technology by steel-making slags: Recent progress and future challenges, *Chemical Engineering Journal* 455 (2023) 140552.

Y.S. Wei and R.J. Sadus, Equations of state for the calculation of fluid-phase equilibria, *AIChE Journal* 46 (2000) 169-196.

Z.Q. Hu, J.C. Yang, Y.G. Li, Crossover SAFT equation of state for pure supercritical fluids, *Fluid Phase Equilibria* 205 (2003) 1-15.